



RESEARCH ARTICLE

Effect of Organophosphate-Pesticide on the Freshwater Fish *Labeo rohita* (Hamilton)

S.Kalaimani¹ and C.Kandeepan^{2*}

¹Department of Zoology, GTN College, Dindigul-624001, Tamilnadu, India.

²Postgraduate & Research Department of Zoology, Arulmigu Palaniandavar College of Arts and Culture, Palani, Tamilnadu, India.

Received: 13 Aug 2017

Revised: 28 Aug 2017

Accepted: 5 Sep 2017

* Address for correspondence

Dr.C.Kandeepan

Postgraduate & Research Department of Zoology,
Arulmigu Palaniandavar College of Arts and Culture,
Palani, Tamilnadu, India.

E.mail: kansbiotech@gmail.com



This is an Open Access Journal / article distributed under the terms of the **Creative Commons Attribution License** (CC BY-NC-ND 3.0) which permits unrestricted use, distribution, and reproduction in any medium, provided the original work is properly cited. All rights reserved.

ABSTRACT

The Indian major carp *Labeo rohita* (Hamilton) was exposed to the organophosphate pesticide Phosalone and 1.5ppm, 2.5ppm and 4.0ppm were determined as sublethal, median lethal and lethal concentrations at 96 hr of exposure. These LC₅₀ values indicate that the Phosalone is highly toxic to fish. The fish were exposed to sub-lethal concentration (1.5ppm) for 4 days and the changes in the biochemical constituents were studied. Significant changes in Respiratory, haematological, Biochemical and enzymological parameters in fish were observed. Several behavioural changes during the period of exposure were also observed and noted. The results obtained were discussed at length with the available literature.

Keywords: Hamilton, Pesticide, Phosalone, Fish.

INTRODUCTION

Pesticides are widely used in modern agriculture to aid in the production of high quality food. However, some pesticides have the potential to cause serious health and environmental damage. Though the pesticides are applied to enhance agricultural production while the indiscriminate and contaminate the biota. Subsequent to the translocation of pesticides to aquatic environment the non-targets such as fish are exposed to low concentration over a long period and affect the efficiency of various life parameters and seem to produce many physiological and Biochemical changes in fish. Fish have been valued for many years as excellent indicators of water quality. High usage of pesticide in the field, it affects both biotic and abiotic environment. The oxygen consumption (biotic) is a very sensitive physiological process and the change in respiratory activity has been used as an indicator of stress in animals exposed to toxicants. A number of investigations on the effect of pesticides on the Oxygen Consumption of





Kalaimani and Kandeepan

fish have been reported (Ram Nayan Singh et al., 2014; Mohammad Illiyas Hussain et al., 2015; Sivakumar 2015). Stresses and pollutants generally cause relatively rapid changes in Blood characteristics of fish (Kandeepan 2013; Deshmukh, 2016). A reduction in haemoglobin content and erythrocyte population resulting in anaemia have also been suggested as reason for drop in Oxygen uptake in fish *Channa punctatus* exposed to lethal Concentration of Deltamethrin (Jayaprakash and Shettu, 2013). Though, the biochemical, Physiological and enzymatic parameters are the common biomarkers of exposed fish to toxicity of pollutant.

Since blood glucose level is an important parameter to assess the stress condition of fish by pesticides. Enzymes play a significant role in food Utilization and Metabolism. Phosphatase plays an important role in synthesis and transport of metabolites across the membrane, secretory activity, and protein synthesis and glycogen metabolism. Pesticide pollution also affects the activity of enzymes and produce metabolic changes at cellular levels. The toxic effects of organophosphorous compounds on the activity of alkaline phosphatase in various tissues of fishes have been worked out by various workers. Dubey et al., (2014) reported significant inhibition of alkaline Phosphatase in liver, intestine and muscle tissues of *Clarias batrachus* when exposed to Dimethoate. The decrease in acid phosphatase in liver suggested the uncoupling of phosphorylation by toxicity. Acid phosphatase were significant decrease in liver tissue when compared to those of muscle and gills in the fish *Labeo rohita* collected from Industrial polluted lake. The effect of Rogor on the activity of alkaline phosphatase was studied by Borah and Yadav (1996).

In view of the paucity of information regarding the effects of pesticide, Phosalone on Respiratory, haematological, Biochemical and enzymological parameters in *Labeo rohita* (Hamilton), were made in this investigation.

MATERIALS AND METHODS

Commercially valuable and edible fresh water fish *Labeo rohita* used in this experiment. The length and weight of the fishes ranged between 10-15 cm and 25-30 g, respectively, were acclimatized to laboratory conditions for 10 days and separated into groups (10 each). During the acclimatized period fishes were fed ad-libitum with rice bran (or) powdered oil cakes. The median lethal concentration (LC₅₀) and sub lethal concentrations were found out by exposing the fish to different concentrations of Phosalone (1.5, 2, and 2.5 PPM) for 4 days and control group was also maintained separately. Pesticide, organophosphate represent one of the most widely used classes of pesticide with high potential for human exposure in field of cultivated area. Phosalone (C₁₂H₁₅CINO₄PS₂) is a broad spectrum organophosphate pesticide widely used to control pests in agricultural crops. It is commercially available organophosphate pesticide and is more toxic to living beings.

Before starting the experiment the Oxygen content of water used in the animal chamber was estimated by Winkler's method. Blood sample was collected from the control and experimental fishes by cardinal vein puncture using an insulin syringe containing 0.1ml of 0.2% EDTA of each group at 1st, 2nd, 3rd and 4th day of experiment. Haemoglobin was estimated by Darbkin's method (Suganthi et al. 2015a). The blood sugar was estimated by O - toluidine method. The alkaline phosphatase was estimated by using the method of Bergmeyer (1963) as modified by Butterworth and Probert (1970).

RESULTS AND DISCUSSION

The mortality of fish can be observed that, mortality did not occur at 1.5 PPM concentration of Phosalone for 96 h exposure. The mortality rate increased as concentration of Phosalone increased (Fig.1). The sub lethal concentration is 1.5 PPM, median lethal concentration (LC₅₀) is 2.5PPM and the lethal concentration is 4 PPM for 96 hrs exposure. The LC₅₀ value differs from species to species for the same pesticide as well as for different pesticides due to their mode of action on fish. Durairaj and Selvarajan (1991) have estimated LC₅₀ value for Quinolphos and Phenthoate and were found to be 7.5 PPM and 2.5 PPM respectively for 96 hours of exposure in *Channa punctatus*. Malathion was



**Kalaimani and Kandeepan**

found to be highly toxic to minnows (LC₅₀ 8.6 ppm) and murels (LC₅₀ 5.93ppm) as summarized by Durkin (2008). The present findings gain support from the work of Anoop et al., (2010) who also recorded LC₅₀ values of Dimethoate in *Heteropeunistic fossilis*. The median lethal concentration (LC₅₀) was calculated by means of probit analysis (Finney 1981) (Table 1).

Fig 2, Shows that, the rate of Oxygen Consumption of *Labeo rohita* exposed to 0.5, 1 and 1.5 PPM concentration of Phosalone for a period of 24, 48, 72 and 96 hrs. The fish treated with different concentration of Phosalone consumption at these increasing duration was decreased in the rate of Oxygen Consumption and it's found to be highly significant at $P < 0.01$ Level compare to control fishes. A similar decrease in oxygen uptake has been reported in *Labeo rohita* (Sivakumar et al., 2013) due to Monocrotophos exposure. Sublethal concentrations of deltamethrin, a pyrethroid, have decreased oxygen consumption in *O. mossambicus* (Nazeemul Khane et al., 1992). The results of this study confirm the earlier report (Saradhamani et al., 2009) on oxygen consumption by fish in pesticide mixed water.

Haemoglobin (Hb) content was estimated in the blood of *Labeo rohita* exposed to LC₅₀ value of Phosalone concentration and presented in table 2. The Hb content of blood was 8.75 g/dl in control fish and it was decreased (6.30 g/dl) when exposed to LC₅₀ concentration of Phosalone. The Hb content was gradually reducing with increasing exposure period. The decreased haemoglobin concentration represents that the fish power to supply adequate oxygen to the tissues is limited considerably and this will result in decline of physical activities (Nussey et al., 1995). The same trend was obtained *Catla catla*, sub lethal concentration of lead nitrate and Mercury chloride toxicity was significantly decreased in Hb content when compared to control fish at 96 hrs exposures (Kandeepan 2013). A clear-cut evidence of reduction of Hb content has been reported by Bhatkar and Dhande (2000) in *Labeo rohita*, when exposed to Furadon. The reduction in Hb content of fish may be due to the effect of pollutant on haemopoietic system. The reduced level of haemoglobin content may be affecting the Oxygen consumption of the fish by way of reduced transportation of Oxygen and this fact can be confirmed in the present study also.

The total blood sugar content increased with increasing concentrations of Phosalone. The blood sugar level which was 54.50 mg/ml in control fish significantly increased to 74.50 mg/ml in LC₅₀ of Phosalone at 96 hrs exposure period (Table 2). The percentage (36.70) of blood sugar level increase is, as a function of exposure period. Such increase in blood sugar has been probably due to increased rate of utilization of blood sugar to meet the excess energy demands imposed by the severe stress of pesticide on the physiological activity of fish. This increase of blood sugar level i.e. hyperglycaemic condition may be due to conversion of stored glycogen into blood glucose (glycogenolysis) by the inducement of adrenal hormones namely glucocorticoids and Catacolamines by pesticides. Christobher et al. (2016) reported increased level of blood sugar when exposed to 1ppm concentration of Phosphamidon treated *Labeo rohita* fishes at 15 days intervals. The present findings were support from the work of Mohammad Illiyas et al., (2015) in Dimethoate- treated *Catla catla* under insecticide toxicity.

Alkaline Phosphatase is responsible for Phosphorylation, biosynthesis, Secretary Activity, mediation of membrane transport, involvement in active transport and good indicator for stress condition of biological system. Hence, the change in the alkaline Phosphatase activity will affect the Physiological and biochemical pathways of metabolism in *Labeo rohita*. In the present study on *Labeo rohita*, the alkaline phosphatase activity has been decreased significantly in intestine and liver tissues with increasing sub lethal concentrations of Phosalone at different exposure period from 24 - 96 hours and this decrease may be due to the inhibition of enzyme activity by the pesticide Phosalone (Table.3). The same result was supported by Saraswati (2015), who observed the significant decrease in the activity of alkaline phosphatase in liver tissue of *Clarias batrachus* exposed Dimethoate pesticide. Baby Shakila et. al., (1993) reported the inhibition of alkaline phosphatase in liver of fish was due to the interaction of chemicals with co-factors and regulators.





Kalaimani and Kandeepan

CONCLUSION

This study concludes that the exposure of various concentrations (0.5 - 4ppm) Phosalone pesticide is toxic to aquatic organisms and severely affects the function of respiratory system, blood tissues, Liver and intestinal tissue of freshwater fish *Labeo rohita* which seriously affects the survival of fish in its habitat. Therefore, it is concluded that Phosalone at sub lethal concentration, can cause considerable deterioration to fish health. For this reason, Phosalone use must be regulated otherwise contaminated runoff from agricultural fields can deteriorate fish health and significantly reduce fish and aquatic organisms productivity of water bodies.

REFERENCES

1. Anoop Kumar Srivastava, Mishra, D, Shrivastava, S, Srivastava, S. K. and Srivastava, A. K. (2010): Acute Toxicity and behavioral responses of *Heteropneustes fossilis* to an organophosphate insecticide, Dimethoate, International Journal of Pharma and Biosciences, 1 (4): B-355- B363.
2. Baby Shakila.I., P.Thangavel and Ramasamy M. 1993. Adaptive trends in tissue acid and alkaline phosphatase of *Sarotherodon mossambicus* (peters) under sevin toxicity. Indian J. Environ. Health. 33:36-39.
3. Bergmeyer, H.U., 1963. Methods of enzymatic analysis. Academic press, New York.
4. Bhatkar, N.V., and R.R. Dhande, 2000. Furadan Induced Haematological changes in the fresh water fish, *Labeo rohita*. J. EcoToxicol. Environ. Monit, 10(3): 193-196.
5. Borah, N., and K.Yadav 1996. Effect of Rogor on the activity of alkaline phosphatase in *Heteropneustes fossilis*, Poll.Res., 5(3):112-115.
6. Butterworth, P.J., and A.J. Probert., 1970. Non specific phosphomono-esterases of *Ascaris suum*. Effect of Inhibitors, activators and chelators. Exp. Parasitol. 28: 555-565.
7. Christobher S, Periyasamy M, Suganthi P, Saravanan TS. (2016). Effect of Phosphamidon on Haematological and Biochemical parameters in freshwater fish *Labeo rohita*, International Journal of Fauna and Biological Studies, 3(1): 114-116.
8. David M, J. Sangeetha, J Shrinivas, ER Harish and VR Naik, 2015. Effect of deltamethrin on haematological indices of indian major carp *Cirrhinus mrigala*. Indian Journal of pure and applied zoology, 3(1): 37-43.
9. Deshmukh D. R. 2016. Hamatological response in a freshwater fish *Channa Striatus* exposed to endosulfan pesticide, Bioscience Discovery, 7(1):67-69.
10. Dubey.S, Shrivastava. R, Chouhan. R, Raghuvanshi.A and Vinoy K. Shrivastava, 2014. Ameliorative role of vitamin-C Against Dimethoate toxicity in air breathing fish, *Clarias batrachus* (LINN.), Global Journal Bioscience and Biotechnology, Vol.3 (1) : 46-50.
11. Durairaj. S., and V.R. Selvarajan 1992, Influence of Quinolphos and organo phosphorous pesticide on the Biochemical constituents of the tissues of *Oreochromis mossambicus*. J. Env. Biol 13(3): 181-185.
12. Durkin PR (2008). Malathion; Human Health and ecological risk assessment. Final report submitted to Paul Mistretta, PCR, USDA/Forest Service, Suthern region, Atlanta Georgia. SERA TR- 052-02-02c, p. 325.
13. Finney DJ. 1981. Probit analysis 3rd edition. Cambridge,United Kingdom: Cambridge Univ. Press.
14. Jayaprakash. C and N. Shettu, 2013. Changes in the hematology of the freshwater fish, *Channa punctatus* (Bloch) exposed to the toxicity of deltamethrin, Journal of Chemical and Pharmaceutical Research, 5(6):178-183.
15. Kandeepan C.(2013), Impact of Mercury Chloride and Lead Nitrate on Haematological Profile of Fresh Water Fish, *Catla catla*. Indian Journal of Natural Sciences, Vol.3(16): 1255-1260.
16. Mohammad Illiyas Hussain, Baidyanath Kumar and Mumtaz Ahmad, (2015). Acute Toxicity, Behavioral response and Biochemical composition of Blood of common carp, *Catla catla* (Hamilton) to an Organophosphate Insecticide, Dimethoate, Int.J.Curr.Microbiol.App.Sci: 4(5): 1189-1199.
17. Nazeemul Khane, K.M.A., R. James and M.Manjula, 1992. Sublethal effect of deltamethrin on the rate of metabolism in *Oreochromis mossambicus*. J. Ecobiol., 4(2): 81-85.





Kalaimani and Kandeepan

18. Nussey G, Van Vuren JHJ, Du Preez HH.(1995). 'Effects of Copper on Haematology and Osmoregulation of the Mozambique Tilapia, *Oreochromis mossambicus* (Cichlidae), Comparative Biochemistry and Physiology. 111:369-380.
19. Ram Nayan Singh (2014). Effects of Dimethoate (EC 30%) on Gill Morphology, Oxygen Consumption and Serum Electrolyte Levels of Common Carp, *Cyprinus Carpio* (Linn), International Journal of Scientific Research in Environmental Sciences, 2(6), pp. 192-198.
20. Saradhamani, N., K. Shanthi, M. Manimegalai and S. Binu Kumari, 2009. Efficacy of herbicide glyphosate on oxygen consumption of a freshwater fish, *Catla catla*. Indian J. Environ. & EcoPlan., 16(1): 239-243.
21. Saraswati Dubey, Renu Shrivastava, Rajendra Chouhan, Arun Raghuvanshi & Vinoy K. Shrivastava, (2015). Ameliorative role of vitamin-c against Dimethoate toxicity In air breathing fish, *Clarias batrachus* (linn.) Global Journal bio-science and biotechnology, vol.3 (1) 2014: 46-50
22. Sivakumar.B., Kumarasamy.P and Muthukumaravel.K, 2013. Impact of pesticide monocrotophos on the oxygen consumption of the freshwater fish *Labeo rohita*. International Journal of Current Zoological Research- Vol.1, Issue, 10, pp.27-30.
23. Suganthi P, Murali M, Sadiq Bukhari A, Syed Mohamed HE, Basu H, Singhal RK. (2015a). Haematological studies on freshwater Tilapia treated with ZnO nanoparticles. Journal of Advanced Applied Scientific Research. 1(1):41-67.

Table 1: Statistical analysis (Log-dose / probit regression line) of the LC₅₀ value of Phosalone on *Labeo rohita* for 96 hours and Chi - Square for LC₅₀ Value

Concentration PPM	Log conc. (X)	No. of fishes used (n)	Mortality rate (r)	P	Exp. Y	W	X	Y	95% CL	
									Upper	Lower
2.000	0.3010	100	30	0.3000	4.4056	0.559008	0.3010	4.3999	4.6284	4.1714
2.500	0.3979	100	50	0.5000	5.1524	0.631005	0.3979	5.1445	5.2845	5.0046
3.000	0.4771	100	80	0.8000	5.7626	0.513448	0.4771	5.7530	5.9212	5.5848
3.500	0.5441	100	90	0.9000	6.2785	0.343638	0.5441	6.2674	6.5130	6.0216

Log LC₅₀ = 0.375, LC₅₀ = 2.394015, Regression Equation Y = 2.086786 +7.68401 x,
 Chi-Square = 2.061623, Tabular Chi - Square at 0.05 = 5.99 - Not significant





Kalaimani and Kandeepan

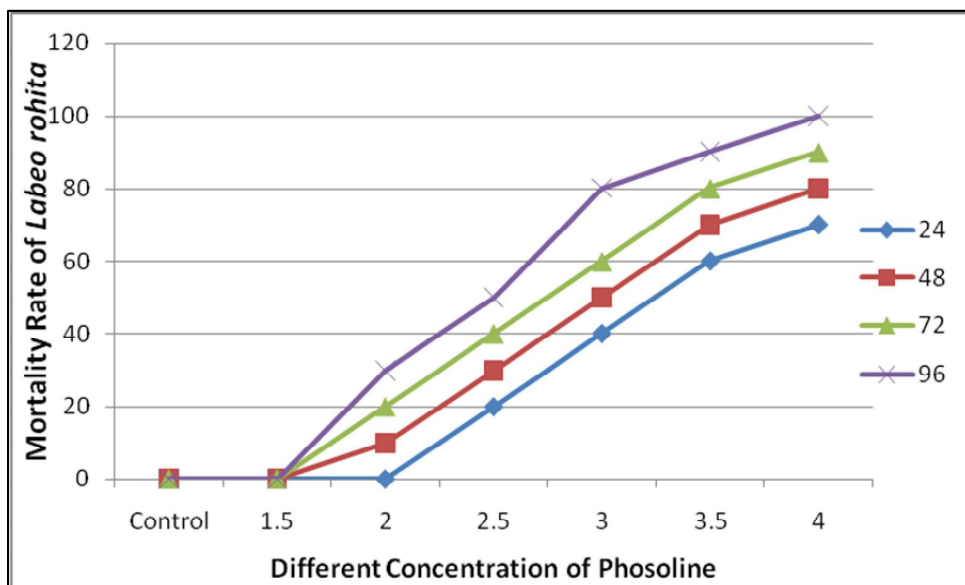


Fig.1: Mortality of *Labeo rohita* when exposed to different concentrations of Phosalone at different durations of exposure.

Table 2: Effect of LC50 2.5PPM of Phosalone on hemoglobin content and Blood glucose level of *Labeo rohita* at different durations of exposure.

Exposure Time (hr)	Haemoglobin Content g / dl		Blood Sugar level mg/ml	
	Control	Experiment LC ₅₀ (2.5 PPM)	Control	Experiment LC ₅₀ (2.5 PPM)
24	8.78±0.005	8.00±0.006	55.10±0.18	61.50±0.43
48	8.75±0.007	7.45±0.007	55.25±0.17	65.25±0.19
72	8.70±0.005	6.85±0.005	54.75±0.16	69.75±0.15
96	8.75±0.006	6.30±0.007	54.50±0.16	74.50±0.3





Kalaimani and Kandeepan

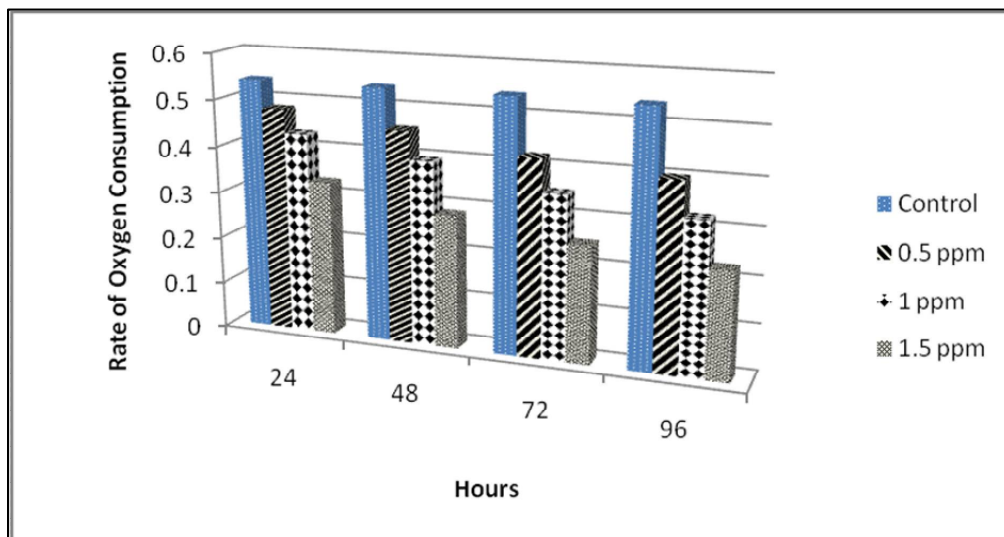


Fig. 2: Effect of Different sub lethal concentrations of Phosalone pesticide on Oxygen consumption of *Labeo rohita* at different time intervals

Table 3: Effect of Different sub lethal concentrations of Phosalone on Intestinal and Liver Alkaline phosphatase activity in *Labeo rohita* at different periods of exposure.(mole PNP / hr / gr of tissue).

Concentrations PPM	Alkaline Phosphatase Activity in Intestinal tissue			
	24 hr	48 hr	72 hr	96 hr
Control	605.5±38.45	603.6±35.43	604.2±31.25	602.5±30.20
0.5	565.4±40.10	555.6±52.2	549.3±42.75	537.6±33.15
1.0	520.5±31.45	508.4±43.44	484.3±25.35	457.7±45.15
1.5	470.6±60	448.4±40.22	409.2±20.15	362.5±12.15
Alkaline Phosphatase Activity in Liver tissue				
Control	571.5±50.24	7570.7±52.32	566.2±50.34	563.5±50.25
0.5	536.4±15.25	530.3±10.50	511.3±30.12	503.5±27.62
1.0	496.6±20.75	485.6±49.45	451.2±26.48	428.6±35.04
1.5	451.5±25.01	430.7±22.10	386.4±21.94	338.3±18.22





Effect of Treated Distillery Effluent and NPK Fertilizers on Soil Available Nitrogen, Potassium, Yield and Uptake of Rice (*Oryza sativa* L.)

Sivasabari.K^{1*} and L.Chithra²

¹Department of Soil Science and Agricultural Chemistry, TNAU, Coimbatore-641003, T.N,India

²Department of Soil Science and Agricultural Chemistry, ADAC&RI, Trichy- 620 009, T.N,India

Received: 10 Aug 2017

Revised: 20 Aug 2017

Accepted: 12 Sep 2017

*Address for correspondence

Sivasabari. K

Ph.D Scholar, Department of Soil Science and Agricultural Chemistry,

Tamil Nadu Agricultural University,

Coimbatore – 641 003, Tamil Nadu, India.

Email:sabarisiva3@gmail.com



This is an Open Access Journal / article distributed under the terms of the **Creative Commons Attribution License** (CC BY-NC-ND 3.0) which permits unrestricted use, distribution, and reproduction in any medium, provided the original work is properly cited. All rights reserved.

ABSTRACT

The long term experiment was conducted since 2008 at Anbil Dharmalingam Agricultural College and Research Institute, Trichy, Tamil Nadu with Rice (TRY-1) as 10th test crop during November, 2012 in the ongoing experiment with an objective to study the effect of treated distillery effluent and NPK fertilizers on soil available nitrogen(N), potassium (P), yield and uptake of rice crop. The treatments were replicated twice in a split plot design. There were four main plots viz., M₁ (Continuous application of TDE), M₂ (TDE application at once in two years), M₃ (TDE application at once in three years) and M₄ (Control) and six fertilizer levels in subplots viz., S₁ (Control), S₂ (100 % recommended doses of NPK), S₃ (50 % N alone), S₄ (50 % N+50 % K), S₅ (100 % N alone) and S₆ (100 % N + 50 % K) . The experimental results revealed that, the soil available N (252- 312 kg ha⁻¹) and K (185-479 kg ha⁻¹) increased from the initial soil status to active tillering stage due to application of treated distillery effluent. The continuous application of TDE along with 100 % RD of NPK (M₁S₂) recorded highest grain yield and straw yield (5745 & 6894 kg ha⁻¹) which was on par with the continuous application of TDE along with 100 % N+ 50 % K (5700 & 6840 kg ha⁻¹) and the continuous application of TDE with 50 % N alone (5670 & 6804 kg ha⁻¹). The control (M₄S₁) recorded the lowest grain and straw yield (2184 & 2228 kg ha⁻¹). Further, the continuous application of TDE along with 100 % RD of NPK recorded the highest uptake of nutrients viz N, P and K in both grain and straw over rest of the treatments. This furnished the cost towards K fertilizer can be reduced by application of TDE thereby the farmers can benefited by saving the fertilizer cost and also increased the yield of rice crop.

Keywords : Treated distillery effluent, Available nitrogen (N), Potassium (K), uptake of rice, Grain and straw yield.





INTRODUCTION

In India there are 579 sugar mills in which 145 M t of sugarcane are crushed annually and 14.5 M t of sugar is produced. There is considerable production of by-product called molasses and it is used for the production of alcohol. In India, there are 319 distilleries producing 3.25 billion litres of alcohol. For every litre of alcohol production, 10 to 15 litres of spent wash is generated (Baskar *et al.*, 2003) and in Tamil Nadu alone contributes around 3.6 billion litres of spent wash. The spent wash is used for power generation resulting in the release of treated distillery effluent (TDE). The Treated Distillery Effluent (TDE) is a by-product of sugarcane based distillery waste material which is non-harmful, bio-degradable and of purely plant origin. The treated distillery effluent contains considerable amount of N and P, rich in K, Ca, Mg, S and trace amount of Fe, Zn, Cu and Mn (Mohammed Haroon and Subash Chandra Bose, 2004). In India, rice is the major staple food and a mainstay for the rural population and their food security. Tamil Nadu is the fifth largest producer of rice and it is grown in an area of 1.85 M ha with the production of 5.67 M t and an average productivity of 3,070 kg ha⁻¹ (Anon, 2009). The use of inorganic fertilizer is becoming costlier day by day. Hence, there is a need to follow nutrient management for long term and sustainable basis to increase the crop yield. In this context, the use of inorganic fertilizers alone is depleting the soil nutrients, especially secondary and micronutrients and thereby the soil health is also deteriorating. To increase the yield of rice and to decrease the burden caused to the farmers by the expenditure towards the fertilizer cost, it is better to go for agro-based waste material as a source of nutrient to the crop. In this situation, the sugarcane based industrial waste material viz., TDE can play a vital role in supplementing the crop nutrition. Keeping the above facts in view, the current study was aimed to find out the effect of TDE along with fertilizers on soil available N, K, yield and uptake of rice in clay loam soil.

MATERIALS AND METHODS

A field experiment was conducted at central farm of Anbil Dharmalingam Agricultural College and Research Institute Trichy, Tamilnadu with latitude of 10° 45' N and longitude of 78° 36' E at an altitude of 85 meters above mean sea levels. The initial characteristics of experimental soil were clay loam in texture with pH of 8.7 and EC of 0.20 dSm⁻¹. The initial soil available NPK content was 252, 22 and 185 kg ha⁻¹, respectively. The experimental plots were randomized based on split plot design with three replications and each experimental plot size was 9 x 7 m. The main plot treatments imposed were Treated Distillery Effluent @ continuous application, once in two years, once in three years and control. The TDE was applied at the quantity of 1.5 lakh litres ha⁻¹. The calculated quantity of fertilizers @ control, 100 % RD of NPK, 50 % N alone, 50 % + 50 % K, 100 % N alone and 100 % N + 5- % K was applied to each subplot. The 30 days old rice variety TRY-1 seedlings were transplanted in the main field with a spacing of 25 x 25 cm @ two seedlings per hill. The grain and straw yield were calculated based on the plot yield at harvest and expressed at 14 per cent moisture. The initial soil pH and EC was determined by using 1:2 soil water suspension and extract using pH meter and conductivity meter, respectively (Jackson, 1973). The soil available N was estimated by alkaline permanganate method (Subbiah and Asija, 1956) and available K was analysed by flame photometer (Jackson, 1973). The uptake was calculated by using nutrient content and DMP (Dry matter production) of grain and straw {Nutrient uptake (kg ha⁻¹) = Nutrient content (%) × DMP (kg ha⁻¹)/100}. The experimental data were subjected to statistical scrutiny by using AGRSS software.

RESULTS AND DISCUSSION

Soil Available N and K

The soil available N and K range increased from the initial soil available N (252 kg ha⁻¹) and K (185 kg ha⁻¹) to active tillering stage soil available N (312 kg ha⁻¹) and K (479 kg ha⁻¹) Table 1. The effect of application of TDE at different time intervals along with different doses of fertilizers was found to be significant. The highest available nitrogen and



**Sivasabari and Chithra**

potassium status was registered in the treatment which received continuous application of TDE with 100 % RD of NPK (M_1S_2). The organic form of N supplied by TDE and inorganic form of N released by fertilizers into the soil available pool and there by increased the available N content of the soil. The soil available K was increased due to the high potassium content of TDE. Increase in the available K content of the surface soil was sustained even after the harvest. These results also agreed with the findings of Janaki (2008). In panicle initiation stage, the availability of N and K in the soil got decreased as the crop growth advanced which could be attributed to the uptake of N and K by the crop (Sivasamy, 2004). There was a marginal decrease in available N content observed at the time of harvest stage, which could be due to loss of nitrogen through volatilization. (Gupta *et al.*, 1986).

Yield of Rice

The results of the field experiment revealed that the grain and straw yield of rice was significantly influenced by treated distillery effluent (TDE) application along with different doses of fertilizers. The grain and straw yield ranged from 2184 to 5745 kg ha⁻¹ and 2228 to 6874 kg ha⁻¹. (Table 2). The highest grain and straw yield (5745 & 6874 kg ha⁻¹) was recorded in the treatment which received continuous application of TDE @ 1.5 lakh litres per ha and recommended doses of NPK fertilizer application (M_1S_2), which was on par with continuous application of TDE along with 100 % N + 50 % K (M_1S_6). The treatment M_4S_1 recorded the lowest grain and straw yield of in the absence of TDE and fertilizer. The increase in grain and straw yield was attributed to the positive influences on the yield and growth parameters viz. number of productive tillers and thousand grain weight of the rice, plant height and number of tillers. The increase in available nutrients viz., N, P, K, Zn, Fe, Cu and Mn as recorded in the TDE applied soils supported the above findings. Similar findings were also reported by saliha (2005) and Rodrigo *et al.* (2008).

NPK Uptake

Data elucidated that application of TDE significantly increased in the nitrogen uptake by paddy grain. The highest N uptake of 101.4 Kg ha⁻¹ was obtained in continuous application of TDE along with 100% RD of NPK over control which recorded only 38.5 kg ha⁻¹. Similar to the grain uptake, the N uptake in straw also gets influenced by the application of TDE with different doses of NPK. The highest N uptake of 127.6 Kg ha⁻¹ in straw was obtained in continuous application of TDE with 100 % RD of NPK over control which recorded 41.2 kg ha⁻¹. The higher uptake of N noticed in TDE applied plots might be due to the higher DMP and also more root growth which might have increased the nutrient absorption. The supply of organic form nitrogen from effluent might have enhanced the vegetative growth and increased the N uptake. Similar results were also reported by Ghosh (1999) and Madhumitha *et al.* (2010). The highest P uptake of 3758 kg ha⁻¹ in grain was observed by the continuous application of TDE with 100 per cent recommended doses of NPK over control which recorded the least uptake of 14.29 kg ha⁻¹. Similar to the uptake of P in grain, the highest P uptake of 51.05 kg ha⁻¹ in straw was also recorded by the continuous application of TDE along with 100 % RD of NPK over control which recorded the lowest uptake of 16.50 kg ha⁻¹. The supply of all essential nutrients by TDE might have increased the dry matter production of the crop which was also responsible for increase in uptake of P. These findings were corroborated with the findings of Patil *et al.* (2000) and Balasubramaniam (2013). The K uptake of rice grains was also increased from 56.3 kg ha⁻¹ to 148.2 kg ha⁻¹. Continuous application of TDE with 100 per cent RD of NPK recorded the highest K uptake of 148.2 kg ha⁻¹ over rest of the treatments. Similarly, the K uptake in straw was also increased from 58.8 to 182.0 Kg ha⁻¹. The highest mean K uptake was recorded in the treatment which received continuous application of TDE (171.4 kg ha⁻¹). In subplot treatments of NPK, the uptake of K by straw was high at 100 per cent RD of NPK (150.8 kg ha⁻¹). The highest K uptake of 182 kg ha⁻¹ in straw was obtained by the addition of continuous application of TDE + 100 per cent NPK over control which recorded the lowest uptake of 58.8 Kg ha⁻¹. In general, the TDE is rich in potassium and used as a K nutrient source. Since this is a long term experiment the continuous application of TDE gradually builds up the potassium content in the soil and the soil pool supplies K when plant needs. These findings were in cope with the finding of Patil *et al.* (2000) and Balasubramaniam *et al.* (2013).



**Sivasabari and Chithra****CONCLUSION**

From the experimental observations, it may be concluded that continuous application of TDE which is every year @ 1.5 lakh litres per ha may serve as a good liquid fertilizer for rice crop. In the potassium skipped plots, the yields were found to be comparable with 100 % RD of NPK. The continuous application of TDE along with 100 % RD of NP could be recommended for rice in fine textured soil (clay loam). Hence, the cost towards K fertilizer can be reduced by application of TDE thereby the farmers can benefited by saving the fertilizer cost.

ACKNOWLEDGEMENTS

The authors gratefully acknowledge the M/S.Chemplast Sanmar Pvt Ltd, Panruti, Tamil Nadu for funding and Department of Soil Science and Agricultural Chemistry, Anbil Dharmalingam Agricultural College and Research Institute, Tamil Nadu Agricultural University (TNAU), Trichy for permitting the research project and providing facilities to carry out study.

REFERENCES

1. Anonymous, 2009-2010. Area, production and productivity of principal crops. Department of Economics and Statistics, Chennai.
2. Baskar, M., C. Kayalvizhi and M. Subash Chandra Bose. 2003. Ecofriendly utilization of distillery effluent in agriculture- A Review. *Agric. Rev.*, 24: 16-30.
3. Gupta, A.P., R.S.Antil and V.K.Gupta. 1986. Effect of pressmud and zinc on the yield and uptake of zinc and nitrogen by corn. *J. Indian Soc. Soil Sci.*, 34: 810-814.
4. Jackson M.L. 1973. Soil Chemical Analysis. Prentice Hall of India (Pvt) Ltd., New Delhi.
5. Janaki.,2008. Utilization of distillery spentwash as manure to crops and its impact on soil,crop and groundwater quality.Ph.D thesis, Tamil Nadu Agricultural university,India.
6. Mohamed Haroon, A. and M. Subash Chandra Bose. 2004. Use of distillery spentwash for alkali soil reclamation, treated distillery effluent for fertigation of crops. *Indian farm.*, 53(11): 48 - 51.
7. Rodrigo B. Badayos, Nertila M. Manalili and Prof. Moises A. 2008. Dorado SEAMEO regional center for graduate study and research in agriculture. **In:** Results and findings on the use of treated distillery wastes as inputs for agricultural production – a waste management approach to cleaner productions. pp. 16.
8. Saliha, B. 2005. Distillery spentwash for sustainable soil health. *Kissan World*, 32:50-51.
9. Sivasamy, N. 2004. Phytoremediation potential of fodder crops in paper mill effluent polluted soil habitat. M.Sc., Thesis, Tamil Nadu Agricultural University, Coimbatore.
10. Subbiah, B. V and C. L. Asija. 1956. A rapid procedure for estimation of available nitrogen in soils. *Curr. Sci.*, 25: 259 - 260.
11. Ghosh, A. K., Pankaj Kumar and N. P. Ray. 1999. Physico-chemical analysis of distillery effluent and their effect on germination of some legumes. *Neo Botanica.*, 7(1):27-32.
12. Madhumita D., H. Chakraborty, R. B. Singandhupe, S. D. Muduli and A. Kumar. 2010. Utilization of distillery wastewater for improving production in unproductive paddy grown area in India. *J. Sci. Ind. Res.*, 69: 560-563.
13. Patil, G. D., Pingat, S. M. and Yelwande, 2000. Effect spentwash levels on soil fertility, uptake, quality and yield of Fodder Maize. *J. Maharashtra Agri. Univ.*, 25: 168-170.





Sivasabari and Chithra

Table 1. Effect of TDE and NPK fertilizers on Soil available N and K at three different stages

Treatments		Active tillering stage		Panicle initiation stage		Post harvest stage	
		N (kg ha ⁻¹)	K (kg ha ⁻¹)	N(kg ha ⁻¹)	K (kg ha ⁻¹)	N (kg ha ⁻¹)	K (kg ha ⁻¹)
M₁	S ₁	340	721	295	690	291	677
	S ₂	355	725	320	700	300	685
	S ₃	348	716	295	692	274	679
	S ₄	347	720	296	698	273	683
	S ₅	353	715	318	694	298	680
	S ₆	355	724	319	699	299	684
Mean		349	720	307	695	289	680
M₂	S ₁	320	565	290	532	275	515
	S ₂	342	582	310	540	290	525
	S ₃	329	570	294	533	262	517
	S ₄	330	585	293	537	263	520
	S ₅	340	571	314	533	291	519
	S ₆	341	581	313	539	292	522
Mean		330	575	300	535	278	519
M₃	S ₁	290	435	276	418	262	410
	S ₂	311	440	302	425	271	420
	S ₃	301	420	286	420	253	412
	S ₄	302	438	288	420	254	415
	S ₅	310	422	301	419	269	414
	S ₆	311	435	302	423	270	417
Mean		304	431	292	420	261	414
M₄	S ₁	250	180	233	170	210	170
	S ₂	275	200	280	180	262	178
	S ₃	267	182	268	172	250	170
	S ₄	268	193	270	175	250	173
	S ₅	275	185	275	173	262	172
	S ₆	274	195	276	177	263	175
Mean		267	189	267	174	247	172
CD = (p=0.05)	M	17.4	4.37	11.5	3.43	10.7	6.55
	S	5.29	9.87	0.37	7.52	0.3	8.70
	M x S	19.8	18.5	11.6	14.1	10.7	17.1
	S x M	10.5	19.7	0.75	15.0	0.6	17.4





Sivasabari and Chithra

Table 2. Effect of TDE and NPK fertilizers on grain and straw yield (kg ha⁻¹)

Treatments		Grain yield (kg ha ⁻¹)	Straw yield (kg ha ⁻¹)
M₁	S ₁	4218	5062
	S ₂	5745	6894
	S ₃	5520	6624
	S ₄	5607	6727
	S ₅	5670	6804
	S ₆	5700	6840
Mean		5610	6491
M₂	S ₁	3820	4508
	S ₂	5311	6267
	S ₃	4620	5334
	S ₄	4565	5387
	S ₅	5164	6095
	S ₆	5231	6173
Mean		4785	5627
M₃	S ₁	3246	3765
	S ₂	4927	5483
	S ₃	3810	4481
	S ₄	3875	4495
	S ₅	4583	5316
	S ₆	4667	5414
Mean		4151	4825
M₄	S ₁	2184	2228
	S ₂	4120	4202
	S ₃	2865	2922
	S ₄	3176	3240
	S ₅	3498	3568
	S ₆	3784	4014
Mean		3271	3362
CD (P=0.05)	M	125.6	150.8
	S	149.7	169.4
	M x S	300.2	343.3
	S x M	299.5	338.9





Sivasabari and Chithra

Table 3. Effect of TDE and NPK fertilizers on nutrient uptake (kg ha⁻¹) at post harvest stage

Main plot treatments	Subplot treatments	Nitrogen uptake		Phosphorus uptake		Potassium uptake	
		Grain	Straw	Grain	Straw	Grain	Straw
Continuous application of TDE (M ₁)	Control (S ₁)	74.4	93.7	27.5	37.4	108.8	133.7
	100 % RD of NPK (S ₂)	101.4	127.6	37.5	51.0	148.2	182.0
	50 % N alone (S ₃)	97.4	122.6	36.1	49.0	142.3	174.9
	50 % N+ 50 % K (S ₄)	98.9	124.5	36.6	49.8	144.6	177.6
	100 % N alone (S ₅)	100.0	125.9	37.0	50.3	146.2	179.7
	100 % N+ 50 % K (S ₆)	100.6	126.6	37.2	50.6	147.0	180.6
Once in two years (M ₂)	Control (S ₁)	67.4	83.4	24.9	33.3	98.5	119.0
	100 % RD of NPK (S ₂)	93.7	116.0	34.7	46.4	137.0	165.5
	50 % N alone (S ₃)	79.7	99.9	29.5	39.9	116.6	142.5
	50 % N+ 50 % K (S ₄)	80.5	99.7	29.8	39.8	117.7	160.9
	100 % N alone (S ₅)	91.1	112.8	33.7	45.1	133.2	160.9
	100 % N+ 50 % K (S ₆)	92.3	114.2	34.2	45.1	134.9	163.0
Once in three years (M ₃)	Control (S ₁)	57.2	69.7	21.3	27.8	83.7	99.4
	100 % RD of NPK (S ₂)	83.4	101.5	30.9	40.6	121.9	144.8
	50 % N alone (S ₃)	68.1	82.9	25.2	33.1	99.6	118.3
	50 % N+ 50 % K (S ₄)	68.3	83.2	25.3	33.2	99.9	140.4
	100 % N alone (S ₅)	80.8	98.4	29.9	39.3	118.2	140.4
	100 % N+ 50 % K (S ₆)	82.3	100.2	30.5	40.0	120.3	143.0
Control (M ₄)	Control (S ₁)	38.5	41.2	14.2	16.5	56.3	58.8
	100 % RD of NPK (S ₂)	72.7	77.8	26.9	31.1	106.2	110.9
	50 % N alone (S ₃)	50.5	54.1	18.7	21.6	73.9	77.1
	50 % N+ 50 % K (S ₄)	56.0	59.9	20.7	23.9	81.9	94.2
	100 % N alone (S ₅)	61.7	66.0	22.8	26.4	90.2	94.2
	100 % N+ 50 % K (S ₆)	66.7	71.7	24.7	28.5	97.6	101.9
CD(P=0.05)	M	3.07	3.70	1.11	1.47	4.50	5.29
	S	0.84	0.78	0.30	0.29	1.25	1.12
	M x S	3.43	3.96	1.26	1.58	5.03	5.66
	S x M	1.70	1.57	0.61	0.61	2.50	2.26





RESEARCH ARTICLE

Evaluating Anti-Anemic Effect of Mesenchymal Stem Cells and Oxymetholone on Aplastic Anemia Induced in Mice

Esraa M.Krair¹, Huda F.Hasan^{2*} and Mohammad M.F.AI-Halbosi³

¹Scholar, Department of Physiology and Pharmacology, College of Veterinary Medicine, University of Baghdad, Iraq.

²Assist. Prof. PhD, Department of Physiology and Pharmacology, College of Veterinary Medicine, University of Baghdad, Iraq.

³Assist. Prof. PhD, Biotechnology Research Center, Al-Nahrain University, Iraq.

Received: 11 Aug 2017

Revised: 23 Aug 2017

Accepted: 11 Sep 2017

*Address for correspondence

Huda F.Hasan

Assist. Prof. PhD, Department of Physiology and Pharmacology,
College of Veterinary Medicine,
University of Baghdad, Iraq.
Email: dr.hudaalqaraghuli@yahoo.com



This is an Open Access Journal / article distributed under the terms of the **Creative Commons Attribution License (CC BY-NC-ND 3.0)** which permits unrestricted use, distribution, and reproduction in any medium, provided the original work is properly cited. All rights reserved.

ABSTRACT

The study was performed to estimate the anti-anemic influence of MSCs and Oxymetholone on aplastic anemia (A.A) induced in mice. A.A was developed after 15 days from the first administration of benzene (1940mg/kg). Twenty eight females mice were alienated into four groups: 1st group (T1) was (A.A) induced and treated with dose (2x 10⁶ cell/kg) of MSCs given I\N once time weekly, 2nd group (T2) was (A.A) induced and treated with Oxymetholone(3mg/kg) B.W given I\N, 3rd group (T3) was (A.A) induced and treated with phosphate buffer saline given I\N, 4th group (T4) not induced (A.A) and left without any handling. PCV%, Hb, RBC, WBC, L%, M%, E%, B%, MCHC % and MCH of T1 and T2 exhibited a significant surge as likened with T3. ALT and AST levels of T1 revealed a significant decline as likened with T2 and T3. Total protein of T1 displayed a significant rise as likened with T2 and T3. GPX and SOD of T1 appeared a significant surge as likened with T2 and T3. Total bone marrow of T1 displayed a significant increase as compared with T2, T3 and T4. Histopathological section of T1 in the bone showed normal endosteum and periosteum and in the liver showed multifocal aggregation of MNCs in the liver parenchyma. Positive immune-reactivity brown for CD44 of both bone and liver tissues as compared with T2 and T3. From this study concluded the MSCs had suppressing effect of A.A devoid of any side effect whereas Oxymetholone drug was credited in healing of A.A with many side effects on tissues.

Keywords: Mesenchymal Stem Cells, Oxymetholone, Aplastic anemia, Benzene.



**Esraa M. Krair et al.**

INTRODUCTION

Mesenchymal stem cells (MSCs) had drawn much attention during the last decade in the arena of renewing medicine, mainly related to their capability to differentiate into explicit cell kinds [1]. MSCs had the ability to migrate to the sites of inflammation and hold effective of immunomodulatory and anti-inflammatory effects through cell. Hundreds of clinical trials have been sprinted by using MSCs for therapy of numerous immune mediated illnesses, e.g., Crohn's disease (CD), Graft versus Host sickness GVHD and aplastic anemia (AA) [2]. MSCs could be form new bone tissue and had the ability to hold up medullary hematopoiesis structural with functional via supplying development features and extracellular matrix, MSC was enhanced animals myelopoiesis and megakaryocytopoiesis and increases the functional hematopoietic microenvironment [3]. Several studies suggested that MSCs are played pivotal roles in the pathogenesis of aplastic anemia by increasing the amount of Tregs (T-cell) in peripheral blood. [4]. A.A is a disease characterized by bone marrow damage lead to incapacity of the stem cells to produce grown blood cells [5]. Aplastic anemia was usually reasoned through contacting to specific chemicals, medicines, rays, contagion, immune disease and exposure to poisons like benzene [6]. Medicinal treatment of aplastic anemia oftentimes included anti-thymocyte globulin (ATG) and different months of therapy by ciclosporin to modify the immune system but contained other toxicity than ATG antibody treatment [7]. Oxymetholone was used to treat the plastic anemia in mice by improving and stimulating the proliferation of hematopoietic stem and progenitor cells but also several side effect was included during the treatment such as liver dysfunction and lipid profile disorders [8]. The drive of the study made to estimate the anti-anemic actions of MSCs and Oxymetholone drug on aplastic anemia induced in mice.

MATERIALS AND METHODS

Isolation and culturing Mesenchymal Stem Cells (MSCs)

The techniques of procedure was done according to [9] as the following: MSCs were taken from the tibiae and femurs BM. of adult male mice, Cells of bone marrow were harvested by pushing 10 ml of Ross Well Park Memorial Institute medium (RPMI, GIBCO/ Italy) to the femurs and tibiae, then the dissolving cells were together calmed by put the suspension into centrifuge (200g) for five minutes to get the discard supernatants (fat and serum layers) and cell pellet. The cell pellets were re suspended in 10 ml RPMI1640 media and placed in 50 cm² flask of culture (falcon) and then 1ml of 10% serum of fetal calf with 1% penicillin-streptomycin were added to cells culture and put in incubator at 37°C and with 5% humidified CO₂ for 72 hrs. The big adherent cells colonies were developed (80% - 90% confluence) which under inverted microscope were examined, while the non adherent hematopoietic cells were get rid, the resulting culture was referred to as first-passage culture. The re sub culture was done by de attaching the adherent cells and the cultures were rinsed two times with PBS, then 2ml of trypsin (0.25%) and 1 mm Ethylene Diamine Tetra Acetate were added to suspension of cells for five min. at 37°C. Next, the cells were dissociated to single cells suspension, then 1 ml of 10% fetal calf serum with ten ml of culture media was applied to Falcon of cells suspension and then put in incubator at 37°C for 72hr. The resultant of culture was referred to as second-passage culture. The culturing of MSCs was done to the third passage. Culture of MSCs was inspected every day to noticed the growth of cells, the photographs was taken daily by using inverted microscope at magnification 40X, the MSCs pictures of growth in third passage were appeared as adhesiveness and fusiform with a spindle-like shape. Anti-CD44 antibodies (kit No: ab157107 and ab64261) was employed to distinguish MSCs according to [10].

Determination of cell count and viability

MSCs was separated from the surface of falcon by using trypsin-versene and the cells were counted by consuming double neubauer ruling counting chamber (slid chamber). Trypan blue stain was used for counting and determination of cells viability. 0.5 ml of cell suspensions was applied to 0.5ml of trypan blue stain which put in the sterile test tube and then incubated at 37°C for 30 mints. 0.02ml of the mix was

12715





Esraa M. Krair et al.

added in counting chamber slides and calculated below light microscope under magnification power 40X. By using the following equation counting cells concentration (cell/ml) = total cells count x dilution factor x 10^4 / number of squares (five squares). Furthermore, the MSCs viability was estimated according to the subsequent equation: cells viability = cell non stained number / cell total number x100, the lifeless cells were stained by the dye while the alive cells were not stained by the dye [11].

Induction of Aplastic anemia

Benzene was used to induce aplastic anemia, twenty six female mice were given orally at daily dose of benzene (1940mg/kg) B.W. and (2ml/kg), which dissolved with corn oil, aplastic anemia was developed after fifteen days [12]. After ending the induction period, five female mice were taken arbitrarily and scarified to study the histopathological changes of bone and liver tissues, in addition to measurement the blood pictures to ensure the induction of aplastic anemia was induced.

Experimental design

Twenty eight female mice were alienated into four similar groups, the animals of the group one (T1) were induced A.A. and treated with MSCs in dose (2×10^6 cell/kg) given I/P once time weekly. The animals of the second group (T2) were induced A.A. and treated daily with Oxymetholone in dose (3mg/kg) B.W given I/P. The animals of third group (T3) were induced A.A. and treated daily with phosphate buffer saline given I/P (positive control group). The animals of the fourth group (T4) were left without any treatment (negative control group).

Detection of blood pictures

After ending the experiment, the mice were anesthetized by diethyl ether and the samples of blood were obtained by cardiac puncture by using disposable syringes of insulin. After that, the samples put in anticoagulant tubes for measurement blood pictures. The hemoglobin test was done by diluting the blood in the solution consisted of potassium ferric cyanide and potassium cyanide; in this test the hemoglobin was rapidly converted into cyanohamogioin by pulling and mixing the blood with 5 ml of Drabkin's Reagent for 5 min. after that, the read was taken by using spectro-photometer [13]. Packed cell volume was determined via using micro-hematocrit capillary tubes, which filled with blood 2 to 3 up to their length. The other part of tubes was closed by clay and set in micro-hematocrit centrifuge for 5 min. the results were taken by micro-hematocrit reader [14]. Thomas's solution was taken for diluting the blood and counting WBCs by using haemocytometer method, the WBCs were counted in four squares (squares of corners) Number of Counted WBCs / $4 \times 20 \times 10 =$ WBCs x 50. [15]. The counting of differential WBCs was measured according to [15], one drop of blood sample was put and spread on each slide, after then the slides were dried and dyed with Leishmans stain for 10 min. then rinsed with tap water, the slides were examined in zigzag like line down and up until 100 cells were counted. While isotonic solution of Hayemsfluid was used to diluting the blood and counting RBCs by haemocytometer method, Number of Counted RBCs x $200 \times 50 =$ RBCs x 10,000, [15].

Detection of blood indices

Blood indices were calculated according to [16] as following equations: MCV: Average volume of RBC in Femtoliters (FL), $MCV = (\text{Hematocrit \%} \times 10) / \text{RBC count}$. MCH: Average weight of Hemoglobin in an RBC expressed in the units of picogram. $MCH = (\text{Hemoglobin} \times 10) / \text{RBC count}$. MCHC: Average concentration of Hemoglobin into each individual RBC expressed in the units gram per deciliter g/L. $MCHC = (\text{Hemoglobin} \times 100) / \text{Hematocrit \%}$.

Determination of total bone marrow cell count

Total bone marrow cells were counted according to [17]. As follows: The femurs of mice were taken, cleaned from muscles, and cut the epiphyses, 1ml of the isotonic saline liquid was injected into the medullary channel of bone and the cells suspension were collected in a glass tube, then $10 \mu\text{l}$ of cell suspension was taken and diluted by using $200 \mu\text{l}$ of Turk's solution. The counting chamber of hematocytometer slide was filled by one drop of diluting bone marrow





Esraa M. Krair et al.

cells suspension, after that the bone marrow cells were counted in 4 corners of the large squares (64 large squares), and multiplied the total count by 50 to get the bone marrow cells count per μl of cells suspension.

Determination of total Protein, Aspartate Transaminase, Alanine Amino-Transferase, Glutathione peroxidase and Superoxide dismutase

Total proteins concentrations in the serums were estimated by consuming of Biuret method described by [18]. The serum of (AST) and (ALT) levels were determined by using IFCC recommended procedure described by [19]. The serum levels of Glutathione peroxidase and superoxide dismutase were performed according to the details given in Biodiagnostic kits instruction, SOD was calculated by using spectrophotometer at 560 nm according to the method of [20], while the GPX was determined spectrophotometrically rendering to the methods of [21].

Histopathological method

After ending the treatment, mice were anesthetized by diethyl ether, animals were sacrificed and tissues samples of bone and liver have been obtained and also clean off from the concerned connective tissue and fat, then preserved in formalin (10%) for fixing, processed habitually in histokinette, cut up at 5mm thickness via microtome and bleached with Eosin and Haematoxylin after that noticed below light microscope [10].

Immunohistochemical staining for the CD44 to detect MSCs

Immuno histochemical staining was used according to [22]. The slides were deparaffinized, rehydrated, immersed in xylene (3 minutes and twice times) and in xylene with 100% ethanol (3 minutes). The slides were rehydrated in a reducing ethanol sequence and diluted with distilled water (100% ,100% ,95% ,75% ,and 50% ,3 minutes each) after this step, the slides in each dilution were rinsed with phosphate buffer saline (PBS). The slides were soaked in cold tap water and put in 100% retrieval buffer citrate in pH 6.0, then the slides were put in the water bath about 5 minute at 95°C . Slides were dried at room temperature and a drop of hydrogen peroxide was put in each slide for 30 minute to block the endogenous activity of peroxidase, then all slides were washed with (PBS). Drop of Protein blocker was put in each slide for 30 minute, then also the slides were rinsed with PBS. After that the drop from primary antibodies was supplemented in each slide and left over night. In the second day, the slides were rinsed with phosphate buffer, the secondary antibody (biotinylated goat antirabbit) was used on each slide for 30 minute after that the slides were rinsed three times with PBS. The drop of streptavidin peroxidase was supplemented in each slide for 30 minute. After preparation of diaminobenzidine chromogen (DAB stain) by taken one drop of DAB in one ml DAB substrate which was transformed into a brown precipitous through peroxidase, the site of antibody binding was visualized after added one drop of DAB stain in each slide, at the end the slides were stained with hematoxyline stain for 10 minute, washed and dried at room temperature and put under microscope to read.

Statistical analysis

The system of Statistical Analysis - one way was applied to all results of parameters in this study. Low significant variation LSD analysis at ($P \leq 0.05$) was used to a momentous comparison among means of the study [23].

RESULTS

Separation and isolation of bone marrow MSCs

The culturing results at first day appeared the majority of BMSCs are hanging as a slim arrows in culture medium under inverted microscopy, figure (1-A), whereas in second day the culturing of MSCs was appeared adhering the cells to the flask of culture thinly and this cells observed as a spindle-like in shape figure (1-B), while in the third day the cells revealed a big colonies and attended to propagated in the media of culture, with a spindle-like in shape, when examined under inverted microscope figure (1-C). Every the development of cells persistent, the colonies of cells progressively extensive in their size and each colony adjacent ones were unified with each other as in culturing of six day figure (1-D). However, the proliferation of cells nearly ceased, fusiform with a spindle-like in shape and





Esraa M. Krair et al.

adhesiveness at nine day. Figure (1-E). The surface antigen CD44 marker revealed the bone marrow MSCs were positive reaction for CD44 marker and deeply stained with brown color of DAB stain figure (1-F).

Count and viability cells results

The viability results of culturing cells after third passage revealed the non-stained and stained cells ratio were 90% and 10% respectively, the cells were adjusted until obtained the concentration 0.2×10^6 cell/ml.

Effect of Benzene on blood pictures after 15 days of first administration

The PCV%, Hb, RBC, total WBC count and differential WBC: Neutrophils(N%), Lymphocyte (L%), Monocyte (M%), Eosinophil (E%), and Basophile (B%) in mice treated with Benzene showed a momentous fall ($P < 0.05$) as likened with negative baseline group as in table (1).

Parameters of blood pictures after 30 days of the treatment

The result of all blood pictures are shown in table (2). The PCV%, Hb, RBC count, WBC count, L%, M%, E% and B%, in T1 and T2 exhibited a significant surge ($P < 0.05$) as likened T3, with no momentous difference ($P < 0.05$) as likened with T4, while the N% in mice preserved with MSCs revealed a momentous decrease ($P < 0.05$) as likened with T3 with no momentous difference ($P < 0.05$) as likened with T4. The N% in mice preserved with Oxymetholone revealed a momentous surge ($P < 0.05$) as equated with T1 and T4. Whereas, all parameters PCV%, Hb, RBC count, WBC count, L%, M%, E% and B%, in T3 revealed a significant decline ($P < 0.05$) as equated with T4, T2 and T1, except the N% in T3 showed a significant rise ($P < 0.05$) as equated with T4, T2 and T1.

Blood indices (MCHC%, MCH and MCV) after 30 days of the treatment

The result of blood indices are shown in table (3). The MCHC % and MCH (pg/cell) in T1 marked a significant surge ($P < 0.05$) as equated with T3, with no momentous difference ($P < 0.05$) as likened with T4 and T2, while the MCV (fl/cell) in T1 exhibited no momentous alteration ($P < 0.05$) when equated with T4, T3 and T2. Furthermore, MCHC percentage, MCH (pg/cell) and MCV (fl/cell) in T2 showed a momentous increase ($P < 0.05$) as equated with T3 with no significant difference ($P < 0.05$) as equated with T4, whereas, the result of MCHC percentage, MCH (pg/cell) and MCV (fl/cell) in T3 displayed significant decrease ($P < 0.05$) as equated with T4.

Alanine aminotransferase (ALT) and aspartate transaminase (AST) and total protein after 30 days of the treatment

The outcomes of the current research revealed that ALT and AST levels in T1 displayed a significant decline ($P < 0.05$) as equated with T2 and T3, with no momentous difference ($P < 0.05$) as likened with T4. Furthermore the ALT, AST levels in T2 and T3 exhibited a significant rise ($P < 0.05$) as equated with T4, furthermore there was no momentous difference ($P < 0.05$) in ALT, AST altitudes between T2 and T3. While the result of total protein level in T1 displayed a momentous increase ($P < 0.05$) as equated with T2 and T3 with no momentous variance ($P < 0.05$) as likened with T4, whereas, the total protein level in T2 and T3 exhibited a momentous decrease ($P < 0.05$) when likened with T4 with no momentous difference ($P < 0.05$) in total proteins level between T2 and T3 as in table (4),

Superoxide dismutase (SOD) and Glutathione peroxidase (GPX) after 30 days of the treatment

The result of GPX (mmol/mg) and SOD (U/ML) levels in T1 appeared a significant rise ($P < 0.05$) as likened with T2 and T3, with no momentous difference ($P < 0.05$) when compared with T4, whereas, the GPX and SOD levels of T2 and T3 exhibited a momentous decrease ($P < 0.05$) when likened with T4 with no momentous variance ($P < 0.05$) in GPX and SOD altitudes between T2 and T3 as in table (5).



**Esraa M. Krair et al.****Total bone marrow (X 10³cell/μL) after 30 days of the treatment**

The outcomes of the total bone marrow count are shown in table (6) and in figures (2A, 2B, 2C and 2D), the mice treated with Mesenchymal stem cells displayed a momentous increase ($P < 0.05$) in total bone marrow count as likened with T4, T3 and T2, while total bone marrow count of T2 showed a momentous increase ($P < 0.05$) when likened with T3 with no momentous variance ($P < 0.05$) as equated with T4, whereas, the T3 displayed a momentous decline ($P < 0.05$) in whole bone marrow count as likened with T4. In addition the T1 showed the best increases in their count and aggregations as in figure (2A) as compared with T2, T3 and T4, while the total bone marrow cells count of T2 revealed normal aggregation under light microscope as in figure (2B), whereas the T3 appeared severe decrease in the bone marrow cells (2C), when equated with T4 (2D).

Histopathological and Immunohistochemistry results

After 15 days of treatment mice with Benzene, the bone tissues showed decrease in the cellularity of bone marrow, mild hemorrhage and neutrophils in the medullary cavity of compact bone as in figure (3). After 30 days the inspected bone tissues from T3 showed severe distraction of compact bone which contained many cavities filled with RBCs and necrotic inflammatory cells, necrosis in the bone marrow and incomplete mineralization of the compact bone as in figure (4) when contrasted with ordinary section of bone tissue in T4 figure (7). While the T1 appeared the best improvement in bone tissues when contrasted with others treated groups, as in figure (5), the bone tissues showed normal endosteum and periosteum, the compact bone showed dilated Haversian canal with RBCs in their lumen, and improvement mineralization of trabecular bone and cellularity. Whereas, the T2 showed normal endosteum and compact bone but irregular periosteum, the compact bone showed normal osteocytes, but there was areas of incomplete mineralization seen in the compact bone, in addition to mild improvement in cellularity of bone marrow and some of cells replaced by fat tissue, as in figure (6). After 15 days of treatment mice with Benzene, the liver tissues showed aggregation of neutrophils and MNCs adjacent to central vein with vacuolar degeneration of the hepatocytes as in figure (8). While following 30 days the inspected liver tissues from T3 showed congestion of blood vessels and severe infiltration of neutrophils as in figure (9). While the T1 revealed mild congestion of central veins and multifocal aggregation of MNCs in the liver parenchyma as in figure (10). Furthermore, the T2 showed vacuolar degeneration of the hepatocytes and dilation of central vein, multifocal aggregation of inflammatory cells mainly MNCs and neutrophils in the liver parenchyma figure (11), as compared with histological section of liver in T4 figure (12). After thirty days the immunohistochemistry of the bone and liver tissues from, T1 showed very deep strong positive brown reaction for CD44 as in figures (13 and 14) respectively. Whereas, the the bone and liver tissues from T2, T3 and T4 revealed a negative immune-staining reaction for CD44 marker as in figures (15, 16, 17) respectively in bone tissues and figures (18, 19 and 20) respectively in liver tissues.

DISCUSSION

The employing of 10% FCS with a culture medium RPMI guide to a successful MSCs compilation from bone marrow, the serum is added to the BM culture to improve factors for the stem cells colony growth, these results are in concurrence with preceding studies reported by [24]. The findings of culturing in first, second and third passages are communicated to results mentioned by [22], who has been seen that numeral of floating cells augmented during the first day and after feeding development, the foundation for this increase may be to exclude the toxic materials consequential from metabolic processes of cells and due to cells action for division and propagation, the ability of MSCs for explosion and increasing in number with their aptitude for attaching in the culture flasks, this result possibly due to the stem cells are alienated to give the progenitor cells, these cells are self-replicate, in addition to, a further cell which is dedicated to final differentiated and certain direction of cells with spindle like shape which had no potential to self-duplicate, this result was in conformity with findings mentioned by previous reports [25]. There has been a common opinion that CD44 are highly specific for MSCs [26]. So the findings of phenotypic analysis of MSCs can be resulted from the capability of Anti-CD44 antibody to recognize MSCs representing to those cells are primarily of Mesenchymal origin through antigen antibody interactions. [27]. The findings of blood pictures in benzene treated mice after 15 days and in T3 after 30 days of treatment may be attributed to Cytotoxic effect of



**Esraa M. Krair et al.**

benzene and its metabolites led to damage of bone marrow stromal cells and failure in synthesis of normal signaling polypeptides resulted in damage to bone marrow pluripotential stem cells, leukopenia or thrombocytopenia and disorders in the immune system such as decline the lymphocytes, increasing the excessive TNF- α and IFN- γ accumulation in the bone marrow and then destructed the normal hematopoiesis with inhibition of Tregs cells lead to decrease the blood cells, loss of together stem cells and cells of bone marrow stroma via reducing DNA synthesis in progenitor cells into the bone marrow and then decrease in cellularity of the BM[28]. The relative increase in neutrophils may be due to a rejoinder to the particular stimulus of benzene metabolites, e.g. hydroquinone, which stimulated the granulocyte-macrophage progenitor cells [29]. The findings of blood picture and blood indices in T1 perhaps due to the role of BM-MSCs in supporting of hematopoiesis and regulating virtually overall immune cells purposealso MSCs had the capacity to migrate to a specific site of wound or damage tissue and then attributed in regeneration, stimulation bone tissue for producing blood cell, improving engraftment of HSCs by suppressing the creation of IFN- γ and TNF- α by CD4 cells, these results agreed with results reported by [30]. The decrease in neutrophils in T1 as compared with T3 may be attributed to the ability of MSCs in attenuated the cytokines e.g. (IL-8, IL-6 and TNF- α , activated neutrophils) with poly mononeuclear neutrophils chemotactic factors (MIP-2), while not affecting on the migration capability, viability with function of neutrophils this results are in agreement with [31]. The increase in number of blood pictures and indices T2 as compared with T3 may be attributed to the Oxymetholone had the ability in increasing reticulocytosis, Hb concentration, an excessive deposition of iron in the marrow reticulum cells, erythroblasts and marrow cellularity. Furthermore, Oxymetholone was stimulated erythropoiesis by enhancing the creation of erythropoietin (EPO) and encouraging the proliferation, regulation of progenitor and hematopoietic stem cells, these results also in agreement with findings recorded by [8]. The increase in ALT and AST and decrease in total protein, GPX and SOD of mice in T3 may be regarded to benzene led to stimulating cellular MDA and LPO furthermore, the chemical ingredients and hydrocarbons of the benzene, are metabolized in the tissues of liver, and interacted with the tissues to reason LPO, increase the actions of plasma ALT with AST levels and leakage of cellular components, in addition to benzene metabolites are bioactivated through myeloperoxidase with another heme protein peroxidase to interactive with semiquinone and quinone, that resulted in the formations the ROS, hydroperoxyl radicals, high reactive hydroxyl radical and hydrogen peroxide resulted in damages of DNA and RNA and genetic modification also, alterations in the functions of important enzymes and proteins [32]. The decrease in ALT and AST levels and increase GPX and SOD of T1 as compared with T3 perhaps due to the ability of BM-MSCs into decreasing of the α -SMA and TGF- β 1 proteins expression, MSCs can be differentiated into hepatocytes and stimulated the renewal of parenchymal cells which migrated to impaired locations and enhanced the fibrous matrix degeneration and then regulated liver enzymes with supported the liver metabolic functions. Furthermore, MSCs had the ability in increasing in the albumin level during the secretion of IL-10 led to increase total protein, those results are in agreement with [33]. MSCs had the ability in free radical scavenging by decreasing MDA and concurrently augmented the effectiveness of SOD and GPX levels in tissues, this result is agreed by [34]. While the increase in ALT and AST levels and decrease of GPX and SOD levels in T2 may be due to capability of Oxymetholone in inducing of MDA in liver tissue which stimulated of hydroperoxides led to degradation tissues by toxic hydroxyl that may be reacted with metals such as copper or iron and form stable aldehydes such as MDA resulted in damage of liver cells and then disturbances in production of liver enzymes, this consequences are in concurrence with [35]. So Oxymetholone may be provided a reduction in GPX and SOD, by its toxicity effect on the cells led to increase free radicals resulted in cells damage through oxidative modification of total proteins, albumins, lipid and DNA, that may be explained the cause of decrease total proteins after 30 days of oxymetholone administration, this results was in agreement with [36]. The decrease of total bone marrow count in T3 may be attributed to the ability of benzene metabolites in decreasing progenitor cells and discriminating hematopoietic cells, resulted by cellular DNA damage and inherited in somatic cell lines led to inability of the cells to react to cytokines and chromosomal aberrations oncogenes activation or antioncogenes inactivation, as well as, the Cytotoxic damage of bones marrow stromal cells resulted in inhibiting the differentiation and propagation of stem cells in addition to failure to synthesize normal signaling polypeptides and caused hematotoxic effect [28]. The increase in total bone marrow of T1 may due to migrated of MSCs to the bone marrow damage and provided its microenvironmental supporting for MSCs and hematopoietic stem cell had the ability in stimulating of PGE2 which played a vital roles





Esraa M. Krair et al.

in the suppression of the creation of TNF- α and IFN- γ . BM-MSCs can be caused the expansion of Treg cells BM-MSCs in animals suffered from AA. [37]. The increase in total bone marrow of T2 as compared with T3 may be attributed to the androgens stimulated the erythropoiesis through an increase in the production of erythropoietin and had a direct effect on bone marrow led to regulation of progenitor and hematopoietic stem cells [38]. The bone and liver tissues changes after 15 days of first administration of benzene and after 30 days of treatment mice with PBS, was possibly due to the benzene metabolites induced haematopoietic toxicity, caused accumulation several metabolites in bones marrow that resulted in the creation of free radicals and destruction of the BM microenvironment and destruction of stem progenitor cells with increase oxidative DNA damage, lipid peroxidation as well as HSCs and MSCs by increasing the excessive TNF- α and IFN- γ accumulation in the bone marrow [39]. Also the chemical ingredients and hydrocarbons of the benzene vapor are probably processed in the tissues of liver, and interacted with the tissues resulted in the deposition of benzene ingredients and their metabolite in liver tissues and cause severe pathological lesion, this result are in agreement with findings recorded by [40]. The improvement in bone tissue changes of T1 may be regarded to MSCs had a proliferative capability to discriminate into various cell kinds indicating these cells may be participated in bone formation lead to hematopoiesis supporting and potent immunoregulation by stimulation the Tregs cells in addition to release of hematopoietic cytokines, including IL-6 which in turn reduced the expression of the transcription factors Runx-1 in early hematopoietic progenitor cells and increased myeloid differentiation and triggered the temporary activation of emergency myelopoiesis [41]. The therapeutic actions of MSCs in liver tissues are based on the liberating of trophic and immunomodulatory factors that change function of hepatic stellate cells, MSCs were capable to decrease the proliferation of stellate cells during the secretion of IL-10, in addition to its ability in scavenging the free radicals then repairing liver tissues [42]. The results of histopathological changes of bone marrow and liver tissues in T2 may be due to Oxymetholone enhancement the bone marrow cellularity and the major site action of androgenic steroids appeared to be into the bone marrow [43]. Oxymetholone had toxic effect on liver cells by increasing free radicals which caused hepatotoxicity and can be also attributed to OXM-induced free radicals in the liver [36]. The positive CD44 reaction in both bone and liver tissues of T1 as compared with other treated groups can be explained by the amalgamation of MSCs into the bone and liver tissues and modification of wronged cells, in addition to the recognition of endogenous MSCs through applied CD44 immuno-reactivity marker by using a specific antigen/antibody reactions and exploiting the labeled avidin-biotin peroxidase, which related to the secondary antibody specifically biotin, the situation of antibody strap was imagined by diaminobenzidine chromogen, lead to revolved into a brown impulsive via peroxidase which is dedicated for distinguishing MSCs and then the CD44-positive cells were materialized as brown deposits in cytoplasm, this outcome is in conformity with study recorded by [44].

CONCLUSION

Mesenchymal stem cells at doses (2×10^6 cell/kg) lead to more protection effect on hematological disorders and bone with liver tissues than Oxymetholone (3mg/kg) BW against the toxic benzene (1940mg/kg).

REFERENCES

1. Zuk PA, Zhu M, Ashjian P, De Ugarte DA, Huang JI, Mizuno H. Human adipose tissue is a source of multipotent stem cells. *Mol Biol Cell*. 2002; 13:12:427-995.
2. Tondreau T, Meuleman N, Delforge A, Dejefeffe M, Leroy R, Massy M. Mesenchymal stem cells derived from CD133-positive cells in mobilized peripheral blood and cord blood: proliferation, and plasticity. *Stem cells J* 2005; 23:8:110-512.
3. Zheng CL, Yang SG, Guo Z.X, Dong CL, Liang L, Chen XJ. Human Multipotent mesenchymal stromal cells from fetal lung expressing pluripotent markers and differentiating into cell types of three germ layers. *Cell Transplant J*. 2009; 18:10:109-3109.
4. Noack S, Seiffart V, Willbold E, Laggies S, Winkel A, and Shahab-Osterloh S. Periostin secreted by mesenchymal stem cells support tendon formation in an ectopic mouse model. *Stem Cells J*. 2014; 23:16:184-457.





Esraa M. Krair et al.

5. Acton A. Aplastic anemia (AA) is a rare bone marrow failure disorder with high mortality rate, which is characterized by pancytopenia and an associated increase in the risk of hemorrhage, infection, organ dysfunction and death. ISBN. 2013; 78-1-36.
6. Peinemann F, Bartel C, and Grouven U. First-line allogeneic hematopoietic stem cell transplantation of HLA-matched sibling donors compared with first-line cyclosporin and/or antithymocyte or antilymphocyte globulin for acquired severe aplastic anemia. *Cell Transplant J.* 2013; 66: 7-19.
7. Tisdale JF, Maciejewski JP and Nunez O. Late complications following treatment for severe aplastic anemia (SAA) with high-dose cyclophosphamide (Cy): follow-up of a randomized trial". *Blood J.* 2002; 100 :13: 4668–4670.
8. Zhang Q, Benedetti E, Deater M, Schubert K, Major A, Pelz C, Impey S, Marquez-Loza L, Rathbun RK, Kato S, Bagby GC and Grompe M. Oxymetholone Therapy of Fanconi Anemia Suppresses Osteopontin Transcription and Induces Hematopoietic Stem Cell Cycling. *Stem Cell Reports.* 2015; 4:1: 90-102
9. Rochefort GY, Vaudin P, Bonnet N, Pages JC, Domenech J, Charbord P and Eder V. Influence of Hypoxia on the Domiciliation of Mesenchymal Stem Cells after Infusion into Rats: Possibilities of Targeting Pulmonary Artery Remodeling via Cells Therapies. *Respiratory Research.* 2005; 6: 125.
10. Bancroft JD and Cook HC. Immunocytochemistry. Manual of histological techniques and their diagnostic applications. Churchill Livingstone. 1994; 263-325.
11. Pollared JW and Walker JM. Cell culture protocols 2nd ed, human press, Inc. Totowa, New Jersey. 1997; 22-30.
12. Ata SI. Induction of aplastic anemia in experimental model. *Coden IJABFP-CAS-USA.* 1997; 7: 1
13. Varlay H, Gonlock AH and Bell M. Practical clinical biochemistry 5th ed. Williu Heinemann .medical books . Ltd. London Wallace J.L. 1997 ; 45-55.
14. Archer RK. Hematological techniques for use in animals. Blackwell, scientific J. 1985; 12: 21-35 .
15. Coles EH. Veterinary clinical histology. 2nd ed. W.B. Saunders company 1974; 3-8 .
16. Bunn HF. Approach to the anemias. in: (Goldman, L. and Schafer, A. I. eds). Goldman's Cecil Medicine. 25th ed. Philadelphia, PA: Elsevier Saunders . 2015; 158.
17. Lezama RV, Escorcia EB, Torres AM and Aguilar RT. A model of the induction of aplastic anemia by subcutaneous administration of benzene in mice. *Toxicology J.* 2001; 1621: 79-191.
18. Gomali A, Bardawill CJ and David MM. Determination of serum proteins by means of the biuret reaction. *J. Biol. Chem.* 1949; 177-751.
19. Bergmeyer HU, Bowers JR, Hörder M, Moss DW. Provisional recommendations on IFCC Methods for the measurement of catalytic concentrations of enzymes. Part 2. IFCC method for aspartate aminotransferase. *Clin Chim Acta* ;1976: 70:19–42
20. Nishikimi M, Appaji Nand Yagi K. The occurrence of superoxide anion in the reaction of reduced phenazine methosulfate and molecular oxygen. *Biochem Biophys Res.* 1972; 31:46:849-54..
21. Paglia DE and Valentine WN. Studies on the quantitative and qualitative characterization of erythrocyte glutathione peroxidase. *Lab Clin Med.* 1967; 70: 158-169.
22. Jing Z, Qiong Z, Yonggang W and Yanping L. Uterine infusion with bone marrow mesenchymal stem cells improves endometrium thickness in a rat model of thin endometrium. *Reproductive Sciences J.* 2015; 22: 2: 181-188.
23. SAS. Statistical Analysis System User's Guide . Statistical . Version 9 . 1st ed , SAS . Inst . Inc . Cary . N . C . USA. 2012
24. Pittenger MF, Mackay AM, Beck SC, Jaiswal RK, Douglas R, Mosca JD, Moorman MA, Simonetti DW, Craig S and Marshak DR. Multilineage potential of adult human mesenchymal stem cells. *Science J* 1999; 284: 143-147.
25. Xu W, Zhang X, Qian H, Zhu W, Sun X, Hu J, Zhou H , Chen Y. Mesenchymal stem cells from adult human bone marrow differentiate into a cardiomyocyte phenotype *in vitro*. *Exp Biol Med.* 2004; 229: 623-631.
26. Boxall SA and Jones E. Markers for characterization of bone marrow multipotential stromal cells. *Stem cells Int.* 2012; 12 :7-15.
27. Afifi N M , Olfat N R . Role of mesenchymal stem cell therapy in restoring ovarian function in a rat model of chemotherapy induced ovarian failure: a histological and immunohistochemical study. *Journal of histology* 2012; 36:144-1126.





Esraa M. Krair et al.

28. Snyder R. Recent developments in the understanding of benzene toxicity and leukemogenesis. *Drug Chem. Toxicol.* 2000; 23:13-25.
29. Macedo SM, Lourenco EL, Borelli P, Fock RA, Ferreira JM and Farsky, SH. Effects of in vivo phenol or hydroquinone exposure on events related to neutrophil delivery during an inflammatory response. *Toxicology J.* 2006; 220:126-135.
30. Shake JG, Gruber PJ, Baumgartner WA, Senechal G, Meyers J, Redmond JM, Pittenger MF, Martin BJ. Mesenchymal stem cell implantation in a swine myocardial infarct model: engraftment and functional effects. *Ann Thorac Surg.* 2006; 73: 1919-1956
31. Tian-Shun L, Zhi-Hong W and Shao-Xi C. Mesenchymal Stem Cell Attenuates Neutrophil-predominant Inflammation and Acute Lung Injury in an *In Vivo* Rat Model of Ventilator-induced Lung Injury. *Chin Med J.* 2015; 128:3: 361–367.
32. Al-Olayan EM, El-Khadragy MF, Aref AM, Othman MS, Kassab RB, Abdel Moneim AE. The potential protective effect of *Physalis peruviana* L. against carbon tetrachloride-induced hepatotoxicity in rats is mediated by suppression of oxidative stress and downregulation of MMP-9 expression. *Oxid Med Cell Longev* 2014; 38-43.
33. Jang YO, Kim MY, Cho MY, Baik SK, Cho YZ and Kwon SO. Effect of bone marrow-derived mesenchymal stem cells on hepatic fibrosis in a thioacetamide-induced cirrhotic rat model. *Gastroenterol J.* 2014; 14: 198.
34. Burova E, Borodkina A, Shatrova A, Nikolsky N. Sublethal oxidative stress induces the premature senescence of human mesenchymal stem cells derived from endometrium. *Oxid Med Cell Longev.* 2013; 47-93.
35. Shodehinde SA, Oboh G. Antioxidant properties of aqueous extracts of unripe *Musa paradisiaca* sodium nitroprusside induced lipid peroxidation in rat pancreas *in vitro*. *Asian pacific journal of tropical biomedicine.* 2013; 3:6: 449-457.
36. Deneke SM, Fanburg BL. Regulation of cellular glutathione. *Am J Physiol* 1989; 257: 163-173.
37. Uccelli A, Moretta L and Pistoia V. Mesenchymal stem cells in health and disease. *Nat Rev Immunol.* 2008; 8 : 9:72-636.
38. Sjoen GG, Beguin Y, Feyen E, Rubens R, Kaufman JM and Gooren L. Influence of exogenous oestrogen or (anti-) androgen administration on soluble transferrin receptor in human plasma. *J. Endocrinol.* 2005; 186:61–67.
39. Niyibizi C, Wang S, Mi Z, Robbins PD. The fate of mesenchymal stem cells transplanted into immunocompetent neonatal mice: implications for skeletal gene therapy via stem cells. *Mol Ther.* 2004; 9: 1525-2016
40. El-Shakour AA, El-Ebiarie AS, Ibrahim YH, Abdel Moneim AE and El-Mekawy AM. Effect of benzene on oxidative stress and the functions of liver and kidney in rats. *J Environ Occup Sci.* 2015; 4:1.
41. Li J, Lu S, Yang S, Xing W, Feng J and Li W. Impaired immunomodulatory ability of bone marrow mesenchymal stem cells on CD4 (+) T cells in aplastic anemia. *Immunol J.* 2012; 2:14-27.
42. Parekkadan B, van-Poll D, Megeed Z. Immunomodulation of activated hepatic stellate cells by mesenchymal stem cells. *Biochem Biophys Res J.* 2007; 363:247–252.
43. Finch C A, Ferrokinetics IN, Gillette PN, Peterson CM, Lu YS and Cerami, A. Sodium cyanate as potential treatment for sickle-cell disease. *N Engl J Med.* 1974; 290: 654.
44. AL-Qaisy BA. In vitro differentiation of mouse bone marrow derived mesenchymal stem cells into islet of langerhans-like cells. 2013; 22-28.

Table 1 :Effect of Benzene (1940 mg/kg) on PCV%, Hb (gm/dl), RBC(cell /cm³), total WBC count (cell /cm³), differential WBC(N%, L%, M%, E% and B%) of mice after 15 days of first administration.

Groups Parameters	Negative control group	Benzene induced group	LSD
PCV	39.9±2.53 A	30.1±1.17 B	5.60
Hb	12.5±3.16 A	7.9±1.31 B	3.9
RBC (X10 ⁶)	6.3±3.13 A	5.1±1.71 B	0.9
WBC(X10 ³)	6.9±3.03 A	4.0±1.58 B	2.1





Esraa M. Krair et al.

N%	55.1±3.08 A	62.3±6.21 B	6.5
L%	32.4±4.14 A	26.5±2.69 B	4.8
M%	6.0±2.73 A	3.9±1.52 B	1.7
E%	3.6±2.11 A	3.0±1.53 B	0.4
B%	0.8±0.5 A	0.4±0.35 B	0.4

*Averages with the various letters in similar row differed statistically (P<0.05).

Table 2 : Effect of Mesenchymal stem cell (2x10⁶ cell/kg), Oxymetholone(3mg/kg) and phosphate buffer saline on blood pictures of mice after 30 days of the treatment.

Parameter groups	PCV%	Hb g/dl	RBCs X10 ⁶ Cell /cm ³	WBCs cell /cm ³	N %	L %	M %	E %	B %
T1	38.2 ±6.09A	12.88 ± 3.15A	6.15 ±1.83A	7.5 ±3.16A	54.09 ±1.5B	35.04 ±3.6A	6.2 ±1.44A	4.0 ±2.44A	0.8 ± 0.5A
T2	42.0 ±4.12 A	13.04± 3.67 A	6.5 ±3.05A	6.1 ±1.52A	58.11 ±3.06 C	32.93 ±2.45A	6.5 ±3.13A	4.0 ±2.54A	1.0 ±0.90A
T3	30.0 ±3.60B	8.01 ±3.66B	5.0 ±1.58B	4.22 ±2.60 B	61.40± 2.91A	28.91±3. 53 B	4.0 ±1.87B	3.1 ±1.21B	0.4 ±0.15B
T4	40.0 ±3.16 A	12.97 ±3.51 A	6.0 ±1.27A	7.1 ±3.08A	55.6 ±3.26B	33.8 ±3.14 A	6.1 ±3.29A	3.9 ±2.53A	0.9 ±0.72A
LSD	4.8	0.19	0.6	1.9	2.5	2.1	1.8	0.9	0.2

*Averages with the various letters in similar columns differed statistically (P<0.05).

Table 3 : Effect of Mesenchymal stem cell (2x10⁶ cell/kg), Oxymetholone(3mg/kg) and phosphate buffer saline on blood indices after 30 days of the treatment.

Parameters Groups	MCHC %	MCH (Pg/cell)	MCV (fl/cell)
T1	33.71 ±1.57A	20.03±4.46A	62.11±2.57 AB
T2	31.04±1.42A	20.06±1.62A	64.61±6.44 A
T3	26.7±1.45 B	16.02±4.12 B	60.00±3.15 B
T4	32.42±3.71A	21.61±2.20 A	66.70±1.59A
LSD	3.29	3.55	4.7

*Averages with the various letters in similar columns differed statistically (P<0.05).





Esraa M. Krair et al.

Table 4 : Effect of Mesenchymal stem cell (2×10^6 cell/kg), Oxymetholone(3mg/kg) and Phosphate buffer saline on Alanine aminotransferase(IU/L) and, Aspartate transaminase(U/L) and total protein (g/dl) after 30 days of the treatment.

Parameters Groups	ALT(IU/L)	AST(U/L)	Total proteins(g/dl)
T1	27.93±3.16 B	28.31±1.99 B	8.01±3.15 A
T2	33.09±2.23 A	36.20±5.10 A	6.02±1.40 B
T3	35.79±1.37 A	38.25±7.07 A	5.93±2.55 B
T4	25.18±3.82 B	26.69±2.02B	8.45±1.63 A
LSD	2.9	3.07	1.46

*Averages with the various letters in similar columns differed statistically ($P < 0.05$).

Table 5 : Effect of Mesenchymal stem cell(2×10^6 cell/kg), Oxymetholone(3mg/kg) and Phosphate buffer saline on Glutathione peroxidase GPX (mmol/mg) and Superoxide dismutase SOD(U/ML) after 30 days of the treatment.

Parameters Groups	GPX(mmol/mg)	SOD(U/ML)
T1	8.99±2.60 A	11.89±5.14A
T2	5.98±3.08 B	7.43±4.10 B
T3	5.30±3.16 B	7.90±1.61 B
T4	8.61±1.36A	11.95±6.08A
LSD	2.91	1.75

*Averages with the various letters in similar columns differed statistically ($P < 0.05$).

Table 6 : Effect of Mesenchymal stem cell (2×10^6 cell/kg), Oxymetholone(3mg/kg) and Phosphate buffer saline on total bone marrow ($X 10^3$ cell/ μ L) after 30 days of the treatment.

Parameters Groups	Total bone marrow ($X 10^3$ cell/ μ l)
T1	9.5±1.69 A
T2	8.6±2.00 B
T3	7.1±3.08 C
T4	8.9±2.78 B
LSD	0.51

*Averages with the various letters in similar columns differed statistically ($P < 0.05$).





Esraa M. Krair et al.

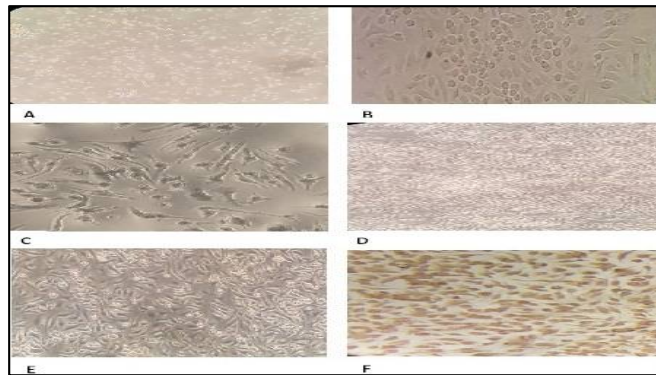


Figure 1: The morphology of BMSCs are floated in culture media a the first day (A). The cells in the second day are adhered to the culture media flask thinly with spindle-like in shape (B). MSCs in the third day appeared as a large colonies of cells (C). MSCs colonies in six day appeared regularly extensive in their size and each nearby colony ones are unified with each other (D). MSCs in the nine day appeared adhesiveness and fusiform with a spindle-like in shape (E). MSCs given positive reaction for CD44 marker and stained with deeply brown color by DAB stain (F).

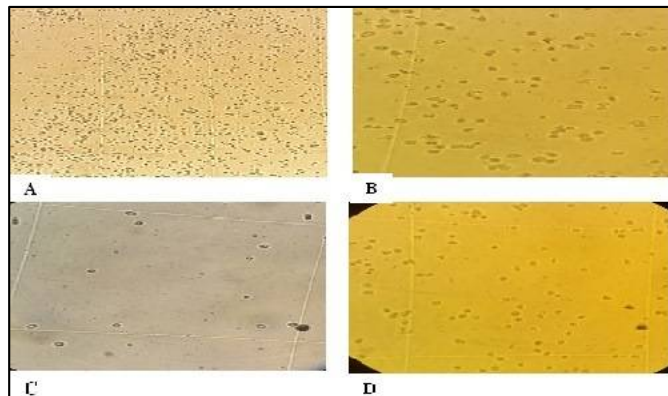
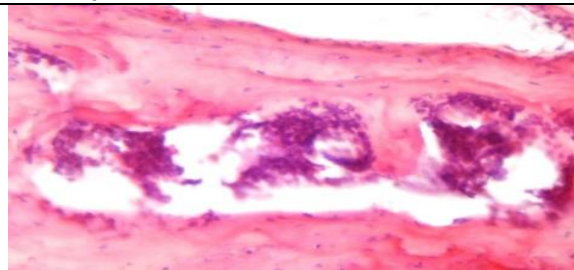


Figure 2: Cells of bones marrow mice treated with MSCs were appeared great enhancement in their count and aggregations (A), while cells of bone marrow in mice treated with Oxymetholonewere appeared normal enhancement in their count and aggregations (B). cells of bone marrow in mice treated with PBS were appeared decrease in their count (C). Bone marrow cells of negative control group were appeared normal count under light microscope (X100).



Figure(3): Histopathological section in the mice bone handled with Benzene, after 15 days of treatment showed decrease in the cellularity of bone marrow, mild hemorrhage and neutrophils in the medullary cavity of compact bone (H and E stain; ×20)



Figure(4): Histopathological section in the bone of T3 after 30 days of treatment showed severe distraction of compact bone which contained many cavities filled with RBCs and necrotic inflammatory cells (H and E stain; ×40).





Esraa M. Krair et al.



Figure(5):Histopathological section in the bone of T1 after 30 days showed normal endosteum and periosteum and improvement mineralization of trabecular bone and cellularity.(H and E; X100).

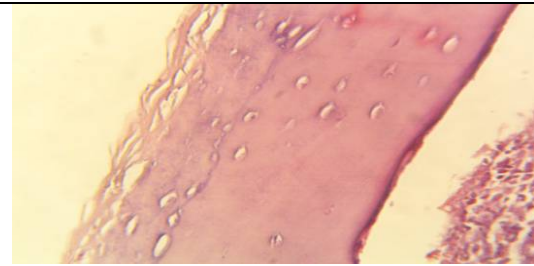


Figure (6):Histopathological section in the bone of T2 after 30 days showed normal endosteum and compact bone but irregular periosteum. There was mild improvement in cellularity of bone marrow (H and E; x 200)

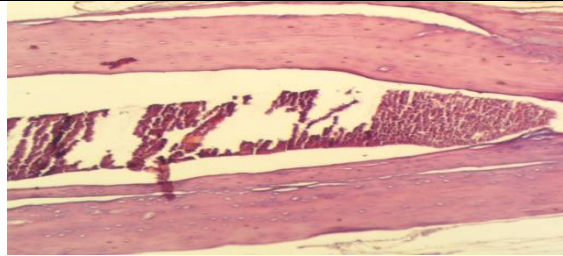


Figure (7) :The histopathological section of bone from normal mice showed normal bone structure . H and E stain (x100).

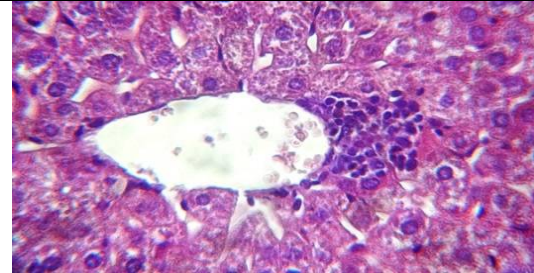
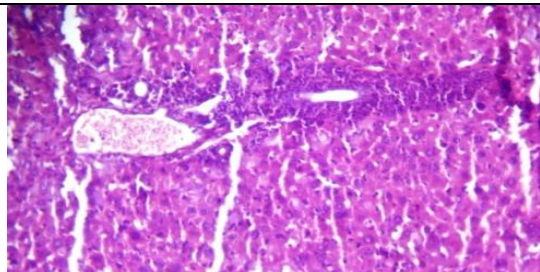
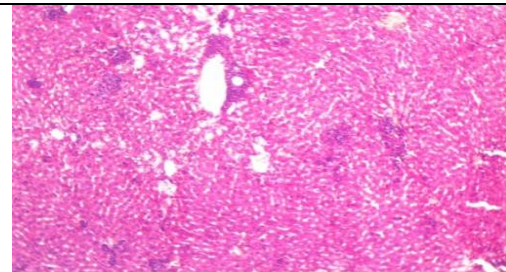


Figure (8):Histopathological section in the liver of mice treated with Benzene after 15 days of treatment showed aggregation of neutrophils and MNCs adjacent to central vein (H and E stain; x40).



Figure(9):Histopathological tissue section in the liver of T3 after 30 days of handling revealed congestion of blood vessels and sever infiltration of neutrophils (H and E stain; x20).

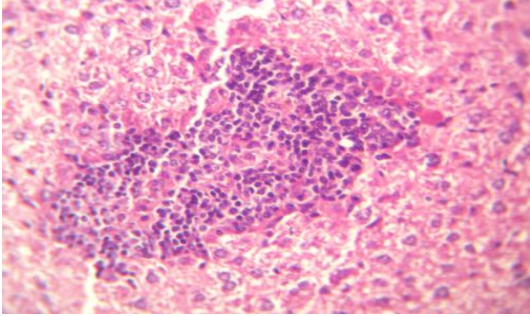


Figure(10):Histopathological section in the liver of T1 after 30 days of treatment showed mild congestion of central veins, and multifocal aggregation in the liver parenchyma(H and E; X100).

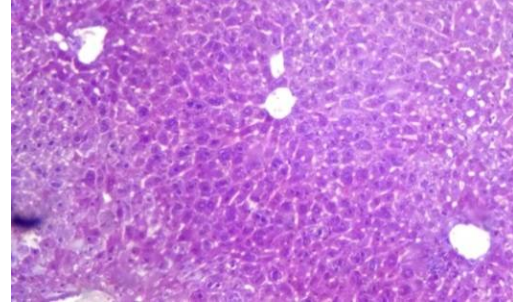




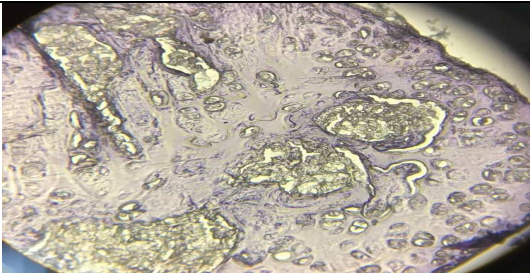
Esraa M. Krair et al.



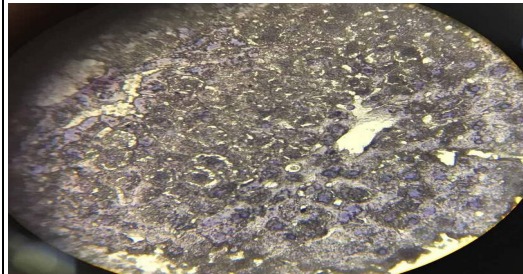
Figure(11):Histopathological tissue section in the liver of T2 revealed vacuolar degeneration of the hepatocytes, dilation of central vein, multifocal aggregation of inflammatory cells and neutrophils in the liver parenchyma(H and E; x200)



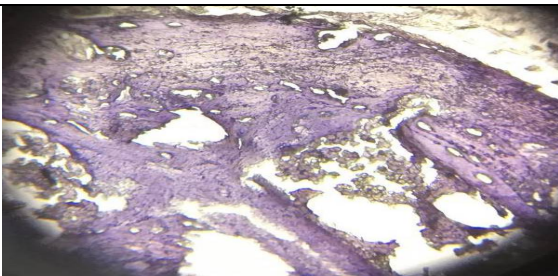
Figure(12) :Histopathological section of liver in basline group, showed ordinary liver architecture (H and E stain; x40).



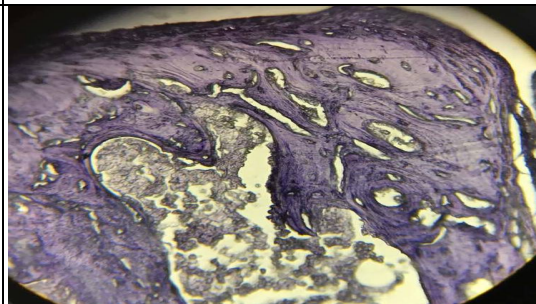
Figure(13):Immunohistograph of bone in T1 showed very strong positive deep reaction for CD44 (DAB stain x40).



Figure(14) :Immunohistograph of liver in mouse treated with T1 showed very strong positive deep result for CD44 (DAB stain ;x40).



Figure(15):Immunohistograph of bone in T2 showed negative result for CD44 (DAB stain x40).

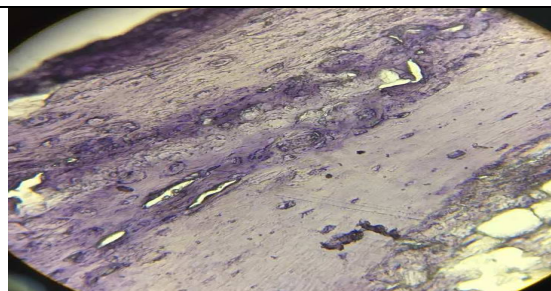


Figure(16):Immunohistograph of bone in T3 showed negative result for CD44 (DAB stain x40).

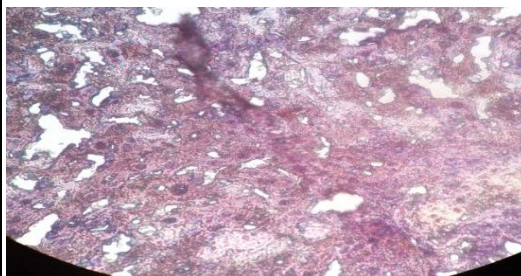




Esraa M. Krair et al.



Figure(17):Immunohistograph of bone in T4 showed negative result for CD44 (DAB stain x40).



Figure(18):Immunohistograph of liver in T2 showed negative result for CD44 (DAB stain ;x40).

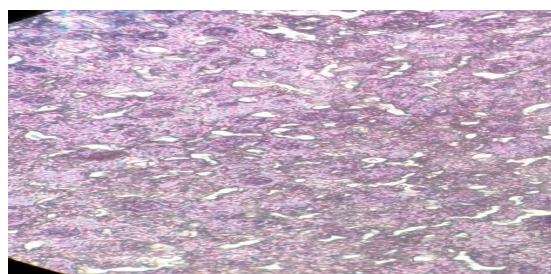


Figure (19):Immunohistograph of liver in T3 showed negative result for CD44 (DAB stain ;x40).



Figure (20):Immunohistograph of liver in T4 showed negative reaction for CD44 (DAB stain ;x40)





Effect of Growth Regulator and Chemicals on Fruit Yield in Tamarind Plantation at Harur Taluk, Dharmapuri, Tamil Nadu, India

C.N.Hari Prasath*, A.Balasubramanian, S.Radhakrishnan, A.Mayavel and S.Manivasakan

Department of Silviculture, Forest College and Research Institute, TNAU, Mettupalayam – 641 301.

Received: 24 May 2017

Revised: 28 June 2017

Accepted: 25 July 2017

*Address for correspondence

C.N.Hari Prasath

Department of Silviculture, Forest College and Research Institute,
TNAU, Mettupalayam – 641 301,
TamilNadu,India.

Email: prasathforestry@gmail.com



This is an Open Access Journal / article distributed under the terms of the **Creative Commons Attribution License** (CC BY-NC-ND 3.0) which permits unrestricted use, distribution, and reproduction in any medium, provided the original work is properly cited. All rights reserved.

ABSTRACT

A field experiment was carried out in 15 year old tamarind plantation at Chinnakupam village, Harur taluk, Dharmapuri district, Tamil Nadu. The tamarind trees were imposed with different growth regulators and chemicals viz., ZnSO₄ (0.5 %) + Boric acid (0.3 %), Planofix (Naphthalene acetic acid 150 ppm), Paclobutrazol, Ethephon and control for enhancing the flowering and fruiting in Tamarind. The maximum tamarind fruit yield was recorded in T₃ (Paclobutrazol) with the value of 42 kg./tree followed by T₂-Planofix (35 kg./tree) and the minimum fruit yield of 12 kg./tree was recorded in T₅ (Control). To conclude the study, the foliar application of Paclobutrazol had a significant increase in the nutrient status and tamarind fruit yield.

Keywords: Tamarind, Growth regulator and Chemicals, Paclobutrazol, Fruit Yield

INTRODUCTION

Bioregulator and chemical mediated biochemical changes have been shown to play a vital role during drought stress (Thakur *et al.*, 2008). Growth regulators such as hormones, chemicals and micronutrients play an important role in improving the growth, yield and quality of the many fruit crops (Rajan, 2013). Paclobutrazol significantly reduce the number of days taken for panicle initiation compare to control. A positive relation between per cent flower bearing capacity and growth regulators was reported by several workers (Majumdar and Mukhejee, 1961). Although tamarind is being planted on large scale plantations, since long time as a species of wide adaptability and amplitude of uses, little has been done for its yield improvement (Reddy *et al.*, 2010) and to reduce its reproductive age which would in turn make its cultivation economically feasible. Tamarind, a suitable species for wasteland and other afforestation programme (Kumar and Reddy, 2007), planted extensively in Tamil Nadu by forest department, farmers



**Hari Prasath et al.**

and other agencies suffers from irregular bearing associated with shy bearing which results in poor fruit yield. It is documented by earlier workers that due to profuse flowering in *Tamarindus indica*, the fruit set was very poor, resulting in large scale abscission of flowers as well as fruits during various stages of development (Laxmi, 2011). Having the above understanding, the study is focused to study the application of growth regulators and chemicals on tamarind trees for enhancing the fruit yield.

MATERIALS AND METHODS

The study was carried out during 2014-2016 in the Chinnakupam village, Harur Taluk, Dharmapuri district, Tamil Nadu, India (12°01'00"N 78°27'38.7" E). The plant material consisted of tamarind trees, planted in 2000 with the spacing of 5 × 5 m were employed for productivity enhancement of tamarind fruit through the application of growth regulators and chemicals.

The experiment was initiated during April, 2014. The trees were selected on the basis of uniform vigor and development. The growth regulators and chemicals applied in the tamarind plantation, viz., ZnSO₄ (0.5 %) + Boric acid (0.3 %), Planofix (Naphthalene acetic acid 150 ppm), Paclobutrazol, Ethepon and Control (No Application). The foliar spray of growth regulators and chemicals were given at the time of new flush formation, peak flowering and pod maturation or fruiting. The observation recorded was fruit yield by the pods harvested from each tree were weighed and expressed in kg tree⁻¹. The data obtained were subjected for statistical analysis to evaluate the possible relationship between the different parameters and analysis of variance employing statistical methods described by Panse *et al.* (1985).

RESULTS AND DISCUSSION

Fruit yield is significantly increased by the application of chemicals with Paclobutrazol and Planofix in tamarind plantation (Table 1). This increase in pod yield might be due to improvement in flowering, pod set and retention and pod weight. Paclobutrazol application has significantly increased the number of fruits per tree compare to control and NAA spray (Siddik *et al.*, 2015). In present study, tamarind fruit yield was registered maximum in T₃ (Paclobutrazol) with the value of 42 kg. followed by T₂-Planofix (35 kg and the minimum fruit yield of 12 kg. was recorded in T₅ (Control). In confirmation with the present investigation, the experimental observation registered that the increased in intensity of flowering, better fruit set and fruit weight in paclobutrazol treated trees have ultimately increased the yield of mango by 42.17 per cent (Reddy and Bhagwan, 2014).

ACKNOWLEDGEMENTS

The foliar application of Paclobutrazol had a significant increase in the tamarind fruit yield and it also plays a major role in enhancing the nutrient status and biochemical constituents. On contrary, the lowest fruit yield and nutrient status was registered in control treatment.

REFERENCES

1. Kumar, Ashok M. and Y.N. Reddy. 2007. Effect of Calcium nitrate and Salicylic acid spray at flowering on transduction of flowering in cv. Baneshan. *Crop Research*, 34(3): 146-149.
2. Laxmi, D.V. 2011. Studies on fruit set, fruit drop and development in seeded and seedless types of tamarind (*Tamarindus indica* L.). M.Sc. Thesis, UAS, Bangalore.
3. Majumder, P.K. and S.K. Mukherjee. 1961. Studies on variability of sex-expression in mango (*Mangifera indica* L.). *Indian J. Horti.*, 18: 12-19.





Hari Prasath et al.

4. Panse, V.G., P.V. Sukhatme and V.N. Amble. 1985. Statistical methods for agricultural workers (Ref. Edn.). ICAR, New Delhi.
5. Rajan, S. 2013. GIS tools for genetic resource management in horticultural crops. In: Geospatial technologies for natural resources management. Soam, S.K., P.D. Sreekanth and N.H. Rao (Eds.). New India Publishing Agency, Pitam Pura, New Delhi, pp. 305-320.
6. Reddy, Pulla C.H., Y.N.Reddy, R.Chandrasekhar and Reddy, P. Narayana, 2010. Effect of precursor microbial interactions on induction of flowering and fruiting in mango. 4th Indian Horticulture Congress, 2010. New Delhi Book of abstract p: 259.
7. Reddy, Y.N. and A. Bhagwan. 2014. Induction of flowering in fruit crops – physiological and plant architectural implications. Souvenir of National Seminar-cum-Workshop on Physiology of Flowering in Perennial Fruit Crops. pp. 24-47.
8. Siddik Md. Abubakar, Mohammad Mahbub Islam, Md. Ashabul Hoque, Shahidul Islam, Suraya Parvin and Mominul Haque Rabin. 2015. Morphophysiological and yield contributing characters and yield of sesame with 1-Naphthalene Acetic Acid (NAA). Journal of Plant Sciences, 3(6): 329-336.
9. Thakur, A., P.S. Thakur and R.P. Singh. 2008. Influence of paclobutrazol and triaccontanol on growth and water relations in olive varieties under water stress. Indian J. Plant Physiology, 8(2): 116-120.

Table 1. Effect of growth regulator and chemicals on fruit yield in tamarind tree

Treatment		Yield (kg.)
T ₁	ZnSO ₄ (0.5 %) + Boric acid (0.3 %)	29
T ₂	Planofix (Naphthalene acetic acid 150 ppm)	35
T ₃	Paclobutrazol	42
T ₄	Ethephon	26
T ₅	Control	12

SEd 1.59

CD (0.05) 3.37





RESEARCH ARTICLE

Investigation of the Ground State Nuclear Density Distributions of Unstable ^{17,18,19,20}F Isotopes

Wasan Z.Majeed and Arkan R.Ridha*

Department of Physics, College of Science, University of Baghdad, Iraq.

Received: 15 Aug 2017

Revised: 25 Aug 2017

Accepted: 25 Sep 2017

*Address for correspondence

Arkan R. Ridha

Department of Physics,

College of Science,

University of Baghdad, Iraq.

Email : wasan_zmz@yahoo.com / arkan_rifaah@yahoo.com



This is an Open Access Journal / article distributed under the terms of the **Creative Commons Attribution License** (CC BY-NC-ND 3.0) which permits unrestricted use, distribution, and reproduction in any medium, provided the original work is properly cited. All rights reserved.

ABSTRACT

Structure of unstable ^{17,18,19,20}F isotopes have been investigated using shell model and Hartree Fock (HF) calculations. Results of the ground proton, neutron and matter density distributions and the corresponding root mean square (rms) radii of these unstable nuclei are studied. Shell model calculations are performed using SDPFNOW interaction. In Hartree-Fock method the selected effective nuclear interactions, namely the Skyrme parameterizations SLy4, Skesσ, SkBsk9 and Skxs25 are used. The results of rms radii obtained by shell model showed good agreement with experimental values, while those of HF showed an overestimation. Besides the elastic charge electron scattering form factors of these nuclei are investigated. The calculated charge form factors in Hartree-Fock calculations show the existence of many diffraction minima in contrary to shell model, which predicts less diffraction minima. The long tail behaviour in nuclear density is noticeable seen in HF more than shell model calculations. The deviation occurs between shell model and HF results are attributed to the sensitivity of charge form factors to the change in the tail part of the charge density.

Keywords: Shell model, Hartree – Fock , electron scattering, rms charge, neutron, and matter radii.

INTRODUCTION

Nuclear size and density distribution are the basic quantities to describe the nuclear properties [1-3]. Electron-nucleus scattering is known to be one of the powerful tools for investigating nuclear charge density distributions. Charge density distributions for stable nuclei have been well studied with this method [4-6]. For unstable nuclei, although studies of electron scattering have not been realized so far, nuclear physicists have already





Wasan Z.Majeed and Arkan R.Ridha

planned to explore the structures of unstable nuclei with electron- nucleus scattering. Therefore it is expected that the information of the charge density distributions for unstable nuclei will soon be available [7]. The nuclear shell model provides a main theoretical tool for understanding all properties of nuclei. It can be used in its simplest single-particle form to give a qualitative understanding, but it can also be used as a basis for much more complex and complete calculations [8]. Basically, to deal with the many-body equations, there are two main types of the shell-model basis: mean-field or Hartree–Fock (HF) models and configuration mixing models [9]. The HF method with an effective interaction with Skyrme forces is widely used for studying the properties of nuclei. This method is successfully used for a wide range of nuclear characteristics such as binding energy, root mean square (rms) radii, neutron and proton density, electromagnetic multipole moments, etc. [10].

Via a shell model calculation using a non central particle-hole potential interaction, the energy spectrum of the non-normal parity state in ^{19}F was determined by Lee et al. [11]. Adelberger et al., [12] have taken into consideration the Beta decays and their relations to parity mixing in ^{18}F and ^{19}F nuclei. Chu yan-Yun et al., [13] studied the electron scattering of unstable ^{17}F , ^{18}Ne , and some neutron rich $N=8$ isotones nuclei using relativistic mean field theory and phase shift analysis. Recently, Radhi et al., [14] used shell model and Hartree- Fock calculations to study the inelastic electron scattering form factors, energy levels and transition probabilities for positive and negative low-lying states of ^{19}F nucleus.

The aim of the present work is to study the nuclear density and elastic electron scattering form factors for $^{17,18,19,20}\text{F}$ nuclei using shell model and Hartree_Fock calculations. The nuclear shell model calculation is performed using SDPF - model space which consist the active shells $2s\ 1d$ and $2p\ 1f$ above the inert ^{16}O nucleus core using SDPFNOW interaction [15]. The radial wave functions for the single- particle matrix elements were calculated by using the harmonic- oscillator potential (HO) and the OBDM elements are computed from the shell model code oxbash [16]. For HF method, the effective nucleon- nucleon interaction Skyrme forces SLy4 [17], SKEσ [18], SkBsk9 [19] and Skxs25 [20] parameters are used.

THEORETICAL FORMULATIONS

The expectation value of the HF Hamiltonian of the system is given by [21]:

$$\langle \phi_{HF} | \hat{H} | \phi_{HF} \rangle = \sum_{i=1}^A \langle \phi_i | \hat{T} | \phi_i \rangle + \frac{1}{2} \sum_{ij}^A \langle \phi_i \phi_j | \bar{v}(i, j) | \phi_i \phi_j \rangle \quad (1)$$

where $\bar{v}(i, j)$ contains all parts of nucleon– nucleon forces. This forces consists of some two-body terms together with a three-body term [22]:

$$\hat{V}_{Skyrme} = \sum_{I \sim J} V_{ij}^{(2)} + \sum_{i < j < k} V_{ijk}^{(3)} \quad (2)$$

with

$$V_{ij}^{(2)} = t_0(1 + x_0 p_\sigma) \delta(\vec{r}) + \frac{1}{2} t_1 [\delta(\vec{r}) \vec{k}^2 + \vec{k}^{-2} \delta(\vec{r})] \\ + t_2 \vec{k} \cdot \delta(\vec{r}) \vec{k} + i W_0 (\vec{\sigma}_i - \vec{\sigma}_j) \cdot \vec{k} \times \delta(\vec{r}) \vec{k} \quad (3)$$

$$V_{ijk}^{(3)} = t_3 \delta(\vec{r}_i - \vec{r}_j) \delta(\vec{r}_j - \vec{r}_k) \quad (4)$$

The relative momentum operators $\vec{k} = (\nabla_i - \nabla_j) / 2i$, acting to the right and $\vec{k}^{-2} = -(\nabla_i - \nabla_j) / 2i$, acting to the left.





Wasan Z.Majeed and Arkan R.Ridha

In the shell model calculations, the ground state density distribution takes the form

$$\rho_{t_z}(r) = \frac{1}{4\pi\sqrt{(2J_i + 1)}} \sum_{\alpha} \sqrt{2j_a + 1} X_{a,a,t_z}^{J_i, J_i, 0} |R_{n_a l_a}(r, b_{t_z})|^2 \quad (5)$$

$R_{n_l}(r)$ is the radial part of the HO wave function and $X_{a,b,t_z}^{J_f, J_i, J}$ is the proton ($t_z = 1/2$) or neutron ($t_z = -1/2$) one body density matrix element.

The matter density distribution of eq. (5) may also be expressed as

$$\rho_m(r) = \rho_p(r) + \rho_n(r) \quad (6)$$

The corresponding rms radii are given by

$$\langle r^2 \rangle_x^{1/2} = \frac{4\pi}{x} \int_0^{\infty} dr r^4 \rho_x(r) \quad (7)$$

where x represents the corresponding number of nucleons.

The neutron skin thickness (t), can be defined as

$$t = r_n - r_p \quad (8)$$

The corresponding elastic scattering $J=0$ form factor (C_0) is written in the following form

$$F_{0,t_z}(q) = \frac{4\pi}{x} \int_0^{\infty} dr r^2 \rho_x(r) j_0(qr) F_{fs}(q) F_{cm}(q) \quad (9)$$

where $F_{fs}(q)$ and $F_{cm}(q)$ are free nucleon form factor and center of mass correction, respectively, given by [23]:

$$F_{fs}(q) = [1 + (q/4.33 \text{ fm}^{-1})^2]^{-2} \quad (10)$$

and

$$F_{cm}(q) = e^{q^2 b^2 / 4A} \quad (11)$$

where A in Eq. (11) represents the mass number of the nucleus under study.

RESULTS AND DISCUSSION

In order to explain the nuclear structure of unstable $^{17,18,19,20}\text{F}$ isotopes nuclei, nuclear radii, nuclear density distributions and form factors are studied using shell model calculations with SDPF- model space which consist the active shells $2s-1d$ and $2p-1f$ above the inert ^{16}O nucleus core. SDPFNOW interaction [15] has been used to provide realistic sdpf- shell wave functions for ground state. Also, self-consistent mean field with selected Skyrem forces





Wasan Z.Majeed and Arkan R.Ridha

(SLy4, Skεσ, SkBsk9 and Skxs25) are used. The HO size parameters for ^{17}F , ^{18}F , ^{19}F and ^{20}F are taken to be 1.7 fm, 1.82 fm, 1.67 fm and 1.77 fm, respectively.

The calculated proton, neutron and matter rms radii with neutron skin thickness (t) are tabulated and compared with available experiment data in Tables (1 to 4) for ^{17}F , ^{18}F , ^{19}F and ^{20}F , respectively. From these Tables, it clear that the calculated rms using shell model calculation gives excellent agreement with experimental data. The results of HF showed an overestimation in the calculated rms radii for ^{17}F , ^{19}F and ^{20}F , while the results for ^{18}F is quite consistent with the experimental values. These Tables give the conclusion that the calculated proton rms with the Skyrme HF has approximately been decreased with increasing number of neutron while, the results of rms of neutron, matter and neutron skin thickness increased with the increasing of number of neutron .

The neutron density distributions of these isotopes are displayed in figures (5,6,7 and 8) . Also, these figures showed that the results of HF calculations are all have the same behavior through the whole range of r and differ from the shell model results at fall-off region. The long tail behaviour is noticeable seen in HF more than shell model calculation. The obtained values of the neutron density for these isotopes at center region increased with increasing number of neutron. The matter density distribution of these nuclei are displayed in figures (9,10,11 and 12).

In figure (13,14,15 and 16), the calculated elastic form factors are plotted. For the sake of completeness of comparison, ^{19}F is chosen as a reference of the stable nucleus, where experimental data of electron scattering form factors are available [25]. These figures give the conclusion that the form factor is not dependent on detailed properties of the distributions of neutron density.

It is apparent from figure (13) that the HF calculations for all Skyrme almost coincide in all range of momentum transfer. The deviation occurs between shell model and HF results at $q \approx 1 \text{ fm}^{-1}$, since the form factors are sensitive to the change in the tail part of the charge density. One can see that both of shell model and experimental data has one diffraction minimum. The location of the minimum of shell results has forward shift as compared with the minimum of HF results. The longitudinal C0 elastic electron scattering form factors of ^{18}F nucleus are shown in figure (14). These form factors are connected with the proton density distribution. It is clear from this figure that all HF results has two diffraction minimum, while shell model results has only one. The location of the minimum of shell results has forward shift as compared with the minimum of HF results. Figure (15) show the calculated electron scattering form factors of ^{19}F . In this figure, all results predicted approximately the same position of the diffraction minimum. Also, it is apparent from this figure that the calculated form factors using shell model and HF are in good agreement with experimental data, except that there is an underestimation in the prediction of the position of first diffraction minimum in comparing with experimental data. At high q The deviation occurs between shell model and HF results. It is apparent from figure (16) that the HF calculations for all Skyrme almost have the same behavior for all range of momentum transfer. The deviation occurs between shell model and HF results at $q \approx 1 \text{ fm}^{-1}$, since the form factors are sensitive to the change of the tail part of the charge density. It is clear from this figure that all HF results has two diffraction minimum, while shell model results has only one.

CONCLUSION

In this study, structure of unstable $^{17,18,19,20}\text{F}$ isotopes have been investigated using shell model and HF calculations. In shell model calculations, results of rms radii showed excellent agreement with experimental data, while HF results showed an overestimation in the calculated rms radii for $^{17,19,20}\text{F}$ and good agreement for ^{18}F . In general, it is found that the calculated rms radii of neutron, matter and neutron skin thickness with the Skyrme HF have approximately been increased with increasing number of neutron. It is clear from the result of the density distribution that the calculated density is quite consistent with all the Skyrme forces and shell model in the central region. Also, the obtained values of the proton density for these isotopes at center region decreased with increasing number of





Wasan Z.Majeed and Arkan R.Ridha

neutron, while the neutron density has increased. The long tail behaviour in neutron density is noticeable in HF more than shell model calculation. Thus, the deviation occurs between shell model and HF results since the form factors are sensitive to the change in the tail part of the charge density. It is clear that each HF results have two diffraction minimum in disagreement with experimental data in contrary to shell model, which predicts less diffraction minima.

ACKNOWLEDGMENTS

The authors would like to express their thanks to Professor B.A. Brown in National Superconducting Cyclotron Laboratory, Michigan State University, for providing computer code OXBASH.

REFERENCES

- [1] A Bohr and B R Mottelson *Nuclear Structure Volume 1: Single-Particle Motion* (World Scientific Publishing Co Pte Ltd) p 138 (1998)
- [2] I Tanihata *J. of Phys. G* 22 (1996) 157
- [3] J W Negele and E Vogt *Adv Nucl Phys.* 19 (1989) 1
- [4] R Hofstadter *Rev. Mod Phys* 28 (1956) 214
- [5] T W Donnelly and I Sick *Rev Mod Phys* 56 (1984) 461
- [6] A H Wapstra G Audi and R Hoekstra *At Data Nucl Data Tables* 39 (1988) 281
- [7] Z Wang Z Ren and Y Fan *Phys Rev C* 73 (2006) 014610
- [8] A H Raheem Ph. D. Thesis (University of Baghdad, Iraq) (2009)
- [9] B A Brown *Nucl Phys A* 704 (2002) 11c.
- [10] E Tel S Okuducu G Tamr et al *Commun Theor Phys* 49 (2008) 696
- [11] T Y Lee C T Chen-Tsai W W Yeh and S T Hsieh *Phys Rev C* 4 (1971) 64.
- [12] E G Adelberger M M Hindi C D Hoyle H E Swanson and R D Von Lintig *Phys Rev C* 27 (1983) 2833
- [13] Y Chu Z Ren Z Wang and T Dong *Commun Theor Phys* 54 (2010) 347
- [14] R A Radhi A A Alzubadi and E M Rashed *Nucl Phys A* 947 (2016) 12
- [15] S Nummela et al *Phys Rev C* 63 (2001) 044316
- [16] B A Brown et al *Oxbash for Windows PC* (MSU-NSCL report number 1289) 1 2005
- [17] E Chabanat P Bonche P Haensel J Meyer and R Schaeffer *Nucl Phys A* 635 (1998) 231
- [18] J Friedrich and P G Reinhard *Phys Rev C* 33 (1986) 335
- [19] S Goriely M Samyn J M Pearson M Onsi *Nucl Phys A* 750 (2005) 425
- [20] B A Brown G Shen G C Hillhouse J Meng and A Trzcinska *Phys Rev C* 76 (2007) 034305
- [21] L. Guo-qiang, *Commun. Theor. Phys.* 13 (1990) 457
- [22] D Vautherin D M Brink *Phys Rev C* 5 (1972) 626
- [23] J P Glickman et al *Phys Rev C* 43 (1991) 1740
- [24] A Ozawa T Suzuki and I Tanihata *Nucl Phys A* 693 (2001) 32
- [25] T. Sakuda *Prog Theor Phys* 87 (1992) 1159





Wasan Z.Majeed and Arkan R.Ridha

Table 1. The values of rms radii in fm of ¹⁷F nucleus.

Model	$\langle r \rangle_p^{1/2} \text{ fm}$	$\langle r \rangle_n^{1/2} \text{ fm}$	$t \text{ fm}$	$\langle r \rangle_m^{1/2} \text{ fm}$	Exp. $\langle r \rangle_m^{1/2} \text{ fm}$ [24]
Sly4	2.825	2.695	- 0.13	2.765	2.54±0.08
Skeσ	2.749	2.642	- 0.107	2.699	
SkBsk9	2.8	2.685	- 0.115	2.747	
Skxs25	2.874	2.714	- 0.16	2.8	
Shell model	2.627	2.55	- 0.077	2.591	

Table 2. The values of rms radii in fm of ¹⁸F nucleus.

Model	$\langle r \rangle_p^{1/2} \text{ fm}$	$\langle r \rangle_n^{1/2} \text{ fm}$	$t \text{ fm}$	$\langle r \rangle_m^{1/2} \text{ fm}$	Exp. $\langle r \rangle_m^{1/2} \text{ fm}$ [24]
Sly4	2.812	2.782	-0.03	2.797	2.81±0.14
Skeσ	2.741	2.713	-0.028	2.727	
SkBsk9	2.786	2.759	-0.027	2.772	
Skxs25	2.897	2.779	-0.098	2.823	
Shell model	2.813	2.813	0.0	2.813	

Table 3. The values of rms radii in fm of ¹⁹F nucleus.

Model	$\langle r \rangle_p^{1/2} \text{ fm}$	$\langle r \rangle_n^{1/2} \text{ fm}$	$t \text{ fm}$	$\langle r \rangle_m^{1/2} \text{ fm}$	Exp. $\langle r \rangle_m^{1/2} \text{ fm}$ [24]
Sly4	2.806	2.852	0.046	2.83	2.61±0.07
Skeσ	2.739	2.772	0.033	2.756	
SkBsk9	2.779	2.824	0.045	2.802	
Skxs25	2.828	2.872	0.044	2.851	
Shell model	2.581	2.646	0.065	2.615	

Table 4. The values of rms radii in fm of ²⁰F nucleus.

Model	$\langle r \rangle_p^{1/2} \text{ fm}$	$\langle r \rangle_n^{1/2} \text{ fm}$	$t \text{ fm}$	$\langle r \rangle_m^{1/2} \text{ fm}$	Exp. $\langle r \rangle_m^{1/2} \text{ fm}$ [24]
Sly4	2.803	2.911	0.108	2.863	2.79±0.03
Skeσ	2.740	2.82	0.08	2.785	
SkBsk9	2.776	2.882	0.106	2.834	
Skxs25	2.816	2.936	0.12	2.882	
Shell model	2.735	2.849	0.114	2.798	





Wasan Z.Majeed and Arkan R.Ridha

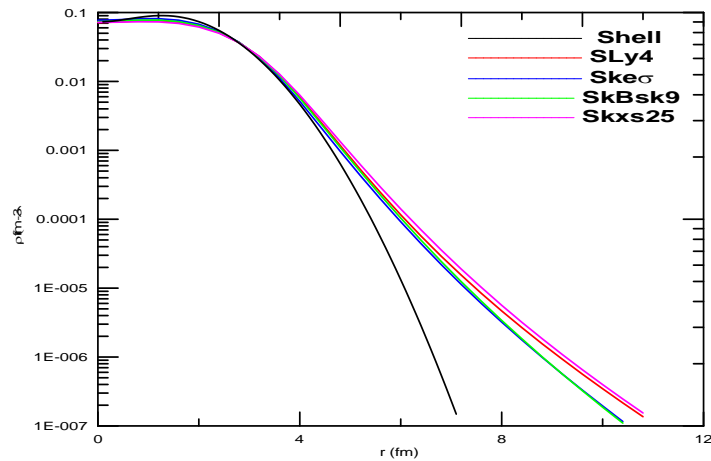


Fig.1.Proton density distributions of ^{17}F

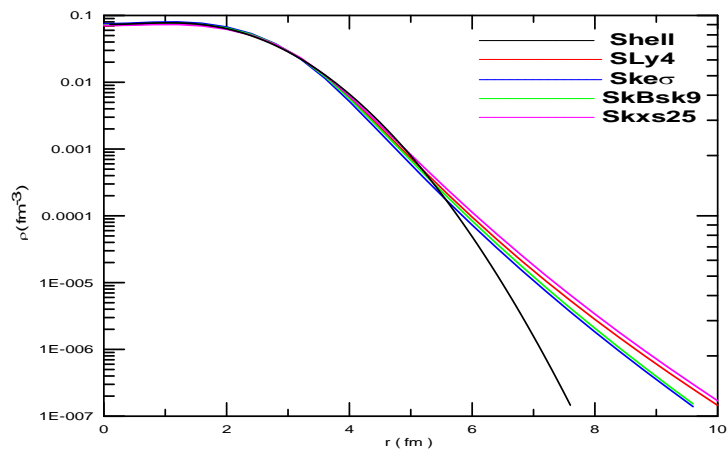


Fig. 2 .Proton density distributions of ^{18}F

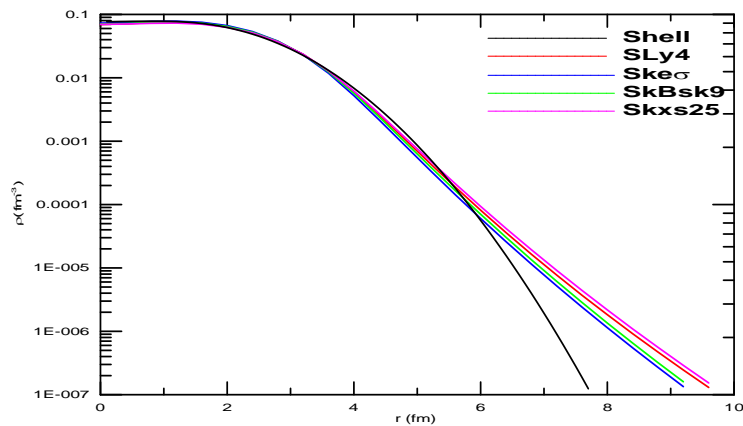


Fig.3.Proton density distributions of ^{19}F





Wasan Z.Majeed and Arkan R.Ridha

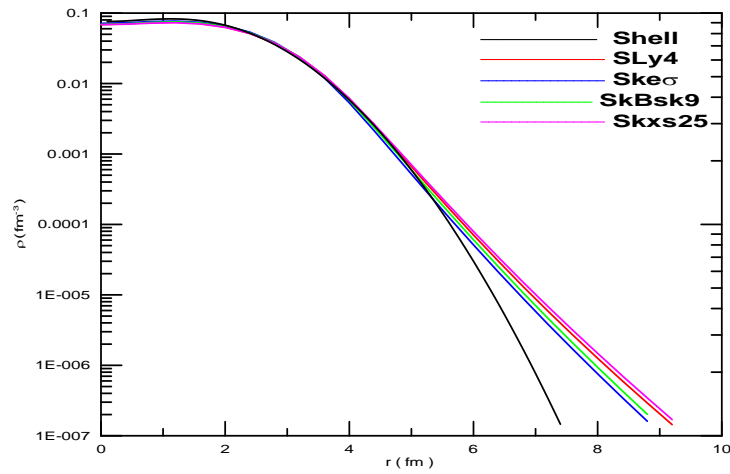


Fig.4.Proton density distributions of ²⁰F

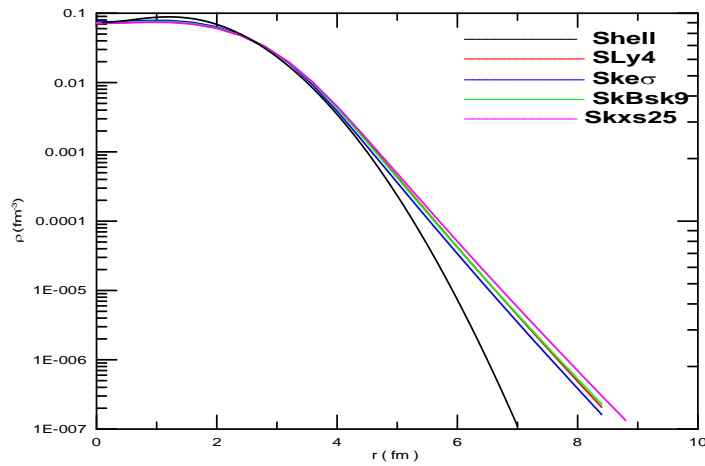


Fig. 5 .Neutron density distributions of ¹⁷F

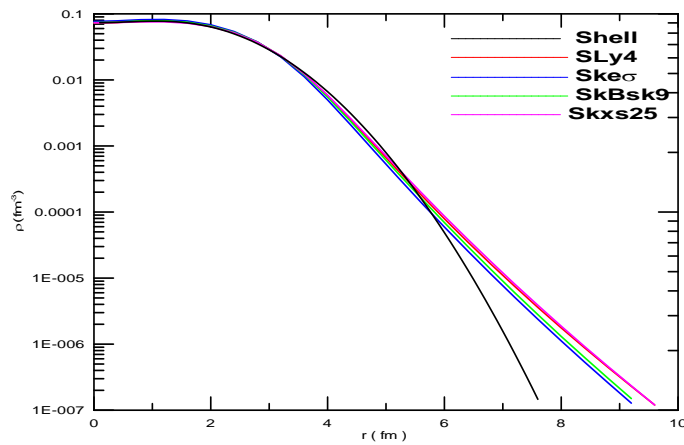


Fig. 6 .Neutron density distributions of ¹⁸F





Wasan Z.Majeed and Arkan R.Ridha

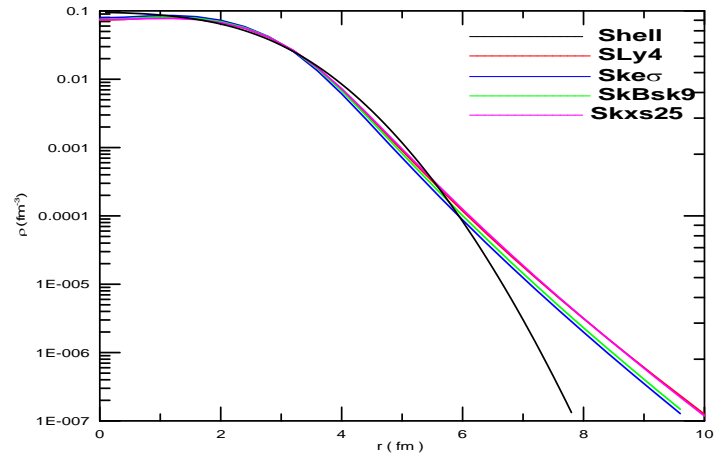


Fig. 7 Neutron density distributions of ¹⁹F

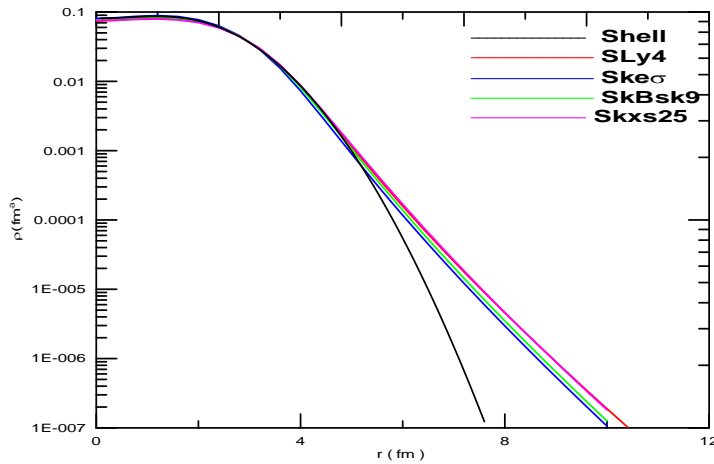


Fig.8.Neutron density distributions of ²⁰F

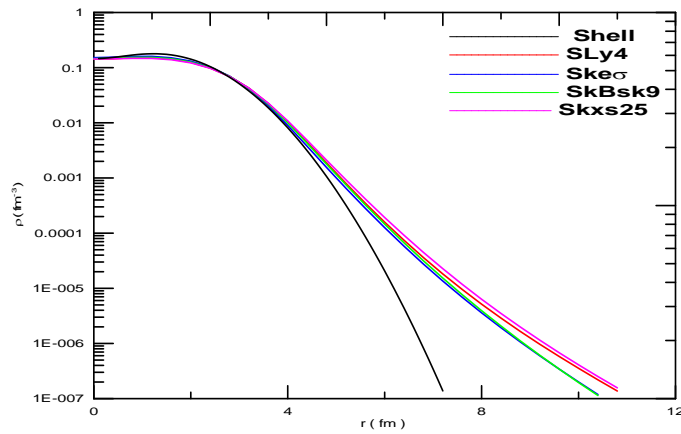


Fig. 9.Matter density distributions of ¹⁷F





Wasan Z.Majeed and Arkan R.Ridha

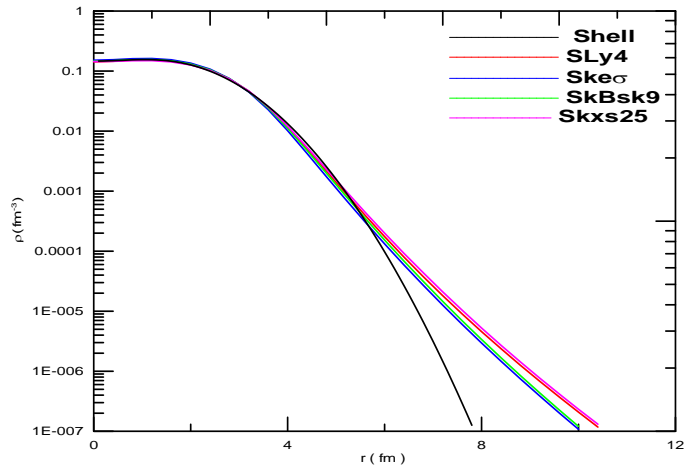


Fig.10.Matter density distributions of ¹⁸F

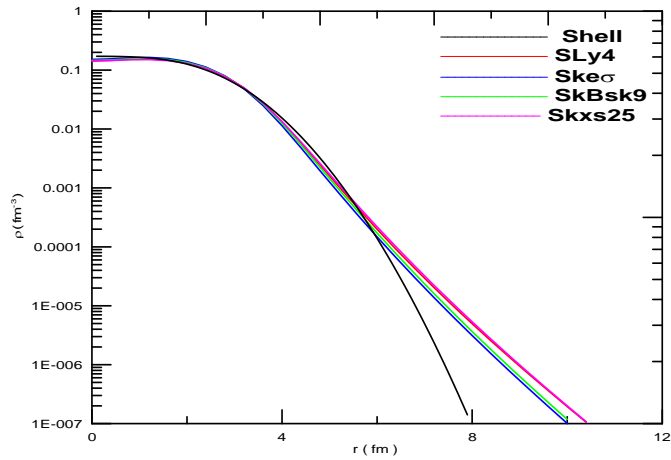


Fig.11.Matter density distributions of ¹⁹F

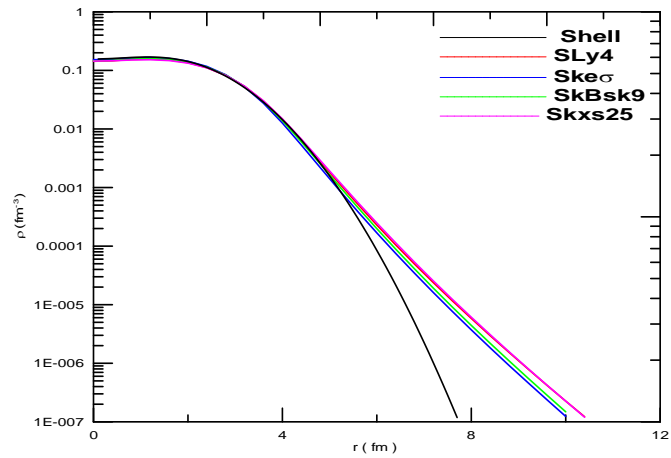


Fig. 12 .Matter density distributions of ²⁰F





Wasan Z.Majeed and Arkan R.Ridha

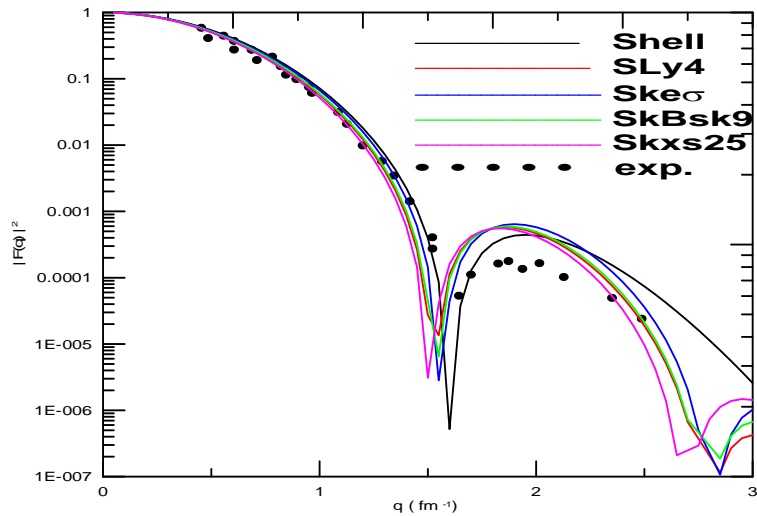


Fig. 13.Elastic charge form factors of ¹⁷F

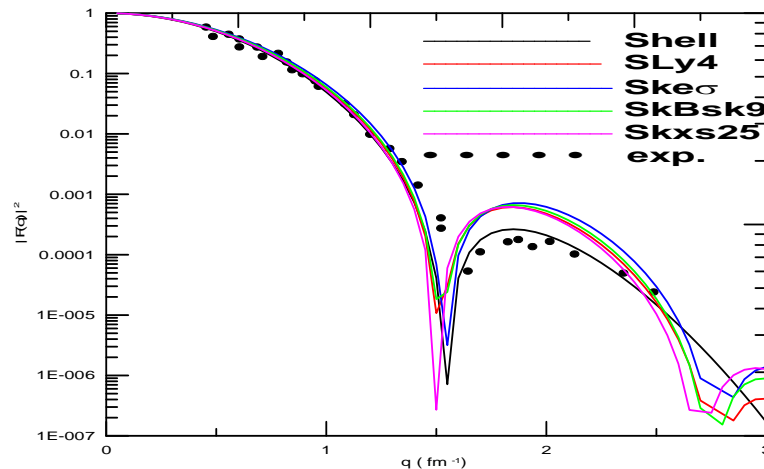


Fig. 14.Elastic charge form factors of ¹⁸F

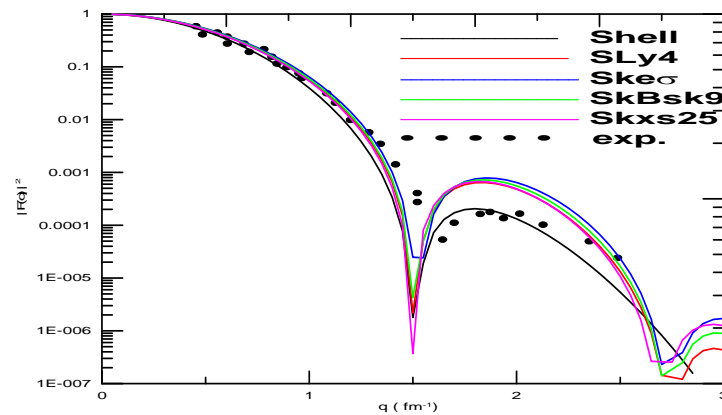


Fig. 15. Elastic charge form factors of ¹⁹F





Wasan Z.Majeed and Arkan R.Ridha

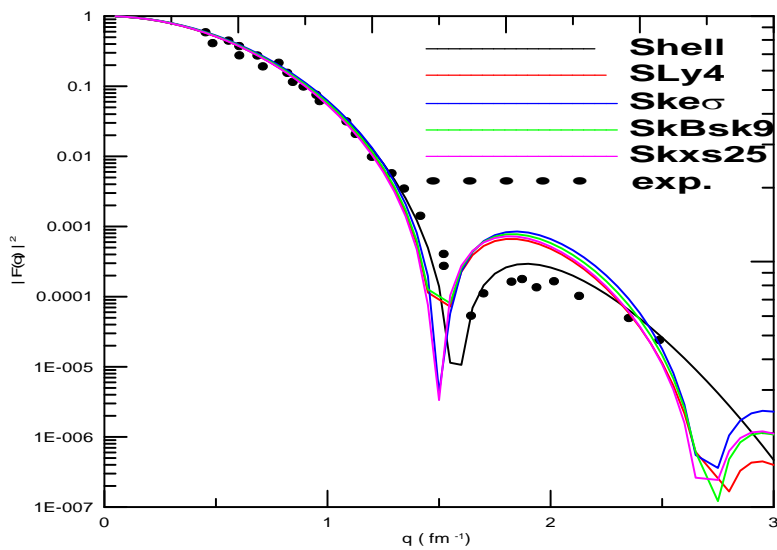


Fig. 16 .Elastic charge form factors of ^{20}F





Studies on Stress Protein Produced by Two Earthworm Speceies after Exposure to Nanoparticles and Microbial Stress

Vinotha.V¹ and Biruntha.M^{2*}

¹Scholar ,Department of Animal Health and management, Alagappa University Karaikudi -630003 .TamilNadu, India.

²Assistant Professor, Department of Animal Health and management, Alagappa University Karaikudi - 630003. TamilNadu, India.

Received: 10 Aug 2017

Revised: 20 Aug 2017

Accepted: 25 Sep 2017

*Address for correspondence

Dr.Biruntha.M

Assistant Professor, Department of Animal Health and Management,
Alagappa University Karaikudi -630003.

TamilNadu, India

.Email: biruntha6675@gmail.com



This is an Open Access Journal / article distributed under the terms of the **Creative Commons Attribution License** (CC BY-NC-ND 3.0) which permits unrestricted use, distribution, and reproduction in any medium, provided the original work is properly cited. All rights reserved.

ABSTRACT

The coelomic fluid protein profiling studies were performed under nanoparticles and microbial challenge condition in two species of earthworms namely *Eudrilus eugeniae* and *L.mauritii*. The AgNPs and ZnNPs (3mg/200g) and *B.suhtilis* and *P.aeruginosa* (400µl/earthworm) were used as an agent to measure the changes in the coelomic fluid protein profile. The changes in protein Sconcentration were identified by SDS-PAGE. The concentration of proteins expressed gets varied between treated (nanoparticles and microbes) and untreated earthworms. The antibacterial activity was analyzed by using well diffusion method zone of inhibition measured at the range of 12mm to18mm in diameter.

Keywords: coelomic fluid protein, *Eudrilus eugeniae* and *L.mauritii*, nanoparticles, *B.suhtilis* and *P.aeruginosa*

INTRODUCTION

Earthworms are an important soil invertebrate that participates in nutrient cycling in terrestrial ecosystems and in the formation of the soil profile from the physical, chemical and microbial point of view [1]. They are found in wide range of habitats throughout the world, having adapted for many different soil types as well as lakes and streams. Earthworms often called night crawlers, garden worms, red worms or simply worms. They provide bait for fishing, a source of protein for food and most importantly, they play a unique and important role in conditioning the soil [2, 3]. Earthworms are in permanent close contact with soil particles via both their highly permeable skin and alimentary



**Vinotha and Biruntha**

tract [4, 5 and 6]. Therefore, they are much affected by pollutants in the soil system and are suitable use in monitoring soil pollution due to heavy metals [7] chemicals and organic pollutants [8, 9]. They contribute 60-80% of the soil biomass [10]. They are widely contributed in standard toxicity tests [11]. Most of the studies have used various parameters such as mortality, growth rate, gross protein concentration and immune function to assay the effects of toxins and infections using the earthworm as an experimental model [12].

Protein profiling of coelomic fluid was analyzed in *Lumbricus terrestris* earthworm by causing bacterial challenge (*Aeromonas hydrophilia*) [13]. The changes occur in the growth, as well as antioxidant and antimicrobial functions of earthworm in response to various concentrations of *Escherichia coli* O157:H7 in artificial soil, then they found that earthworms can inhibit the growth of *E.coli* O157:H7 [14]. Among all tested micro-organism suspensions, earthworms *E. fetida* were stressed by *E. cloacae* UCMA 10580 (culture broth) and *L. monocytogenes* UCMA 6115 (culture broth and supernatant). Furthermore, the filter paper contact test OECD might be used as a tool to evaluate the response of *E. fetida* to biotic stresses [15].

AgNPs, are widely used in medicine, physics, chemistry and material sciences, for the development of nanotechnology [16, 17 and 18]. Until the arrival of AgNPs cure wound infection [19]. Due to the greater production and integration with the consumer products, experts expect that AgNPs will provide an increasing plenty of anthropogenic Ag into the environment [20]. AgNP toxicity has been mostly attributed to the generation of reactive oxygen species (ROS) in cells [21, 22 and 23]. Soil represents a major recipient of nanoparticles entering the environment [24]. Asha Rani et al., (2009) [25] found that the cells can take NPs up to bind with DNA when they come in contact by a variety of mechanisms. This can lead to the activation of cellular signaling processes producing reactive oxygen species (ROS), inflammation and eventually cell cycle arrest or cell death [26]. ZnNPs are widely used in sun care products [27] as well as self cleaning coatings [23]. ZnO₂ are applied as antibacterial in dentistry and largely used in toothpaste, beauty products, and sunscreen [28, 29]. Wang et al. [30] determined that ZnO NPs were toxic, inhibiting growth and reproduction in a soil nematode (*Caenorhabditis elegans*).

Bacillus subtilis, known also as the hay *bacillus* or *grass bacillus*, is a Gram-positive, catalase-positive bacterium, found in soil and the gastrointestinal tract of ruminants and humans. It is one of the bacterial champions in secreted enzyme production and used on an industrial level by means of biotechnological companies. They were used as biopesticides to control plant diseases and to increase yield. *Pseudomonas aeruginosa* is a common Gram-negative, rod-shaped bacterium that can cause disease in plants and animals, including humans. *P. aeruginosa* typically infects the airway, urinary tract, burns, and wounds, and also causes other blood infections. *P.aeruginosa* is used for the control of plant pathogens.

Man-made nanoparticles have a wide range of application due to the exclusive properties compared with their bulk counter parts [31]. On the other hand there is a growing concern regarding the safety of NPs in relation to their toxicity. Several studies reported the potential risk to human health from NPs, based on evidences of inflammatory reactions caused by the ferric oxide NPs in rats [32] and toxic effect of silica NPs on fibroblast and tumor cells [33]. In earthworm *Eisenia fetida*, the toxicity of TiO₂ and ZnO NPs were evaluated [34] and Maria J. Ribeiro et al [35] studied the effect of AgNP (AgNM300k) in terms of oxidative stress in the soil worm *Enchytraeus crypticus*, using a range of biochemical markers. The ecotoxicity of AgNPs was measured on *Aporrectodea caliginosa* earthworm [24].

The standard tests [36] are followed for the qualitative analysis of essential and non essential amino acids present in the coelomic fluid of earth worm. The amino acid profile of four species of earthworms from Nigeria namely *Eudrilus eugeniae*, *Hyperiadrilus africanus*, *Alma millsoni* and *Libyodrillus violaceus* have been evaluated. The proteins were isolated from coelomic fluid of earthworm, *Lumbricus terrestris* and have analyzed by polyacrylamide gel electrophoresis in sodium dodecyl sulphate (SDS-PAGE). The proteomic profile expressed in earthworm coelomic fluid, a component of the earthworm's immune system should prove to be worthwhile in advancing immunotoxicity biomarker based assays [13].





Vinotha and Biruntha

The antimicrobial activity of coelomic fluid of earthworms was performed against gram positive and gram negative bacteria. Antibacterial activity of earthworm's coelomic fluid was carried out by using well diffusion method [37]. The nutrient agar plate was used for this antibacterial activity of coelomic fluids collected from treated animals as well as control animal (untreated). *Enterococcus aureas*, *Pseudomonas aeruginosa*, *Klebsilla pneumonia* and *E.coli* are used to test antibacterial activity of coelomic fluids.

In this study, protein profiling of coelomic fluid before and after exposure to nanoparticles (AgNPs and ZnNPs) and microbial (*Bacillus subtilis* and *pseudomonas aeruginosa*.) stress. There are two types of earthworms used as a model organism for this study. They are, 1. *Eudrilus eugeniae* and 2. *Lampito mauritii*.

MATERIALS AND METHODS

Experimental animals

The clitellate earthworms of *Eudrilus eugeniae* (African species) and the *Lampito mauritii* (native species) were selected as the test animals for the present study. Earthworms were obtained from our Department Vermiculture Unit. The selected clitellate earthworms were transfer to experimental set up and then allowed to acclimatize for ten days.

Test materials

The silver nanoparticles, and zinc nanoparticles were obtained from the Department of Industrial Chemistry, Alagappa University. Then it was used for the experiment. The microbial cultures were obtained from our laboratory. The *B. subtilis* and *P. aeruginosa* were getting from our laboratory culture collection, and then it was cultured in Nutrient Agar (NA) medium. The individual colony were isolated and cultured again in a nutrient agar medium to obtain pure culture. Then the pure culture colony were picked and transferred to 500ml of nutrient broth to get a large culture for the injection. After 48h, the broth culture was centrifuged at 3000 rpm for 10min in cooling centrifuge. The supernatant was discarded and then the cells were washed with 1xPBS. The cells were centrifuged for washing cells to remove broth with PBS solution at 3000 rpm for 10 min. Then the cell transferred to 1x PBS for the injection [13].

Preparation of earthworm bed

All the experiments were carried out under laboratory conditions. The earthworms were exposed to Ag NPs as in the form of AgNO₃, Zn NPs, and the microbes used in this study are *B. subtilis* and *p. aeruginosa* in artificial soil as described by OECD guidelines (1984) [38]. An artificial soil was prepared using 70% industrial soil, 20% kaolin clay and 10% sphagnum peat moss and the p^H was adjusted to 6.0± 0.5 by the addition of CaCO₃. The dry artificial soil was moistened with distilled water. Five trays were maintained with artificial soil for each species. The first tray contains one Kg of artificial soil and earthworms without any mixture and it was maintained as control. In second tray, 3mg of AgNO₃ was added with 200mg of artificial soil and earthworms. In third tray, 3mg of ZnNPs were added with 200mg of artificial soil and earthworms. In fourth and fifth tray, the earthworms were injected with microbial cultures *B. subtilis* and *P. aruginosa* respectively. Worms were injected at post-clitellum with 400 µl of microbes with PBS. For injection earthworms were immobilized by wrapping them lengthwise on a plastic cling wrap sheet [13]. The soils were mixed thoroughly to ensure a homogenous mixture. Temperature was maintained at 28±2 °C throughout the study period.





Vinotha and Biruntha

Collection of coelomic fluid from earthworms

The coelomic fluid was collected from the control earth worms and as well as from the tested animals by puncturing them at post clitellum segment of the coelomic cavity with a help of Pasteur micropipette and by using ice cold method after 5th and 10th days and then samples were kept at 4°C [3]. Coelomic fluid from each treatment was centrifuged for ten minutes at 13x g and the supernatant was collected and re-centrifuged for ten minutes at 13x g to remove remaining particulates which are contaminating the coelomic fluid. Then a final five minutes centrifugation at 16x g was performed to ensure sample contain no solid matter. Then the samples were stored at □ 20°C [13and3].

Determination of coelomic fluid protein concentration

Total crude coelomic fluid protein concentration for samples collected from control and experimental organisms was determined according to the Lowry's method [39].

Qualitative amino acid analysis

A number of tests were performed to analyze the both essential and non essential amino acids present in the coelomic fluid of earthworms [36]. They include the followings;

- Ninhydrin test (for all amino acids)
- Nitroprusside test (for cysteine, cystine and methionine)
- Xanthoproteic test (for tryptophan)
- Million's test (tyrosine)
- Lead sulfide test (for cysteine and cystine)
- Ehrlich test (tryptophan and glycine)
- Hopkin's cole test (tyrosin)

SDS-PAGE (sodium dodecyl sulphate-polyacrylamide gel electrophoresis)

Polyacrylamide gel electrophoresis is the widely used gel system in laboratories for the analysis of proteins. The protein separation was accomplished using 10% SDS run at 100V for two hours. Gels were removed from the plate carrier following separation and placed in a plastic tray which containing staining solution (contains 80ml of methanol, 20ml of acetic acid 100ml of distilled water and 0.24g of coomassie brilliant blue) for two hours. Then the staining solution was discarded and destaining solution (contains 80ml of methanol, 20ml of acetic acid and 100ml of distilled water) was added. The destaining solution was changed two to three times until the bands get clearly visible. The destain was removed and gels were washed with distilled water to remove any remaining destaining solution. Then the gel is stored in 10% acetic acid and photographed [40].

Bacterial strains

Gram positive *Enterococcus faecalis* and gram negative *P.aeruginosa*, *Klebsiella pneumoniae* and *E.coli* were used in the experiment to evaluate the antibacterial activity of coelomic fluid collected from treated and untreated animals. The cultures were getting from our laboratory culture collection and maintained in slant of nutrient agar at 4°C. Active culture for experiment were prepared by transferring a loopful culture to the test tubes containing Nutrient Broth (NB) and incubated for 24 hrs at 37°C.



**Vinotha and Biruntha****Antibacterial assay**

Antibacterial activity of earthworm's coelomic fluid was carried out by using well diffusion method. The nutrient agar plate was used for this antibacterial activity of coelomic fluids collected from treated animals as well as control animal (untreated). *E.faecalis*, *P.aeruginosa*, *K. pneumonia* and *E.coli* were used to test antibacterial activity of coelomic fluids. 15µl of each samples were added to each well. The plates were then incubated at 37°C for 24h. The zone of inhibition was measured in millimeter (mm).

RESULTS**Survival and growth of experimental animal**

During this study, mortality and avoidance behavior were not noted in the earthworms exposed to nanoparticles and microbial stress treated beds, there was no significant alteration in body weight of earthworms with respect of the control for the specific period of expose.

Determination of coelomic fluid protein concentration

Coelomic fluid protein concentration was determined by Lowry et al (1951) method. Fig. 3 showed the differential concentration of protein of *E.euginea* 5th and 10th days after exposing to test materials (AgNPs, ZnNPs, *B.suptilis* and *P.aeruginosa*). Fig. 4 showed the difference in concentration of protein of *L.mauritii* 5th and 10th days after exposing to test materials (AgNPs, ZnNPs, *B.suptilis* and *P.aeruginosa*). There was increased amount of protein were recorded in bacterial challenged animal at 10th day after exposure.

Qualitative analysis of amino acids

The qualitative analysis of amino acids was carried out to identify the both essential and non-essential amino acids present in the coelomic fluid of earthworm at different stress conditions (nanoparticles and microbes). Ten essential amino acids namely Arginine, Valine, Histidine, Isoleucine, Leucine, Lysine, Methionine, Phenylalanine, Threonine, Tryptophan and nine non-essential amino acids namely Aspartic acid, Serine, Glutamic acid, Proline, Glycine, Tyrosine, Asparagine, Cysteine, Cystine were recorded in this study for each species of earthworm. Note worthy changes were observed in the concentration of amino acids of control as well as stressed earthworms.

SDS-PAGE (Sodium dodecyl sulphate-poly acrylamide gel electrophoresis)

The SDS-PAGE showing protein expression profile of coelomic fluid from control, nanoparticles (AgNPs and ZnNPs) and microbial (*B.suptilis* and *P.aeruginosa*) stressed earthworms of two species. The number of proteins expressed gets varied between normal and stress induced earthworms. The protein bands are observed in the range of 25 to 40 K Da.

Antibacterial activity

Antibacterial activity of coelomic fluid against gram positive *Enterococcus faecalis* and gram negative *P.aeruginosa*, *K.pneumonia* and *E.coli* was done by using well diffusion method. Fig8. Shows antibacterial activity of coelomic fluid of *E.euginea* that range from 12mm to 19mm in all samples from treated and untreated animals against *E.faecalis*, *P.aeruginosa*, *K.pneumonia* and *E.coli*. Fig 9 shows more than 16mm in antibacterial activity of *L.mauritii* all samples from treated and untreated animals against *E. faecalis*, *P. aeruginosa*, *K. pneumonia* and *E.coli*.



**Vinotha and Biruntha****DISCUSSION**

Aim of this work is profiling of protein of *E.euginea*, *L.mauritii*, before and after exposing to test materials such as AgNPs, ZnNPs, *B.suptilis* and *P.aeruginosa* for future use in immunotoxicity studies. In this study, coelomic fluid was collected by using puncturing at clitellum method and ice cold method. Then the fluids were examined for the estimation of total crude protein, qualitative analysis of amino acids, SDS-PAGE and then for antibacterial assay. The results getting from protein estimation showed reduction in treated animal when compared to control at 5th day. But in 10th day sample there is slight increase in the amount of protein in the microbes treated animal and in nanoparticle treated animal there is decrease in concentration when compared to control. It is due the presence of stress protein secreted by induction of test materials. Likewise in *L.mauritii* at 5th day protein concentration was getting decreased than the *B. suptilis* treated animal when compared to control. At 10th day, AgNPs, and ZnNPs showed little bit increase in the amount of protein but in microbes treated animal's samples exhibit large amount of protein were increased. The Qualitative analyses of amino acids were carried out to identify the both essential and non-essential amino acids present in the earthworm coelomic fluid at different stress conditions. The proteomic analysis was done on earthworm *Eisenia fetida* during *E.coli* 0157:H7 stress and Cadmium exposure. The study of protein expression profile of Coelomic fluid in earthworm *Lumbricus terrestris* was also done following bacteria, *Aeromonas* and metal and pesticide challenged earthworm. Thus, as the bacterial challenge demonstrates, the protein profile of earthworm coelomic fluid can be used to assay the proteomic response following exposure to external agents. There is no significant difference in antibacterial activity of coelomic fluid of treated earthworms when compared to untreated earthworms. More or less equal amount of zone of inhibition range from 13mm to 18mm was recorded in all treated and untreated earthworms.

CONCLUSION

The protein profiling of coelomic fluid was successfully performed with coelomic fluid of treated and untreated earthworms. Nanoparticles and microbial stress increases the synthesis of protein, essential and non essential amino acid in treated earthworms when compared to untreated earthworms. SDS-PAGE analysis showed the changes occur in the treated earthworms than to untreated earthworms. Antibacterial activity does not shows significant changes. These approaches have yielded much useful information, emerging technologies that allow complete protein profiles provide a powerful tool to study the innate immune response in earthworms. These results will provide important information about the effects of nanoparticles and microbial toxicity, and expand the potential use of this experimental animal as a biomarker model organism.

REFERENCES

1. Bartlett, M.D., Briones, M.J.I., Neilson, R., Schmidt, O., Spurgeon, D., Creamer, R.E., 2010. A critical review of current methods in earthworm ecology: from individuals to populations. *Eur. J. Soil. Biol.* 46, 67e73.
2. Lee, K.E., 1985. *Earthworms – Their Ecology and Relationships with Soils and Land use.* Australia: Academic press
3. Jeyanthi .V, J. Arockia John Paul, B. Karunai Selvi, M. Biruntha, N. Karmegam, 2016. Coelomic fluid protein profiling and heavy metal accumulation of three earthworms after exposure to pesticide and metal stress. *Int. J. Adv. Multidiscip. Res.* (2016). 3(2): 84-91.
4. Jager, T., Fleuren, R.H., Hogendoorn, E.A., de Korte, G., 2003. Elucidating the routes of exposure for organic chemicals in the earthworm, *Eisenia andrei* (Oligochaeta). *Environ. Sci. Technol.* 37, 3399e3404.
5. Saxe, J.K., Impellitteri, C.A., Peijnenburg, W.J., Allen, H.E., 2001. Novel model describing trace metal concentrations in the earthworm, *Eisenia andrei*. *Environ. Sci. Technol.* 35, 4522e4529.





Vinotha and Biruntha

6. Radka Roubalova, Jirí Dvorka, Petra Prochazkova, Dana Elhottova, Pavel Rossmann, Frantisek Skanta, Martin Bilej, 2014. The effect of dibenzo-p-dioxin- and dibenzofuran-contaminated soil on the earthworm *Eisenia andrei*. *Environmental Pollution* 193 (2014) 22e28.
7. Nahmani, J., Hodson, M.E., Black, S., 2007. A review of studies performed to assess metal uptake by earthworms. *Environ. Pollut.* 145, 402e424.
8. Jager, T., van der Wal, L., Fleuren, R.H., Barendregt, A., Hermens, J.L., 2005. Bioaccumulation of organic chemicals in contaminated soils: evaluation of bioassays with earthworms. *Environ. Sci. Technol.* 39, 293e298.
9. Shang, H., Wang, P., Wang, T., Wang, Y., Zhang, H., Fu, J., Ren, D., Chen, W., Zhang, Q., Jiang, G., 2013. Bioaccumulation of PCDD/Fs, PCBs and PBDEs by earthworms in field soils of an E-waste dismantling area in China. *Environ. Int.* 54, 50e58.
10. Rida, A.M.A., 1994. Les vers de terre et l'environnement. *La recherche* 25, 260–267.
11. Van-Straalen, N.M., Leeuwangh, P., Stortelder, P.B.M., 1994. Progressing limits for soil ecotoxicological risk assessment. In: Donker, M.H., Eijsackers, H., Heimbach, F. (Eds.), *Ecotoxicology of Soil Organisms*. Lewis, London and Tokyo, pp. 397–409.
12. Goven, A.J., Venables, B.J. and Fitzpatrick, L., 2005. Earthworms as Ecosentinel for Chemical-Induced Immunotoxicity. In: Tryphonas, H., Fournier, M., Blakley, B.R., Smits, J.E.G., Brousseau, P. (Eds.) *Investigative Immunotoxicology*, Chapter 7. Taylor and Francis, Boca Raton. 91- 102.
13. Geoffrey, B.S., 2006. Coelomic fluid protein profile in earthworms (*Lumbricus terrestris*) following bacterial challenge. Thesis prepared for the degree of Master of Science, Submitted to University of North Texas, America.
14. Xuelian Liu, Zhenjun Sun, Wang Chong, Zhentao Sun, Changkun He 2009. Growth and stress responses of the earthworm *Eisenia fetida* to *Escherichia coli* O157:H7 in an artificial soil, *Microbial Pathogenesis* 46 (2009) 266–272.
15. Toualy S. Ouina, Jean-Michel Panoff, Marina Koussémon and Tia J. Gonnety 2016. Effect of pesticides and micro-organisms on earthworm *Eisenia fetida* (Savigny, 1826), *African Journal of Agricultural Research*, ISSN 1991-637X.
16. Sharma, G., Sharma, A.R., Kurian, M., Bhavesh, R., Nam, J.S., Lee, S.S., 2014. Green synthesis of silver nanoparticle using *Myristica fragrans* (nutmeg) seed extract and its biological activity. *Dig. J.Nanomater. Biostructures* 9, 325–332.
17. Zhang, H., Zhang, C., 2014. Transport of silver nanoparticles capped with different stabilizers in water saturated porous media. *J. Mater. Environ. Sci.* 5, 231–236.
18. Murphy, M., Ting, K., Zhang, X., Soo, C., Zheng, Z., 2015. Current development of silver nanoparticle preparation, investigation, and application in the field of medicine. *J. Nanomater.* 2015, 1–12.
19. Edwards-Jones, V., 2009. The benefits of silver in hygiene, personal care and healthcare. *Lett. Appl. Microbiol.* 49, 147–152.
20. Blaser, S.A., Scheringer, M., MacLeod, M., Hungerbuhler, K., 2008. Estimation of cumulative aquatic exposure and risk due to silver: contribution of nanofunctionalized plastics and textiles. *Sci. Total Environ.* 390, 396–409.
21. Ahamed, M.; AlSalhi, M.S.; Siddiqui, M.K.J., 2010. Silver nanoparticle application and human health. *Clin. Chim. Acta* 411, 1841–1848.
22. Arora, S.; Jain, J.; Rajwade, J.M.; Paknikar, K.M. Cellular responses induced by silver nanoparticles: *In vitro* studies. *Toxicol. Lett.* **2008**, 179, 93–100
23. Choi, J.E.; Kim, S.; Ahn, J.H.; Youn, P.; Kang, J.S.; Park, K.; Yi, J.; Ryu, D.-Y. Induction of oxidative stress and apoptosis by silver nanoparticles in the liver of adult zebrafish. *Aquat. Toxicol.* **2010**, 100, 151–159.
24. Abdelmonem M. Khalil 2016. Physiological and genotoxic responses of the earthworm *Aporrectodea caliginosa* exposed to sublethal concentration of Ag NPs., *The Journal of Basic & Applied Zoology* (2016) 74, 8–15.
25. AshaRani, P.V., Mun, G.L.K., Hande, M.P., Valiyaveetil, S. Cytotoxicity and genotoxicity of silver nanoparticles in human cells. *ACS Nano* 2009, 3, 279–290.
26. Ahamed, M.; Posgai, R.; Gorey, T.J.; Nielsen, M.; Hussain, S.M.; Rowe, J.J. Silver nanoparticles induced heat shock protein 70, oxidative stress and apoptosis in *Drosophila melanogaster*. *Toxicol. Appl. Pharmacol.* **2010**, 242, 263–269.



**Vinotha and Biruntha**

27. Serpone, N., Dondi, D., Albini, A., 2007. Inorganic and organic UV filters: their role and efficacy in sunscreens and sun care product. *Inorganica Chimica Acta* 360, 794e802.
28. Federici, G., Shaw, B.J., Handy, R.D., 2007. Toxicity of titanium dioxide nanoparticles to rainbow trout (*Oncorhynchus mykiss*): gill injury, oxidative stress, and other physiological effects. *Aquatic Toxicology* 84, 415e430.
29. Kahru, A., H. Dubourguier, I. Blinova, A. Ivask and K. Kasemets, *Sensors*, 2008, 8(8), 5153–5170.
30. Wang, H., R. L. Wick and B. Xing, *Environ. Pollut.*, 157, pp. 1171–1177
31. Nel, A., Xia, T., Madler, L., Li, N., 2006. Toxic potential of materials at the nanolevel. *Science* 311, 622e627.
32. Zhu, M.T., Feng, W.Y., Wang, B., Wang, T.C., Gu, Y.Q., Wang, M., Wang, Y., Ouyang, H., Zhao, Y.L., Chai, Z.F., 2008. Comparative study of pulmonary responses to nano and submicron-sized ferric oxide in rats. *Toxicology* 247, 102e111.
33. Chang, J.S., Chang, K.L.B., Hwang, D.F., Kong, Z.L., 2007. In vitro cytotoxicity of silica nanoparticles at high concentrations strongly depends on the metabolic activity type of the cell line. *Environmental Science and Technology* 41, 2064e2068.
34. C.W. Hu., M. Li., Y.B. Cui., D.S. Li., J. Chen., L.Y. Yang 2010. Toxicological effects of TiO₂ and ZnO nanoparticles in soil on earthworm *Eisenia fetida*. *Soil Biology & Biochemistry* 42 (2010) 586e591.
35. Maria J. Ribeiro, Vera L. Maria, Janeck J. Scott-Fordsm and Mónica J. B. Amorim. Oxidative Stress Mechanisms Caused by Ag Nanoparticles (NM300K) are Different from Those of AgNO₃: Effects in the Soil Invertebrate *Enchytraeus crypticus* *Environmental Research and Public Health* ISSN 1660-4601.
36. Jayaraman, J., 1968. Laboratory manual in biochemistry. Wiley Eastern Limited, New Delhi 1968.
37. Dedeke, G.A., Owa, S.O. and Olurin, K.B., 2010. Amino acid profile of four earthworm species from Nigeria. *Agriculture and Biology Journal of North America* 1 (2):97-102.
38. Shobha SV, Kale RD. In-vitro studies on control of soil-borne plant pathogens by earthworm *Eudrilus eugeniae* exudates. *Green Pages*, 2008. <http://www.eco.web.com/editorial/080106.html>.
39. Sims, R.W., 1967. Earthworms (Acanthodrilidae and Eudrilidae) from Gambia. *Bulletin of the British museum of natural history*. 16:1-43.
40. Sulata Maity, Sonali Roy, Shibani Chaudhury, Shelley Bhattacharya., 2007. Antioxidant responses of the earthworm *Lampito mauritii* exposed to Pb and Zn contaminated soil. *Environmental Pollution* 151 (2008) 1e7.
41. OECD, 1984. OECD guidelines for testing of chemicals: earthworm, acute toxicity test. *OECD Guidel.* 207, 15.
42. Lowry, O.H., Rosebrough, N.J., Farr, A.L. and Randall, R.J., 1951. Measurement of protein with the folin phenol reagent. *Journal of biological chemistry*. 193:265-275.
43. Plummer, D.T., 1977. An Introduction to practical biochemistry. Tata McGraw Hill, Bombay.
44. Wang, X., Chang, L., Sun, Z. and Zhang, Y., 2010 b. Comparative Proteomic analysis of differentially expressed proteins in the earthworm *Eisenia fetida* during *Escherichia coli* O157:H7 stress. *Journal of Proteome Research*. 9 (12):6547-6560
45. Wang, X., Chang, L., Sun, Z. and Zhang, Y., 2010 a. Analysis of earthworm *Eisenia fetida* proteomes during cadmium exposure: An ecotoxicoproteomics approach. *Proteomes*. 10(24): 4476-4490.
46. Kahru, A., H. Dubourguier, I. Blinova, A. Ivask and K. Kasemets, *Sensors*, 2008, 8(8), 5153–5170.
47. Jager, T., Fleuren, R.H., Hogendoorn, E.A., de Korte, G., 2003. Elucidating the routes of exposure for organic chemicals in the earthworm, *Eisenia andrei* (Oligochaeta). *Environ. Sci. Technol.* 37, 3399e3404.
48. Sharma, G., Sharma, A.R., Kurian, M., Bhavesh, R., Nam, J.S., Lee, S.S., 2014. Green synthesis of silver nanoparticle using *Myristica fragrans* (nutmeg) seed extract and its biological activity. *Dig. J. Nanomater. Biostructures* 9, 325–332.





Vinotha and Biruntha

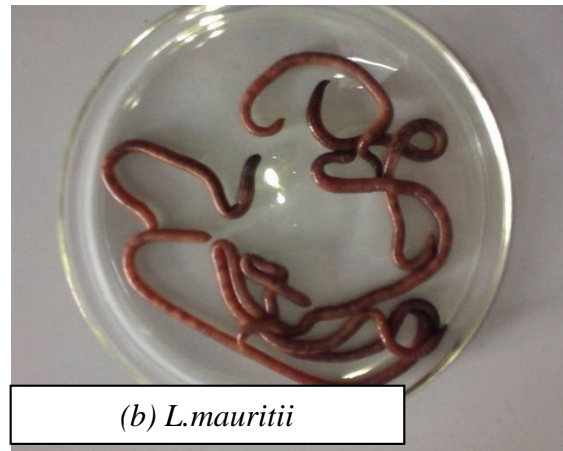
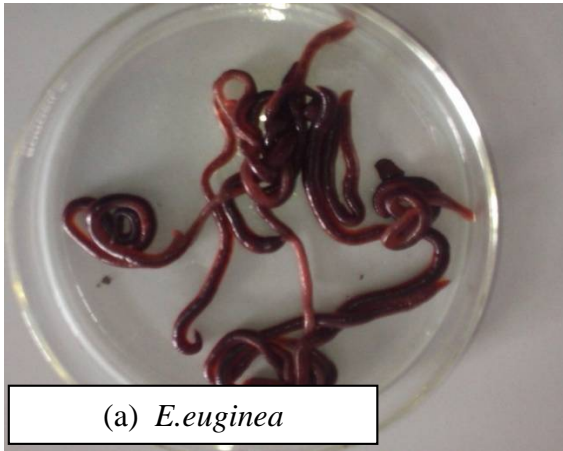
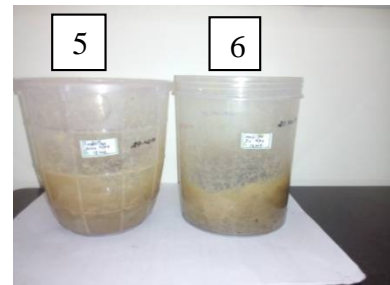
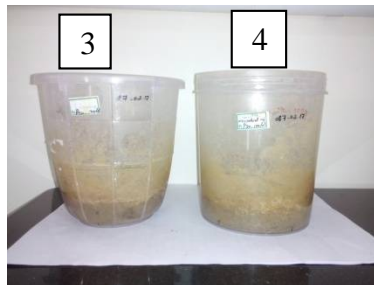


Fig1: Experimental Animals



Fig2: Collection of Coelomic Fluid by Ice Cold Method.





Vinotha and Biruntha

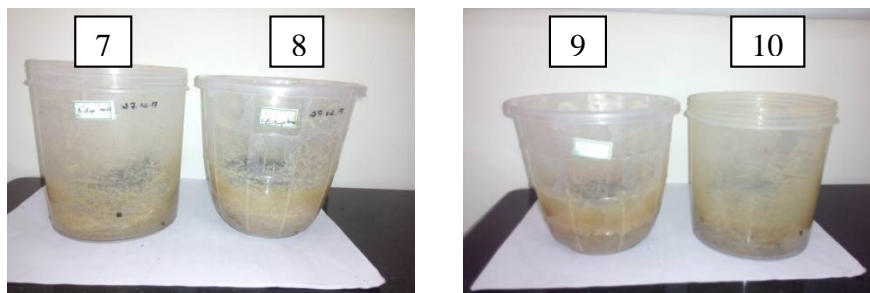


Fig3: experimental set up containing earthworms with artificial soil and test materials.

1.Artificial soil + 10 earthworms of *E.euginea* (control), 2.Artificial soil + 10 earthworms of *L.mauritii* (control) 3.Artificial soil + 10 earthworms of *E.euginea* + AgNPs, 4.Artificial soil + 10 earthworms of *L.mauritii* + AgNPs, 5.Artificial soil + 10 earthworms of *E.euginea* + ZnNPs, 6.Artificial soil + 10 earthworms of *L.mauritii* + ZnNPs 7.Artificial soil + 10 earthworms of *E.euginea* + *B.suptilis*,8.Artificial soil + 10 earthworms of *L.mauritii* + *B.suptilis*, 9.Artificial soil + 10 earthworms of *E.euginea* + *P.aeruginosa*, 10.Artificial soil + 10 earthworms of *L.mauritii* +*P.aeruginosa*

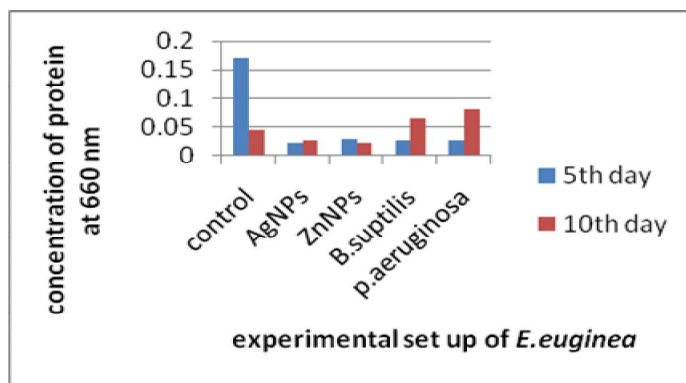


Fig 4: concentration of protein of *E.euginea* before and after exposing to test materials (AgNPs, ZnNPs, *B.suptilis* and *p.aeruginosa*).

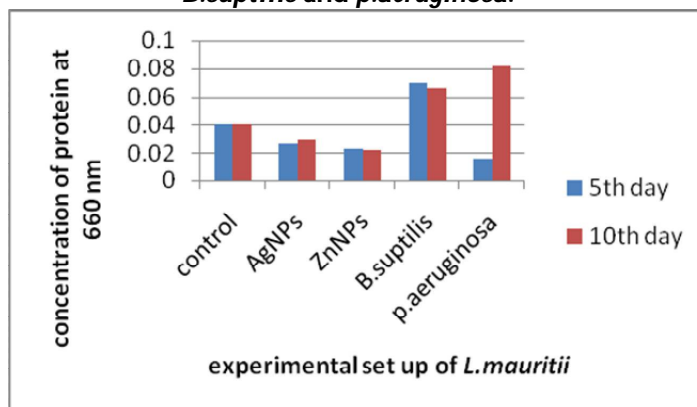


Fig 5: The concentration of protein of *L.mauritii* before and after exposing to test materials (AgNPs, ZnNPs, *B.suptilis* and *P.aeruginosa*).





Vinotha and Biruntha

Table 1: comparison of qualitative analysis of coelomic fluid of *E.euginea* after exposing to AgNPs, ZnNPs, *B.suptilis* and *P.aeruginosa*.

AMINO ACIDS	<i>E.euginea</i>				
	control	Ag NPs	Zn NPs	<i>B. suptilis</i>	<i>P.aeruginosa</i>
ESSENTIAL AMINOACIDS					
Arginine	**	**	***	*	*
Valine	***	*	***	**	**
Histidine	*	*	***	*	**
Isoleucine	*	**	*	**	*
Leucine	**	***	**	**	**
Lysine	*	*	**	**	***
Methionine	*	**	***	*	*
Phenylalanine	**	*	**	**	**
Threonine	***	**	**	***	**
Tryptophan	***	*	**	***	***
NON ESSENTIAL AMINOACIDS					
Aspartic acid	**	**	**	*	**
Serine	***	**	**	*	***
Glutamic acid	*	*	*	**	**
Proline	*	**	**	**	*
Glycine	*	**	*	***	**
Alanine	**	***	**	**	*
Cystine	***	**	***	*	**
Tyrosine	**	**	*	***	*
Asparagine	***	***	**	***	**

*** = Highly present;

** = Moderately present;

* = less amount





Vinotha and Biruntha

Table 2: Comparison of qualitative analysis of coelomic fluid of *L.mauritii* after exposing to AgNPs, ZnNPs, *B.suptilis* and *P.aeruginosa*.

AMINO ACIDS	<i>L.mauritii</i>				
	Control	Ag NPs	Zn NPs	<i>B. suptilis</i>	<i>P.aeruginosa</i>
ESSENTIAL AMINOACIDS					
Arginine	**	**	**	*	*
Valine	***	*	***	**	**
Histidine	*	*	*	*	**
Isoleucine	*	**	***	**	*
Leucine	**	*	**	***	**
Lysine	*	*	*	**	***
Methionine	*	**	**	*	*
Phenylalanine	**	*	**	***	**
Threonine	***	**	***	**	**
Tryptophan	***	**	**	***	*
NON ESSENTIAL AMINO ACIDS					
Aspartic acid	**	**	**	*	**
Serine	***	**	**	*	***
Glutamic acid	*	*	*	**	**
Proline	*	**	**	**	*
Glycine	*	**	*	***	**
Alanine	**	***	**	**	*
Cystine	***	**	***	*	**
Tyrosine	**	**	*	***	*
Asparagine	***	***	**	*	**

*** = Highly present;

** = Moderately present;

* = less amount





Vinotha and Biruntha

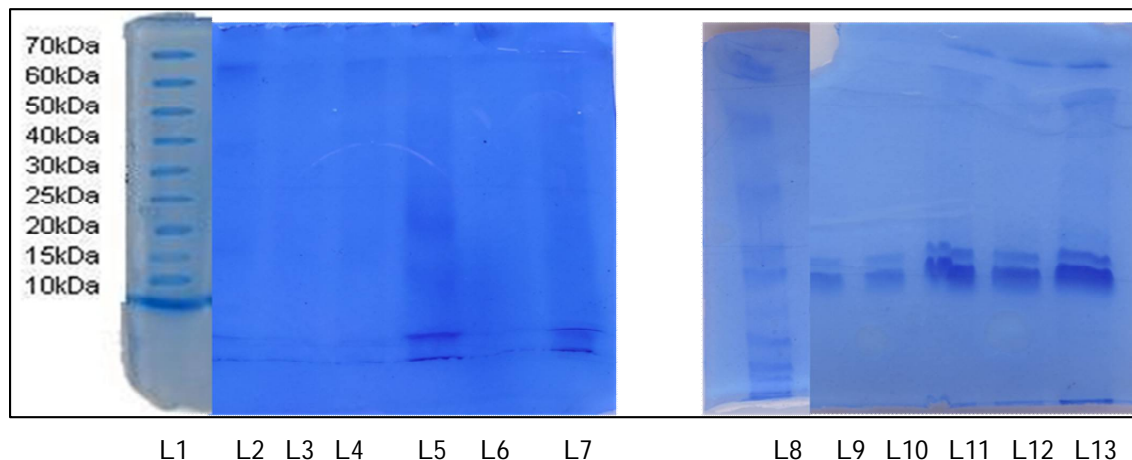


Fig.6.SDS-PAGE shows protein expression of *E.euginea* after exposing to nanoparticles and bacterial challenges.

- L1 and L8 stands for standard protein markers
- L2 and L9 stands for control
- L3 and L10 stands for AgNPs stressed earthworm
- L4 and L11 stands for ZnNPs stressed earthworm
- L5 and L12 stands for *B.sputilis* stressed earthworm
- L6 and L13 stands for *P.aeruginosa* stressed earthworm

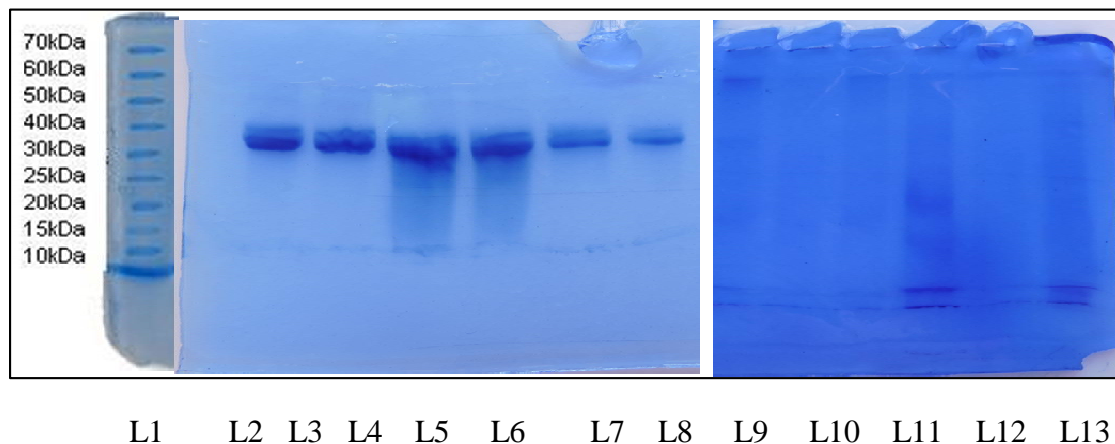


Fig 7.SDS-PAGE shows protein expression of *L.mauritii* after exposing to nanoparticles and bacterial challenges.

- L1 and L8 stands for standard protein markers
- L2 and L9 stands for control
- L3 and L10 stands for AgNPs stressed earthworm
- L4 and L11 stands for ZnNPs stressed earthworm
- L5 and L12 stands for *B.sputilis* stressed earthworm
- L6 and L13 stands for *P.aeruginosa* stressed earthworm





Vinotha and Biruntha

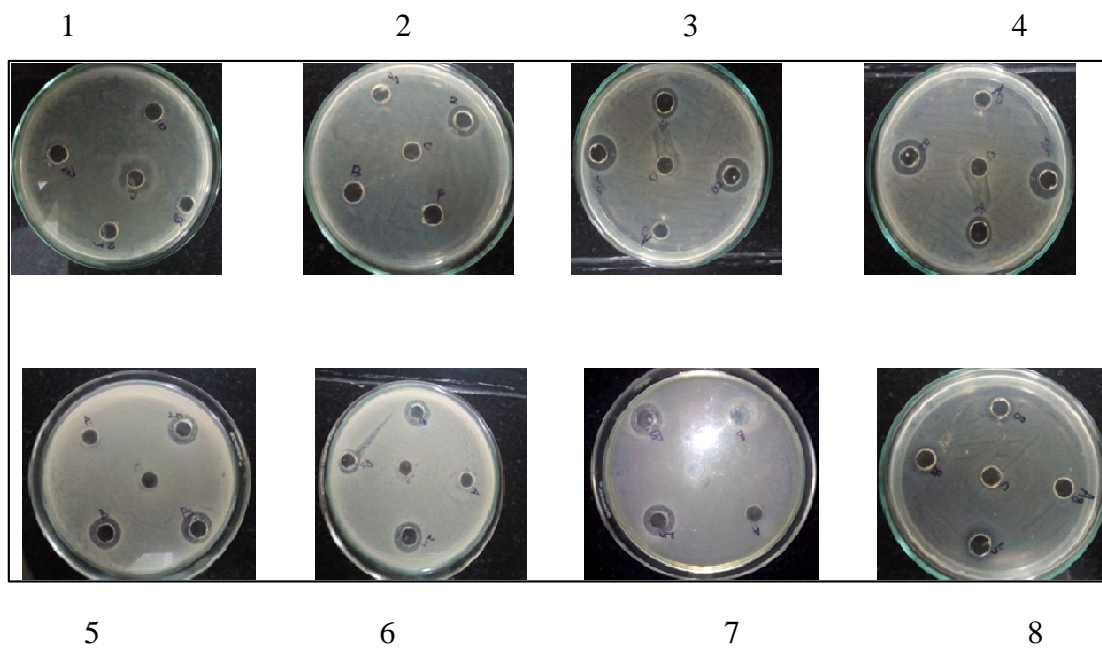


Fig 8.1 and 2: antibacterial activity of coelomic fluid against gram positive bacteria *E.faecalis*
3 and 4: antibacterial activity of coelomic fluid against gram negative bacteria *P.aeruginosa*
5 and 6: antibacterial activity of coelomic fluid against gram negative bacteria *K.pneumonia*
7 and 8: antibacterial activity of coelomic fluid against gram negative bacteria *E.coli*





RESEARCH ARTICLE

Seasonal Variations in the Protein Profile and Characterization of Proteins of the Kidney with Special Reference to Renal Sexual Segment in the Lizard, *Eutropis carinata*.

S.Samson¹, M. Bhagya^{1*}, B.K.Chandrasekhar Sagar² and R. Medini¹

¹Department of Studies in Zoology, Manasagangotri, University of Mysore, Mysuru, 570006, Karnataka, India.

²Department of Neuropathology, Electron Microscopy Laboratory, National Institute of Mental Health and Neuro Sciences (NIMHANS), Bengaluru, 560029, Karnataka, India.

Received: 13 Aug 2017

Revised: 25 Aug 2017

Accepted: 30 Sep 2017

Address for correspondence

Dr. M. Bhagya

Professor in Zoology

Department of Studies in Zoology,

University of Mysore, Manasagangotri,

Mysuru, 570006, Karnataka, India.

Email: bhagya.uomzoology@gmail.com



This is an Open Access Journal / article distributed under the terms of the **Creative Commons Attribution License** (CC BY-NC-ND 3.0) which permits unrestricted use, distribution, and reproduction in any medium, provided the original work is properly cited. All rights reserved.

ABSTRACT

Seasonal variations in the electrophoretic protein profiles of the kidney and the Renal Sexual Segment (RSS) in the lizard, *Eutropis carinata*, were investigated for the first time during successive phases of the annual sexual cycle. The synchronization of weight and total protein content of the kidney with that of RSS cycle is discussed. The sequential change in the protein profile across the reproductive cycle reveals a total of 18 protein bands during post breeding and regressed phases, 20 protein bands during regenerative phase and 22 bands during breeding phase of the reproductive cycle. The addition of two new protein bands during regenerative phase with the molecular weight of 96.5KDa and 45.2KDa persists until the end of the breeding phase and protein with the weight of 45.2KDa reacts positively with PAS. The protein profile of the kidney during breeding season shows the addition of two more new proteins with the molecular weight of 63.4KDa and 34.8KDa. One of these proteins with the molecular weight of 63.4KDa is PAS positive. The activities of the androgen dependent enzymes viz., acid phosphatase, alkaline phosphatase and α -glucosidase that parallels with the seasonal cycle of the RSS is discussed.

Keywords: Renal sexual segment, Protein profile, *Eutropis carinata*.



**Samson et al.**

INTRODUCTION

The kidney of the mature male snakes and lizards (Squamates) has gained reproductive significance due to the presence of an accessory sex structure called Renal Sexual Segment (RSS) (Sever *et al.*, 2012). The RSS is the hypertrophied region of the nephron (kidney tubules) initially described by Gampert (1866) in the grass snake, *Natrix natrix*. However, this hypertrophied portion of the nephron was termed "Segment Sexual" by Regaud and Policard (1903) in the same snake. Since then this seemingly important accessory reproductive structure has been extensively studied in various species of snakes and lizards (Regaud and Policard, 1903; Bons and Saint Girons, 1963; Prasad and Reddy, 1972; Saint Girons, 1972; Fox, 1977; Gabri, 1983; Sarkar and Shivanandappa, 1989; Sever *et al.*, 2002; Krohmer, 2004; Sever *et al.*, 2008; Aldridge *et al.*, 2011; Rheubert *et al.*, 2011). The location of the RSS varies considerably among squamates, it encompasses distal portion of the nephron, collecting ducts and/or portions of ureter (Saint Girons, 1972; Fox, 1977; Sever and Hopkins, 2005; Rheubert *et al.*, 2011). Studies have confirmed that the RSS display varying degrees of hypertrophy and regression that occurs in a cyclic pattern corresponding to different seasons throughout the annual sexual cycle. Also, castration experiments done on snakes and lizards have given solid evidence that the seasonal cycle of RSS is greatly influenced by circulating androgens and testicular activity. Studies carried out on lizards to date have shown that the hypertrophy of RSS occurs only during the periods of sexual activity and during sexual quiescence it becomes indistinguishable from adjacent renal tubules (Forbes, 1941; Kehl, 1944; Volsoe, 1944; Bishop, 1959; Burtner *et al.*, 1965; Fox, 1965; Arvy, 1969; Weil and Aldridge, 1981; Krohmer and Aldridge, 1985; Krohmer *et al.*, 1987; Sarkar and Shivanandappa, 1989; Aldridge, 1993, 2002; Aldridge and Brown, 1995; Van Wyk, 1995; Krohmer, 2004; Rojas *et al.*, 2013; Norris, 2013; Meesook *et al.*, 2016). However, seasonal changes occurring in the RSS of snakes are not as dramatic as in lizards (Volsoe, 1944; Pandha and Thapliyal, 1964; Krohmer and Aldridge, 1985; Krohmer *et al.*, 1987; Clesson *et al.*, 2002; Sever *et al.*, 2002; Krohmer, 2004; Aldridge *et al.*, 2008; Mathies *et al.*, 2010).

The histological characteristic feature of RSS involves the presence of monolayer of columnar epithelium which is secretory in nature and the epithelial cells are heavily loaded with conspicuous secretory granules with basally positioned nuclei (Krohmer *et al.*, 1987; Sarkar and Shivanandappa, 1989; Van Wyk, 1995; Krohmer, 2004; Sever and Hopkins, 2005; Sever *et al.*, 2008; Siegel *et al.*, 2009; Mathies *et al.*, 2010; Sever *et al.*, 2012; Rheubert *et al.*, 2015). The physical nature (cytological appearance) of the secretory granules of the RSS in squamates is well described through ultrastructural studies, although such studies are very limited in number (Furieri and Lanzavecchia, 1959; Del Conte and Tamoya, 1973; Kuhnel and Krisch, 1974; Gabri, 1983; Sever *et al.*, 2002; Krohmer, 2004; Sever and Hopkins 2005; Sever *et al.*, 2008; Siegel *et al.*, 2009; Sever *et al.*, 2012; Rheubert *et al.*, 2011; Rheubert *et al.*, 2015). Our earlier ultrastructural study on the RSS shows the existence of seasonal variations in the formation, maturation and regression of different types of secretory granules accompanied by the dramatic variations in the organelles of the epithelial cells of the RSS that corresponds with the circulating androgens during annual sexual cycle in the lizard, *Eutropis carinata* (data communicated).

Numerous histochemical and biochemical studies have been done in several squamate species to understand the biochemical make up of the secretory granules of the RSS. These studies indicate that the secretory granules of RSS contains mucopolysaccharides, glycogen, neutral glyco- or mucoproteins, neutral carbohydrates, lipids, phospholipids, choline, peptide containing high amount of tyrosine, tryptophan, disulphide residues and acid phosphatase (Bishop, 1959; Deb and Sarkar, 1963; Burtner *et al.*, 1965; Misra *et al.*, 1965; Sanyal and Prasad, 1966; Kuhnel and Krisch, 1974; Weil, 1984; Weil and Aldridge, 1981; Sarkar and Shivanandappa, 1989; Sever and Hopkins, 2005; Sever *et al.*, 2008; Rheubert *et al.*, 2011; Sever *et al.*, 2012; Rojas *et al.*, 2013).

The secretions of the RSS are presumed to have variety of functions, some of the proposed functions include: to provide nutrient medium for spermatozoa and an activating agent in the semen, increasing the viscosity of the seminal fluid (Bishop, 1959; Cuellar, 1966; Prasad and Reddy, 1972; Kuhnel and Krisch, 1974; Sever *et al.*, 2008); the



**Samson et al.**

possibility of forming a vaginal plug, which may prevent sperm leakage from the vagina of the female (Volsoe, 1944; Devine, 1975; Ross and Crews, 1977); to flush the sperm from the sulcus spermaticus of the hemipenis into the vagina (Volsoe, 1944); to induce posterior uterine muscle contraction (Nilson and Andren, 1982); to induce sex pheromone production in the female (Shine *et al.*, 2000) and provide sustenance for mature sperm (Cuellar *et al.*, 1972; Prasad and Reddy, 1972). The direct experimental evidence which suggests that the secretions of the kidney enhance sperm motility is shown in the lizard, *Anolis carolinensis* (Cuellar, 1966) and in the snake, *Crotalus durissus* (Moura *et al.*, 2014). Our earlier study in *Eutropis carinata*, also suggests that the secretions of the RSS enhances epididymal sperm motility (unpublished data). Also, studies have shown that the secretions of the RSS (secretory granules) are transported by the ureter and mixes with the sperms from the ductus deferens during copulation and they are seen along with the sperms in the vagina-uterus of the mated female lizards (Sanyal and Prasad, 1966; Sarkar and Shivanandappa, 1989). However, even after decades of interest and investigation to date, the exact functions of the RSS secretion are still not clearly understood (Siegel *et al.*, 2009). Besides, even though histochemical and biochemical studies on snakes and lizards have shown that the secretions of the RSS constitutes mixture of various biochemical components, the most basic and major biochemical component appears to be proteins, no attempts have been made so far to isolate/characterize proteins that are secreted by the RSS. This is crucial in understanding the precise biological/physiological role of the secretions of the RSS. Therefore, to isolate the protein(s) that are secreted by the RSS, it is essential to generate an electrophoretic protein profile of the kidney. However, such attempts have been made to isolate the proteins of the epididymal luminal fluid of various lizards (although such studies are not done on snakes) since epididymal proteins are vital for spermatozoa to attain physiological maturation during their transit through epididymis (Depeiges and Dacheux, 1985; Depeiges and Dufaure, 1980).

Therefore in the present study, for the first time, the electrophoretic protein profile of the kidney is generated during all the successive phases of the annual sexual cycle in the Indian grass skink, *Eutropis carinata*. The study also reveals the seasonal variations that occur in the weight and total protein content of the kidney, proteins of the kidney that are exclusive to breeding season and their biochemical composition, as well as the activities of certain enzymes that corresponds with the expression of the kidney proteins. Information available on this aspect in squamates of India, including *E. carinata* is very scarce and fragmentary. The present study provides insight on the proteins of the RSS in male squamates, particularly lizards.

MATERIALS AND METHODS

Sexually mature male lizards, *Eutropis carinata* (Asian *Mabuya carinata* is now known as *E. carinata* (Mausfeld *et al.*, 2002)) were collected from woody areas in and around Mysore University Campus that stretches over 739 acres of pristine woody habitat, in Mysuru district, Karnataka, India (12° 18' N latitude, 76° 12' E longitude). The collection of lizards (four lizards per reproductive phase) was carried out during regenerative (Aug-Sep), breeding (Oct-Dec), post breeding/regressive (Jan-Mar) and regressed (Apr-Jul), phases of the reproductive cycle (Sarkar and Shivanandappa, 1989). The protocols followed in handling and sacrifice of animals were approved by Institutional Animal Ethics Committee of University of Mysore and CPCSEA. The lizards were etherized and body weights were recorded. Blood was drawn, cold centrifuged (-4°C) at 4000 g for 10 min and serum was separated and utilized for the enzyme assays. The lizards were sacrificed and kidneys were removed free from connective tissue and blood. The weight of the kidneys was recorded and homogenized with cold phosphate buffer (pH 7.4), cold centrifuged (-4°C) at 8000 g for 10 min and the supernatant was utilized to determine total protein content following Lowry *et al.*, (1951) method, for gel electrophoresis and for enzyme assays.

Gel Electrophoresis

One dimensional electrophoresis was performed in the presence of sodium dodecylsulphate (SDS) in 12.5% (w/v) acrylamide and 0.1% bisacrylamide in Tris-glycine buffer pH 8.3 according to the method of Laemmli (1970). Standard medium range molecular weight marker ranging from 14.3KDa to 97.4KDa (Sigma chemicals, USA) was



**Samson et al.**

loaded into first lane of the gel. Kidney homogenates corresponding to each phase of the reproductive cycle containing 20µg of protein were loaded into subsequent lanes. The electrophoresis was carried out and the gels were stained with Coomassie brilliant blue (CBB-R250) and de-stained using methonal, acitic acid solution. Molecular weight of the protein bands were determined using image lab software.

For two dimensional electrophoresis (2DE), protein samples were precipitated overnight with cold acetone. The precipitate was cold centrifuged at 10,000 g for 15min, pellet recovered was resuspended in lysis buffer. Insoluble components were removed by centrifugation and the protein content was estimated following modified Bradford's method (Ramagli L, 1999). The standard IPG strips (Bio-Rad) with linear pH range 3-11 was actively rehydrated, loaded onto PROTEAN IEF system (Bio-Rad) and focused at 20°C with increasing linear voltage from 1,000- 60,000V for 12 hrs. The strips were equilibrated for 15 min. in 500mM Tris-HCl buffer with pH 8.8. The strips were transferred into 12% SDS-PAGE for electrophoresis, medium range SDS-PAGE standard molecular weight marker ranging from 14.3KDa to 97.4KDa (Sigma chemicals USA) was loaded beside the strip. The electrophoresis was carried out and the gels were stained with Coomassie brilliant blue (CBB-R250) as described by Wang *et al.*, (2012). Molecular weight of the protein spots were determined using PDQuest software.

PAS test

The SDS-PAGE gels that were subjected for PAS test contained BSA in the first lane as positive control, kidney homoginate in the subsequent lanes followed by a lane of Tripsin as negative control. The concentration of 20µg of protein was loaded in all the lanes. PAS staining was performed by a slight modification of the procedure reported by Dubray and Bezard (1982). The gels were soaked in 7.5% (v/v) acetic acid for 30 min. and with 0.2% (w/v) periodic acid and with the Schiff reagent for 1 hr. When the reddish-pink bands of stained glycoprotein gradually begin to appear the gels were rinsed and soaked in 7.5% cold acetic acid, photographed and the gels were subsequently stored in distilled water.

Native PAGE (12.5% gel): The native PAGE was performed following the method of Laemmli (1970), for localization of enzymes, acid phosphatase and alkaline phosphatase. The kidney homogenate was prepared using cold 40% sucrose and loaded into the gel. The electrophoresis was carried out at 4°C. The gels were incubated in the reaction mixture containing 125mg polyvinyl pyrrolidone, 25mg of sodium-1-naphthyl phosphate, fast blue RR salt, 15mg of MgCl₂ MnCl₂ and 50mg of NaCl₂ in 25ml of 0.125M sodium acetate buffer (pH 5.0) for acid phosphatase and 25ml of 0.5M Tris HCl buffer (pH 8.5) for alkaline phosphatase for 2-4 hrs at 37 °C. The gels were rinsed in distilled water and localized protein band was compared against standard protein marker.

Enzyme assay

Phosphatases:The activity of Phosphatases was determined by following the method of Linhardt & Walter (1963). For acid phosphatase, 0.1ml of kidney homogenate and serum was added separately to 0.9ml of reaction mixture containing, 1.25mM of para-Nnitrophenol phosphate (PNP) in 0.05M Citrate buffer (pH 4.0). For Alkaline phosphatase, 0.1ml of kidney homogenate and serum was added separately to 0.9ml of reaction mixture containing, 1.25mM of para-Nnitrophenol phosphate in 0.05M Tris HCl buffer (pH 8.5). The contents were incubated at 37°C for 30 min. The enzyme reaction was arrested by adding 2ml of 0.1N NaOH and the optical density was measured at 405nm. The activity of the enzyme is expressed as µmoles of p-nitrophenol liberated/30min./mg protein.

α-glucosidase:The activity of α-glucosidase (AGH) was determined by a slight modification of the procedure reported by Sawada *et al.*, (1993), in which 0.9ml of the enzyme reaction mixture of 0.05M phosphate buffer (pH 6.8) containing 0.1M NaCl, 1.35mM paranitrophenol α-D-glucopyranoside (PNP-G) was added to 0.1ml of kidney homogenate and serum separately. The contents were incubated at 37°C for 15 min. The enzyme reaction was arrested by adding 2ml of 0.5M Tris solution. The absorbance of PNP released from PNP-G at 400nm was measured



**Samson et al.**

using spectrophotometer. The activity of the enzyme is expressed as μ moles of p-nitrophenol liberated/30min./mg protein.

Statistical analysis

Primary numerical data were analysed using SPSS software version 14.0. Comparison of numerical data and significant correlations were assessed using standard procedures of ANOVA post hoc parametric tests followed by Tukey's test. A probability level of $P \leq 0.05$ was used to determine statistical significance.

RESULTS

Weight and total protein content of the kidney

The mean weight of the kidney/100g body weight during regenerative phase (Aug.-Sep.) were significantly low ($M=293.1\text{mg}$) when compared to breeding phase (Oct.-Dec.), but were significantly greater than post breeding (Jan.-Mar.) and regressed phases (Apr.-Jul). The mean weight of the kidney attained maximum during breeding phase ($M=293.1\text{mg}$), hence it was significantly greater than other three phases of the reproductive cycle. The mean weight of the kidney during post-breeding phase ($M=191.8\text{mg}$) were significantly low when compared to breeding phase but significantly greater than regressed phase. The lowest mean kidney weight were recorded during regressed phase ($M=145.9\text{mg}$) hence it was significantly least when compared to other three phases of the reproductive cycle. On the other hand, the mean total protein content of the kidney during regenerative phase were significantly low ($M=20.6\text{mg/gm}$) when compared to breeding phase, but were significantly greater than post breeding and regressed phases. The mean total protein content of the kidney reached maximum during breeding phase ($M=53.3\text{mg/gm}$), hence it was significantly greater than other three phases of the reproductive cycle. Whereas, the mean total protein content of the kidney during post-breeding ($M=6.4\text{mg/gm}$) and regressed ($M=5.1\text{mg/gm}$) phases were almost equivalent, hence it did not show significant difference between these two season but they were significantly low in comparison with breeding phase (Fig. 1 & 2).

Gel electrophoresis

One dimensional electrophoretic protein profile of the kidney during regenerative phase (Aug.-Sep.) showed a total of 20 protein bands with the molecular weight ranging from 14.3 to 96.5KDa. The protein band with the molecular weight of 96.5KDa is reduced to 95.7KDa during breeding season accompanied by marked reduction in the density of the band (it becomes less prominent during breeding season). However this protein band disappears during post breeding and regressed phases. Another band with the molecular weight of 45.2KDa that appears during regenerative phase persists during breeding phase and disappears during post breeding and regressed phases. Out of 20 protein bands that appear during regenerative phase, 18 were common to other three phases of the reproductive cycle. There is no protein band/s that is unique to regenerative phase. The number of protein bands increased to 22 during breeding phase with the molecular weight ranging from 14.3 to 95.7KDa. Protein bands with the molecular weight of 63.4KDa and 34.8KDa are unique to breeding phase. The number of protein bands decreased to 18 during post breeding and regressed phases with the molecular weight ranging from 14.3 to 87.2KDa. There is no protein band/s that is unique to these phases (Fig. 3 and Table-1).

The kidney protein profile during breeding season were further resolved in two dimensional electrophoresis and differentially expressed protein spots were detected between pI range of 3 to 11 and a mass range of 14.4 KDa to 97KDa. The protein band with a molecular weight of 96.5KDa which reduced to 95.7KDa during breeding season, further resolved into two spots with a molecular weight of 47.1 KDa and 48.6 KDa with the pI 5.06 and 5.15 respectively suggesting that it is a cluster of two protein complex. Whereas, the protein band from the regenerative phase with a molecular weight of 45.2KDa that persisted only during breeding season remained as a single spot.

12763



**Samson et al.**

Also the two proteins that were specific to breeding season with the molecular weight of 63.4KDa and 34.8KDa did not resolve separately in two dimensional electrophoresis but remained as a single spot suggesting that these proteins are solitary (Fig. 4).

PAS test

The electrophoretic kidney protein profile during all the four phases of the reproductive cycle when subjected to PAS test, only a few protein bands that appeared during regenerative and breeding phases showed moderate reaction to PAS, whereas protein bands that appeared during post breeding and regressed phases showed very weak reaction for PAS. However, among the two protein bands that were unique to breeding season (63.4KDa and 34.8KDa), the band with the molecular weight of 63.4KDa showed positive reaction for PAS. Among the two protein bands that were present only during regenerative and breeding phase (95.7KDa and 45.2KDa) the band with the molecular weight of 45.2KDa showed positive reaction for PAS which suggests that these protein bands are glycoproteins (proteins with carbohydrate moiety) (Fig. 5).

Native PAGE: The enzymes, acid and alkaline phosphatases were localized in the kidney homogenate during all the four successive phases of the annual sexual cycle. The molecular weights of these enzymes were 51.7KDa and 26.1KDa respectively. These localised protein bands (enzyme bands) were among the 18 protein bands that were common to all the four successive phases of the annual sexual cycle (Fig.6).

Enzyme assay

The mean activity of acid phosphatase in kidney homogenate and serum during regenerative phase were $M=0.042\mu\text{mol}$ and $M=0.053\mu\text{mol}$ respectively. In comparison with regenerative phase, the mean activity of this enzyme did not show a significant increase during breeding phase though it slightly increased to $M=0.049\mu\text{mol}$ and $M=0.057\mu\text{mol}$ in kidney homogenate and serum respectively. During post breeding phase, the mean activity of this enzyme in kidney homogenate and serum decreases significantly to $M=0.012\mu\text{mol}$ and $M=0.024\mu\text{mol}$ respectively. In comparison with post breeding phase, The activity of acid phosphatase in kidney homogenate and serum did not show a significant increase during regressed phase though it slightly increased to $M=0.019\mu\text{mol}$ and $M=0.030\mu\text{mol}$ respectively (Fig. 7).

The mean activity of alkaline phosphatase in kidney homogenate and serum during regenerative phase were $M=0.022\mu\text{mol}$ and $M=0.029\mu\text{mol}$ respectively. In comparison with regenerative phase, the mean activity of this enzyme did not show a significant increase during breeding phase though it slightly increased to $M=0.031\mu\text{mol}$ and $M=0.035\mu\text{mol}$ in kidney homogenate and serum respectively. During post breeding phase, the mean activity of this enzyme in kidney homogenate and serum decreases significantly to $M=0.011\mu\text{mol}$ and $M=0.019\mu\text{mol}$ respectively. The activity of acid phosphatase in kidney homogenate and serum did not show a significant decrease during regressed phase though it slightly decreased to $M=0.007\mu\text{mol}$ and $M=0.011\mu\text{mol}$ respectively (Fig. 8).

The activity of α -glucosidase in serum and kidney homogenate was significant throughout the reproductive cycle. The mean activity of α -glucosidase in kidney homogenate and serum during regenerative phase ($M=0.026\mu\text{mol}$ and $M=0.033\mu\text{mol}$ respectively) was significantly lower than breeding phase, but significantly higher than post breeding and regressed phases. The peak mean activity of this enzyme in kidney homogenate and serum was recorded during breeding phase ($M=0.046\mu\text{mol}$ and $M=0.053\mu\text{mol}$ respectively) hence it was significantly high compared to all other phases of the reproductive cycle. The mean activity of α -glucosidase in kidney homogenate and serum during post breeding phase ($M=0.003\mu\text{mol}$ and $M=0.004\mu\text{mol}$ respectively) was significantly lower than regenerative and breeding phases but higher than regressed phase. The lowest mean activity of this enzyme in kidney homogenate and serum was recorded during regressed phase ($M=0.001\mu\text{mol}$ in both kidney and serum) hence it was significantly least compared to all other phases of the reproductive cycle (Fig. 9).





Samson et al.

DISCUSSION

In the lizard *E. carinata*, the weight and the total protein content of the kidney exhibit seasonal variations during the annual reproductive cycle. Based on the histological, histochemical and ultrastructural evidences from our previous study (data communicated), a correlation can be assessed between these two parameters that reflect the physiological status of the kidney across reproductive cycle. The ultrastructural and histochemical examinations have shown that, the regenerative phase marks the onset of RSS hypertrophy and the synthesis of secretory granules whose major biochemical composition is proteins (data communicated). This implies rapid protein synthesis and increase in the kidney weight; hence there is a parallel increase in these two parameters during regenerative phase. The hypertrophy of RSS and the synthesis of secretory granules that forms the bulk of the protein content of the kidney culminates during breeding season; hence the weight and the total protein content of the kidney shows a parallel increase during this phase and it is significantly greater than any other phases of the reproductive cycle. The hypertrophy of the RSS gradually reduces during post breeding phase (the cells of the RSS becomes low columnar) and the hypertrophy is lost (the cells of the RSS becomes cuboidal) completely during regressed phase.

This is reflected in the gradual, yet significant reduction in the weight of the kidney during post breeding and regressed phases. In contrast, the total protein content of the kidney falls abruptly during post breeding phase and remains almost the same during regressed phase. This is due to the cessation of the synthesis of secretory granules of the RSS soon after breeding phase; this in turn implies the lack of rapid protein synthesis which results in the significant decrease in the protein content of the kidney during post breeding and regressed phases. Thus, it is evident that the weight and the total protein content of the kidney rests on the cycles of the RSS. Besides, studies have shown that the weight of the reproductive organs among snakes and lizards increase significantly during peak breeding season and opposite is true during peak non breeding season. A study on the snake *Trimeresurus s. stejnegeri* (Chinese green tree viper) shows that, the mass of the kidney is concomitant with RSS hypertrophy and also mating activities (Tein-Shun Tsai and Ming- Chung Tu, 2000). Studies among female lizards, *Calotes versicolor* and *Psammophilus dorsalis* have shown that, the secretory activity of RSS coincides with the increase in the weight of the kidney, though RSS is poorly developed unlike in the males (Sarkar and Shivanandappa, 1989). However, the study does not assess the protein content of the kidney.

The electrophoretically generated kidney protein profile during all the successive phases of reproductive cycle in the lizard, *E. carinata* has revealed that, number of protein bands remain same during post breeding and regressed phase, which suggest the lack of protein synthesis during these phases. However, the addition of two new protein bands with a molecular weight of 96.5KDa and 45.2KDa during regenerative phase suggests that these proteins are synthesised during this phase, but it is not unique to regenerative phase since it is also present during breeding phase. Further addition of two new protein bands that are unique to breeding phase with a molecular weight of 63.4KDa and 34.8KDa suggests rapid protein synthesis during this phase. Since the synthesis of the two proteins that are confined to regenerative and breeding phase and two other proteins that are unique to breeding phase, synchronizes with the hypertrophy and secretory activity of the RSS, it is more likely that these proteins are the product of RSS secretions. The two dimensional electrophoretic characterization has revealed that, the protein band with a molecular weight of 96.5KDa that appeared during regenerative phase, is a protein complex made up of two protein conjugates with a molecular weight of 47.1KDa and 48.6KDa possessing different isoelectric points (pI). Attempts have been made to isolate the proteins secreted by the epididymis among mammals and lizards to elucidate their biochemical and functional significance (Bedford, 1975; Toshimori, 2003; Dacheux et al., 1989, 1998, 2003; Jones, 1998; Nirmal and Rai, 2000; Aranha et al., 2006). Depeiges and Dufaure (1980) fractionated conspicuous secretory granules of epididymis in the lizard, *Lacerta vivipara* through one dimensional electrophoretic characterization. Their study revealed that the core of the secretory granule constitutes a major protein with molecular weight of 70KDa. In another study on the same lizard, Depeiges et al., (1987) during reproductive period through the electrophoretic protein profile of the epididymal luminal fluid revealed a solitary protein that is



**Samson et al.**

extremely androgen sensitive with the molecular weight of 19KDa which is designated as 'L' protein. This protein seems to have greater physiological significance since its expression is concomitant with the acquisition of maximum motility of spermatozoa in the epididymis. However, such studies have not been reported so far for reptilian kidney. Kidney protein profile subjected to test for PAS suggests that most of the proteins irrespective of any phase of reproductive cycle possess carbohydrate moiety even though they show faint reaction with PAS. However, among the two proteins that appeared during both regenerative and breeding phases, one of the proteins showed positive reaction with PAS and the other did not. Similarly, among the two proteins that were unique to breeding phase, only one of the protein reacted with PAS. This suggests that the secretory product of the RSS differs in their staining properties because they differ in their biochemical make up (histochemical examination of the RSS secretory granules in our previous study has revealed that the secretory granules react moderately with PAS but doesn't react with Alcian blue which suggests the lack of glycosaminoglycans). The selective reaction of protein bands with PAS shows that, not all secretory products (secretory granules) of the RSS are glycoproteins, which in turn proves that secretory products of RSS are more than one type. This strongly corroborates our previous finding which has revealed the presence of three different types of secretory granules in the RSS of the lizard, *E. carinata* (data communicated).

The present study provides the first report on the protein profile of the kidney, its seasonal variations throughout the sexual cycle and one of its biochemical compositions. Such findings are not reported in any of the squamates studied thus far. Studies on lizards through histochemical localization have shown that the enzymes acid and alkaline phosphatases are the major constituents of the kidney tubules. Deb and Sarkar (1962) showed that the RSS of the lizard, *Calotes versicolor* showed negligible amount of the enzyme alkaline phosphatase whereas acid phosphatase was markedly high in RSS than in other tubules of the kidney. Their study also showed that, just before the hibernation when the RSS is not fully atrophied, the fall in the concentration of acid phosphatase occurs. Prasad and Reddy (1972) showed that in the lizard, *Hemidactylus flaviviridis* the secretory granules of the RSS react positively for acid phosphatase and negatively for alkaline phosphatase. In the lizard *M. carinata* it is shown that the activity of acid phosphatase is much higher in sexual segment than in other tissues of the lizard and its activity disappears along with secretory granules after breeding season. It is also shown that castration abolishes the activity of acid phosphatase and upon testosterone administration the enzyme activity is replenished (Sarkar and Shivanandappa, 1989). Though the enzymes acid and alkaline phosphatase are androgen dependent, their activities have to be assessed in both kidney and serum throughout the sexual cycle to know if these enzymes serve as indices for the secretory activity of the RSS. Thus, in the present study it is shown that there is a significant increase in the activity of the enzyme acid phosphatase in serum and kidney during regenerative phase and the activity peaks during breeding phase suggesting that the activity of this enzyme is concomitant with that of secretory activity of RSS during these two phases. However, the activity of this enzyme does not cease, but only reduces markedly in serum and kidney during post breeding phase and the activity begins to increase slightly during regressed phase. This suggests that the abolition of the secretory granules (secretory activity) of the RSS after breeding phase doesn't abolish the activity of acid phosphatase. Thus the activity of acid phosphatase is not completely parallel to RSS hypertrophy and its secretory activity.

The activity of alkaline phosphatase, in serum and kidney during regenerative phase and breeding phase is also concomitant with that of the secretory activity of RSS during these two phases. However, a gradual, yet significant decrease in the activity of this enzyme occurs during post breeding and regressed phases which are in parallel with the regression of the RSS and abolition of its secretory activity. Thus the peak activity of alkaline phosphatase reflects the peak secretory activity of the RSS and the lowest activity of alkaline phosphatase reflects abolition of RSS. Hence, this enzyme serves as an index for the secretory activity of the RSS. The localization of the enzymes acid and alkaline phosphatase in the native gel revealed the molecular weight of these enzymes (proteins) that are common throughout the sexual cycle. Thus, the activity of these enzymes are not only specific to RSS but to the other kidney tubules.



**Samson et al.**

Cuellar *et al.*, (1972) has shown the evidence for sperm sustenance by secretions of the RSS in the lizard, *Anolis carolinensis*. Their study revealed that the kidney homogenate of breeding season significantly increases sperm motility. Similarly, crude extracts of the RSS of the snake, *Crotalus durissus* on bovine (dog) semen showed a significant increase in sperm total motility (Moura *et al.*, 2014). It is also shown that, the kidney homogenate during breeding season enhances sperm motility in the lizard, *E. carinata* (unpublished data). However, the actual component of the kidney that induced sperm motility in reptiles is not known. In the present study for the first time the activity of α -glucosidase is assessed throughout the reproductive cycle in the kidney and serum in *E. carinata*, since this enzyme is well known to cause sperm motility (Fourie *et al.*, 1991; Loko *et al.*, 1997; Xu *et al.*, 2006; Ponzio *et al.*, 2011). Interestingly, the activity of this enzyme is markedly high during regenerative and breeding phases and extremely negligible during postbreeding and regressed phases. Since its activity synchronizes precisely with the production of secretory granules of the RSS, this enzyme is the more likely candidate that induces sperm motility. RSS being one of the most important male accessory reproductive structures, like epididymis and vas deferens, exhibit seasonal variations and secrete products required for reproduction. The physiological importance of the new proteins secreted during regenerative phase and also proteins unique to breeding season as revealed in the present study has to be elucidated. Since this is the first study on the characterization of reptilian kidney proteins, such studies have to be carried out in other squamates to understand the exact role of the secretions of the RSS in reproduction as RSS in reptiles are regarded similar to prostate gland of mammals (Prasad and Reddy, 1972).

ACKNOWLEDGEMENTS

The authors wish to thank University Grants Commission for financial assistance (No. 40-367/2011).

REFERENCES

1. Aldridge, RD., Brown, WS. 1995. Male reproductive cycle, age at maturity, and cost of reproduction in the timber rattle snake (*Crotalus horridus*). *Journal of Herpetology*. 29: 399-407.
2. Aldridge, RD., Jellen, BC., Allender, MC., Dreslik, MJ., Shepard, DB., Cox, JM., and Phillips, CA. 2008. Reproductive biology of the Massasauga (*Sistrurus catenatus*) from South-central Illinois. *Biology of the Rattlesnake*: 403-412.
3. Aldridge, RD., Jellen, BC., Siegel, DS., and Wisniewski, SS. 2011. The sexual segment of the kidney. In: Aldridge RD, Sever DM, editors. *Reproductive Biology and Phylogeny of Snakes*, vol. 9. Boca Raton: Science publishers CRC press: 477-509.
4. Aldridge, RD. 2002. The link between mating season and male reproductive anatomy in the rattle snakes *Crotalus viridis oregonus* and *Crotalus viridis helleri*. *Journal of Herpetology*. 36: 295-300.
5. Aldridge, RD., 1993. Male reproductive anatomy and seasonal occurrence of mating and combat behavior of the rattlesnake *Crotalus v. viridis*. *Journal of Herpetology*, 27(4): 481-484.
6. Aranha, I., Bhagya, M., Yejurvedi, HN. 2006. Ultrastructural study of the epididymis and the vas deferens and electrophoretic profile of their luminal fluid proteins in the lizard *Mabuya carinata*. *Journal of submicroscopic cytology and pathology*. 38(1): 37-43.
7. Arvy, L. 1969. Contribution à l'étude du rein des Reptiles: données histoenzymologiques sur le rein des Colubridés. *Cells Tissues Organs*. 73: 27-39.
8. Bedford, JM., 1975. Maturation transport and fate of spermatozoa in the epididymis.
9. Bishop, KE. 1959. A histological and histochemical study of the kidney tubule of the common garter snake *Thamnophis sirtalis* with special reference to the renal segment in the male. *Journal of Morphology*. 104: 307-358.
10. Bons, J., and Saint Girons, H. 1963. Ecologie et cycle sexuel des amphisbeniens du Maroc. *Bulletin de la Société des Sciences Naturelles et Physiques du Maroc* 43: 117-158.
11. Burtner, HJ., Floyd, AD., and Longley, JB. 1965. Histochemistry of the "sexual segment" granules of the male rattlesnake kidney. *Journal of Morphology*. 116: 189-195.





Samson et al.

12. Clesson, D., Bautista, A., Baleckaitis, DD., and Krohmer, RW. 2002. Reproductive biology of male eastern garter snakes (*Thamnophis sirtalis sirtalis*) from a denning population in central Wisconsin. The American midland naturalist. 147: 376-386.
13. Cuellar, O. 1966. Oviductal anatomy and sperm storage structures in lizards. Journal of Morphology. 119: 7-19.
14. Cuellar, HS., Roth, JJ., Fawcett, JD., and Jones, RE. 1972. Evidence for sperm sustenance by secretions of the renal sexual segment of male lizards. *Anolis carolinensis*. Herpetologica: 53-57.
15. Dacheux, JL., Dacheux, F. and Paquignon, M. 1989. Changes in sperm surface membrane and luminal protein fluid content during epididymal transit in the boar. Biology of reproduction, 40(3): 635-651.
16. Dacheux, JL., Druart, X., Fouchecourt, S., Syntin, P., Gatti, JL., Okamura, N. and Dacheux, F. 1998. Role of epididymal secretory proteins in sperm maturation with particular reference to the boar. Journal of Reproduction and Fertility-Supplement-, 99-107.
17. Dacheux, JL., Gatti, JL. and Dacheux, F. 2003. Contribution of epididymal secretory proteins for spermatozoa maturation. Microscopy research and technique. 61(1): 7-17.
18. Deb, C., and Sarkar, C. 1963. Histochemistry of renal sex segment in the garden lizard, *Calotes versicolor*. Proceedings of the National Institute of Sciences of India. 29: 197-202.
19. Del Conte, E., and Tamayo, JG., 1973. Ultrastructure of the RSS of the kidneys in male and female lizards, *Cnemidophorus l. lemniscatus* (L.). Zeitschrift für Zellforschung und mikroskopische Anatomie. 144: 325-327.
20. Depeiges, A., and Dacheux, J.L. 1985. Acquisition of sperm motility and its maintenance during storage in the lizard, *Lacerta vivipara*. Journal of reproduction and fertility, 74(1): 23-27.
21. Depeiges, A., and Dufaure, J.P. 1980. Major proteins secreted by the epididymis of *Lacerta vivipara*: Isolation and characterization by electrophoresis of the central core. Biochimica et Biophysica Acta (BBA)-General Subjects, 628: 109-115.
22. Depeiges, A., Force, A., and Dufaure, J.P., 1987. Production and glycosylation of sperm constitutive proteins in the lizard *Lacerta vivipara*. Evolution during the reproductive period. Comparative Biochemistry and Physiology Part B: Comparative Biochemistry, 86(2): 233-240.
23. Devine, MC. 1975. Copulatory plugs in snakes: enforced chastity. Science 187: 844-845.
24. Dubray, G., and Bezar, G. 1982. A highly sensitive periodic acid-silver stain for 1, 2-diol groups of glycoproteins and polysaccharides in polyacrylamide gels. Analytical biochemistry. 119(2): 325-329.
25. Forbes, TR. 1941. Observations on the urogenital anatomy of the adult male lizard, *Sceloporus*, and on the action of implanted pellets of testosterone and of estrone. Journal of Morphology. 68: 31-69.
26. Fourie, M.H., Toit, D.D., Bornman, M.S., Van Der Merwe, M.P. and Du Plessis, D.J., 1991. α -Glucosidase, sperm ATP concentrations, and epididymal function. Archives of andrology, 26(3): 139-141.
27. Fox, H. 1977. The urinogenital system of reptiles. In: Gans C, Parsons TS, editors. Biology of the Reptilia, vol. 6. Morphology E. New York: Academic Press: 1-157.
28. Fox, W. 1965. A comparison of the male urogenital systems of blind snakes, Leptotyphlopidae and Typhlopidae. Herpetologica 21: 241-256.
29. Furieri, P., and Lanzavecchia, G. 1959. Le secrezione dell' epididimo e del renesessualeirettili. Studio al microscopioelettronico. Arch. Ital. Anat. Embriol 64: 357-379.
30. Gabri, MS. 1983. Seasonal changes in the ultrastructure of the kidney collecting tubules in the lizard *Podarcis taurica*. Journal of Morphology. 175: 143-151.
31. Gampert, O. 1866. Über die Niere von *Tropidonotus natrix* und der Cyprinoiden. Zeit. Wissen. Zool. 16: 369-373.
32. Jones, RC. 2002. Evolution of the vertebrate epididymis. In The Epididymis: From Molecules to Clinical Practice, Springer US. : 11-33
33. Kehl, R. 1944. Etude de quelques problèmes d' endocrinologie genitale chez certaine reptiles du Sud Algerien. Revue Canadienne De Biologie. 3: 131-219.
34. Krohmer, RW., and Aldridge, RD. 1985. Male reproductive cycle of the lined snake (*Tropidoion lineatum*). Herpetologica. 41: 33-38.
35. Krohmer, RW., Grassman, M., and Crews, D. 1987. Annual reproductive cycle in the male red-sided garter snake, *Thamnophis sirtalis parietalis*: field and laboratory studies. General and comparative endocrinology. 68: 64-75.





Samson et al.

36. Krohmer, RW. 2004. Variation in seasonal ultrastructure of sexual granules in the renal sexual segment of the northern water snake, *Nerodia sipedon sipedon*. Journal of Morphology. 261: 70–80.
37. Kuhnel, W., and Krisch, B. 1974. On the RSS of the kidney in the snake (*Natrix natrix*). Cell and Tissue Research. 148: 412–429.
38. Laemmli, UK., 1970. Cleavage of structural proteins during the assembly of the head of bacteriophage T4. Nature, 227(5259): 680-685.
39. Linhardt, K., and Walter, K. 1963. Phosphatase. Methods of Enzymatic Analysis. (Ed. Bergmeyer HU). Academic Press, New York : 799.
40. Loko, F., Alihonou, E., Goufodji, B., Fagla, B. and Hounton, M., 1997. Neutral alpha-glucosidase, a specific marker for epididymal secretion in seminal pathology. Contraception, fertillite, sexualite, 25(12): 939-941.
41. Lowry, OH., Rosebrough, NJ., Farr, AL., and Randall, RJ. 1951. Protein measurement with the Folin phenol reagent. Journal of biological chemistry. 193(1): 265-275.
42. Mathies, T., Cruz, JA., Lance, VA., Savidge, JA., 2010. Reproductive biology of male brown tree snakes (*Boiga irregularis*) on Guam. Journal of Herpetology. 44: 209-221.
43. Mausfeld, P., Schmitz, A., Bohme, W., Misof, B., Vrcibradic, D., and Rocha, CF. 2002. Phylogenetic affinities of *Mabuya atlantica* Schmidt, 1945, endemic to the Atlantic Ocean archipelago of Fernando de Noronha (Brazil): Necessity of partitioning the genus *Mabuya* Fitzinger, 1826 (Scincidae: Lygosominae). Zoologischer Anzeiger-A Journal of comparative zoology. 241: 281-93.
44. Meesook, W., Artchawakom, T., Aowphol, A., and Tumkiratiwong, P. 2016. Reproductive pattern and sex hormones of *Calotes emma* Gray 1845 and *Calotes versicolor* Daudin 1802 (Squamata; Agamidae). Turkish Journal of Zoology. 40: 1508-53.
45. Misra, UK., Sanyal, MK., and Prasad, MRN., 1965. Phospholipids of the sexual segment of the kidney of the Indian house lizard, *Hemidactylus flaviviridis* (Ruppell). Life Science 4: 159–166.
46. Moura, CS., Silva, CC., Silva, SV., Cordeiro, E., Silva, B., Bezerra, RS., and Guerr, MMP. 2014. Activity of crude extract of the sexual renal segment from *C. Rotalus durissus* on spermatic kinematics of thawed dog semen. BioMed Central. Vol. 8 (4): 150.
47. Nilson, G., and Andrén, C., 1982. Function of renal sex secretion and male hierarchy in the adder, *Vipera berus*, during reproduction. Hormones and Behavior. 16: 404-413.
48. Nirmal, BK., and Rai, U., 2000. Epididymal protein secretion and its androgenic control in wall lizards *Hemidactylus flaviviridis* (Ruppell).
49. Norris, DO., 2013. Comparative aspects of vertebrate reproduction In: David O. Norris and James A. Carr, editors. Vertebrate Endocrinology, vol. 5. Tokyo, Japan: Elsevier Academic Press: 416-423
50. Pandha, SK., and Thapliyal, JP. 1964. Effect of male hormone on the renal sex segment of castrated males of the lizard *Calotes versicolor*. Copeia 1964: 579-581.
51. Prasad, MRN., and Reddy, PRK., 1972. Physiology of the sexual segment of the kidney in reptiles. General and Comparative Endocrinology. 3: 649-662.
52. Ponzio, M.F., Roussy-Otero, G.N., Ruiz, R.D. and de Cuneo, M.F., 2011. Seminal quality and neutral alpha-glucosidase activity after sequential electroejaculation of chinchilla (*Ch. lanigera*). *Animal reproduction science*, 126(3): 229-233.
53. Ramagli, L S., 1999. Quantifying protein in 2-D PAGE solubilization buffers. 2-D Proteome analysis protocols. : 99-103.
54. Regaud C, Policard A. 1903. Recherchessur la structure du rein de quelquesophidiens. Archives d' Anatomie Microscopique. 6: 191–282.
55. Rheubert, JL., Murray, CM., Siegel, DS., Babin, J., and Sever, DM., 2011. The sexual segment of *Hemidactylus turcicus* and the evolution of sexual segment location in Squamata. Journal of Morphology. 272: 802–813.
56. Rheubert, Sever, Siegel, and Trauth. 2015. Male reproductive anatomy: the gonadoducts, sexual segment of the kidney, and cloaca. In Reproductive Biology and Phylogeny of Lizards and Tuatara (eds. JL Rheubert, DS Siegel, and SE Trauth). Pp 253-301. CRC Press.





Samson et al.

57. Rojas, CA., Barros, VA., and Almeida Santos, SM., 2013. The reproductive cycle of the male sleep snake *Sibynomorphus mikanii* (Schlegel, 1837) from southeastern Brazil. *Journal of morphology*. 274: 215-228.
58. Ross, P., and Crews, D., 1977. Influence of the seminal plug on mating behaviour in the garter snake. *Nature*: 344-345.
59. Saint Girons, H., 1972. Morphologiecomparee du segment sexuel du rein des squamates (Reptilia). *Archives d'Anatomie Microscopique et de Morphologie Experimentale*. 61: 243-266.
60. Sanyal, MK., and Prasad, MRN., 1966. Sexual segment of the kidney of the Indian house lizard, *Hemidactylus flaviviridis* (Ruppell). *Journal of Morphology*. 118: 511-527.
61. Sarkar, HBD., Shivanandappa, T., 1989. Reproductive cycles of reptiles. In: Saidapur S.K., editors. *Reproductive Cycles of Indian Vertebrates*. Bombay: Allied Publishers: 225-272.
62. Sawada, Y., Tsuno, T., Ueki, T., Yamamoto, H., Fukagawa, Y., and Oki, T., 1993. Pradimicine q, a new pradimicine aglycon, with α -glucosidase inhibitory activity. *Journal of Antibiotics*. 46: 507-510.
63. Sever DM., and Hopkins, WA. 2005. Renal sexual segment of the ground skink, *Scincella laterale* (Reptilia, Squamata, Scincidae). *Journal of Morphology*. 266: 46-59.
64. Sever, DM., Rheubert, JL., Gautreaux, J., Hill, TG., and Freeborn, LR. 2012. Observations on the sexual segment of the kidney of snakes with emphasis on ultrastructure in the yellow bellied sea snake, *Pelamis platurus*. *Journal of Anatomical Record*. 295: 872-882.
65. Sever, DM., Ryan, TJ., Stephens, R., and Hamlett, WC. 2002. Ultrastructure of the reproductive system of the black swamp snake (*Seminatrix pygaea*). III. Sexual segment of the male kidney. *Journal of Morphology*. 252: 238-254.
66. Sever, D.M., Siegel, D.S., Bagwill, A., Eckstut, M.E., Alexander, L., Camus, A., and Morgan, C., 2008. Renal sexual segment of the cottonmouth snake, *Agkistrodon piscivorus* (Reptilia, Squamata, Viperidae). *Journal of Morphology*. 269(6): 640-653.
67. Shine, R., Olsson, MM., and Mason, RT., 2000. Chastity belts in garter snakes: the functional significance of mating plugs. *Biological Journal of the Linnean Society*. 70: 377-390.
68. Siegel, DS., Aldridge, RD., Clark, CS., Poldemann, EH., and Gribbins, KM. 2009. Stress and reproduction in *Boiga irregularis* with notes on the ultrastructure of the sexual segment of the kidney in squamates. *Canadian Journal of Zoology*. 87: 1138-1149.
69. Toshimori, K., and Ito, C. 2003. Formation and organization of the mammalian sperm head. *Archives of histology and cytology*. 66(5): 383-396.
70. Tsai, T.S., and Tu, M.C. 2000. Reproductive cycle of male Chinese green tree vipers, *Trimeresurus s. stejnegeri*, in northern Taiwan. *Journal of Herpetology*: 424-430.
71. Van Wyk, JH., 1995. The male reproductive cycle of the lizard, *Cordylus giganteus* (Sauria: Cordylidae). *Journal of Herpetology*: 522-535.
72. Volsoe H., 1944. Structure and Seasonal Variation of the Male Reproductive Organs of *Vipera Berus (L.) spolia*. *Zoologica. Musei. Hauniess*. 5: 1-157.
73. Wang, QH., Kalantar-Zadeh, K., Kis, A., Coleman, JN., and Strano, MS. 2012. Electronics and optoelectronics of two-dimensional transition metal dichalcogenides. *Nature nanotechnology*. 7(11): 699-712.
74. Weil. MR., and Aldridge, RD. 1981. Seasonal androgenesis in the male water snake *Nerodia sipedon*. *General and comparative endocrinology*. 44: 44-53.
75. Weil, MR., 1984. Seasonal histochemistry of the RSS in male common water snakes, *Nerodia sipedon (L.)*. *Canadian Journal of Zoology*. 62: 1737-1740.
76. Xu, H.R., Lu, J.C., Chen, F., Huang, Y.F., Yao, B. and Lu, N.Q., 2006. The effect of chymotrypsin on the determination of total alpha-glucosidase activity in seminal plasma and the correlation between alpha-glucosidase level and semen parameters. *Archives of andrology*, 52(6):441-446





Samson et al.

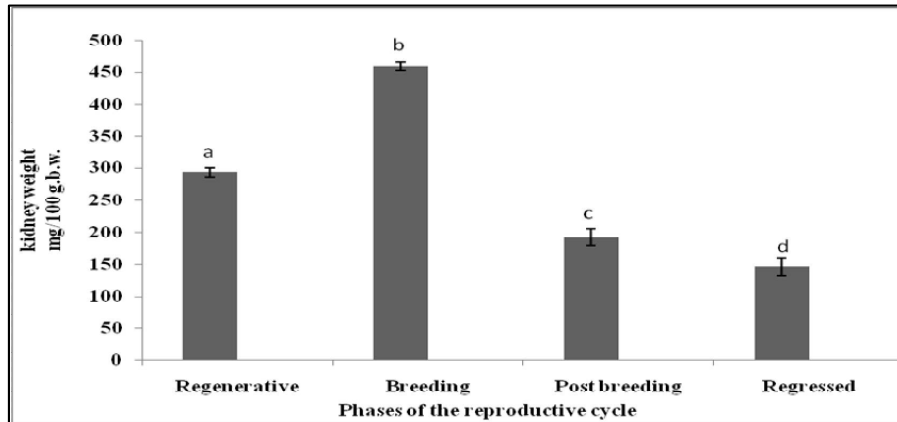


Fig. 1: Weight of the kidney during successive phases of the reproductive cycle in the lizard, *Eutropis carinata*.

Note: Values with same superscript letters are not significantly different, whereas those with different superscript letters are significantly ($P < 0.05$) different as judged by ANOVA Post hoc parametric test followed by Tukey's test.

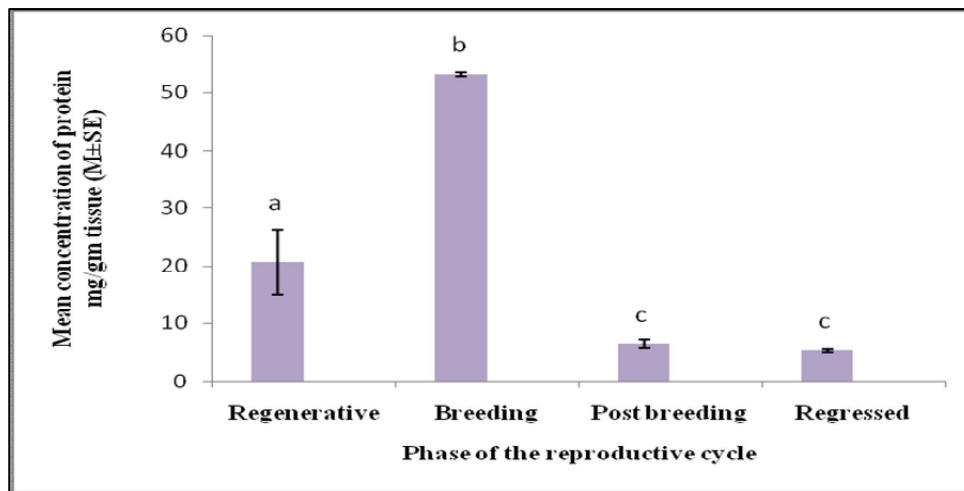


Fig. 2: Mean protein concentration of the kidney during successive phases of the reproductive cycle in the lizard, *Eutropis carinata*.

Note: Values with same superscript letters are not significantly different, whereas those with different superscript letters are significantly ($P < 0.05$) different as judged by ANOVA Post hoc parametric test followed by Tukey's test.





Samson et al.

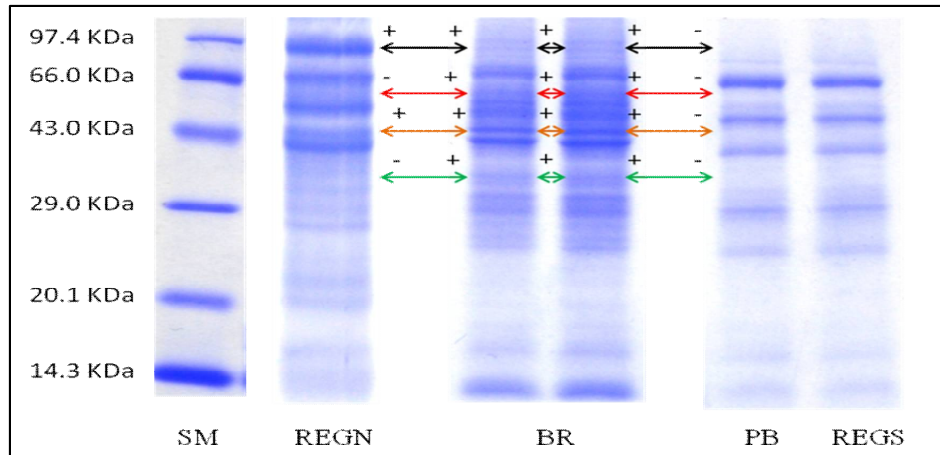


Fig.3: Electrophoretic protein profile of the kidney in the lizard, *Eutropis carinata* during successive phases of the reproductive cycle.

Note: Arrows indicate the position of the bands, '+' sign on the arrow heads indicate presence of the band, '-' sign on the arrow head indicates absence of the band and different colour of the arrows indicates different molecular weights of the band. Black arrow- 96.5KDa (weight is reduced to 95.7KDa during breeding phase. Present during regenerative and breeding phase) , Red arrow- 63.4KDa (unique to breeding phase), Orange arrow- 45.2KDa (Present during regenerative and breeding phase)

Green arrow-34.8KDa (unique to breeding phase), SM= standard marker; REGN= regenerative phase; BR= breeding phase; PB= post breeding phase; REGS= regressed phase.

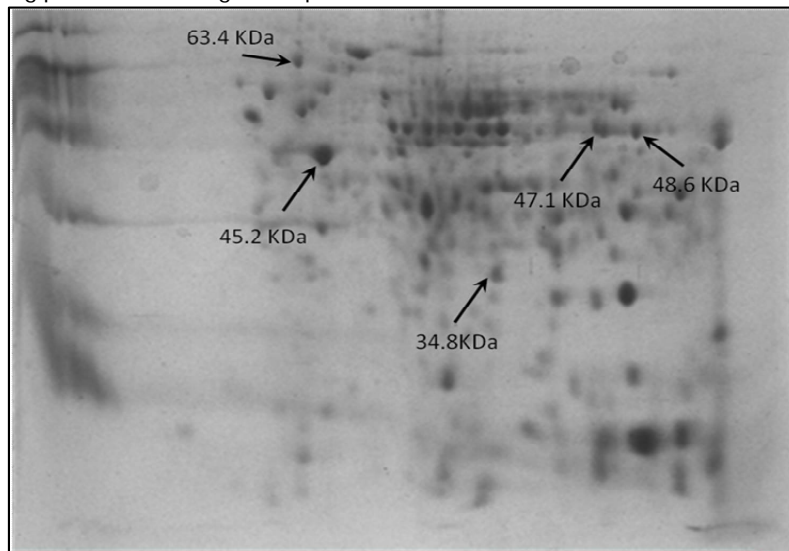


Fig.4:Two dimensional electrophoretic protein profile of the kidney in the lizard, *Eutropis carinata* during breeding phases of the reproductive cycle. Arrows shows protein spots that are unique to breeding phase and protein spots that are that are common to both regenerative and breeding phases.

Note: Protein spots 63.4KDa and 34.8KDa are unique to breeding phase; protein spots 45.2KDa are common to both regenerative and breeding phases and protein spots 47.1KDa and 48.6KDa corresponds to single protein that appeared in regenerative phase with the molecular weight of 96.5KDa.





Samson et al.

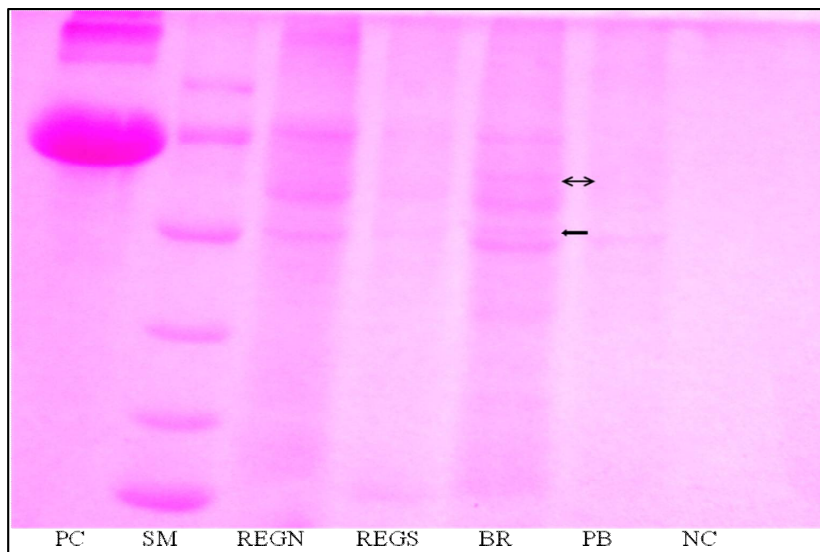


Fig.5: Electrophoretic profile of the kidney proteins of the lizard, *Eutropis carinata* during successive phases of the reproductive cycle subjected to PAS test for glycoproteins.

Note: Double headed arrow indicates protein with molecular weight of 63.4KDa and single head arrow, 45.2KDa. PC= positive control (BSA); SM= standard marker; REGN= regenerative phase; REGS= regressed phase; BR= breeding phase; PB= post breeding phase; NC= negative control (Tripsin).

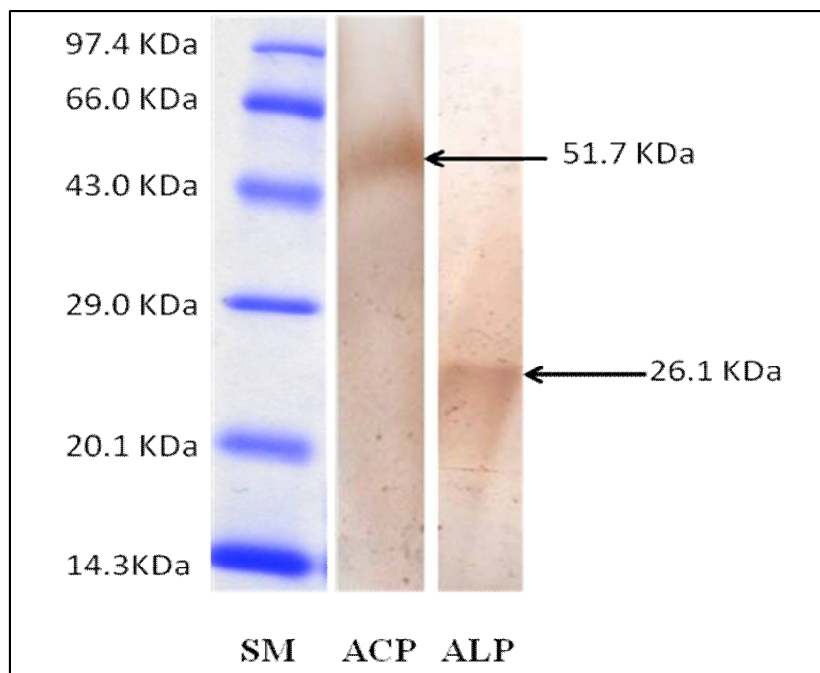


Fig.6: Localization of enzymes in the kidney proteins of the lizard, *Eutropis carinata*.

Arrows bearing molecular weights points towards the localized enzyme. SM=standard marker; ACP= acid phosphatase; ALP= alkaline phosphatase.





Samson et al.

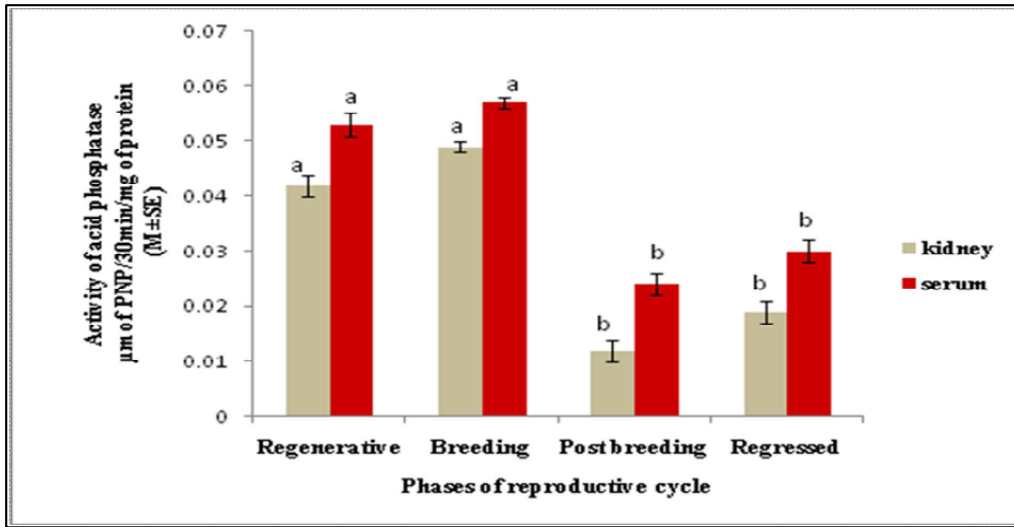


Fig.7: The activity of acid phosphatase in the kidney and serum of the lizard, *Eutropis carinata* during successive phases of the reproductive cycle.

Note: Values with same superscript letters are not significantly different, whereas those with different superscript letters are significantly ($P < 0.05$) different as judged by ANOVA Post hoc parametric test followed by Tukey's test.

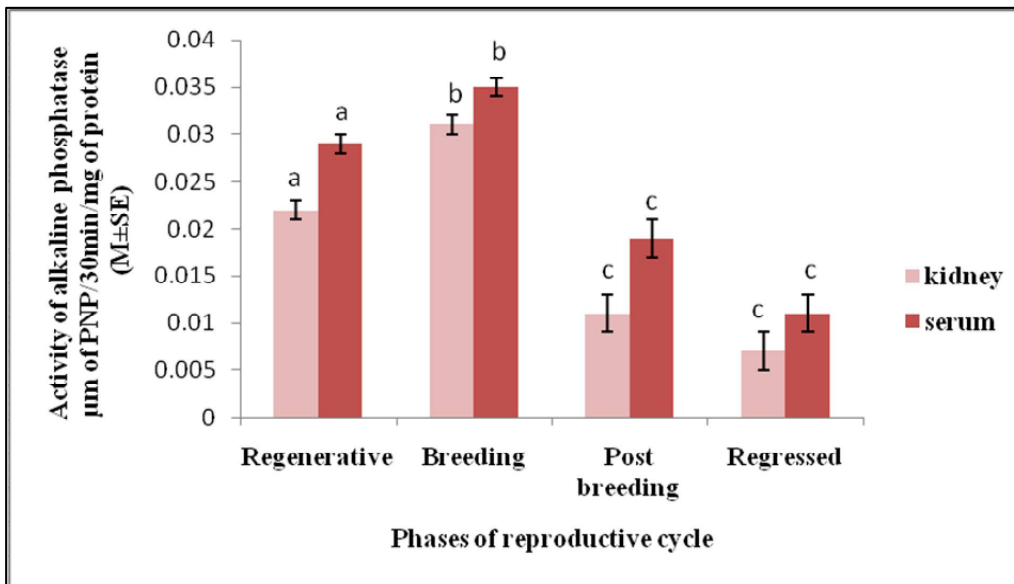


Fig.8: The activity of alkaline phosphatase in the kidney and serum of the lizard, *Eutropis carinata* during successive phases of the reproductive cycle.

Note: Values with same superscript letters are not significantly different, whereas those with different superscript letters are significantly ($P < 0.05$) different as judged by ANOVA Post hoc parametric test followed by Tukey's test.





Samson et al.

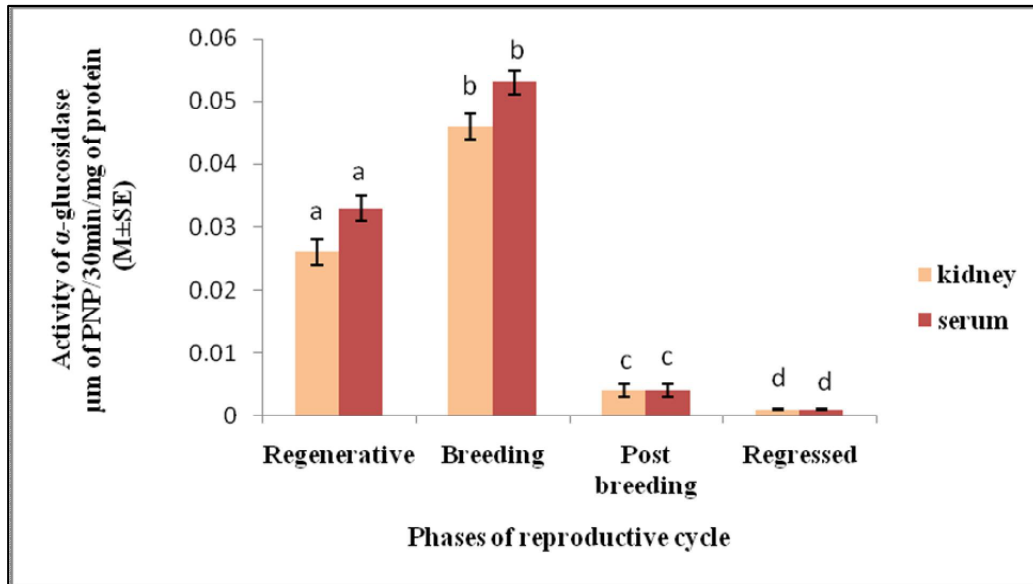


Fig.9: The activity of α -glucosidase in the kidney and serum of the lizard, *Eutropis carinata* during successive phases of the reproductive cycle.

Note: Values with same superscript letters are not significantly different, whereas those with different superscript letters are significantly ($P < 0.05$) different as judged by ANOVA Post hoc parametric test followed by Tukey's test.





Samson et al.

Table-1. Molecular weight of each protein in the kidney protein profile during Successive phases of the reproductive cycle in the lizard, *Eutropis carinata*.

SI. No.	Standard marker	Regenerative phase	Breeding phase	Post-breeding phase	Regressed phase
1.	97.4	<u>96.5</u>	<u>95.7</u>	-	-
2.	-	87.2	87.2	87.2	87.2
3.	-	71.3	71.3	71.3	71.3
4.	66.0	66.0	66.0	66.0	66.0
5.	-	-	<u>63.4</u>	-	-
6.	-	60.7	60.7	60.7	60.7
7.	-	59.3	59.3	59.3	59.3
8.	-	56.2	56.2	56.2	56.1
9.	-	<u>51.5</u>	<u>51.7</u>	<u>51.7</u>	<u>51.5</u>
10.	-	<u>45.2</u>	<u>45.2</u>	-	-
11.	43.0	43.0	43.0	43.0	43.2
12.	-	37.1	37.1	37.1	37.2
13.	-	-	<u>34.8</u>	-	-
14.	-	31.3	31.3	31.3	31.3
15.	29.0	29.0	29.0	29.0	29.0
16.	-	<u>26.1</u>	<u>26.1</u>	<u>26.1</u>	<u>26.1</u>
17.	-	24.8	24.8	-	-
18.	-	23.2	23.2	23.2	23.3
19.	20.1	20.1	20.1	20.2	20.1
20.	-	18.6	18.5	18.6	18.5
21.	-	17.8	17.8	17.7	17.8
22.	14.3	14.3	14.3	14.3	14.3
Total No. of bands	6	20	22	18	18

Note: The molecular weights of the proteins are expressed in KDa.





Livelihood Pattern of Rural Youth in Agriculture

Indumathy.K¹ and Rajasekaran.R^{2*}

¹Assistant Professor, Department of Agricultural Extension, Adhiparasakthi Agricultural College, G.B.Nagar, Kalavai-632506, Tamil Nadu, India.

^{2*}Assistant Professor, Department of Agricultural Extension, Don Bosco College of Agriculture, Sagayathottam, Vellore district, Tamil Nadu-631 151, India.

Received: 10 Aug 2017

Revised: 22 Aug 2017

Accepted: 27 Sep 2017

Address for correspondence

Rajasekaran.R

Assistant Professor, Department of Agricultural Extension,
Don Bosco College of Agriculture,
Sagayathottam, Vellore district, Tamil Nadu-631 151, India.
Email: rajasekaranextension@gmail.com



This is an Open Access Journal / article distributed under the terms of the **Creative Commons Attribution License** (CC BY-NC-ND 3.0) which permits unrestricted use, distribution, and reproduction in any medium, provided the original work is properly cited. All rights reserved.

ABSTRACT

The study was conducted to assess the livelihood pattern of rural youth in agriculture. The study was undertaken at Vaniyambaditaluk, Alangayam block in Vellore district of Tamil Nadu. Totally 90 respondents were composed through random sampling method. A survey was conducted and interview schedule was used to collect the data. Based on the collected data, the variables were analysed by using SPSS software and the results are predicted. The results show that the majority of the farm youth education were upto higher secondary followed by middle level. Majority 73.00 per cent of the respondents belong to joint family followed by 26.70 per cent of the respondents were nuclear family.

Keywords: livelihood pattern, SPSS software, nuclear family.

INTRODUCTION

Youth are the most potent segment of the population of a country. They are the hopes of tomorrow and the backbone of the country. "Youth possess dynamic energies, creative activities and adventurous spirit. They undergo psychological and physiological changes as they grow". The development of youth determines the development of the country. There are over one billion youth (aged 15-24 years) in the world today. Among 99 percent of the world population, eighty per cent of them are youth live in the developing world. India is a land of youth and constitutes a numerically dominant potential, resourceful and also adventurous segment of the population. According to 2011 census, youth population in India with the age group of 15 to 35 years is around 43,02,28,000 (35.36%) of the total population. Out of this, 70 percent (301 million) are rural youth and the remaining 30 per cent (129 million) are urban



**Indumathy and Rajasekaran**

youth. As the majority of the youth comes from rural areas and they are considered as the nation builders of tomorrow. (Marimuthu, P. 2001). Hence the present study is taken up with the following specific objectives.

- Socio economic characteristics of rural youth
- Participation of rural youth in agriculture

METHODOLOGY

The present study was conducted in Vellore district of Tamil Nadu. Totally, 20 blocks in Vellore district. From the total block, Alangayam block was selected. In Alangayam block, Vaniyambaditaluk was selected. From the selected taluk, 9 villages were selected. Hence the total sample size of 90 was composed for the study. Well structured interview schedule was prepared to collect data. Expost facto research design was applied to conduct this experiment.

RESULTS AND DISCUSSION**Educational status**

As shown in table 1, majority 37.00 per cent of the respondents had education up to higher secondary schooling, which was followed by 27.00 per cent were middle education, 19.00 per cent were primary education and 6.00 per cent of the respondents were collegiate education. This is in line with the studies conducted by Model and Yadav (2013). Significant relationship was found between education and income generating activities. Majority of the youth were literates they were largely depend on non agricultural income generating activities like construction, teaching etc.

Type of family

Table 2 reveals that majority 73.00 per cent of the respondents belong to joint family followed by 26.70 per cent of the respondents were nuclear family.

Farm size

It could be seen from the table 3 that majority 41.00 per cent of the respondents were marginal farmers followed by 40.00 per cent were small farmers and only meagre 19.00 per cent of the respondents were big famers. This is in line with the studies conducted by Ovwigho (2014).

Mass media exposure

Exposure to mass media like newspaper, TV, radio, magazines would have made the respondents to contribute in agricultural sector. The data presented in table 4 reveals that 84.40 percent of the farmers were regularly watching television. Three fourth 84.40 per cent of the respondents never read agricultural magazines and 32.20 percent of the respondents never read newspapers. It could be inferred that TV was the most preferred media among the respondents.

Extent of involvement of rural youth in agricultural activities

In this section, to find out the extent of involvement of farm youth in agricultural activities was observed. There were eighteen statements in extent of involvement in agriculture activities were included. A list of activities with varying degrees of agricultural has been administered and relevant data have been collected. The results are presented in the Table 5. The responses were collected on three point continuum as low, medium and high with scores ranging from



**Indumathy and Rajasekaran**

three, two and one. The study operationalized to study the youth involvement in agricultural activities. The responses were categorized into low, medium and high. From the data, it could be inferred that the rural youth have major role in harvesting followed by fertilizer and manure application and irrigation management. Further it could be inferred that the farm activities in which involvement of youth obtained highest score in harvesting (68.90 %) followed by irrigation management (52.20 %) and manures and fertilizer application (47.80 %) and least scores was obtained in marketing (93.30 %) followed by seed processing (92.20 %) and grain/seed storage (90.00 %).

Extent of participation of rural youth in agricultural income generating activities

Rural youth are facing difficulty in maintaining livelihoods and consequently, poverty remains pervasive among them. The income generating activities should be emphasized for the development of rural livelihoods. This section (table 6) have been investigated into nine major components viz., cereals production, oilseed production, pulse production, goat production, poultry production, milk production, fish production and vegetable production.

It could be observed, pulse production, oilseed production and milk production ranked first, second and third respectively. We have also found out that fish production, fruit production and poultry farming scored least. From this we have overall conclusion that the rural youth are actively engage in pulse production and oilseed production in agricultural income generating activities. These findings are in conformity with that of Mangal (2009) who reported crop production as the most participated agricultural income generating activities among rural youth.

CONCLUSION

This study carried out an assessment participation and involvement of Youth in Agriculture and income generating activity through practicing agriculture. The study can be used by various agencies and organizations interested in youth empowerment through agriculture to identify the areas of concerns for effective participation in agriculture. Based on the findings of this research, participation in soil testing, selection of varieties, storage, seed processing and marketing were identified as very low. Hence, there is a need in creating awareness among the youth on importance of technologies in agriculture.

REFERENCES

1. Ovwigho, B O. (2014). Factors Influencing Involvement in Non-farm income generating Activities among Local farmers: The case of Ughelli South local government area of delta state, Nigeria, Sustainable Agriculture Research, 3(1): 76-84
2. Mangal H. (2009). Best practices for Youth in Agriculture: The Barbados, Grenada and Saint Lucia Experience. Final report.
3. Marimuthu, P. 2001. Indigenous Tribal Wisdom for Rural Development: A Multidimensional Analysis. Unpub. Ph.D. Thesis, TNAU, Coimbatore.





Indumathy and Rajasekaran

Table 1. Distribution of respondents based on educational status

SI.No	Categories	Frequency	Percent
1	Illiterate	10	11.00
2	Primary	17	19.00
3	Middle	25	27.00
4	Secondary	34	37.00
5	Collegiate	5	6.00
TOTAL		90	100.00

Table 2. Distribution of respondents based on types of family

SI.No	Categories	Frequency	Percent
1.	Joint family	66	73.30
2.	Nuclear family	24	26.70
TOTAL		90	100.00

Table 3. Distribution of respondents based on farm size

SI.No	Categories	Frequency	Percent
1	Marginal farmer	37	41.00
2	Small farmer	36	40.00
3	Big farmer	17	19.00
TOTAL		90	100.00

Table 4. Distribution of respondents based on mass media

SI.No	Categories	Regularly		Rarely		Never	
		Frequency	%	Frequency	%	Frequency	%
1.	Reading newspaper	48	53.30	13	14.40	29	32.2
2.	Listening radio	55	61.10	6	6.70	29	32.00
3.	Watching TV	76	84.40	5	5.60	9	10.00
4.	Reading magazine	5	5.5	9	10.00	76	84.40





Indumathy and Rajasekaran

Table 5. Distribution of respondents based on extent of involvement in agricultural activities

SI.No.	Area of activity	Extent of involvement in agriculture					
		Low		Medium		High	
		Frequency	%	Frequency	%	Frequency	%
1.	Soil testing	78	86.70	6	6.70	6	6.67
2.	Soil treatment	82	91.10	3	3.30	5	5.60
3.	Preparation of land	68	75.60	14	15.60	8	8.90
4.	Selection of seed variety	70	77.80	12	13.30	8	8.90
5.	Seed treatment	14	56.60	13	14.40	63	17.00
6.	Sowing	56	62.20	9	10.00	25	27.80
7.	Manure and fertilizer application	32	35.60	14	15.60	43	47.80
8.	Irrigation management	33	36.70	10	11.10	47	52.20
9.	Weeding	81	90.00	6	6.70	3	3.30
10.	Plant protection	70	77.80	6	6.70	14	15.60
11.	Harvesting	15	16.70	13	14.40	62	68.90
12.	Collection of harvested crops	47	52.20	18	20.00	25	27.80
13.	Threshing process	74	82.20	4	4.40	12	13.30
14.	Winnowing process	82	91.10	0	0.00	8	8.90
15.	Grain storage	81	90.00	1	1.10	8	8.00
16.	Seed processing	83	92.20	3	3.30	4	4.40
17.	Seed storage	81	90.00	6	6.60	3	3.30
18.	Marketing	84	93.30	3	3.30	3	3.30

Table 6. Distribution of respondents based on agricultural income generating activities

SI.No	Particulars	Mean	Rank
1.	Cereal production	1.12	VIII
2.	Pulse production	1.67	I
3.	Oilseed production	1.52	II
4.	Fruit production	1.26	IV
5.	Goat rearing	1.06	X
6.	Poultry farming	1.11	IX
7.	Milk production	1.13	III
8.	Fish production	1.34	VII
9.	Vegetable production	1.18	VI





RESEARCH ARTICLE

Rice Area Estimation in Tiruvarur District of TamilNadu using VV Polarized Sentinel 1A SAR Data

Mugilan Govindasamy Raman*, Ragunath Kaliaperumal and Sellaperumal Pazhanivelan

Department of Remote Sensing and GIS, Tamil Nadu Agricultural University, Coimbatore -641003, Tamil Nadu, India.

Received: 12 Aug 2017

Revised: 24 Aug 2017

Accepted: 27 Sep 2017

Address for correspondence

Mugilan Govindasamy Raman

Scholar, Department of Remote Sensing and GIS,
Tamil Nadu Agricultural University,
Coimbatore -641003, Tamil Nadu, India.
Email: mugilantnau@gmail.com



This is an Open Access Journal / article distributed under the terms of the **Creative Commons Attribution License** (CC BY-NC-ND 3.0) which permits unrestricted use, distribution, and reproduction in any medium, provided the original work is properly cited. All rights reserved.

ABSTRACT

A research study on 'Rice Area estimation in Tiruvarur district of Tamil Nadu using VV Polarized Sentinel 1A SAR data' was conducted during *rabi* 2016 (Samba season) to estimate rice area in Tiruvarur district. Multi temporal Sentinel 1A satellite data with VV polarization at 20 m spatial resolution was acquired between September, 2016 and January, 2017 at 12 days interval and processed using MAPscape-RICE software. Continuous monitoring was done for crop parameters and validation exercise was done for accuracy assessment. Spectral dB curve of rice was generated using temporal Sentinel 1A SAR data. The dB values showed a minimum at agronomic flooding and a peak at maximum tillering stage and decreased thereafter. A total rice area of 106773 ha was estimated in Tiruvarur district during samba season 2016-17 using VV polarization.

Keywords: Rice, Sentinel 1A SAR, VV Polarization, Spectral dB curves

INTRODUCTION

The importance of agriculture for the Indian society can be hardly be over emphasized, as its role in the economy, employment, food security, national self reliance and general well being, does not need reiteration. The need for timely and reliable information on crop area and production for tactical and strategic decision making by all the stake holders in agriculture, such as producers, processors, resource managers, marketing finance and the government is well known. Crop growth and yield are determined by a number of factors such as genetic potential of crop cultivar, soil, weather, cultivation practices (date of sowing, amount of irrigation and fertilizer) and biotic stresses. Accurate crop identification can achieve a good estimation for crop sown acreage, planting structure and spatial distribution, as well as provide key input parameters for crop yield estimation. Hence study on crop identification is important for making national food policy and economy plan. With the launch and continuous



**Mugilan et al.**

availability of multi-spectral (visible, near-infrared) sensors on polar orbiting earth observation satellites (LANDSAT, SPOT, IRS, etc) remote sensing (RS) data has become an important tool for area and yield estimation. Remote sensing data provide timely, accurate, synoptic and objective estimation of crop identification, crop monitoring, acreage and yield estimation. In view of the advantages of high temporal resolution, wide coverage and low cost, remote sensing has been used in a wide range of earth observation activities and thus provides a useful tool for crop recognition and planting acreage monitoring at a large scale. Since the 1980's, optical remote sensing has been widely used to identify various crops, however, optical images are not often available in the key growth period of crops, owing to the cloudy and rainy weather. Thus, it has a negative effect on the accuracy and timeliness of crop area monitoring. As a new technology with an advantage of all weather, all-time, high resolution and wide coverage, Synthetic Aperture Radar (SAR) has been widely applied in agricultural condition monitoring which provides a strong complement and support for crop identification in data and technology aspect. As the updating and improvement of function parameters and performance index of radar sensors, it has been an important field of agriculture remote sensing in getting the information of crop sown acreage, growing condition and yield by SAR. In order to increase the accuracies of crop identification and area estimation, we need to have a better understanding of the crop and the underlying soil characteristics that influence the radar backscatter throughout the growing season and identify the suitable methodologies to extract crop information from SAR imagery and evaluate the multi temporal SAR data for crop identification.

MATERIALS AND METHODS

Synthetic Aperture Radar (SAR) has the advantage of operating at wavelengths not impeded by cloud cover or a lack of illumination and can acquire data over a site during day or night time under all weather conditions. Sentinel-1A, with its C-SAR instrument, can offer reliable, repeated wide area monitoring. Sentinel-1A is a European radar imaging satellite launched in 2014. It is the first Sentinel 1 satellite launched as part of the European Union's Copernicus programme. It provides dual polarization capability, very short revisit times and rapid product delivery. For each observation, precise measurements of spacecraft position and attitude are available. The satellite carries a C-band Synthetic Aperture Radar which will provide images in all light and weather conditions with VV (Vertical-Vertical) and the data obtained at twelve days interval. Sentinel1-A has four standard operational modes, designed for interoperability with other systems. Level-1 ground range (GRD) product obtained by interferometric wide (IW) swath mode (1) of High Resolution (HR) is used for this research. The characteristics of IW1-GRD-HR product are given in Table1. In order to have a full coverage during the crop growing period of rice, the satellite data were downloaded for 19th September 2016 to 17th January 2017 at 12 days interval from <https://scihub.copernicus.eu/dhus/>.

GIS and other softwares viz., MAPscape-RICE, ArcGIS, QGIS, RiceYES and ORYZA growth model will be used in the study to perform different operations to achieve results. A fully automated processing chain developed by Holecz *et al.* (2013) will be used to convert the multi-temporal space-borne SAR SLC data into terrain-geocoded σ° values. The processing chain is a module within the MAPscape-RICE software.

The multi-temporal stack of terrain-geocoded σ° images was input to a rule-based rice detection algorithm in MAPscape-RICE. The temporal evolution of σ° was analyzed from an agronomic perspective, which also required *a priori* knowledge of rice maturity, calendar and duration and crop practices from field information and knowledge of the study location. The temporal signature was frequency and polarization dependent and also relied on the crop establishment method and, to some extent, on crop maturity. This implied that general rules could be applied to detect rice, but that the parameters for these rules needed to be adapted according to the agro-ecological zone, crop practices and rice calendar. The Rule-based rice detection algorithm for multi-temporal C-band σ° is presented in Fig.1 with the parameters used in the MAPscape-RICE software.





Mugilan et al.

The choice of parameters a, b, c, d, e and f was guided by a simple statistical analysis of the temporal signature of σ° values in the monitored fields. The criteria used to guide the selection of parameters. The mean, minimum, maximum and range of σ° were computed for the temporal signature of each monitored field. Then, we computed the minima and maxima of those mean σ° values across fields, the maxima of the minimum σ° values across fields, the minima of the maximum σ° value across fields and the minimum and maximum of the range of σ° values across fields (Holecz *et al.*, 2013). These six statistics, which we call temporal features, concisely characterize the key information in the rice signatures of the observed fields, and each one relates directly to one parameter. Hence, the value of the six temporal features from the monitoring locations at each site can be used to guide the choice of the six parameter values as shown in Table 2.

The Error matrix and Kappa statistics are used for evaluating the accuracy of the estimated rice area. The class allocation of each pixel in classified image is compared with the corresponding class allocation on reference data (Crop Cutting Experiment data) to determine the classification accuracy. The pixels of agreement and disagreement are compiled in the form of an error matrix, where the rows and columns represent the number of all classes and the elements of matrix represent the number of pixels in the testing dataset (Lillesand 1994). The accuracy measures, such as overall accuracy, producer's accuracy and user's accuracy are estimated from the error matrix (Congalton, 1991). The overall accuracy, which is the percentages of correctly classified cases lying along the diagonal, was determined as follows:

$$\text{Overall Accuracy} = \frac{\sum (\text{Correctly classified classes along diagonal})}{\sum (\text{Row Total or Column Total})}$$

The producer's accuracy (errors of omission) of each class was computed by dividing the number of samples that were classified correctly by its total number of reference samples as follows:

$$\text{Producer's Accuracy} = \frac{\text{Number of correctly classified classes in a column}}{\text{Total number of items verified in that column}}$$

The user's accuracy (errors of commission) of each class was computed by dividing the number of correctly classified samples of that class by its total number of samples that were verified as belonging to the class as follows:

$$\text{User's Accuracy} = \frac{\text{Number of correctly classified item in a row}}{\text{Total number of items verified in that row}}$$

Another measure of classification accuracy is the kappa coefficient, which is a measure of the proportional (or percentage) improvement by the classifier over a purely random assignment to classes (Richards, 1993). The kappa coefficient can be estimated from the formula given below.

$$\hat{K} = \frac{NA - B}{N^2 - B}$$

For an error matrix with r rows, and hence the same number of columns,

Where,

A = the sum of r diagonal elements, which is the numerator in the computation of overall accuracy

B = sum of the r products (row total x column total)

N = the number of pixels in the error matrix (the sum of all r individual cell values)

Field observations will be performed throughout the rice and non-rice fields within the study area. Monitoring sites will be fixed in major rice growing blocks of the study area and these fields will be selected with the farmers' consent, prior to the start of the rice season and the image acquisition schedule. Observations will be made on or as



**Mugilan et al.**

close to the image acquisition date as possible. Observations will include latitude and longitude from hand held GPS receivers, descriptions and photos of the status of the field, plant height, water depth, weather conditions and crop stage. A validation exercise will be conducted for each footprint to assess the accuracy of the rice classification.

Random stratified sampling method will be adopted to collect land cover information at approximately 106 locations throughout the district with these points split 12/94 between non-rice points and rice points. Map validation assessments will be conducted in season, in the reproductive or ripening stage before harvesting. Locations will be chosen such that the land cover was homogeneous in a 50 m radius around each GPS point for 20 m resolution imagery.

RESULTS AND DISCUSSION

This study on 'Rice Area estimation in Tiruvarur district of Tamil Nadu using VV Polarized Sentinel 1A SAR data' has attempted to estimate the rice area using SAR images from Sentinel 1A satellite, which is a freely available data. Single (VV) polarized data are available from these sensors, which pave way to explore the interaction of the polarizations to determine crop characteristics. The strength of different polarization in rice area estimation was studied and the results on the characteristics of the study area, rice area mapping for VV polarization, rice area map are discussed in this Chapter.

A dB stack was generated using eleven sets of Sentinel-1A data (Table 3) acquired after basic processing viz., orbital and radiometric correction, geo-coding, mosaicking and speckle filtering. Temporal signatures were extracted in VV polarization for each monitoring field and used to generate the dB curves for rice fields for VV polarization. The temporal signature for a selected representative pixel in VV polarization was generated to visualize the resulting rule based classification (Fig.2). A detailed analysis of temporal signatures of rice for VV polarization were done separately for deriving parameters used to classify rice pixels in MAPscape-RICE software. The eleven parameters derived from the temporal signatures of VV polarization for analysis were, mean value of Built-up area, minimum value at tillering, minimum and maximum crop cycle duration, maximum value at start of season, start of season to last acquisition, minimum primary and secondary variation, maximum value and days of temporary water. The temporal signatures for the selected rice pixels in VV polarization are presented in Fig.3 and the parameters used for classification are given in the Table 4.

VV polarization signatures showed a minimum dB value at agronomic flooding and a peak at maximum tillering stage. At flooding, minimum dB value from -13.64 to -12.18 was recorded with an average of -12.55 and the average maximum value at peak tillering stage was found to be -10.47 with a range of -8.67 to -11.41 in VV polarization (Table 5), Rice crop shows significant temporal behaviour and a large dynamic range (-14.4 to -8.41dB) during its growth period (Inoue *et al.*, 2002, Suga and Konishi, 2008, Oh *et al.*, 2009 and Kim *et al.*, 2009). The Minimum primary variation was found to be 1.3 dB corresponding to growth at vegetative and maximum tillering stage in VV polarization.

The lowest values at emerging were due to less back scattering from less vegetation cover with rougher surface which was the moment to capture the start of the season for each pixel. This might be the due to soil moisture variation or sowing which made the soil surface smoother (Karjalainen *et al.*, 2004). Nelson *et al.*, 2014 recorded a similar minimum at early stage of rice crop with X-band (TerraSAR-X and CosmoSmed) SAR data across Asia in Philippines and Thailand. Rice map generated from VV polarization of Sentinel 1A SAR data recorded a total area of 106773 ha (Fig.04). Block wise statistics were derived for Tiruvarur district. Total rice area in the blocks ranged from 6625 ha to 17348 ha, were Kottur block recorded the largest area followed by 13033 ha in Thiruthuraiipoondi, 12399 ha in Muthupettai and 11932 ha in Needamangalam block. The lowest area was found in the Tiruvarur block



**Mugilan et al.**

followed by Kudavasal with 7931 ha and Koradacheri block with 8096 ha. The other blocks viz., Mannargudi and Valangaiman had 9596 ha and 8508 ha respectively (Table.6)

The generated rice area map was validated using ground truth points collected throughout Tiruvarur district during different time of visit coinciding with crop stages and satellite pass. Both rice and non-rice points were collected with latitude and longitude values during the visits. There were 106 points collected which includes 94 rice points and 12 non-rice points. The number of non-rice points collected was less, since in Tiruvarur district the major crop grown is rice and very less area with other crops. The ground truth points collected for validation are depicted in the Fig.5.

Validation was carried out using confusion matrix and classification accuracy was calculated. The two classes of Rice and Late rice available in the rice area map were considered as a single class for map accuracy. The accuracy assessments in the field were generally conducted in season, in the reproductive or ripening stage before harvesting, but in some cases the field assessment was conducted post season and rice stubble and farmer survey were used to confirm that the observed post harvest situation reflected the presence of a rice crop during the monitoring season. The results of the confusion matrix showed that the number of true positives (actual rice that are classified as rice) was 71 points, the number of false positives (actual non rice that classified as rice) was 1 point. The number of false negatives (actual rice that classified as non rice) was 23 points and the number of true negatives (actual non rice that classified as non rice) was 22 points. The user accuracy of Rice and Non rice points were 75.5% and 95.7% respectively. The Producers accuracy of Rice and Non rice points were 98.6% and 48.9% respectively. The overall accuracy of both rice and non rice points was 79.5%. The average accuracy and reliability was about 85.6% and 73.8% respectively. The overall Kappa index was 0.59 which was low (Table 7). There were more misclassified pixels in the southern parts of the district where more of direct seeding has taken place. The rice area in Mannargudi, Thiruthuraiipoondi, Kottur and Nannilam blocks as found in ground truth collection were classified as non-rice area in VV polarization, clearly indicating the capability of missing direct seeded rice area. The transplanted rice in other blocks and double crop were well classified.

REFERENCES

1. Congalton, R.C. 1991. A review of assessing the accuracy of classifications of remotely sensed data. *Remote Sensing Environment*, 37, pp. 35-46.
2. De Zan, F. and A. M. Guarnieri. 2006. TOPSAR: Terrain Observation by Progressive Scans. *IEEE Transactions on Geoscience and Remote Sensing*, 44(9), pp. 2352–2360.
3. Holecz, F., M.F.L. Barbieri, A. Collivignarelli, T.D.M. Gatti, Nelson, G. Setiyono, Boschetti, P.A.B. Manfron, J.E. Quilang. 2013. An operational remote sensing based service for rice production estimation at national scale. In: *Proceedings of the Living Planet Symposium*, Edinburgh, UK, 9-11.
4. Inoue, Y. T. Kurosue, H. Maeno, S. Uratsuka, T. Kozu, K. Dabrowska-Zielinska, J. Qi. 2002. Season - long daily measurements of multifrequency (Ka, Ku, X, C, and L) and fullpolarization backscatter signatures over paddy rice field and their relationship with biological variables. *Remote Sens. Environ.*, 81: 194–204.
5. Karjalainen, M., H. Kaartinen, J. Hyypä, H. Laurila and R. Kuittinen. 2004. The Use of ENVISAT Alternating Polarization SAR Images in Agricultural Monitoring in Comparison with RADARSAT-1 SAR Images. *XXth ISPRS Congress*, July 12-23, 2004 Istanbul, Turkey. XXXV (B7), pp. 132-137.
6. Kim, Y.H., S.Y. Hong and Y. H. Lee, 2009. Estimation of paddy rice growth parameters using L-, C-, X-bands polarimetric scatterometer. *Korean J. Remote Sens.*, 25, 31–44.
7. Lillesand, T.M. and Kiefer, R.W., 1994. *Remote sensing and photo interpretation*. John Wiley and Sons: New York, p.750.
8. Nelson, A., Setiyono, T., Rala, A.B., Quicho, E.D., Raviz, J.V., Abonete, P.J., Maunahan, A.A., Garcia, C.A., Bhatti, H.Z.M., Villano, L.S. and Thongbai, P. 2014. Towards an operational SAR-based rice monitoring system in Asia: Examples from 13 demonstration sites across Asia in the RIICE project. *Remote Sensing*, 6(11), pp.10773-10812.





Mugilan et al.

9. Oh, Y, S.Y., Hong, Y. Kim, J.Y. Hong and Y.H. Kim. 2009. Polarimetric backscattering coefficients of flooded rice fields at L- and C-bands: Measurements, modeling, and data analysis. *IEEE Trans. Geosci. Remote Sens.*, 47, 2714–2721. on 1 June 2014).

10. Richards, J.A. 1993. *Remote Sensing Digital Image Analysis*. Springer, Heidelberg, New York. Suga, Y. and Konishi, T. 2008, October. Rice crop monitoring using X, C and L band SAR data. In *SPIE Remote Sensing* (pp. 710410-710410). International Society for Optics and Photonics.

Table 1. Characteristics of Sentinel1-A (IW1-GRD-HR) Data (DeZan and Guarnieri., 2006)

Parameters	Characteristics
Pixel value	Magnitude detected
Coordinate system	Ground range
Polarization options	Single(HH or VV) or Dual (HH+HV or VV+VH)
Resolution (range x azimuth in meters)	20.4x21.7
Pixel spacing (range x azimuth in meters)	10x10
Incidence angle (degree)	32.9
Radiometric resolution	1.7 dB
Ground range coverage (km)	251.8
Absolute location accuracy (m) (NRT)	7
Equivalent Number of Looks (ENL)	4.4
Number of looks (range x azimuth)	5 x 1
Range look bandwidth (Hz)	14.1
Azimuth look bandwidth (Hz)	327
Look overlap (range, azimuth)	0.250, 0.000
Bits per pixel	16

Table 2. Site-specific parameters for the rule-based classification and the criteria used to select them based on temporal features.

Parameter	Relationship between Parameter and Temporal Feature
a = lowest mean	a < (i) minima of the mean σ° across all rice signatures
b = highest mean	b > (ii) maxima of the mean σ° across all rice signatures
c = maximum variation	c > (vi) maxima of the range in σ° across all rice signatures
d = max value at SoS	d > (iii) highest minima in σ° across all rice signatures
e = min value at peak	e < (iv) lowest maxima in σ° across all rice signatures
f = minimum variation	f < (v) minima of the range in σ° across all rice signatures





Mugilan et al.

Table 3. Sentinel 1A data acquisition dates during Samba 2016 for Tiruvarur district

S.No	Date of Acquisition	S.No	Date of Acquisition
1	19 Sep 2016	7	30 Nov 2016
2	01 Oct 2016	8	12 Dec 2016
3	13 Oct 2016	9	24 Dec 2016
4	25 Oct 2016	10	05 Jan 2017
5	06 Nov 2016	11	17 Jan 2017
6	18 Nov 2016		

Table 4. Classification parameters used for rice pixel delineation in VV polarization data

S.No	Parameter	VV
1.	Mean Value of Water (dB)	-17.00
2.	Max Value of Temporary Water (dB)	-15.00
3.	Days of Temporary Water (days)	65
4.	Mean Value of Built up Areas (dB)	-7.00
5.	Max Value at Start of Season (dB)	-11.00
6.	Min Primary Variation (dB)	1.30
7.	Min Secondary Variation (dB)	0.50
8.	Min Value at Tillering (dB)	-11.50
9.	Minimum Cycle Duration (days)	60
10.	Maximum Cycle Duration (days)	150
11	SOS to Last Acquisition (days)	40





Mugilan et al.

Table 5. Temporal dB values of Rice fields across Tiruvarur district (VV Polarization)

Satellite Pass no.	Field 1	Field 2	Field 3	Field 4	Field 5	Field 6	Field 7	Field 8	Average
19-Sep-2016	-11.28	-10.19	-11.37	-10.58	-10.18	-10.85	-8.75	-11.66	-10.6075
01-Oct-2016	-12.18	-12.23	-12.69	-12.70	-12.31	-12.45	-12.22	-13.64	-12.5525
13-Oct-2016	-13.32	-11.09	-11.45	-12.10	-10.88	-12.98	-10.92	-12.94	-11.96
25-Oct-2016	-12.52	-10.19	-10.33	-11.60	-9.81	-11.83	-9.10	-11.67	-10.8813
06-Nov-2016	-11.65	-10.17	-9.85	-10.10	-9.55	-10.58	-8.42	-10.76	-10.135
18-Nov-2016	-10.33	-10.67	-10.10	-9.83	-9.58	-10.45	-8.54	-10.90	-10.05
30-Nov-2016	-10.38	-11.26	-10.74	-10.15	-9.87	-10.66	-8.67	-11.41	-10.3925
12-Dec-2016	-10.56	-11.12	-10.42	-10.95	-10.37	-10.89	-9.47	-11.48	-10.6575
24-Dec-2016	-10.67	-10.99	-10.52	-10.81	-10.92	-11.14	-10.45	-11.56	-10.8825
05-Jan-2017	-10.99	-10.73	-10.97	-11.14	-11.01	-10.95	-10.63	-11.70	-11.015
17-Jan-2017	-11.81	-10.48	-11.73	-11.41	-11.10	-10.78	-10.82	-11.85	-11.2475



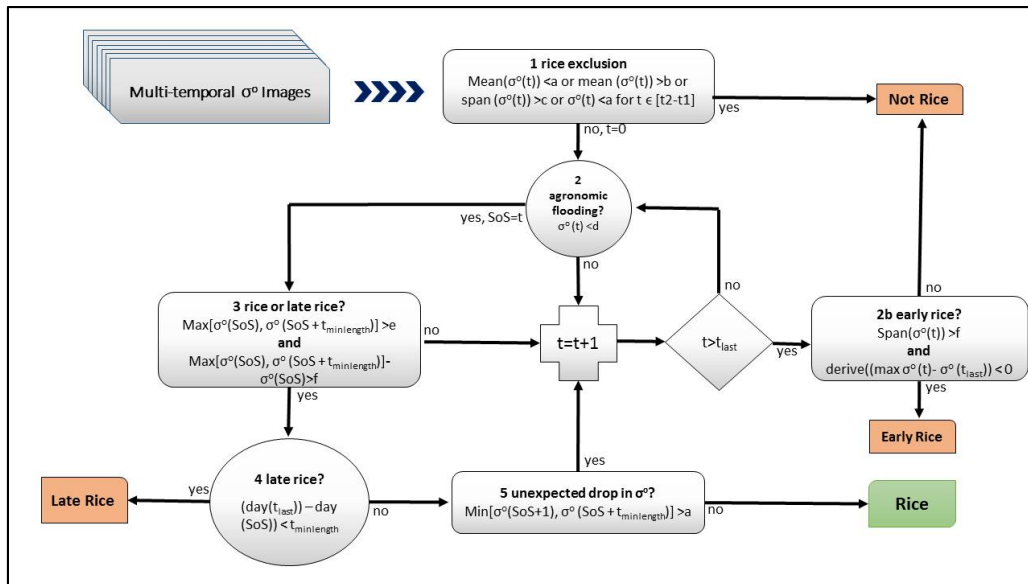


Fig.1.Rule-based rice detection algorithm for multi-temporal C-band σ^0 in MAPscape-RICE

a = lowest mean

b = highest mean

c = maximum variation

d = maximum value at SoS

e = minimum value at maximum peak

f = minimum variation

t = time

t₂-t₁ = maximum time under water

t_{min} length= minimum number of days of season length

t_{max} length= maximum number of days of season length

t_{last} = date of the last acquisition

SoS = Start of Season

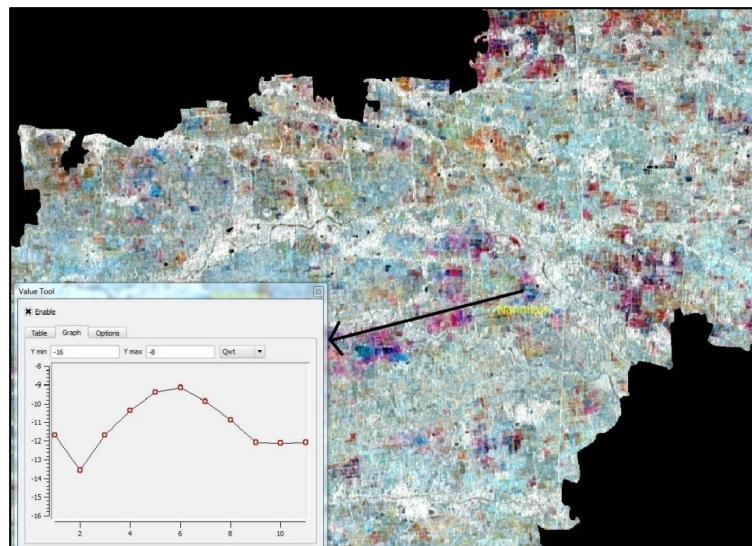


Fig.2.dB stack generate with Sentinel 1A data and Rice temporal curve VV





Mugilan et al.

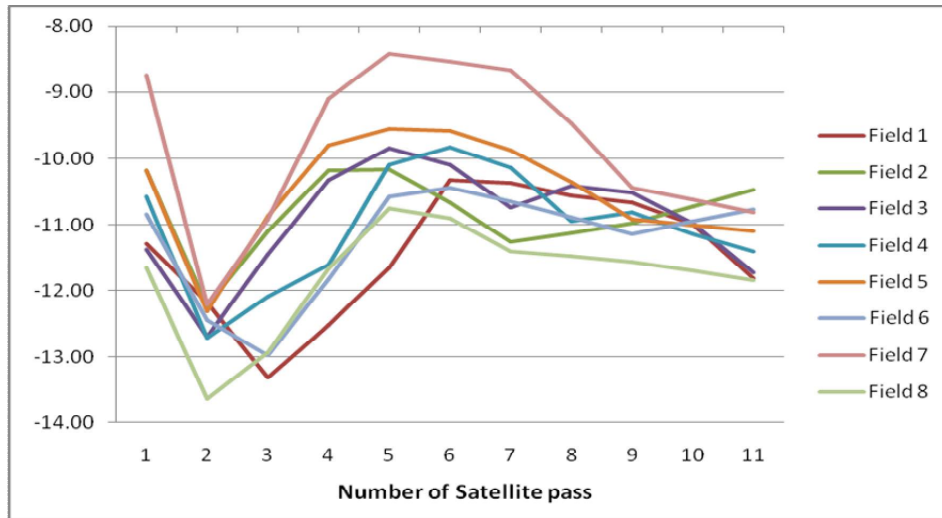


Fig.3.Temporal dB curves for rice at selected sites VV

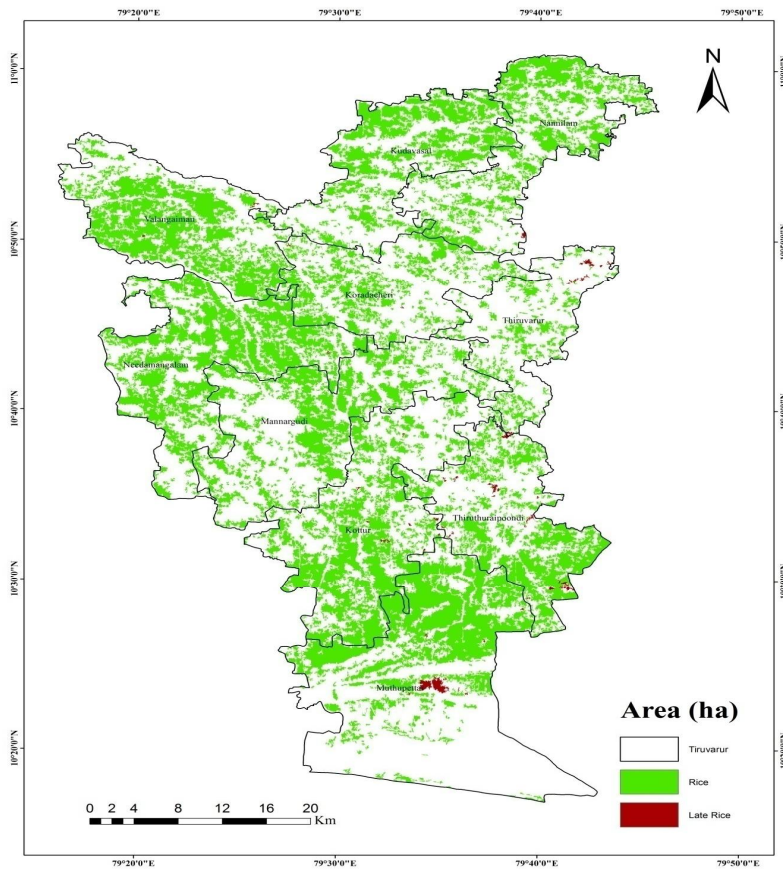


Fig.4.Rice area map of Tiruvarur district generated using VV Polarization





Mugilan et al.

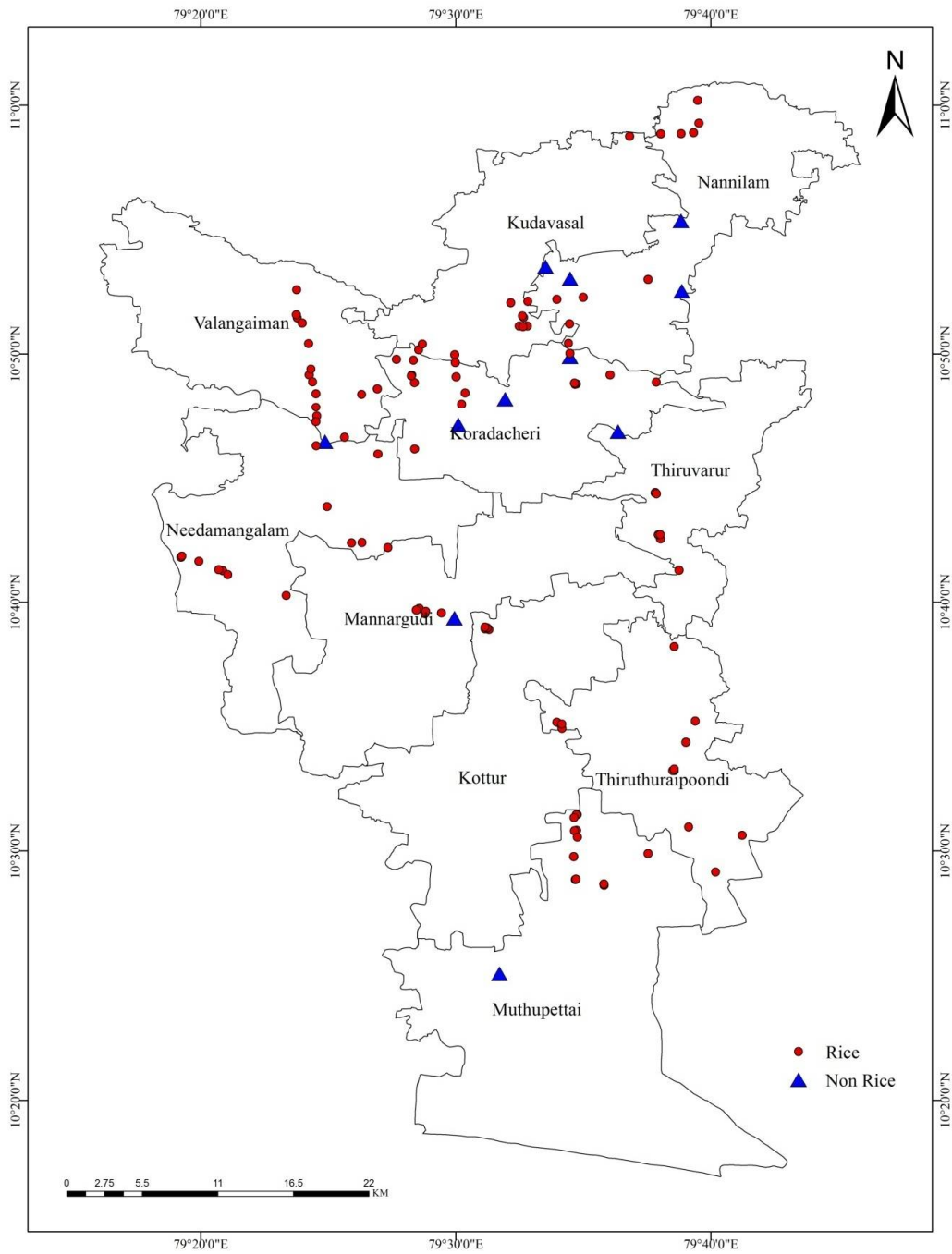


Fig5.Rice area map validation points (rice and non-rice) across Tiruvarur district





A Review on Phytochemicals Based Extraction and their Qualitative Screening Protocols

Ranjith D^{1*} and Maria L²

¹Assistant Professor, Dept. of Veterinary Pharmacology and Toxicology, College of Veterinary and Animal Sciences, Pookode, Wayanad, Kerala, India.

²Research Assistant, Dept. of Veterinary Pharmacology and Toxicology, College of Veterinary and Animal Sciences, Pookode, Wayanad, Kerala, India.

Received: 20 Aug 2017

Revised: 27 Aug 2017

Accepted: 28 Sep 2017

Address for correspondence

Dr.Ranjith.D

Assistant Professor,
Department of Veterinary Pharmacology and Toxicology,
College of Veterinary and Animal Sciences,
Pookode, Wayanad, Kerala, India.
Email: ranjith946@gmail.com



This is an Open Access Journal / article distributed under the terms of the **Creative Commons Attribution License** (CC BY-NC-ND 3.0) which permits unrestricted use, distribution, and reproduction in any medium, provided the original work is properly cited. All rights reserved.

ABSTRACT

Plants produce a wide variety of secondary metabolites which serve them as defense compounds against herbivores, and other plants and microbes, but also as signal compounds. In general, Secondary metabolites exhibit a wide array of biological and pharmacological properties. Because of this, some plants or products isolated from them have been and are still used to treat infections, health disorders or diseases. This review provides evidence of importance of secondary metabolites in plants, their extraction protocols including multifarious identification tests for different classes of phyto constituents responsible for pharmacological activity in plants.

Keywords: Secondary metabolites, Pharmacological activity, Phyto constituents.

INTRODUCTION

India, with its diverse agro-climatic conditions and regional topography, has been considered as the treasure house of plant genetic resources with one of the world's top 12 mega diversity nation. Although there are around 8,000 medicinal plant species used by different communities in India across different ecosystems, only around 10% of them are in active trade (Singh., 2005). Among these, around 48 species are exported in the form of raw drugs and extracts, while around 42 species are imported. The wild populations of about 100 of the traded species are known to have declined, thereby making them to be considered threatened (Vijayalatha., 2004).



**Ranjith and Maria**

Phytochemicals, the term generally used to describe chemicals from plants that enhance health status of organisms, but are not essential nutrients (Chessbrough., 2001). The primary metabolite like chlorophyll, amino acids, nucleotides, simple carbohydrates or membrane lipids have roles in photosynthesis, respiration, solute transport, translocation, nutrient assimilation and differentiation (Taiz and Zeiger., 2006). Secondary metabolites are synthesized by the plants as part of the defense system (Phan *et al.*, 2001) which includes alkaloids, terpenoids, tannins, saponins and phenolic compounds (Edeoga *et al.*, 2005). Correlation between the phytoconstituents and the bioactivity of plant is known for the synthesis of compounds with specific activities to treat various health ailments and chronic disease (Pandey *et al.*, 2013). It is well-known that plants produce these chemicals to protect themselves, but recent researches demonstrate that many phytochemicals can also protect human and animals against diseases (Narasinga., 2003). Phytochemicals may reduce the risk of coronary heart disease by preventing the oxidation of low-density lipoprotein (LDL) cholesterol, reducing the synthesis or absorption of cholesterol, normalizing blood pressure and clotting, and improving arterial elasticity (Mathai., 2000). The physiological properties of relatively few phytochemicals are well understood and many more research has focused on their possible role in preventing or treating cancer and heart disease (Meagher., 1999). Phytochemicals have also been promoted for the prevention and treatment of diabetes, high blood pressure and macular degeneration (Meagher., 1999). An individual compound may have more than one biological function serving as both an antioxidant and antibacterial agent (Narasinga., 2003).

Extraction is the separation of medicinally active portions of plant tissues using selective solvents through standard procedures. These include classes of preparations known as decoctions, infusions, fluid extracts, tinctures, pilular (semisolid) extracts or powdered extracts (Remington., 2000). During extraction, solvents diffuse into the solid plant material and solubilize compounds with similar polarity (Ncube *et al.*, 2008). These products contain complex mixture of many medicinal plant metabolites, such as alkaloids, glycosides, terpenoids, flavonoids and lignans (Handa *et al.*, 2008). The factors affecting the choice of solvent are quantity of phytochemicals to be extracted, rate of extraction, diversity of different compounds extracted including inhibitory compounds, ease of subsequent handling of the extracts, toxicity of the solvent in the bioassay process, potential health hazard of the extractants (Elof., 1998). Different solvent systems are available to extract the bioactive compound from natural products. For extraction of more lipophilic compounds, dichloromethane or a mixture of dichloromethane/methanol in ratio of 1:1 are used. In some instances, extraction with hexane is used to remove chlorophyll (Cosa *et al.*, 2006).

EXTRACTION PROCEDURES

Maceration: This is the simplest method of crude drug extraction. In this process, the material to be extracted is placed in a closed vessel and suitable solvent (menstruum) is added and left for 7 days with occasional shaking. The liquid is then strained off and the solid residue (Marc) is pressed to remove the solution as much as possible. The strained and expressed liquids are mixed and clarified by filtration. Occasional shaking brings about rapid equilibrium between intra and extra cellular fluids there by bringing fresh menstruum to the particle surface for further extraction (Jain & Sharma., 2000).

Types of maceration

Modified maceration

It is essentially used for extracting unorganized drugs. Ex: gums, resins etc. This process is quick because the soluble constituents are directly exposed to menstruum due to lack of cellular structure. The process includes, Comminute the drug with menstruum, place in closed vessel for 2-7 days, agitate the mixture occasionally, strain and filter the strained liquid, wash the Marc with fresh menstruum.



**Ranjith and Maria****Multiple maceration**

Multiple maceration is aimed at achieving maximum extraction by using portions of total volume of menstruum for successive maceration.

Vacuum extraction

This process employs a specially designed maceration vessel with arrangement for connecting it to vacuum line. This process increases the permeability of the cell walls considerably and facilitates extraction in a much shorter time.

Infusion

An infusion is a very simple chemical process used with plants that are volatile and dissolve readily or release their active ingredients easily, in water, oil or alcohol. They are typically dried herbs, flowers or berries. The liquid is typically boiled (or brought to another appropriate temperature) and then poured over the herb, which is then allowed to steep in the liquid for a period of time. The liquid may then be strained or the herbs otherwise removed from the liquid. The amount of time the herbs are left in the liquid depends on the purpose for which the infusion is being prepared. Usually steeping for not more than 15 to 30 minutes, or until the mix cools, will create a beverage with optimal flavor. A common proportion used is 28 g (one ounce) of herb to 0.5 L (one pint) of liquid (Azwanida., 2015).

Digestion

Digestion is a form of maceration with slight warming during the extraction process, provided that the temperature does not alter the active ingredients of plant material and so there is greater efficiency in the use of menstruum. The most used temperatures are between 35° and 40°C., although can rise to no higher than 50°C. This process is used with the tougher plant parts or those that contain poorly soluble substances (Bimkr., 2010).

Decoction

The decoction is used for active ingredients that doesn't modify with temperature. In this process the plant is boiled in water for 15 to 60 minutes (depending on the plant or the active ingredient to extract), it's cooled, strained and added enough cold water through the plant to obtain the desired volume. Depending on the consistency of the parts to extract, decoction times will be more or less long; generally, roots, leaves, flowers and leafy stems are boiled in water for about 15 minutes, while the branches and other hard parts can require up to an hour, during this time the evaporated water must be replaced (Das *et al.*, 2010).

Percolation

Percolation is an extraction process that involves the slow descent of a solvent through a powdered substance until it absorbs certain constituents and drips out through the filtered bottom of the container. The main advantages of percolation are a more complete extraction of constituents, shorter processing time, and increased flexibility in processing (David., 1998).





Ranjith and Maria

Soxhlet Extraction

Soxhlet extraction is only required where the desired compound has a limited solubility in a solvent and the impurity is insoluble in that solvent. The advantage of this system is that instead of many portions of warm solvent being passed through the sample, just one batch of solvent is recycled. This method cannot be used for thermo labile compounds as prolonged heating may lead to degradation of compounds (Nikhil *et al.*, 2010).

Supercritical Fluid Extraction (SFE)

Supercritical Fluid Extraction (SFE) involves use of gases, usually CO₂ and compressing them into a dense liquid. This liquid is then pumped through a cylinder containing the material to be extracted. From there, the extract-laden liquid is pumped into a separation chamber where the extract is separated from the gas and the gas is recovered for re-use (Patil and Shettigar., 2010).

Microwave-Assisted Extraction (MAE)

It simply termed as microwave extraction, that combines microwave and traditional solvent extraction. Heating the solvents and plant tissue using microwave increases the kinetic of extraction, is called microwave-assisted extraction. The target for heating in dried plant material is the minute microscopic traces of moisture that occurs in plant cells. The heating up of this moisture inside the plant cell due to microwave effect, results in evaporation and generates tremendous pressure on the cell wall. The cell wall is pushed from inside due to the pressure and the cell wall ruptures. Thus, the exudation of active constituents from the ruptured cells occurs, hence increasing the yield of Phytoconstituents (Delazar *et al.*, 2012).

Solvents Used For Extraction

Water: Water is universal solvent, used to extract plant products with antimicrobial activity. Though traditional healers use primarily water but plant extracts from organic solvents have been found to give more consistent antimicrobial activity compared to water extract. Also, water-soluble flavonoids (mostly anthocyanins) have no antimicrobial significance and water soluble phenolics only important as antioxidant compound (Das *et al.*, 2010).

Acetone: Acetone dissolves many hydrophilic and lipophilic components from the two plants used, is miscible with water, is volatile and has a low toxicity to the bioassay used, it is a very useful extractant, especially for antimicrobial studies where more phenolic compounds are required to be extracted. A study reported that extraction of tannins and other phenolics was better in aqueous acetone than in aqueous methanol (Eloff, 1998). Both acetone and methanol were found to extract saponins which have antimicrobial activity (Ncube., 2008).

Alcohol: The higher activity of the ethanolic extracts as compared to the aqueous extract can be attributed to the presence of higher amounts of polyphenols as compared to aqueous extracts. It means that they are more efficient in cell walls and seeds degradation which have unipolar character and cause polyphenols to be released from cells. Moreover, water is a better medium for the occurrence of the micro-organisms as compared to ethanol (Lapornik *et al.*, 2005). The higher concentrations of more bioactive flavonoid compounds were detected with ethanol 70% due to its higher polarity than pure ethanol. By adding water to the pure ethanol up to 30% for preparing ethanol 70% the polarity of solvent was increased (Bimakr., 2010). Additionally, ethanol was found easier to penetrate the cellular membrane to extract the intracellular ingredients from the plant material (Wang., 2010). Since nearly all of the identified components from plants active against microorganisms are aromatic or saturated organic compounds, they are most often obtained through initial ethanol or methanol extraction (Cowan., 1999). Methanol is more polar





Ranjith and Maria

than ethanol but due to its cytotoxic nature, it is unsuitable for extraction in certain kind of studies as it may lead to incorrect results.

Chloroform: Terpenoid lactones have been obtained by successive extractions of dried barks with hexane, chloroform and methanol with activity concentrating in chloroform fraction. Occasionally tannins and terpenoids will be found in the aqueous phase, but they are more often obtained by treatment with less polar solvents.

Ether: Ether is commonly used selectively for the extraction of coumarins and fatty acids

Dichloromethanol: It is another solvent used for carrying out the extraction procedures. It is specially used for the selective extraction of only terpenoids [Nur., 2012].

RESULTS AND DISCUSSION

Test for Alkaloids

- ✓ **Dragendroff's test:** The extract is treated with few drops of Dragendroff's reagent. The Orange brown precipitate Coloration / Dark orange color is observed.
(Preparation of Dragendroff's Reagent → Solution A: Pour 0.5 g of bismuth nitrate into an empty beaker. Add about 10 ml of distilled water. The mixture should be like a suspension. Add 10 ml of concentrated hydrochloric acid. Stir the resulting mixture.
Solution B: Pour 4 g of potassium iodide into another beaker, add a little water and stir until KI is completely dissolved. Mix solution A and B in equal quantity (Soni and Sheetal., 2013)
- ✓ **Wagner's test:** The extract is treated with few drops of Wagner's reagent. The reddish-brown precipitate is observed which confirms the presence of alkaloids in the extract.
(Preparation of Wagner's Reagent → 1.27g of iodine and 2g of potassium iodide was dissolve in 5 ml of water and the volume was made 100ml with distilled water)
- ✓ **Mayer's test:** The extract is treated with few drops of Mayer's reagent. The White or pale precipitate is observed / A creamy- white colored precipitation appeared giving a positive result.
(Preparation of Mayer's Reagent → Solution A → 1.36 g of mercuric chloride is dissolved in 60ml of distilled water. Solution B → 5g of potassium iodide is dissolved in 20ml of distilled water. Solution A and B are mixed and the volume was adjusted to 100 ml with distilled water)
- ✓ **Hager's Test** – Test solution was treated with few drops of Hager's reagent (**saturated picric acid solution**). Formation of yellow precipitate would show a positive result for the presence of alkaloids (Brain and Turner., 1975).

Test for Flavonoids

- ✓ With aqueous solution of sodium hydroxide blue to violet colour (Anthrocyanins), yellow colour (Flavones), yellow to orange (Flavonones).
- ✓ With concentrated sulphuric acid yellowish orange colour (Anthrocyanins), orange to crimson colour (Flavonones).
- ✓ **Shinoda's test:** The extracts were dissolved in alcohol, to that a piece of magnesium turnings and followed by concentrated hydrochloric acid was added drop wise and heated. Appearance of magenta colour shows the presence of flavonoids.





Ranjith and Maria

- ✓ **Ferric chloride test:** Test solution when treated with few drops of Ferric chloride solution would result in the formation of blackish red color indicating the presence of flavonoids (Rajaram and Ashvin., 2013).
- ✓ **Alkaline reagent Test:** Test solution when treated with sodium hydroxide solution, shows increase in the intensity of yellow color which would become colorless on addition of few drops of dilute Hydrochloric acid, indicates the presence of flavonoids.
- ✓ **Lead acetate solution Test** – Test solution when treated with few drops of lead acetate (10%) solution would result in the formation of yellow precipitate.
- ✓ **Wolf am test for Isoflavonoids:** The extract is treated with sodium amalgam and conc. HCl. The pink colour formation is observed.
- ✓ A small quantity of the extract is heated with 10 ml of ethyl acetate in boiling water for 3 minutes. The mixture is filtered and the filtrates are used for the following test.
 - Ammonium Test:** The filtrate was shaken with 1 ml of dilute ammonia solution (1%). The layers were allowed to separate. A yellow coloration was observed at ammonia layer which indicates the presence of the flavonoid from the plant extract.
 - Aluminum Chloride Test:** The filtrates were shaken with 1 ml of 1% aluminum chloride solution and observed for light yellow color, the light yellow colour indicates the presence of flavonoid and when dilute NaOH and HCl is added the yellow solution turns colorless (Harbourne., 1973).

Test for Phenolic Compounds

- ✓ **Ferric Chloride test:** The extract (50 mg) is dissolved in 5 ml of distilled water. To this few drops of neutral 5% ferric chloride solution are added. A dark green colour or blue colour indicates the presence of phenolic compound.
- ✓ **Gelatin test:** The extract (50 mg) is dissolved in 5 ml of distilled water and 2 ml of 1% solution of Gelatin containing 10% NaCl is added to it. White precipitate indicates the presence of phenolic compounds.
- ✓ **Lead acetate test:** The extract (50 mg) is dissolved in of distilled water and to this 3 ml of 10% lead acetate solution is added. A bulky white precipitate indicates the presence of phenolic compounds.
- ✓ **Ellagic Acid Test:** The test solution was treated with few drops of 5% (w/v) glacial acetic acid and 5% (w/v) NaNO₂ solution. The absence of muddy or Niger brown precipitate indicates the presence of phenols in the extract.

Test for Tannins

- ✓ **Lead acetate test:** The Ethanolic extract is treated with few drops of 1% lead acetate solution. The Yellow or red precipitate formation is observed.
- ✓ **Ferric chloride test:** The Ethanolic extract is treated with 2ml of FeCl₃ solution. The Blue or Black precipitate or greenish to black colour formation is observed which indicates the presence of tannins.
- ✓ **Lead Sub Acetate Test:** 1ml of the different filtrate was added with three drops of lead sub acetate solution. A creamy gelatinous precipitation, indicates positive test for Tannins
- ✓ **Gelatin Test:** To the extract, 1% gelatin solution containing sodium chloride was added. Formation of white precipitate indicates the presence of tannins (Kokate., 1998).

Test for Glycosides

- ✓ For 50 mg of extract is hydrolyzed with concentrated hydrochloric acid for 2 hours on a water bath, filtered and the hydrolysate is subjected to the following tests.
- ✓ **Borntreger's test:** To 2 ml of filtered hydrolysate, 3 ml of chloroform is added and shaken, chloroform layer is separated and 10% ammonia solution is added to it. Pink colour indicates presence of glycosides



**Ranjith and Maria**

- ✓ **Modified Borntrager's Test:** Extracts were treated with Ferric Chloride solution and immersed in boiling water for about 5 minutes. The mixture was cooled and extracted with equal volumes of benzene. The benzene layer was separated and treated with ammonia solution. Formation of rose-pink colour in the ammonical layer indicates the presence of anthranol glycosides.
- ✓ **Legal's test:** 50 mg of extract is dissolved in pyridine, sodium nitroprusside solution is added and made alkaline using 10% NaOH. Presence of glycoside is indicated by pink colour.
- ✓ **Modified Legal's Test:** Extracts were treated with sodium nitroprusside in pyridine and sodium hydroxide. Formation of pink to blood red colour indicates the presence of cardiac glycosides.
- ✓ **Keller-Kiliani Test:** In 2 ml plant extract, glacial acetic acid, one drop of 5% FeCl₃ and conc. H₂SO₄ were added. Reddish brown color appears at junction of the two liquid layers and upper layer appears bluish green, confirming the presence of cardiac glycosides (Kokate., 2006).
- ✓ **Bromine water test** - Test solution was dissolved in bromine water and observed for the formation of yellow precipitate to show a positive result for the presence of glycosides.

Test for Saponins

- ✓ To the Ethanolic extracts add sodium bicarbonate and shake well, honey comb froth formation is observed which indicates the presence of saponins.
- ✓ **Foam Test:** The extract was diluted with 20 ml of distilled water and it was shaken in a graduated cylinder vigorously. A two-cm layer of foam indicates the presence of saponins which is stable for 10 minutes indicates positive result.
- ✓ **Hemolysis Tests:** - Add leaves extract to one drop of blood placed on a glass slide. Appearance of Hemolytic zone confirms the presence of saponins in the extract (Setty *et al.*, 2011).

Test for Carbohydrates

- ✓ **Molish's test:** To 2 ml of plant sample extract, two drops of alcoholic solution of α -naphthol added. The mixture is shaken well and few drops of concentrated sulphuric acid is added slowly along the sides of test tube. A purple or violet coloured ring at the junction indicates the presence of carbohydrates.
- ✓ **Fehling's Test:** Fehling A and Fehling B reagents were mixed and few drops of extract is added and boiled. A brick red coloured precipitate of cuprous oxide forms, indicating the presence of carbohydrates.
- ✓ **Starch test:** The aqueous extract 5ml was treated with the reagent of the starch (iodine). Any shift to blue violet indicates the presence of starch.
- ✓ **Benedict's test:** Test solution was mixed with few drops of Benedict's reagent (alkaline solution containing cupric citrate complex) and boiled in water bath, observed for the formation of reddish brown precipitate to show a positive result for the presence of carbohydrate (Kandelwal, 2000, Brain & Turner, 1975 and Harborne, 1973).

Test for Terpenoids

- ✓ The extract is treated with 1ml of 2, 4- dinitrophenyl hydrazine in 2M HCl. The Yellow orange color formation confirms the presence of terpenoids.
- ✓ **Salkowski test:** The extract was mixed with 2ml of chloroform and concentrated H₂SO₄ (3ml) is carefully added to form a layer. A reddish-brown coloration of the interface is formed to show positive result of the presence of terpenoids (Krishnaiah *et al.*, 2009).
- ✓ **Noller's test:** The extract is warmed with tin and thionyl chloride. Pink coloration indicates the presence of triterpenoids.





Ranjith and Maria

- ✓ **Liebermann Burchard test** - Extracts were treated with chloroform and filtered. The filtrate was mixed with few drops of acetic anhydride, boiled and cooled. Concentrated sulphuric acid was then added from the sides of the test tube and observed for the formation of a brown ring at the junction of two layers. Green coloration of the upper layer and the formation of deep red color in the lower layer would indicate the presence of sterols and triterpenoids respectively (Krishnaveni *et al.*, 1984).
- ✓ **Detection of Diterpenes:**
 - **Copper acetate Test:** Extracts were dissolved in water and treated with 3-4 drops of copper acetate solution. Formation of emerald green colour indicates the presence of Diterpenes.

Test for Phytosterols

- ✓ **Liebermann Burchard's test:** Extracts were treated with chloroform and filtered. The filtrates were treated with few drops of acetic anhydride, boiled and cooled. Conc. Sulphuric acid was added. Formation of brown ring at the junction indicates the presence of phytosterols.
- ✓ **Salkowski test:** In 2 ml of plant extract, 2ml of chloroform and 2 ml of concentrated H₂SO₄ was added and shaken well. Chloroform layer appeared red and acid layer greenish yellow fluorescent. This confirms the presence of sterols (Suman Kumar *et al.*, 2013).

Test for protein and amino acids

The extract (100 mg) is dissolved in 10 ml of distilled water and filtered through Whatman No. 1 filter paper and the filtrate is subjected to test for following tests:

- ✓ **Millon's test:** To 2 ml of filtrate few drops of Millon's reagent is added. A white precipitate or red colour indicates the presence of proteins.
- ✓ **Biuret test:** Equal volume of 5% solution of sodium hydroxide and 1% copper sulphate were added. Appearance of pink or purple or violet colour indicates the presence of proteins and free amino acids.
- ✓ **Test for Free Amino Acids: Ninhydrin Test:** Test solution when added and boiled with 0.25% w/v solution of Ninhydrin, would result in the formation of purple / blue color suggesting the presence of free amino acids.
- ✓ **Xanthoproteic Test:** The extracts were treated with few drops of conc. Nitric acid. Formation of yellow colour indicates the presence of proteins (Makkar *et al.*, 1993).

Tests for Lignin

- ✓ The extract was added with phloroglucinol and 1 ml of conc. HCl. The formation of red colour indicates the presence of lignin.

Tests for Gums and Mucilage's

- ✓ The extract (100 mg) is dissolved in 10 ml of distilled water and to this 2 ml of absolute alcohol is added with constant stirring. White or cloudy precipitate indicates the presence of Gums and Mucilages.

Tests for Volatile Oils

- ✓ For volatile oil estimation 50 mg of powdered material (crude drug) is taken and subjected to hydro-distillation. The distillate is collected in graduate tube of the assembly, wherein the aqueous portion automatically separated out from the volatile oil (Harbourne., 1973).



**Ranjith and Maria****Tests for Fixed Oil and Fats**

- ✓ **Spot test:** A small quantity of extract is pressed between two filter papers. Oil stain on the paper indicates the presence of fixed oils.
- ✓ **Saponification test:** A few drops of 0.5 N alcoholic potassium hydroxide solution is added to a small quantity of extract along with a drop of phenolphthalein. The mixture is heated on a water bath for 2 hours. Formation of soap or partial neutralization of alkali indicates the presence of fixed oils and fats (Obdoni and Ochuko, 2001).

Test for Emodols

- ✓ Evaporate 3 ml of etheric extract. Dissolve the dry residue in 1 ml of concentrated NH_4OH and treating the solution with the reagent Borntrager's. Appearance of a bright color ranging from orange red to purple indicates the presence of emodols.

Test for Anthracenosids

- ✓ Eight ml (8 ml) of the extract solution treated with the reagent Borntrager's, a positive test is revealed the appearance of a bright color change from orange red to purple.

Test for Anthocyanosids

- ✓ The presence of anthocyanosids is revealed by a color change as a function of pH due to titration of the acidic aqueous solution with a solution of NaOH . If the solution turns a red color, the pH is less than 3, if against a blue color; the pH is between 4 and 6 (Arumugam *et al.*, 2006).

Test for Coumarins

- ✓ Evaporate 5 ml of ethanolic solution, dissolve the residue in 1-2 ml of hot distilled water and divide the volume into two parts. Take half the volume as a witness and to add another volume of 0.5 ml 10% NH_4OH . Put two spots on filter paper and examined under UV light. Intense fluorescence indicates the presence of coumarins (Burden. 1983).

Test for Vitamin C

- ✓ **DNPH Test:** Test solution was treated with Dinitrophenyl hydrazine dissolved in concentrated sulphuric acid. The formation of yellow precipitate would suggest the presence of vitamin C.

REFERENCES

1. Singh, S. Medicinal plants-A Natural gift to mankind. *Agriculture today* 2005.3(3): 58-60 pp.
2. Vijayalatha, S.J. An Ornamental garden with medicinal plants an indirect approach for conservation of medicinal plants. *Indian J. Arecanut, spices and medicinal plants*. 2004. 6(3): 98-107.
3. Chessbrough M. Medicinal laboratory manual for tropical countries, Lianacre Houses. Volume II: Microbiology. Chap. 200;44:289-311. Butterworth-Heinemann Ltd., Linacre House, Jordan. Hill, Oxford.
4. Taiz Q and Zeiger E. Plant physiology 4th Edn. 2006;13: PP 315-344





Ranjith and Maria

5. Phan TT, Wang L, See P, Grayer RJ, Chan SY and Lee ST. Phenolic Compounds of *Chromolaena odorata* Protect Cultured Skin Cells from Oxidative Damage: Implication for Cutaneous Wound Healing. *Biol. Pharm. Bull.* 2001; 24(12):1373-1379.
6. Edeoga HO, Okwu DE and Mbaebie BO. Phytochemical constituents of some Nigerian medicinal plants. *Afr J Biotech.* 2005.4:685-688.
7. Pandey P, Mehta R and Upadhyay R. 2013. Physico-chemical and preliminary phytochemical screening of *Psoralea corylifolia*. *Arch Appl Sci Res.*, 5:261-265.
8. Narasinga Rao. Bioactive phytochemicals in Indian foods and their potential in health promotion and disease prevention. *Asia Pacific Journal of Clinical Nutrition*, 2003; 12 (1): 9-22
9. Mathai K. Nutrition in the Adult Years. In Krause's Food, Nutrition, and Diet Therapy, 10th ed., ed. L.K. Mahan and S. Escott-Stump, 2000; 271: 274-275.
10. Meagher E, Thomson C. Vitamin and Mineral Therapy. In Medical Nutrition and Disease, 2nd ed., G Morrison and L Hark, Malden, Massachusetts: Blackwell Science Inc, 1999; 33- 58.
11. Narasinga Rao. Bioactive phytochemicals in Indian foods and their potential in health promotion and disease prevention. *Asia Pacific Journal of Clinical Nutrition*, 2003; 12 (1): 9-22.
12. Remington JP. Remington: The science and practice of pharmacy, 21st edition, Lippincott Williams & Wilkins, 773-774.
13. Ncube NS, Afolayan AJ, Okoh AI. Assessment techniques of antimicrobial properties of natural compounds of plant origin: current methods and future trends. *African Journal of Biotechnology* 2008; 7 (12): 1797-1806.
14. Handa SS, Khanuja SPS, Longo G, Rakesh DD. Extraction Technologies for Medicinal and Aromatic Plants. International centre for science and high technology, Trieste, 2008, 21-25.
15. Eloff JN. Which extractant should be used for the screening and isolation of antimicrobial components from plants. *J of Ethnopharmacology* 1998; 60: 1–8.
16. Cosa P, Vlietinck A J, Berghe D V, Maes L. Anti-infective potential of natural products: How to develop a stronger in vitro 'proof-of-concept' *J Ethnopharmacol.* 2006;106:290–302
17. Cowan MM. Plant products as antimicrobial agents. *Clinical microbiology reviews* 1999; 12(4): 564-582.
18. N.K.Jain and Sharma. Text book of Professional Pharmacy. pg. 115
19. Azwanida NN. A Review on the Extraction Methods Use in Medicinal Plants, Principle, Strength and Limitation. *Med Aromat Plants.* 2015. 4:196. doi:10.4172/2167-0412.1000196.
20. Bimakr M. Comparison of different extraction methods for the extraction of major bioactive flavonoid compounds from spearmint (*Mentha spicata* L.) leaves. *Food Bioprod Process* 2010; 1-6.
21. Das K, Tiwari RKS, Shrivastava DK. Techniques for evaluation of medicinal plant products as antimicrobial agent: Current methods and future trends. *Journal of Medicinal Plants Research* 2010; 4(2):104-111.
22. David Milbradt L.Ac. Making Herbal Tinctures. 1998. Percolation Method
23. Nikhal SB, Dambe PA, Ghongade DB, Goupale DC. Hydroalcoholic extraction of *Mangifera indica* (leaves) by Soxhletion. *International Journal of Pharmaceutical Sciences* 2010; 2 (1): 30-32.
24. Patil PS, Shettigar R. An advancement of analytical techniques in herbal research *J Adv Sci Res.* 2010; 1(1):08-14.
25. Delazar A, Nahar L, Hamedeyazdan S, Sarker SD. Microwave-assisted extraction in natural products isolation. *Methods Mol Biol.* 2012; 864:89-115
26. Das K, Tiwari RKS, Shrivastava DK. Techniques for evaluation of medicinal plant products as antimicrobial agent: Current methods and future trends. *Journal of Medicinal Plants Research* 2010; 4(2): 104-111.
27. Eloff JN. Which extractant should be used for the screening and isolation of antimicrobial components from plants. *Journal of Ethnopharmacology* 1998; 60: 1–8.
28. Ncube NS, Afolayan AJ, Okoh AI. Assessment techniques of antimicrobial properties of natural compounds of plant origin: current methods and future trends. *African Journal of Biotechnology* 2008; 7 (12): 1797-1806.
29. Lapornik B, Prosek M, Wondra, A. G. Comparison of extracts prepared from plant by-products using different solvents and extraction time. *Journal of Food Engineering* 2005; 71: 214–222.
30. Bimakr M. Comparison of different extraction methods for the extraction of major bioactive flavonoid compounds from spearmint (*Mentha spicata* L.) leaves. *Food Bioprod Process* 2010; 1-6.



**Ranjith and Maria**

31. Wang GX. In vivo anthelmintic activity of five alkaloids from *Macleaya microcarpa* (Maxim) Fedde against *Dactylogyrus intermedius* in *Carassius auratus*. *Veterinary Parasitology* 2010; 171: 305–313.
32. Cowan MM. Plant products as antimicrobial agents. *Clinical microbiology reviews* 1999; 12(4): 564-582.
33. Nur Ain Binti. Effect of Different types of solvents on extraction of phenolic compounds from *Cosmos caudatus*, Faculty of Chemical Engineering & Natural Resources. Universiti Malaysia Pahang 2012.
34. Soni Anjali and Sosa Sheetal., 2013. Phytochemical Analysis and Free Radical Scavenging Potential of Herbal and Medicinal Plant Extracts. *Journal of Pharmacognosy and Phytochemistry* 2013; 2 (4): 22-29.9.
35. Brian and Turner (1975) Brian K.R. and Turner T.D., *Practical Evaluation of Phytochemicals*. Wright Scentechical, Bristol, UK, 1975; Pp. 57-59.
36. Rajaram S. S. and Ashvin G. G., *Asian Journal of Plant Science and Research*, 2013, 3(1):21-25.
37. Harbourne J.B. (1973). *Phytochemical methods of Analysis*, Jackmann and Hall, London, 64- 90.
38. Kokate C.K. (1998). *Qualitative Chemical Examination of Plant Constituents*, VallabhPrakashan, Mumbai, 92-93.
39. Kokate C.K., Purhohit A.P., Gokhale S.B. (2006). *Text book of Pharmacognosy*, NiraliPrakashan, Mumbai, 35-39.
40. Venkata Kullai Setty N., Santhosh D., Narasimha Rao D., 2011. Preliminary phytochemical screening and anti diabetic activity of *Zingiber officinale* rhizomes. *Intl J of Pharm& Life Sci.* 2(12).
41. Khandelwal, K. R. *Practical Pharmacognosy: Techniques and Experiment*. (V. Sethi, Ed.) (20th ed., pp. 25.1–25.9). Pune, India. 2000: NiraliPrakashan.
42. Brain, K.R., and T.D. Turner. *The practical evaluation of phytopharmaceuticals*, Wrightscience technical, 1st Ed , 1975. Bristol Britain., 144.
43. Harbone, J.B., 1973. *Phytochemical methods*. London. *Chapman and Hall, Ltd.*, 49-188.
44. Krishnaiah, D., T. Devi, A. Bono and R. Sarbatly. Studies on phytochemical constituents of six Malaysian medicinal plants. *J. Med. Plants. Res.* 2009. 3(2): 67-72.
45. Krishnaveni, S., B. Theymoli., S. Sadasivam, 1984. Phenol Sulphuric acid method. *Food chain.*, 15: 229
46. R. Suman Kumar, C. Venkateshwar , G. Samuel, S. Gangadhar Rao. Phytochemical Screening of some compounds from plant leaf extracts of *Holoptelea integrifolia* (Planch.) and *Celestrus emarginata* (Grah.) used by Gondu tribes at Adilabad District, Andhrapradesh, India. 2013.2(8).65-70.
47. Makkar H, Bluemmel M, Borowy N, Becker K. Gravimetric determination of tannins and their correlations with chemical and protein precipitation methods. *J Sci Food Agric* 1993; 61:161-165.
48. Harborne JB. *Phytochemical Methods*. Chapman and Hall Ltd., London; 1973; 49-188.
49. Obdoni BO, Ochuko PO. Phytochemical studies and comparative efficacy of the crude extracts of some Homostatic plants in Edo and Delta States of Nigeria. *Glob J Pure Appl Sci.* 2001; 8b: 203-208.
50. Arumugam P, Ramamurthy P, Santhiya ST, Ramesh A. Antioxidant activity measured in different solvent fractions obtained from *Mentha spicata* Linn: An analysis by ABTS, decolorization assay. *Asia Pac J Clin Nutr.* 2006; 15(1):119- 124.
51. Van-Burden T, Robinson W. Formation of complexes between protein and Tannin acid. *J. Agric. Food Chem* 1981; 1: 77.





Study of the Effect of the Conventional and Novel Insecticides on the Collembolan Population of Mango Ecosystem

Shinde M.P^{1*}, M. Raghuraman¹ and Chikte P.B².

¹Department of Entomology and Agriculture Zoology, Institute of Agricultural Sciences, Banaras Hindu University, Varanasi. – 221005, India.

²Agriculture Technology Information Centre, Dr. PDKV, Akola, India.

Received: 10 Aug 2017

Revised: 20 Aug 2017

Accepted: 27 Sep 2017

*Address for correspondence

Shinde M.P.,

Department of Entomology and Agriculture Zoology,
Institute of Agricultural Sciences,
Banaras Hindu University,
Varanasi. – 221005, India.

Email: mak.shinde2008@gmail.com, raghu_iari@yahoo.com, bhumi369@gmail.com



This is an Open Access Journal / article distributed under the terms of the **Creative Commons Attribution License** (CC BY-NC-ND 3.0) which permits unrestricted use, distribution, and reproduction in any medium, provided the original work is properly cited. All rights reserved.

ABSTRACT

Collembolan diversity enriches the soil health of an agro-ecosystem by degrading the soil litter. Little work has been done on the biodiversity of collembola in mango ecosystem, where the organic matter is rich due to fall of leaf litter. Various insecticides are being used to control the insect pests in Mango. Present investigation deals with the study of use of such insecticides, impacting non-target organism collembola. In present study the analysis based on the completely randomized block design reveals that Conventional and Inorganic insecticides show the significant effect on the population. For the study five insecticides (organic and inorganic), were used in different concentration viz. Monocrotophos (0.05% SL), Imidacloprid (0.005%), Nimbecidine (0.03% w/w), Cypermethrin (0.003% EC), and Thiamethoxam (0.25%) with Treatment treating from T1 to T5 respectively with T6 as control. While the recovery in the population of the collembola from 30.33/m² to 31.94/m² after the insecticide spray found in case organic insecticides (Thiamethoxam). *Entomobrya* sp., *Folsomia* sp., *Folsomides* sp., *Hypogastrura* sp., *Isotomorus* sp., *Onychiurus* sp., *Pseudosalina* sp., *Salina* sp. and *Sminthurus* sp. declined to average to low in quantity. *Anurophorus* sp., *Neelus* sp., *Sinella* sp., *Xenylla* sp. declined to low or no population was observed after the insecticide spray. *Cryptopygus* sp., *Lepidocyrtus* sp., did not respond much to the insecticides.

Keywords: Collembola, Mango, Ecosystem, organic and inorganic insecticides.



**Shinde et al.**

INTRODUCTION

Collembolans are important soil insect degrade the soil organisms by consuming the harmful algae, fungi, bacteria, actinomycetes, etc., reducing the growth of the moulds and add the faecal matter in the soil. Insecticides used for the control of insect pests on Mango, affect the population of collembola. Certain species of collembola are able to perceive insecticides, and it has been documented that *Folsomia fimetaria* avoids contact by retreating from insecticide contaminated sites (Fabian and Petersen, 1994 and Petersen and Gjelstrup, 1998). Campiche *et al.* (2006) evaluated the effect of several insect growth regulators (IGRs) on the nontarget soil arthropod *Folsomia candida* (Collembola). Fabian and Petersen (1994) evaluated the short-term effects of the insecticide Dimethoate on activity and spatial distribution of the soil-inhabiting Collembola. Joy and Chakravorty (1991) found that the density of total micro arthropods and major groups Acarina and Collembola found significant and persistent decline in Aldrin 30 EC and Endosulfan 35 EC treated wheat fields. In the present study the effect of the insecticides by considering mean population density derived against completely randomized block design. Five insecticides used for the evaluating the effect of the insecticides viz. Monocrotophos, Imidacloprid, Nimbecidine, Cypermethrin, and Thiamethoxam.

MATERIALS AND METHODS

For the present study five insecticides organic and inorganic, were used in different concentration viz. Monocrotophos (0.05% SL), Imidacloprid (0.005%), Nimbecidine (0.03% w/w), Cypermethrin (0.003% EC), and Thiamethoxam (0.25%) with Treatment treating from T1 to T5 respectively with considering T6 as control. These insecticides are sprayed in five different treatment plots of size 12 × 3m plots and other plot was kept Control. The total area under the experimentation was 252 m² which was under cover of Mango plantation. The soil samples were collected with the iron sampler and extracted by Tullgren's funnel (Plate 1).

The samples were exposed initially to less intensity of the lights for giving the low heat for the period of 12 hours and later on these samples exposed to the light and heat with increased temperature for full extraction of the soil biota. The biota was fully extracted with the help of illumination timer and light intensity controller. The specimen count was done by sampling on 1st, 2nd, 5th, 7th, 14th and 21st day. The mouth aspirator was also used for the counting the surface population of collembola.

RESULTS AND DISCUSSION

The collembolans are very sensitive soil arthropods to the Organic and Non Organic chemicals and can be included in risk assessments for improving risk prediction for soil invertebrate communities. The statistical analysis for evaluation of effect of insecticides on the population of Collembola was done by using Completely Randomized Block Design. It was observed that the mean population density of Collembola in the treatment T1 significantly decreased from the 1st day after spraying up to 7th day after spraying which was observed as 26.94/m² on 1st day after spraying and 21.17/m² on the 7th day after spraying. This value was observed comparatively lower than the population before insecticide spray which was observed 42.05/m².

During the study as the slight increase in population was observed in 14 days after spraying and on the 21st days after spraying it was near to initial population of Collembola before spraying. The same effect was observed in treatment T2 (Imidacloprid), T5 (Thiamethoxam) respectively. But in T3 (Nimbecidine) and T4 (Cypermethrin) there was increase in population growth of Collembola was observed from the 1st day after spraying. However in the control plot, the slight decrease in population was observed which was not significant. Data reveals a significant effect of insecticides on the population of Collembola. The effect of insecticides on the population increased from the 1st day after spraying up to the 14th day but on the 21st day the recovery in the population of Collembola was observed.



**Shinde et al.**

A similar trend was observed in the second spray of insecticides. In this evaluation, the population count of 21st day after first spray was taken as base observation and the subsequent observations were noted similarly (Table1 & Graph1). The significant effect of insecticides was observed in all the insecticidal treatments T1 (Monocrotophos), T2 (Imidacloprid), T3 (Nimbecidine), T4 (Cypermethrine) during the second spray (Table2 & Graph2). The regeneration of the soil fauna started earlier following Imidacloprid treatment then after the Carbofuran treatment. But the T5 (Thiamethoxam) showed slight effect of insecticides on the population. The recovery of population was 31.94/m² which was near about equal to the population before insecticide spray which was observed as 30.33/m². T2 (Imidacloprid) had a moderate effect on their population.

Some Collembolan species such as *Entomobrya* sp., *Folsomia* sp., *Folsomides* sp., *Hypogastrura* sp., *Isotomorus* sp., *Onychiurus* sp., *Pseudosalina* sp., *Salina* sp. and *Sminthurus* sp. which was present in higher amount, declined to average to low in quantity after the Insecticides spray. But some species such as *Anurophorus* sp., *Neelus* sp., *Sinella* sp., *Xenylla* sp. which was present in average in quantity before the insecticide spray, declined to low or no population was observed after the insecticide spray. Some species such as *Cryptopygus* sp., *Lepidocyrtus* sp., did not respond much to the insecticides as their population was not affected significantly by insecticides.

The overall conclusion of the work states that the recovery of Collembola was faster in insecticidal treatments Nimbecidine followed by Imidacloprid. According to the Stark (1992) Neem based formulations are ecofriendly and less detrimental to the soil fauna as compared to synthetic insecticides. The following data reveals the effect of the insecticides over the population of the collembola during the study.

ACKNOWLEDGEMENTS

The authors gratefully acknowledge the Indian Council of Agricultural Research Network Project on Insect Biosystematics for providing financial assistant.

REFERENCES

1. Campiche, S.; Becker-van Slooten, K.; Ridreau, C.; Tarradellas, J. (2006) *Ecotoxicology and Environmental Safety*, 63: 2, 216-225.
2. Fabian and H. Petersen. (1994). Short-term effects of the insecticide dimethoate on activity and spatial-distribution of a soil inhabiting collembolan *Folsomia fimentaria* Linné Collembola, Isotomidae, *Pedobiologia* 38: 289–302.
3. Frampton, G. K. (2000). Recovery responses of soil surface Collembola after spatial and temporal changes in long-term regimes of pesticide use. *Pedobiologia*. 44:3/4, 489-501.
4. Joy, V. C. Chakravorty, P. P. (1991). Impact of insecticides on nontarget microarthropod fauna in agricultural soil. *Ecotoxicology and Environmental Safety*. 22: 1, 8-16.
5. Stark, J.D. (1992). Comparison of the impact of a neem seed-kernel extract formulation 'Margosan-O' and chlorpyrifos on no-target invertebrates inhabiting turf grass, *Pesticide Science*. 36 : 293–299.





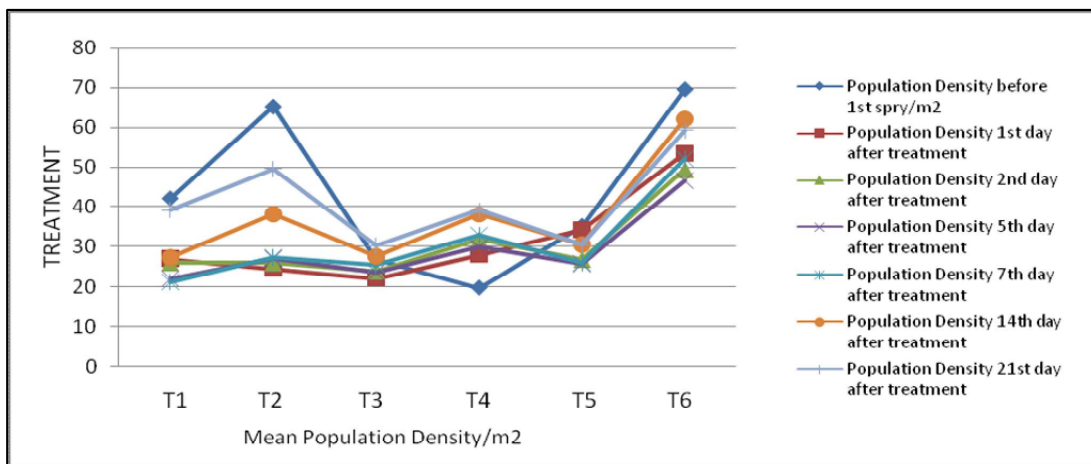
Shinde et al.



Plate 1: Tullgren's dry funnel soil biota extractor

Table 1: Population density of Collembola after 1st spray

Treatment	Population Before 1 st spray/m ²	Mean population/m ² of collembola (days after treatment)					
		1 st	2 nd	5 th	7 th	14 th	21 st
T1	42.05	26.94	26.04	22.00	21.17	27.17	39.14
T2	65.28	24.61	25.93	27.03	27.23	38.07	49.51
T3	26.97	22.11	23.88	23.67	25.48	27.51	30.17
T4	19.73	27.83	31.77	29.83	32.87	37.98	39.03
T5	35.07	34.12	26.83	25.70	25.80	30.33	30.33
T6	69.59	53.43	49.38	46.67	52.08	62.20	59.23
CD	18.60	6.90	3.59	6.59	4.82	5.06	7.18
SEm _±	8.54	3.17	1.65	3.03	2.21	2.32	3.29



Graph1: Effect of Insecticidal spray on population of Collembola after 1st spray

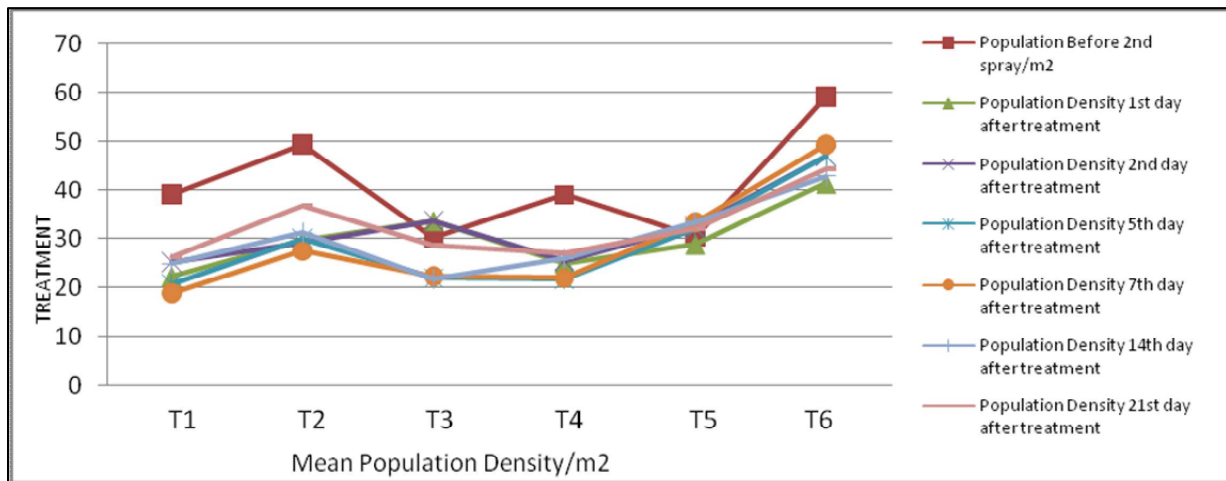




Shinde et al.

Table 2. Population density of Collembola Before 2nd spray

Treatment	Population Before 2 nd spray/m ²	Mean population/m ² of collembola (days after treatment)					
		1 st	2 nd	5 th	7 th	14 th	21 st
T1	39.14	22.33	25.10	20.76	18.76	24.82	26.15
T2	49.51	29.53	29.07	30.07	27.40	31.07	36.65
T3	30.17	33.64	33.64	21.97	22.30	21.64	28.64
T4	39.03	25.07	25.47	21.83	21.83	25.80	27.03
T5	30.33	28.83	32.48	31.99	33.33	33.33	31.94
T6	59.23	41.39	47.02	47.02	49.35	42.72	44.40
CD	7.18	9.11	8.08	6.06	7.15	6.04	9.23
SEm _±	3.29	4.18	3.71	2.78	3.28	2.77	4.24



Graph 2: Effect of Insecticidal spray on population of Collembola after 2nd spray





Purification and Characterisation of Gelatin Binding Proteins from Vechur Bull Seminal Plasma

Mahalingeshwara H.S^{1*}, Abdul Azeez C.P²., Hiron M.Harshan², K.Promod³ and Manoj M⁴.

¹M.V.Sc. Scholar, Department of Animal Reproduction Gynaecology and Obstetrics, College of Veterinary & Animal Sciences, Pookode, Waynad-673576, Kerala, India.

²Assistant Professor,, Department of Animal Reproduction Gynaecology and Obstetrics, College of Veterinary & Animal Sciences, Pookode, Waynad-673576, Kerala, India.

³Assistant Professor and Head (i/c), Dept. of Animal Reproduction, Gynaecology and Obstetrics. College of Veterinary & Animal Sciences, Pookode, Waynad-673576, Kerala, India.

⁴Assistant Professor, Dept. of Animal Genetics and Breeding, College of Veterinary & Animal Sciences, Mannuthy, Kerala, India.

Received: 12 Aug 2017

Revised: 21 Aug 2017

Accepted: 26 Sep 2017

Address for correspondence

Mahalingeshwara H.S

M.V.Sc. Scholar, Department of Animal Reproduction Gynaecology and Obstetrics,
College of Veterinary & Animal Sciences,
Pookode, Waynad-673576, Kerala, India.
Email: mahalingeshwara007@gmail.com



This is an Open Access Journal / article distributed under the terms of the **Creative Commons Attribution License** (CC BY-NC-ND 3.0) which permits unrestricted use, distribution, and reproduction in any medium, provided the original work is properly cited. All rights reserved.

ABSTRACT

Seminal plasma collected from three Vechur bulls, were subjected to Gelatin affinity chromatography to purify Gelatin binding fraction of seminal plasma proteins. The total seminal plasma protein and GBP content was estimated by Lowry's method. The molecular weight of isolated GBP was determined by SDS-PAGE. The mean content of whole seminal plasma protein in Vechur bull semen was 126.48 ± 7.36 mg/ml, while GBP accounted for 50.19 per cent of the total seminal plasma protein.

Keywords: Gelatin affinity Chromatography, Seminal plasma protein, SDS-PAGE profile, Vechur bull seminal plasma.

INTRODUCTION

Binder of sperm protein (BSP), represents the major class of proteins in seminal plasma of ungulates. The proteins have been reported to play a major role in multiple aspects of fertilization including capacitation and sperm reservoir formation. In addition, they have been reviewed to influence the cryopreservability of bovine semen. The bovine seminal plasma has four distinct BSP proteins, designated as BSP-A1, BSP-A2, BSP-A3 and BSP-30 kDa. (Chandonnet *et al.*, 1990). These proteins interact with choline phospholipids on the spermatozoal membrane and

12810



**Mahalingeshwara et al.**

plays a vital role in the membrane stabilization and subsequent destabilization process (Manjunath *et al.*, 2002). BSP proteins show presence of two type-II domains, similar to gelatin binding domains of fibronectin (Ecshtet *et al.*, 1983). These proteins form reversible complexes with collagen and its denatured derivative, gelatin (Manjunath *et al.*, 1987). This binding property has been used to isolate BSP's from seminal plasma. Homologues of BSP proteins have been demonstrated in buffalo, pure bred and cross bred cattle, stallion, boar and buck but not in Vechur bulls. The present study was therefore undertaken with the objectives of isolating and characterizing the BSP proteins based on their gelatin binding property in Vechur bull seminal plasma.

MATERIALS AND METHODS

Experimental animals and source of semen

Nine ejaculates were obtained from three adult healthy breeding Vechur bulls maintained at CAS AGB, College of Veterinary and Animal Sciences, Mannuthy, Thrissur. Ejaculates were supplemented with a protease inhibitor cocktail (10µl/ml) immediately post collection and centrifuged (1000×g for 30 min at 5°C) to separate seminal plasma and sperm cells. The supernatant plasma was collected and re-centrifuged (10,000×g for 10 min at 5°C) further to clarify the plasma from cell debris and stored at -80°C until analysis.

Protein purification by Gelatin-Sepharose affinity chromatography

The purification of gelatin binding fraction of seminal plasma was carried out as per the method described by Manjunath *et al.* (1987). Five ml of coupled gelatin-Sepharose media was loaded on to chromatography column and regenerated by washing with buffers of alternating high pH (0.1 M Tris-HCl, 0.5 M NaCl, pH 8.5) and low pH (0.1 M sodium acetate, 0.5 M NaCl, pH 4.5) five times. The column was equilibrated with 20 bed volumes of equilibration buffer [50 mM Tris-HCl (pH 7.6), 0.15 M NaCl, 10 mM EDTA, 2mM PMSF and 0.025% sodium azide]. Clear seminal plasma was diluted 3× with equilibration buffer and loaded onto the equilibrated gelatin-Sepharose column. Following a holding period of 30 min, the column was extensively washed with 20 bed volumes of equilibration buffer to remove unadsorbed proteins. The unbound fraction obtained from the Gelatin-agarose column before elution of gelatin binding protein (GBP), was cycled again in the column to obtain a fraction completely free of GBP fraction. The adsorbed gelatin binding proteins were eluted in 3 ml fractions with elution buffer [50 mM Tris-HCl buffer (pH 7.4), 10 mM EDTA, 2mM PMSF, 0.025% sodium azide and 8 M urea]. The column was washed thoroughly with the equilibration buffer and stored in storage buffer at 5°C. The eluted fractions were monitored in spectrophotometer at 280 nm. The GBP and Non-Gelatin binding protein (NGBP) fractions were pooled separately and dialysed at 4°C against 50 mM ammonium bicarbonate, lyophilized and stored at -20°C.

Quantification of protein

Protein concentration of whole seminal plasma, NGBP fraction and GBP fraction was determined as per the protocol of Lowry *et al.* (1951).

SDS-PAGE profiling of seminal plasma proteins

Discontinuous SDS-PAGE was carried out in according to Laemmli (1970) in 12 % polyacrylamide gel. Around 15 -20 µL of protein samples and standard molecular weight marker (Merck, Perfect Protein Mkr, 15-150kDa.) were loaded into the well and run at a constant voltage of 80 V. The gel was stained with Coomassie brilliant blue R 250 dye. Apparent molecular mass was determined by Gel documentation and analysis-system (ChemiDoc™ MP Imaging System, Bio-Rad, USA).



**Mahalingeshwara et al.**

RESULTS AND DISCUSSION

Gelatin-Sepharose affinity chromatography profile of Vechur bull seminal plasma is represented in Fig.1. The mean concentration of total protein in crude seminal plasma was found to be 126.48 ± 7.36 mg/ml (range 94.25 to 157.78 mg/ml), which was in agreement with the earlier results reported by Noolvi (2015) and Karthikeyan (2015) in Vechur bulls. Overall mean concentration of GBP and NGBP was 45.54 and 47.23 mg/ml, which represented 49.09 per cent and 50.91 percent of total protein in seminal plasma respectively. Manjunath *et al.* (2002) earlier reported BSP proteins in seminal plasma accounts for 40 to 57 per cent of proteins in bovine semen. Buffalo bulls were reported to have a much lower gelatin binding protein concentration of 3.25 mg/ml (Arangasamy *et al.*, 2005). Concentration and composition of seminal plasma protein vary with animals and environmental factors such as season, nutrition and pre-coital stimulus (Juyena. *et al.*, 2012). Separation pattern of crude seminal plasma on SDS-PAGE indicated presence of 15 protein bands in the range of 12–180 kDa, out of which 12 were NGBP bands. Three major GBP bands were isolated in the molecular weight range of 14 kDa, 16 kDa and 26 kDa with 16 kDa band being intense. The bands representing BSP-A1/A2 were very close and observed as a single thick band on 12% gel slab. (Fig. 2, lane 1,2,3).

Arangasamy *et al.* (2005) observed 18 bands in crude seminal plasma of buffalo. Gelatin-agarose affinity chromatography is a single step affinity purification method developed by Manjunath *et al.* (1987) for the isolation of Fn-2 type of proteins from bovine seminal plasma. BSP proteins have been shown to have fibronectin type-II domains, similar to gelatin binding domains of fibronectin (Esch *et al.*, 1983). Gelatin binding property of BSP-like antigens have also been reported in the seminal plasma of rat, mouse, hamster, porcine, human (Leblond *et al.*, 1993), goat (Villemure *et al.*, 2003) and buffalo (Harshan *et al.*, 2006). Homologous proteins from porcine (pB1) and equine (HSP-1 and HSP-2) seminal fluids have been isolated. (Calvete *et al.*, 1995). The technique was proved to be simple and reliable for isolation and purification of Fn-2 type proteins from seminal plasma. Fn-2 type proteins have been found to have deleterious effects on the freezability of semen. Thus, validating the presence of Fn-2 type proteins in seminal plasma of Vechur bull seminal plasma opens up vistas to improve freezability of Vechur bull semen.

ACKNOWLEDGEMENTS

Authors are thankful to the staff of Artificial Insemination centre and Department of Animal Reproduction Gynaecology & Obstetrics, CVAS, Pookode for infrastructural support. The support provided by the Dean, CVAS, Pookode and The Director (Academics and Research), KVASU are acknowledged.

REFERENCES

1. Arangasamy, A., Singh, L.P., Ahmad, N., Ansari, M.R., Ram, G.C., 2005. Isolation and characterization of heparin and gelatin binding buffalo seminal plasma proteins and their effect on cauda epididymal spermatozoa. *Anim. Reprod. Sci.* 90, 243–254.
2. Calvete, J.J., Mann, K., Schafer, W., Sanz, L., Topfer-Petersen, E. 1995. Amino acid sequence of HSP-1, a major protein of stallion seminal plasma: effect of glycosylation on heparin- and gelatin-binding capabilities. *Biochem. J.*, 310:615-622.
3. Chandonnet, L., Roberts, K.D., Chapdelaine, A., Manjunath, P., 1990. Identification of heparin-binding proteins in bovine seminal plasma. *Mol. Reprod. Dev.* 26, 313–318.
4. Esch, F.S., Ling, N.C., Bohlen, P., Ying, S.Y. and Guillemin, R. 1983. Primary structure of PDC-109, a major protein constituent of bovine seminal plasma. *Biochem. Biophys. Res. Commun.*, 113:861-867
5. Harshan, H.M., Singh, L.P., Arangasamy, A., Ansari, M.R., Kumar, S., 2006. Effect of buffalo seminal plasma heparin binding protein (HBP) on freezability and in vitro fertility of buffalo cauda spermatozoa. *Anim. Reprod. Sci.* 93 (1-2), 124–133.
6. Juyena, N.S. and Stelletta, C., 2012. Seminal plasma: an essential attribute to spermatozoa. *Journal of andrology*, 33, pp.536-551.





Mahalingeshwara et al.

7. Karthikeyan, K., 2015. Isolation and characterization of pdc-109 like protein(s) from Vechur bull seminal plasma. *M. V. Sc. Thesis*, Kerala Veterinary and Animal Sciences University, Pookode, 35p.
8. Laemmli, V.K., 1970. Cleavage of structural proteins during the assembly of the head of bacteriophage T4. *Nature (London)* 227, 660–685.
9. Leblond, E., Desnoyers, L. and Manjunath, P. 1993. Phosphorylcholine-binding proteins from the seminal fluids of different species share antigenic determinants with the major proteins of bovine seminal plasma. *Mol. Reprod. Dev.* 34: 443-449.
10. Lowry, O.H., Rosenbrough, N.J., Farr, A.L., Randall, R.J., 1951. Protein measurement with the folin phenol reagent. *J. Biol. Chem.* 193, 265–275.
11. Manjunath, P. and Sairam, M. R. 1987. Purification and biochemical characterization of three major acidic proteins (BSP-A1, BSP- A2, and BSP A3) from bovine seminal plasma. *Biochem. J.* 241: 685–69.
12. Manjunath, P., Chandonnet, E., Leblond, E., Desnoyers, S.L., 1994. Major proteins of bovine seminal vesicles bind to spermatozoa. *Biol. Reprod.* 50, 27–37.
13. Manjunath, P., Nauc, V., Bergeron, A. and Menard, M. 2002. Major proteins of bovine seminal plasma bind to the low-density lipoprotein fraction. *Biol. Reprod.*, 67:1250-1258.
14. Noolvi, A. 2015. Isolation and characterization of major fertility-associated proteins from seminal fluid of Vechur and crossbred bulls. *M. V. Sc. Thesis*, Kerala Veterinary and Animal Sciences University, Pookode, 36p.
15. Villemure, M., Lazure, C. and Manjunath, P. 2003. Isolation and characterization of gelatin-binding proteins from goat seminal plasma. *Reprod. Biol. Endocrinol.* 1: 39.

Table 1. Concentration of protein in Vechur bull seminal plasma

Bull no.	Average total protein (mg/ml)	NGBP (mg/ml)	GBP (mg/ml)
1 (n = 3)	103.86±4.97	37.605±1.77	39.975±3.77
2 (n = 3)	134.23±10.74	47.84±2.20	46.30±5.08
3 (n = 3)	141.36±10.61	51.19±1.45	54.86±2.80
Overall mean ± SE	126.48±7.36	45.54±2.24	47.23±3.01

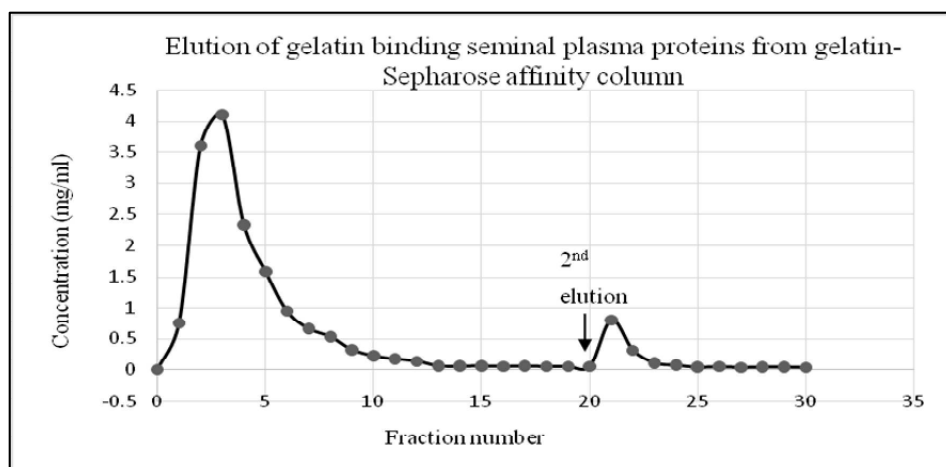


Fig.1: Gelatin-agarose affinity chromatography profile of Vechur Seminal plasma proteins. Clear bovine seminal plasma was loaded on the column. After washing the column, the adsorbed proteins were eluted with 8M urea.



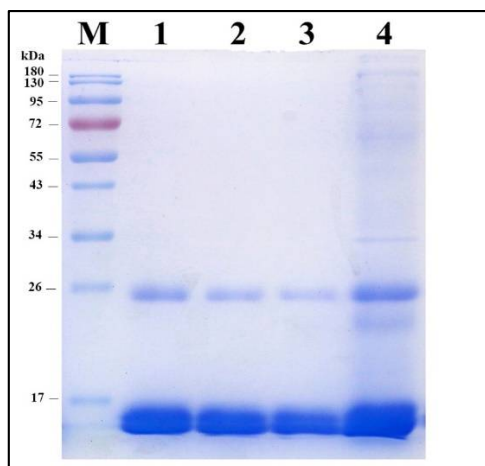


Fig. 2

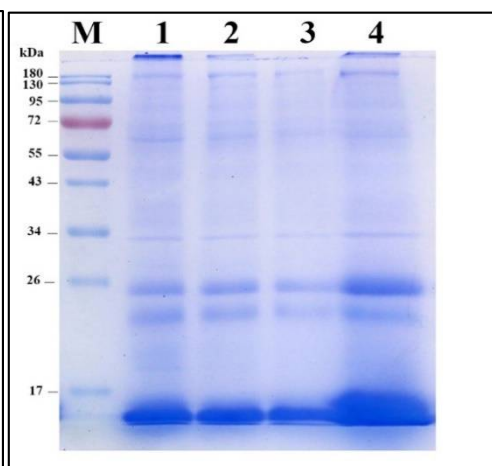


Fig. 3

Electrophoretic pattern of whole seminal plasma protein, GBP and NGBP fraction of Vechur bull seminal plasma. Approximately 5 μ g of denatured protein under reduced condition was loaded in each well in 12% gel cast. (Fig. 2. M: marker; 1,2,3: GBP; 4 crude protein) (Fig. 3; M: marker; 1,2,3 NGBP; 4 crude protein)





RESEARCH ARTICLE

Impact of Climate Change on Length of Growing Period in Western Zone of Tamil Nadu

MugilanGovindasamy Raman*, RagunathKaliaperumal and S.Shanmugapriya

Department of Remote Sensing and GIS, Tamil Nadu Agricultural University, Coimbatore -641003, Tamil Nadu, India.

Received: 15 Aug 2017

Revised: 29 Aug 2017

Accepted: 29 Sep 2017

Address for correspondence

Mugilan Govindasamy Raman

Scholar, Department of Remote Sensing and GIS,
Tamil Nadu Agricultural University,
Coimbatore -641003, Tamil Nadu, India.
Email: mugilantnau@gmail.com



This is an Open Access Journal / article distributed under the terms of the **Creative Commons Attribution License** (CC BY-NC-ND 3.0) which permits unrestricted use, distribution, and reproduction in any medium, provided the original work is properly cited. All rights reserved.

ABSTRACT

Climate change is a long-term shift in the statistics of the weather for a given place and time of year, from one decade to the next. Records have shown that future climate change will negatively affect crop production in low latitude countries, while effects in northern latitudes may be positive or negative. Climate change will probably increase the risk of food insecurity. There are numerous potential effects of climate change. Extensive research is being done around the world to determine the extent to which climate change is occurring, how much it affects the agriculture and its potential impacts. The one way of assessing the climate change impact is by determining the length of growing period of crops (LGP). LGP can be combined with or compared to other aspects of projected climate change such as temperature changes to create a more detailed picture of how climatic shifts could affect crop growth and development. The study area covers 16 districts falling to the Western Zone of Tamil Nadu. The processing of satellite data and other products require tedious iterations and involve raster calculations. Length of growing period requires two products viz., Rainfall and Evapotranspiration. The project aims in estimating the changes in LGP over years at block level. Hence the block map of Tamil Nadu available with the department of Remote Sensing and GIS, TNAU will be used for the purpose. The shift and change in the LGP as ascertained from this project for the western districts of Tamil Nadu reveal that there is certain shift in both positive and negative direction. The blocks with positive shift like increase in LGP with not much change in the start of season are potential areas for diversifying crops and possibilities of crop intensification whereas, the blocks that show negative trend with major shift in the start of season and reduction in the LGP are areas of major concern, where alternate crop planning is important.

Keywords: Climate change, length of growing period of crops (LGP), satellite data, Remote Sensing and GIS.



**Mugilan et al.**

INTRODUCTION

Climate change is a long-term shift in the statistics of the weather for a given place and time of year, from one decade to the next. Climate change and agriculture are interrelated processes, both of which take place on a global scale. Climate change affects agriculture in a number of ways, including changes in average temperatures, shift in rainfall patterns and climate extremes. Records have shown that future climate change will negatively affect crop production in low latitude countries, while effects in northern latitudes may be positive or negative. Climate change will probably increase the risk of food insecurity. The last decade of the 20th Century and the beginning of the 21st have been the warmest period in the entire global instrumental temperature record, starting in the mid-19th century. Along with increases in temperature, global warming is associated with changes in large-scale hydrological cycle elements such as an increase in atmospheric water vapour, shifting precipitation patterns, changes in precipitation intensity and extreme events, reduced snow cover and extensive melting of ice, and variations in soil moisture content and runoff. Studies have shown that precipitation has generally increased from 1900 to the 1950s, but has declined after 1970 to present. There are numerous potential effects of climate change. Extensive research is being done around the world to determine the extent to which climate change is occurring, how much it affects the agriculture and its potential impacts. The one way of assessing the climate change impact is by determining the length of growing period of crops (LGP). The correct choice of planting time is one of the most important decisions that a producer needs to make. The climatic requirements of the crop should be matched to the expected conditions applicable to the specific production site selected, if a successful crop is to be produced. In order for plant growth to take place during favourable conditions and when aiming to harvest at a specific time, it is essential to know approximately how long it will take the crop to reach market maturity, as well as the length of the cropping season. The length of growing period (LGP) is the period (in days) during a year when precipitation exceeds half the potential evapotranspiration ($P > 0.5PET$). Such a period meets the full evapotranspiration demands of crops and replenishes the moisture definite of soil profile. The growing season often determines which crops can be grown in an area, as some crops require long growing seasons, while others mature rapidly. A period required to 2 evapotranspire an assumed 100mm of water from excess precipitation stored in the soil profile is sometimes added. The spatial distribution of crops and farming systems in any region is determined by LGP. Studies show that climate change may significantly increase or decrease the length of growing periods (LGP) of crops. Changes in the length of the growing season can have both positive and negative effects. Moderate warming can benefit crop and pasture yields in mid to high-latitude regions, yet even slight warming decreases yields in seasonally dry and low latitude regions. A longer growing season could allow farmers to diversify crops or have multiple harvests from the same plot. However, it could also limit the types of crops grown, encourage invasive species or weed growth, or increase demand for irrigation. Temperature increases and rainfall changes could push some of these areas to a point where cropping may fail in most years. Some farmers may be able to adapt to shorter growing seasons by planting varieties that mature more quickly other farmers may need to change to more drought and heat-tolerant crops. Increase in LGP may present more growing opportunities, but it is uncertain how the change in growing time would impact soil moisture. As climate changes, the distribution of crop pests and diseases may change too. LGP can be combined with or compared to other aspects of projected climate change such as temperature changes to create a more detailed picture of how climatic shifts could affect crop growth and development. The conventional method of estimating LGP from Meteorological stations data have become obsolete on a spatial scale due to restrictions and unavailability of data. Remote Sensing based estimates of meteorological parameters have now gained momentum due to its availability and easy access. In NOAA-AVHRR satellites (Bella, 2000; Boni et al., 2001; Jiang and Islan, 2001), the image-derived surface temperature was in establishing the regression equation with evapo-transpiration. However, this scheme cannot represent the regional variation of evapotranspiration either. Kuo, et al., (2005) demonstrated a novel scheme applying remote sensing data in estimating evapo-transpiration with Penman method. The required variables of Penman method were derived from the AVHRR satellite images by regression analysis. By this method, the remote sensing application could estimate the regional evapo-transpiration, without using the atmospheric data observed at ground level.



**Mugilan et al.**

Brigitte Mueller, et al., (2015) investigated the annual temperature-based index and the growing season length (number of days with temperature above 5 °C). The analyses also showed that climate change has increased the probability of extremely long growing seasons by a factor of 25, and decreased the probability of extremely short growing seasons. An expansion of areas with more than 150 days of growing season into the northern latitudes makes more land potentially available for planting wheat and maize. The alternative to current practices is double cropping in areas with very long growing seasons. The results suggested that there is a strong impact of anthropogenic climate change on growing season length.

MATERIALS AND METHODS

Study area Tamil Nadu is located in Southern India with latitude of 11.1271oN and longitude of 78.6569oE with a total geographical area of 130,058 sq.kms bordered by Kerala to the west, Karnataka to the northwest, Andhra Pradesh to the north, the Bay of Bengal to the east and the Indian Ocean to the south. The study area covers 16 districts falling to the Western Zone of Tamil Nadu (Fig.1), which lies between 77.67° and 80.35° E latitude and 8.32o and 13.56° N longitude with a total geographical area 64.71 lakh hectares.

Software's and Programming language

The processing of satellite data and other products require tedious iterations and involve raster calculations. Hence a Geographic Information System software ArcGIS version 10.1 will be use used for the vector and raster based calculations. Python language which is compatible with ArcGIS will also be involved in extracting of the downloaded data to .img format (Compatible Raster format with ArcGIS software) and for doing iterative complex calculations in estimation of PET.

Remote Sensing Products

Length of growing period requires two products viz., Rainfall and Evapotranspiration. Precipitation product from Tropical rainfall measuring mission (TRMM) satellite at 0.25o (approx. 25 km) will be downloaded from NASA website using the Warehouse Inventory Search Tool. Evapotranspiration products for direct free download are limited and moreover available at courser scale. Hence PET is estimated from a set of meteorological products estimated through remote sensing. Data for four years viz., 2000, 2005, 2010 and 2013 will be processed.

Extraction to points

The project aims in estimating the changes in LGP over years at block level. Hence the block map of Tamil Nadu available with the department of Remote Sensing and GIS, TNAU will be used for the purpose. LGP Raster processed will be of 25 km grid output. Hence to convert the information at block level, Zonal statistics will be calculated at block level to consolidate the values followed by extracting the values to point file representing each block for further processing. The temporal 8 days composite LGP data generated from processing will be transferred to point file using Extract Multi values to point tool of ArcGIS.

Change detection and Delineation of Risk Zones

The data extracted to points will be analyzed year wise for 2000, 2005, 2010 and 2013 separately to find out the starting and ending of growing periods for different blocks. Apart from this the No. of seasons for each block will also be determined. From the individual year growing period, comparison will be done to determine the changes in the length of growing period in relation to the start and ending of the period. Finally the blocks will be classified to zones of risk for growing rainfed crops based on the LGP.





RESULTS AND DISCUSSION

Growing Seasons

A growing season is the period of the year when crops and other plants grow successfully. The length of a growing season varies from place to place. Most crops need a growing season of at least 50 days. Hence a minimum of 50 days is considered as a season for the delineation. For each year under investigation, the number of seasons (grouping of continuous number of days above 50% PET) was determined. The blocks were grouped according to the number of seasons. Analysis for determining growing seasons for the years under investigation revealed that, there were no significant correlations between years on number of seasons, as there was no trend in season identified. In the year 2000, there were 2 seasons with one season area dominating followed by lesser areas of two seasons. Some blocks were also found to have no predominant season. During 2005, the situation was completely different, showing equal areas of single and double season areas. Few blocks were found to have three growing seasons. Similar trend was also reflected during the 2010 year, except for the shift in seasons of different blocks. Few blocks in 2010 were also found with no prominent season. The year 2013, reflected a similar condition of 2000 with major area of one season and few blocks with two seasons and also no season condition. The irregular trend reflected through the analysis clearly depicts the situation of shifts in normal patterns of meteorological parameters viz., rainfall and PET. The abnormalities in the trend can be attributed to the changing climatic parameters (Fig. 2,3,4,5).

Length of Growing Season

LGP is useful in determining crop cycle lengths and calendars under average conditions. Actual years may sometimes depart significantly from the average. Based on the temporal analysis of 8 day composite, LGP maps were created by reclassifying the number of days to 6 classes viz., less than 50, 50-70, 70-100, 100-120, 120-150 and above 150 days. Season wise length of growing period for the years under study the major season for each year is mapped and used for the change detection studies. The LGP maps are presented in the fig 6, 7, 8 & 9. The LGP for Western Zone during the year 2000 showed that the most of the area having growing season between 70-100 days. Few blocks were found to fall between 50-70, 100-120 and 120-150. There were good areas under above 150 days. During the year 2005, 16 most of the area has growing season between 100-120 days. There were also some areas with 50-70, 100-120, 120-150 and above 150 days. Considering the two years, 2005 was found to be good year for crop growth as most of the blocks had a LGP of more than 70 days.

The LGP during the year 2010 and 2013 shows most of the area with growing season more than 150 days indicating a good rainfall and favorable cropping year except for increased area during the year 2013, which fall under less than 50 days of LGP. Keeping the year 2000 as standard, the Length of Growing period over the years has shown both positive and negative trend. There was increase in the LGP in the blocks of western parts of the zone while a decreasing trend in the southern and mid parts of the zone (Fig. 6,7,8,9).

Change detection

The changes in the length of growing period starting from year 2000 to 2013 were analyzed and the trend was determined. The results show that there were blocks which show an increased LGP and also areas with reduction in the LGP. Most blocks were found to have no change in the LGP (21.07 lakh hectares). About 27.44 lakh hectares of area was found have increased LGP days of more than 20 days over the past and about 12.40 lakh hectares have reduction in the LGP of more than 20 days (Table. 2). The increased LGP can have a positive impact on the crop diversification and crop selection. The reduction in the LGP can have an adverse effect on the existing cropping system in those areas. Although there were both positive and negative changes in the days of LGP as revealed from the analysis, the changes on the start of growing season is considered to be one of the important factor for better management of crop (Crop planning and crop selection). A slight shift in the start of the season is determinant for



**Mugilan et al.**

crop growth. Based on this importance, the change in start of season was analyzed with 2000 as standard year. Two types of classification were carried out with difference in number of shifting days. First classification was based on the shift of more than 50 days. The shift in start of season from 2000 year was found to be on both sides. Classification showed that major area falls under the category of backward shift more than 50 days followed by area under No change and forward shift of more than 50 days category. Second classification was based on shift of number of weeks. The results reveal that, major area was under No change category followed by forward shift of more than 2 weeks (Fig.10,11).

CONCLUSION

Length of Growing Season is useful in determining crop cycle lengths and calendars under average conditions. Actual years may sometimes depart significantly from the average. The calculation of the growing period is based on a simple water balance model, comparing water availability with crop water demand (precipitation with PET), using monthly values. A "normal" growing period is characterized by a dry period, a moist period and a wet period. In tropical regions, where it is warm year-round, the growing season can last the entire year. However in some tropical places, the growing season is interrupted by a rainy season. Understanding the phenomena with respect to climate change is one need of the hour to manage the crop growing situations. The changes in the rainfall pattern viz., quantity of rainfall and distribution and temperature variation in the climate change scenario influence the LGP. The shift and change in the LGP as ascertained from this project for the western districts of Tamil Nadu reveal that there is certain shift in both positive and negative direction. The blocks with positive shift like increase in LGP with not much change in the start of season are potential areas for diversifying crops and possibilities of crop intensification whereas, the blocks that show negative trend with major shift in the start of season and reduction in the LGP are areas of major concern, where alternate crop planning is important.

Future Thrust

1. Detailed studies on the causes for the shift in LGP are needed to understand the phenomena and manage effectively.
2. Continuous monitoring of changes in the phenomena is to be carried out to predict the future scenario.

REFERENCES

1. Mueller, B., Hauser, M., Iles, C., Rimi, R.H., Zwiers, F.W. and Wan, H., 2015. Lengthening of the growing season in wheat and maize producing regions. *Weather and Climate Extremes*, 9, pp.47-56.
2. Di Bella, C.M., Rebella, C.M. and Paruelo, J.M., 2000. Evapotranspiration estimates using NOAA AVHRR imagery in the Pampa region of Argentina. *International Journal of Remote Sensing*, 21(4), pp.791-797.
3. Jiang, L. and Islam, S., 2001. Estimation of surface evaporation map over southern Great Plains using remote sensing data. *Water resources research*, 37(2), pp.329-340.
4. KUO, C., Du, R.H., Lin, C.Y. and Yu, P.S., 2005, November. Using Penman-Monteith method to estimate potential evapotranspiration in Taiwan by using AVHRR and MODIS satellites remote sensing data. In *The 26th Asian Conference on Remote Sensing, Hanoi, Vietnam, NSC-91-2211-E-006-038*





Mugilan et al.

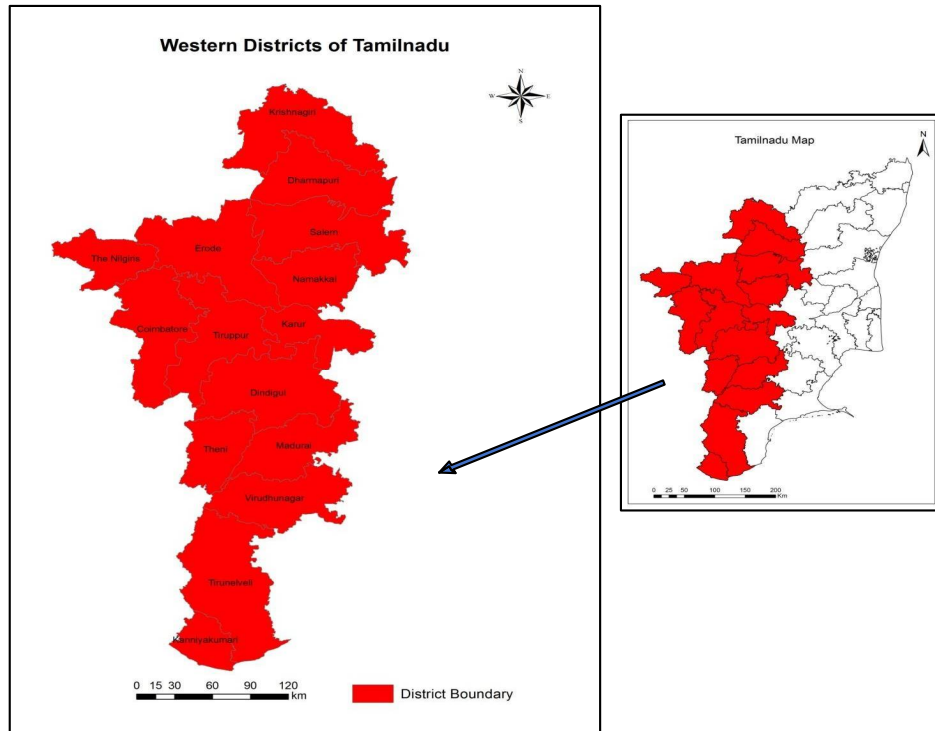


Fig.1. Location Map of the Study Area

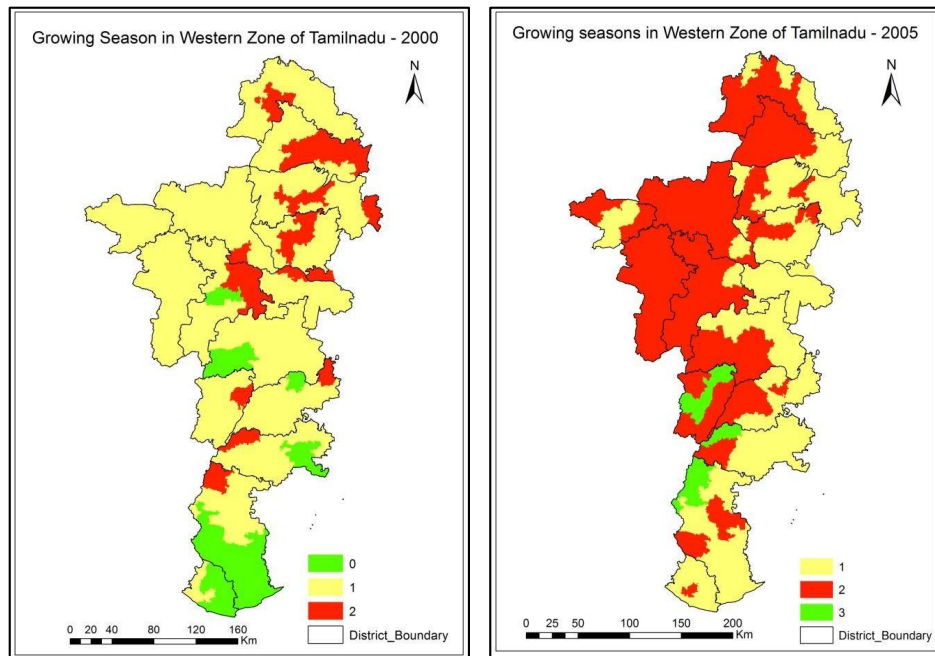


Fig.2 & 3. Growing Season in Western Zone of Tamil Nadu-2000 & 2005





Mugilan et al.

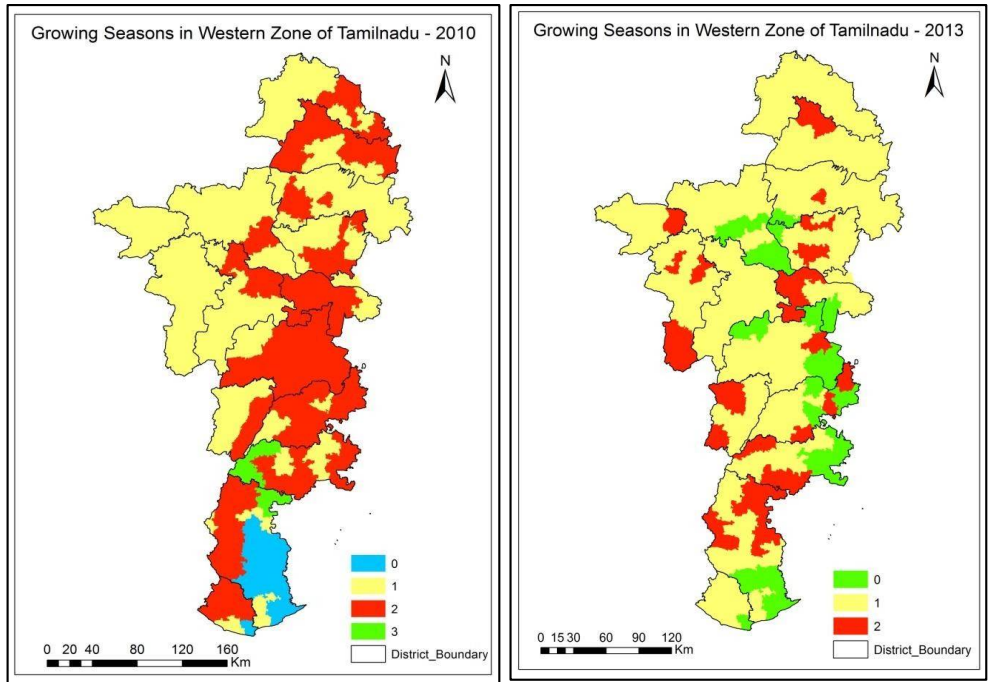


Fig 4 &5. Growing Season in Western Zone of Tamilnadu-2010 &2013

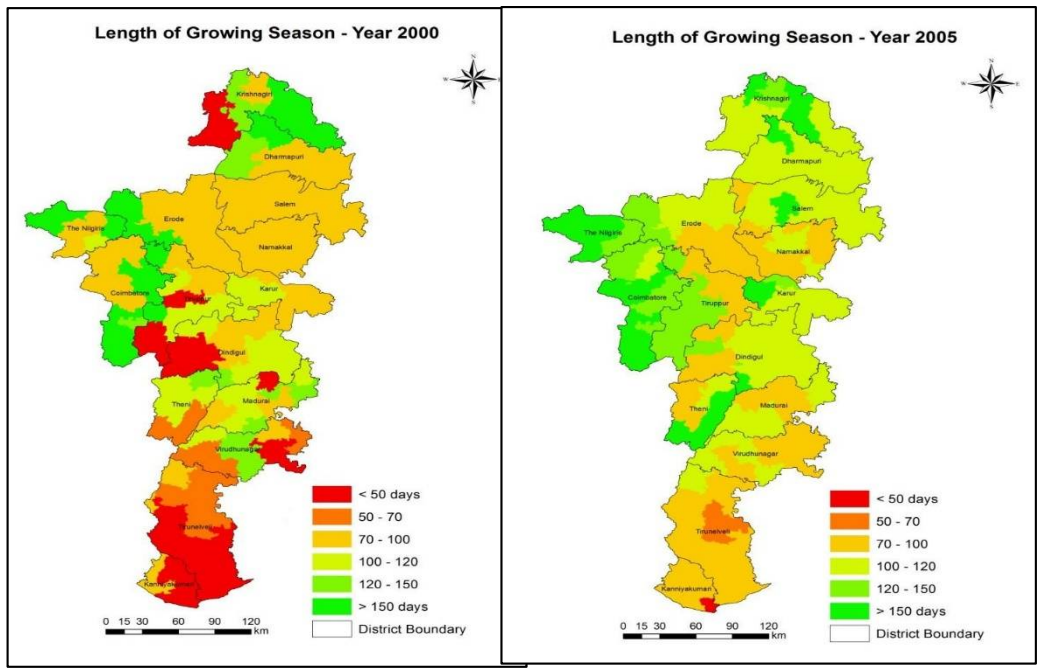


Fig 6 & 7. LPG in Western Zone of Tamilnadu-2000 &2005





Mugilan et al.

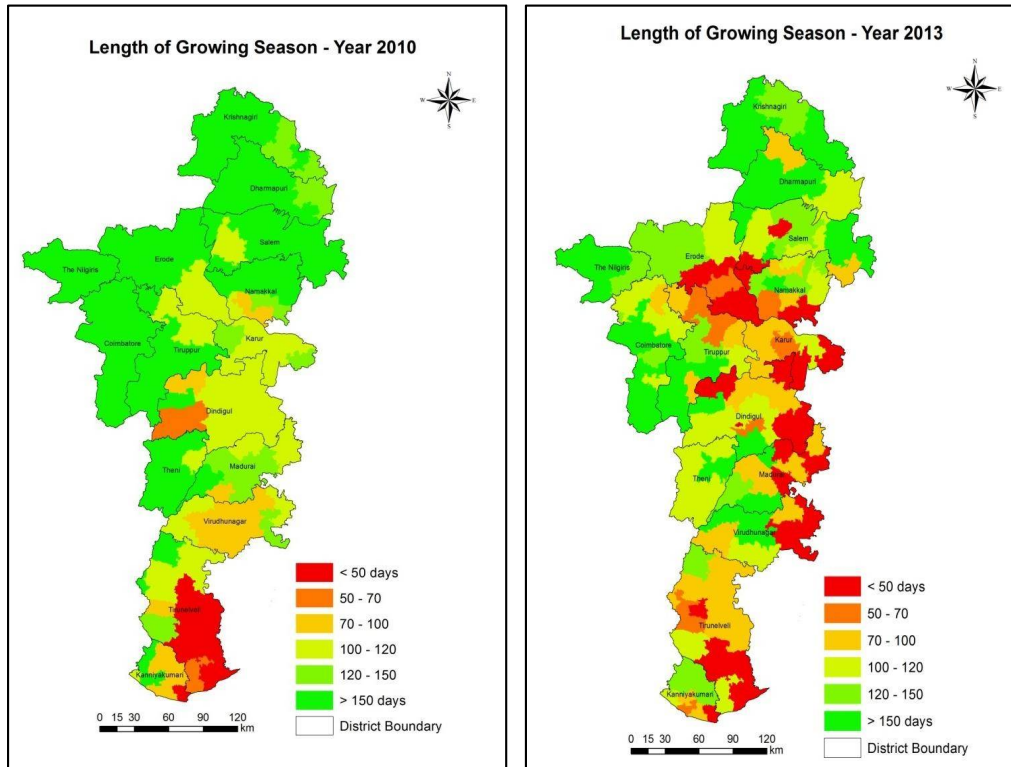


Fig 8 &9. LPG in Western Zone of TamilNadu-2010 &2013

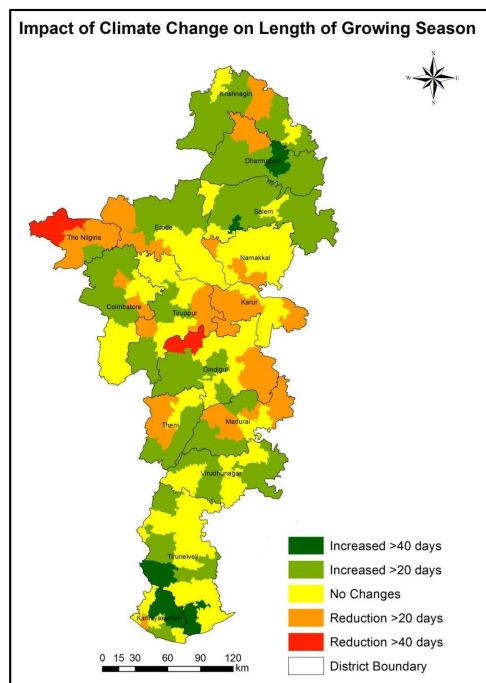


Fig 10. Impact of Climate Change on LGP





Mugilan et al.

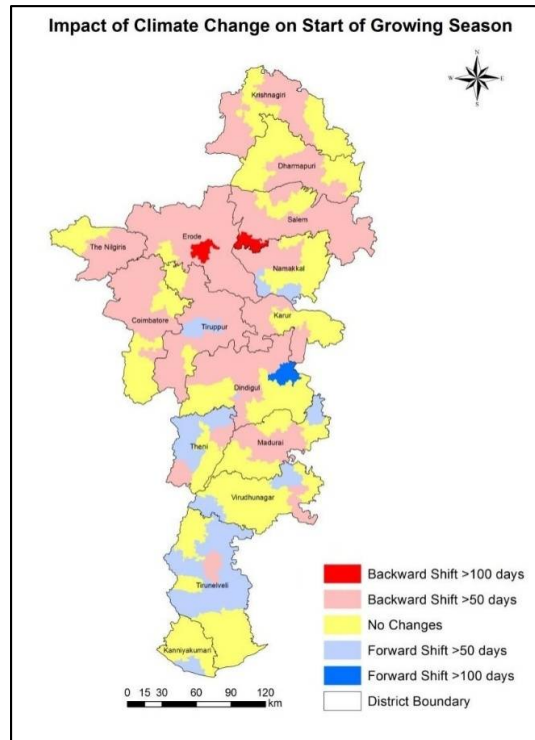


Fig.11. Impact of Climate Change on start of Growing Season in days.

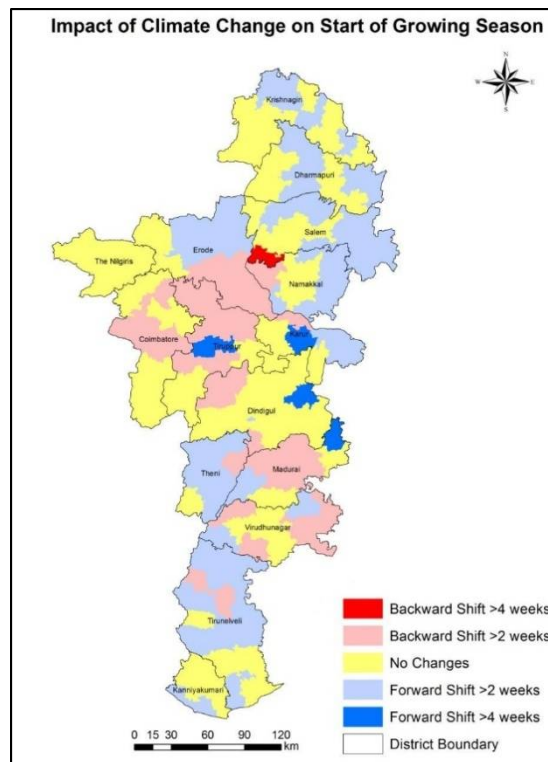


Fig 12. Impact of Climate Change on start of Growing Season in week





Mugilan et al.

Table 1. Area distribution of LGP in the classified categories (Area in Lakh hectares)

LGP	Year 2000	Year 2005	Year 2010	Year 2013
< 50 days	10.10	0.00	3.14	9.70
50 – 70	4.91	1.13	1.49	3.12
70 – 100	27.08	20.94	5.15	11.02
100 – 120	9.14	25.75	14.56	13.29
120 – 150	4.86	8.21	6.05	9.79
> 150 days	8.62	8.69	34.33	17.79

Table 2. Area distribution of LGP Change

LGP	Area (lakh Hectares)
Increased >40days	2.40
Increased >20days	27.44
No Changes	21.07
Reduction >20 days	12.40
Reduction >40 days	1.42

Table 3& 4 Area distribution on start of growing season in days & weeks.

Start of Season	Area(lakh_ha)
Backwardshift>100days	0.55
Backwardshift>50days	31.61
NoChanges	25.02
Forwardshift>50days	7.19
Forwardshift>100days	0.35

Start of Season	Area(lakh_ha)
Backwardshift>4weeks	0.29
Backwardshift>2weeks	13.54
NoChanges	28.39
Forwardshift>2weeks	21.02
Forwardshift>4weeks	1.48





Development of Soil and Soil Nutrient Map Based Integrated Fertilizer Recommendation Tool

Subashini Girivel*, Balaji Kannan and Raguath Kaliaperumal

Department of Remote Sensing and GIS, Tamil Nadu Agricultural University, Coimbatore -641003, Tamil Nadu, India.

Received: 12 Aug 2017

Revised: 20 Aug 2017

Accepted: 27 Sep 2017

Address for correspondence

Subashini Girivel

Scholar, Department of Remote Sensing and GIS,
Tamil Nadu Agricultural University,
Coimbatore -641003, Tamil Nadu, India.
Email: subagannz@gmail.com



This is an Open Access Journal / article distributed under the terms of the **Creative Commons Attribution License** (CC BY-NC-ND 3.0) which permits unrestricted use, distribution, and reproduction in any medium, provided the original work is properly cited. All rights reserved.

ABSTRACT

The study was conducted for integrating soil test based crop response (STCR) equations for the different crops with map inputs and developing a customized tool for automation of interpretation classes and fertilizer recommendation. An investigation was carried out on the test area namely, Parambikulam command area. The customized tool for the Interpretative and Fertilizer recommendation was developed in Python v. 2.7 open source environment using the site packages. The criteria for the interpretative classification viz., Land capability, Land Irrigability and Crop suitability of the area were derived from literatures and an excel sheet containing these criteria were formed which was used as a database for deriving the classification for a particular data using the customized tool. The tool generated for the Land Capability Class of 2, Land Irrigability of 1 and Crop suitable as Maize with high level of suitability indicated by 'S1' for the selected point from Map input. STCR based fertilizer recommendation is also done in manual input routine of the tool. The manual outputs of this test area was displayed as described as Land capability classification of III, Land irrigability classification of II, Crop suitability classification = 'Maize' – S1, Nutrition recommendation N = 187 kg/ ha; P = 88 kg/ha; K= 105 kg/ha. This customized tool is intended to reduce the time in classifying a soil to different interpretative classes and also the personal bias in classification.

Keywords: STCR, Land Irrigability, Land Capability, Crop Suitability, Python.

INTRODUCTION

Decreasing soil fertility has raised concerns about the sustainability of agricultural production at current levels. Future strategies for increasing the agricultural productivity will have focus on using the nutrient resources more



**Subashini et al.**

efficiently and effectively than in the past. Though continuous application of inorganic fertilizers results in higher yield but usually this has resulted in the destruction of inherent soil properties. So greater emphasis should be given to Soil Protection against erodibility of both physical and chemical fertility. Total organic farming though most desirable, may be feasible only under subsistence farming and not under commercial agriculture. This problem can be mediated through Integrated Nutrient Management.

Integrated Nutrient management is an approach that seeks to both increase in production and sustain the environment for future generations. The approach involves the judicious and integrated use of organics, inorganic and biofertilizers. When fertilizer recommendations are developed based on soil tests, balanced nutrition concept, integrated plant nutrient system that maintain soil fertility to sustain high crop yields or cropping system they become rationalized doses of fertilizers for crops.

Farmers' knowledge regarding the right product, dosage, time and method of application is very limited, leading to inefficient use of fertilizers. The blanket recommendation does not take into consideration of the fertility status of the soil and hence resulted in indiscriminate use of fertilizers. The continued use of unbalanced fertilizers results in depletion of nutrient supplying power of soil, provided through the fertilizers and consequent decline in fertilizer response.

With the continuous and steady increase in the use of fertilizers and considerable escalation in their prices, the need to utilize every available unit of plant nutrient in the most productive and profitable manner has become all the more essential. There has been a genuine concern over low nitrogen use efficiency for economic as well as environmental reasons. There are three ways by which fertilizer use efficiency can be increased *viz.*, (i) by adoption of better agronomic practices, (ii) use of more efficient fertilizer materials and (iii) integrated nutrient management involving combined use of fertilizers, organic manures, bio-fertilizers, etc. Agronomic practices such as choice of right crops and their varieties, right type of fertilizer, correct dose, appropriate time and method of fertilizer application, weed control and water management that result in increased yield and also increases fertilizer use efficiency. Applying the recommended dosage in installments at the right stage of plant growth would improve fertilizer use efficiency and crop productivity.

MATERIALS AND METHODS

Parambikulam Aliyar Project (PAP), a multi-purpose, multi-reservoir project, situated in between Kerala and Tamil Nadu states consists of seven reservoirs. Water is released for Aliyar and Thirumoorthy reservoirs. The Parambikulam main canal starts from Thirumoorthy dam irrigating a total area of 1,70,443 ha. The study area falls to the Eastern side of main canal starting from Thirumoorthy dam to Udumalpet, which lies between 77° 15' and 77°-30' E latitude and 10°-30' and 10°-40' N longitude with a total geographical area of 10,550 hectares. The location of the study area is represented in the Figure 1. The major cultivated crops include sorghum, sesame and pulses in rainfed conditions and sugarcane, onion, maize and coconut under irrigated conditions. The natural vegetations observed in the test area are prosopis, neem, grasses and some other thorny bushes.

The data was obtained from the Ph.D. thesis on the topic "Soil resource and land use studies in eastern Parambikulam Aliyar Project command area using remote sensing and GIS techniques" (Ragunath, 2003). The criteria for the interpretative classification *viz.*, Land capability, Land Irrigability and Crop suitability of the area were derived from literatures and an excel sheet containing these criteria were formed which was used as a database for deriving the classification for a particular data using the customized tool.

Python v. 2.7 was used in this study for writing the code to develop the customized tool. Also libraries like GDAL (Geospatial Data Abstraction Library) and OGR for handling spatial data, xlrd (Excel Read module) for accessing excel data, Numpy (Numerical Python) for numerical computations and Matplotlib (Mathematical Plotting Library) for plotting data. Python is a modern, powerful programming language which has efficient high level data structures, a simple but effective approach to object oriented programming and is easy to learn and highly extensible. Python's elegant syntax, together with its dynamic nature, makes an excellent language for scripting and rapid



**Subashini et al.**

application development. Another advantage of Python is that it completely hides technical details with which users of system programming languages need to concern themselves. The list of packages used in the programming is given in Table 1.

PyQt4 is used to write all kinds of GUI applications, from accounting applications, to visualization tools used by programmer. It is used to design and build graphical user interface of the stand-alone tool. The design of the application had been split into different modules to enable easy development and better maintenance. Different python modules used for specific purposes during the coding interface. Modules viz. PyQt, Xlrd, Numpy, Matplotlib, OGR and GDAL packages were installed. The versions of the module and their utilities, descriptions are detailed in Table 1. Crop suitability, Land capability, Land irrigability classification and nutrient recommendation criteria were collected for developing the database for using with the tool. These criteria's were entered in MS Excel format and used as the database. These data resides in backend process of the application. Then the database was queried by python interface using xlrd module to extract necessary data from Microsoft Excel spreadsheet files.

Fertilizer Recommendation helped to translate a nutrient recommendation into correct amounts of different fertilizers needed to make up the right amount of nutrients. The tool was designed to quickly get the nutrient recommendation for various type of soil and crop on specific growing season. The four different interpretative classes used in the tool are.

- Land Capability Classification (LCC)
- Land Irrigability Classification (LIC)
- Crop Suitability Classification (CSC)
- Nutrient Recommendation (N, P,K)

Land capability is a qualitative methodology to classify land resources based on soil, topography and climate parameters without taking into account the yield and socio-economic conditions. The classification based on soil protection and it evaluated the most suitable kind of land use to achieve this target like rain-fed agriculture, extensive grazing, or forestry. Land was classified mainly on the basis of permanent limitations. Based on the criteria data referred to, soil depth, texture, drainage, slope, erosion risk, elevation, rainfall, salinity, rockout crops, gravel, cobbles and stoniness were created in table format using MS excel and LCC at a particular unit in map can be identified by comparing the input data from map and existing data in excel file.

The suitability of land for irrigation depended on physical factors like quality and quantity of irrigation water and socio-economic factors like land development costs provision of drainage facilities production costs of individual crops. Irrigability classification of parameters were created in the database such as soil depth, texture, drainage, slope, gravels, rockout crops, soil permeability, coarse fragment, salty, salinity and available water holding capacity.

The adaptability of crops in one or the other area was the interaction between existing edaphic conditions and fitness of the cultivar under these conditions. The crop suitability for defined uses and the impact of the uses on environment were determined by land conditions and land qualities. The sustainable land use depends on soil resilience. It depended on a balance between soil restorative and soil degradation processes. Ecologically every factor of environment exerted directly or indirectly a specific effect upon the growth and development of a plant or a crop. In a habitat, the water, temperature, sunlight, soil aeration and availability of plant nutrients directly acted on crop growth. These vary from habitat to habitat and determined largely the suitability of plant to any particular environment.

The land evaluation involved the formulation of climatic and the soil and site criteria to meet the requirements of crops and rating of these parameters for highly suitable S1 (S1-with no or slight limitations), moderately suitable S2 (S2-moderate limitation) and marginally suitable S3 (S3-severe limitation) and unsuitable (N) classes.



**Subashini et al.**

Limitations based on the crop suitability parameters were crops, soil depth, soil drainage, slope, texture, mean temperature, elevation, rainfall, pH, EC, CEC, calcareous, organic carbon, gravel and coarse fragment. These parameters were retrieved from the database. The output on percentage of the nitrogen, potassium, phosphorus and target yield depending on the crops, seasons, soil series was obtained from Soil test crop response (STCR) approach. The equation from STCR was used as a basis for predicting fertilizer doses for specific yield targets for varied soil available nutrition levels under inorganic fertilizers alone and with Integrated Plant Nutrition System (IPNS).

Nutrient recommendation, Crop suitability, Land Capability, Land Irrigability classification criteria were collected for developing the database. Classifications criteria were created in excel format and that was added into this database. These data resides in backend process of the application. Data regarding crop suitability classification were collected for agricultural and horticultural crops. Similarly LCC and LIC were generated with that criteria and parameters. Two different kinds of data inputs were provided for the user. One is manual based input and second one, providing inputs in map format.

The customized tool was designed and developed in such a way to select the map of choice to be given the input map is .shp file format. Based on the region of interest, dynamically the features available for the region *viz.*, classifications were identified from the catalogue. A dynamic map file was generated and later manipulated for customization. Maps were presented in an applet form so that the user can perform the zooming operations (zoom in, zoom out, pan) on the map. Those operations allow the user to see the map at own magnification scale. Map can be added layer by layer into the mapping framework. The user can select maps from the application that were generated dynamically based on the geographic location.

In manual input, the various criteria in classifications were selected for particular location. The manual process created by selection of soil order based recommending fertilizer for the crops, soil characteristics and interpretative classification. Input data queried from the database for Crop suitability, land irrigability and land capability classification's parameters and nutrient recommendation. Then proceed button was used to view the output under different classifications and Fertilizer recommendation. Parambikulam was selected as a test area to investigate the Crop Suitability, Land Irrigability, Land Capability and recommendation of nutrients to the crops.

RESULTS AND DISCUSSION

Interpretative groupings *viz.*, Land capability classification, Land irrigability classification and Crop suitability classification are critical in getting information about a soil and for proper management and decision making. These are based on the morphological, physical and chemical properties on individual soils which are arrived at by careful computation as per the standard scientific procedures. Till date these classifications are made by trained persons or scientist with their experience and soil analysis data taken from profiles and ancillary data like climatic parameters of the area. This imparts more of bias in classification methods and hence the final output differs with person to person who does the classification. This study attempts an automated classification of soils by building an open source customized tool into different classes according to the classification methods.

The main layout of the the tool is shown in Figure 2. The menu bar consists of two dropdowns *viz.*, File and Help menu. The File menu consists of options like OPEN, SAVE, SAVE AS, PRINT and CLOSE. These options help in the file management for the tool. The HELP menu consists of two options like ABOUT and CONTENTS. The ABOUT option describes the tool and its version, while the content option describes the modality of the tool.

The main frame contains a tab widget with two tabs *viz.*, FROM MAP and MANUAL, which indicates the forms of input for data to analyse with the tool. The developed tool helps in classifying the input data into Land Capability Class, Land Irrigability Class, Crop Suitability Class and Fertilizer Recommendation. The land capability classes output range from 1 to 7. The land irrigability class output range from 1 to 6. For crop suitability the level of suitability *viz.*, S1, S2, S3 and NS will be displayed along with the suitable crop. For fertilizer recommendation, N, P and K recommended levels will be displayed. The STCR based fertilizer recommendation is provided only in the Manual





Subashini et al.

input window, since the input parameters required to calculate the fertilizer recommendation is not available as map form. The tool can be improved in subsequent versions enabling fertilizer recommendation through map input.

In the Map input tab, input data has to be provided in ESRI shape file format. Necessary browsing options for selecting the file has been provided (Figure 2). The input data in .shp file format should be in WGS84 Geographic coordinates. This is a prerequisite for the tool because the backend raster data (in .tif file format) viz., SRTM elevation data, TRMM rainfall data, Length of Growing Period and Mean Air Temperature are provided in the above said geographic co-ordinate system. Since all these files are having similar spatial reference system they are overlaid upon each other for extracting values for any location from the map. Once the map is selected for display, automatically the map with a random colour palette will be displayed as shown in Figure 3. The geographical coordinates of any point in the selected map is dynamically displayed when mouse is moved over the map (Figure 3). In the Map displaying window, a toolbar is provided for altering the display properties of the map window as shown in Figure 4. A tooltip is also provided to each of the icons in the display toolbar. The following options are provided in the display tool bar:

	Reset original view
	Back to previous view
	Forward to next view
	Pan axes with left mouse and zoom with right
	Zoom to rectangle
	Configure subplots
	Save the figure
	Edit curve line and axes parameters

A sample output of the result in the map window resembles as shown in Figure 5. The results include the Land Capability Class of 2, Land Irrigability of 1 and Crop suitability as Maize with high level of suitability indicated by 'S1' for the selected point.

The Manual Input Window in turn has four different tabs, viz., Crop Suitability, Land Capability, Land Irrigability and Fertilizer Recommended as shown in Figure 6. The Land Capability tab has all the criteria with their specific drop down lists (Figure 7) and only one element of the list can be selected by the user for each criteria. The drop down list for each criterion is provided in the Table 2. The Land Irrigability tab has all the criteria with their specific drop down lists (Figure 8) and only one element of the list can be selected by the user for each criteria. The drop down list for each criterion is provided in the Table 3. The Crop Suitability tab has all the criteria with their specific drop down lists (Figure 9) and only one element of the list can be selected by the user for each criteria. The drop down list for each criterion is provided as shown in Table 4. A text box is provided for manually entering temperature value in degree Centigrade. Check is also provided so that no alphabets or symbols are entered in to the Temperature criterion.

The Fertilizer Recommendation tab has all the criteria with their specific drop down lists (Figure 10) and only one element of the list can be selected by the user for each criteria. The available nutrients in kg/ha has to be entered by the user against their corresponding textboxes provided in the Fertilizer Recommendation tab. The N, P and K value of the selected green manure will be picked up the tool itself and displayed in the corresponding text box as shown in Figure 11. The values of these textboxes cannot be edited and has read only property. The drop down list for each criterion is provided in the Table 5. After completing all the tabs in the Manual Input window, if the final Proceed button provided in the Fertilization Recommendation tab, then the results will displayed as shown in the Figure 12. An investigation was carried out on the test area Eastern Parambikulam Aliyar command area, a multi-purpose, multi-reservoir project (PAP), situated between Kerala and Tamil Nadu states consists of seven reservoirs and the Interpretative classes and STCR



**Subashini et al.**

equations were employed to generate fertilizer recommendations for the study area. The outputs from map for the test area was displayed as mentioned here below:

Land capability classification class = 2

Land irrigability classification class = 1

Crop suitability classification = 'Maize' – S1

The manual outputs of this test area was displayed as described as follows:

Land capability classification = 3

Land irrigability classification = 2

Crop suitability classification = 'Maize' – S1

Nutrition recommendation N = 187 kg/ ha;

P = 88 kg/ha;

K= 105 kg/ha

The criterion used for calculating the Land capability classification of a soil is done with the available information of the area either as a map input or through the selection of values in appropriate categories. The criteria are listed in the Table 6. There were not many reports associated with tool development for the Land capability classification, whereas Sachin Panhalkar (2011) manually did the classification with the help of GIS techniques to integrate spatial information.

The criterion used for calculating the Land irrigability classification of a soil is done with the available information of the area either as a map input or through the selection of values in appropriate categories. The criteria are listed in the Table 7. Mateos *et al.* (2002) reported results for integrated GIS with the tool namely Scheme Irrigation Management Information System (SIMIS) in order to simulate different crops and irrigation scenario for water delivery schedule, and also to compare existing situation for improvement irrigation.

The criterion used for calculating the Crop Suitability classification of a soil is done with the available information of the area either as a map input or through the selection of values in appropriate categories. The criteria are listed in the Table 8. Based on the soil properties, botany and agronomy of the crop, economy of water and nutrient usage, previous experience of farmers on performance of crops in a particular soil, marketing facility, socio-economic status of the farmers, climate etc., the crop suitability to the individual soil series has been judged and semi-quantitatively arrived at in the light of guidelines given by Dhanapalan Mosi *et al.* (1977) and reports of Anandkrishnan (1998) and Kadambavanasundaram (2000).

Similar results were reported a decision and planning support tool ALSE (Agricultural land suitability evaluation) used VB script that allows for standardizing a framework for characterizing geo-environmental conditions (e.g. climate, soil, erosion, flood and topographic) relevant for production of major crops (e.g. mango, banana, papaya, citrus, and guava). The ALSE identified crop-specific conditions and systematically computed the spatial and temporal data with maximum potential (Ranya *et al.* 2013). Instead of VB script, this study involves the development of tool using Python which has unique features of open source application; map visualization and stand alone segregation. There is more scope for developing the tool with the present Interpretative classes *viz.*, inclusion of sub classes and modifiers in the respective classification and also to include the other interpretative classes available like Fertility Capability Classification, Productivity potential rating, Water balance models etc. This tool is indented to reduce the time in classifying a soil to different interpretative classes and also the personal bias in classification.





Subashini et al.

REFERENCES

1. Adornado, H. A., and M. Yoshida. 2008. Crop Suitability and Soil Fertility Mapping using Geographic Information System (GIS), *Agricultural Information Research*, 17(2), pp. 60 – 68.
2. Anandakrishnan, B. 1998. Pedology and resources of soils in Tamil Nadu Agricultural University Research Station farm, Vaigaidam, Theni District, Tamil Nadu, M.Sc. (Ag.) Thesis, Tamil Nadu Agricultural University, Madurai.
3. Anjana Dasai and Chandra Subramanian. 1999. Land use planning based on land capability using GIS technique and remote sensing. *ISRS national symposium on remote sensing application for natural resources retrospective and prospective*, Jan. 19- 21, Bangalore, pp. 101.
4. Buresh, R. J. 2008. Management made easy: A new decision-making tool is helping rice farmers optimize their use of nutrient inputs. *International Rice Research Institute, Rice Today*, Philippines.
5. Chinene, V. R. N. 1991. The Zambian Land Evaluation System (ZLES). *Soil use and management*, 7, pp. 21 - 30.
6. Chinene, V. R. N. and V. Shitombanuma. 1998. Land evaluation proposed Musaba state farm in Samfya district, Zambia. *Soil survey and land evaluation*, 8, pp. 179 - 182.
7. Dampney, P. M. R. and E. Sagoo. 2008. PLANET– the national standard decision support and record keeping system for nutrient management on farms in England. In *Agriculture and Environment VII–Land Management in a Changing Environment. Proceedings of the SAC and SEPA Biennial Conference*, pp. 239 - 245.
8. Dhanapalan Mosi, A., K. Subramanian, M. Jayaraman and S. N. Vivekanandan. 1977. Soil survey interpretations for suitability for low land rice cultivation. Seminar on response of crops to application of P and K and soils' fertility evaluation at A.C. & R.I., Coimbatore. 3, pp. 112 - 151.
9. Fairhurst, T. H., A. Dobermann and C. Witt. 2005. Fertilizer Chooser. Lincoln, NE: University of Nebraska-Lincoln, Singapore: Pacific Rim Palm Oil Limited and Potash & Phosphate Institute/Potash & Phosphate Institute of Canada (PPI/PPIC) & International Potash Institute (IPI).
10. Kadambavanasundaram, 2000. Pedology, Resources and Management of Bench Mark soils in the plains of Dindigul District, Tamil Nadu, M.Sc. (Ag.) Thesis, Tamil Nadu Agricultural University, Madurai.
11. Mateos, L., I. Lopez and J. A. Sagardoy. 2002. SIMIS: the FAO decision support system for irrigation scheme management. *ELSEVIER, Agricultural Water Management*, 56(3), pp. 193 - 206.
12. Ranya Elsheikh, Abdul Rashid B. Mohamad Shariff, Fazel Amiri, Noordin B. Ahmad, Siva Kumar Balasundram and Mohd Amid Mohd Soom. 2013. Agriculture Land Suitability Evaluator (ALSE): A decision and planning support tool for tropical and subtropical crops. *Computers and Electronics in Agriculture*, 93, pp. 98 - 110.
13. Sachin Panhalkar. 2011. Land Capability Classification for Integrated Watershed Development by applying Remote Sensing and GIS techniques. *ARPN Journal of Agricultural and Biological Science*, 6(4), pp. 46 - 55.

Table 1. List of Python packages used for application development

Modules	Version	Description
Numpy	1.8.2 win-32 bit	General purpose multi-dimensional array processing and math library
GDAL	1.11.1.win32	Geospatial Data Abstraction Library
PyQt4	4.11.3- gpl- Py2.7- Qt4.8.6	Cross-platform application and GUI framework
Xlrd	0.9.3.win32	Extract data from Microsoft Excel spreadsheet files
Matplotlib	1.1.0.win32	Python 2D plotting library





Subashini et al.

Table 2. Drop down list for each criteria in the Land Capability tab of the tool

S.No.	Criteria	Elements of the drop down list
1	Soil depth	90-999; 65-90; 50-65; 35-50; 20-35; 10-20; 0-10
2	Texture	Medium to heavy clays; CL,LC; L,SIL,SCL; SL
3	Drainage	Well; Well / Rapidly; Moderate well; Imperfectly; Poorly; Very Poorly; Swamp
4	Slope	0-1; 1-5; 5-12; 12-18; 18-28; 28-56; 56-999
5	Erosion Risk	Nil; Very Low; Low; Moderate; High; Very High; Extreme
6	Elevation	0-180; 180-260; 260-380; 380-500; 500-600; 600-900; 900-9999
7	Rainfall	850-1300; 1300-1500; 1500-1700; 1700-1850; 1850-2000; 2000-2500; >2500
8	Salinity	0-1; 1-2; 2-4; 4-8; 8-16; 16-32; >32
9	Gravel	0-2; 2-20; 20-35; 35-50; 50-70; 70-90; 90-999
10	Cobble	0-2; 2-10; 10-20; 20-35; 35-70; 70-90; 90-999
11	Stone	NIL; 0-10; 10-20; 20-35; 35-50; 50-90; 90-999
12	Rockout Crop	N/A; 0-2; 2-10; 10-20; 20-50; 50-90; 90-999

Table 3. Drop down list for each criteria in the Land Irrigability tab of the tool

S.No.	Criteria	Elements of the drop down list
1	Soil depth	0-7.5; 7.5-22.5; 22.5-45; 45-90; 90-999
2	Texture	SL/CL; LS/C; S/SC
3	Drainage	Well; Moderate; Poor
4	Slope	0-1; 1-3; 3-5; 5-10
5	Gravels	0-15; 15-35; 35-55; 55-75; 75-999
6	Rockout Crop	40; 20; 15; 5
7	Soil Permeability	5-50; 1.3-5; 0.3-1.3; <0.3
8	Coarse fragment	0-5; 5-15; 15-35; 35-65; 65-999
9	Salinity	0-4; 4-8; 8-12; 12-16; 16-999
10	Available W.H.C	12-999; 9-12; 6-9; 2-6; 0-2
11	Salt	0-2; 2-50; 50-999

Table 4. Drop down list for each criteria in the Crop Suitability tab of the tool

S.No.	Criteria	Elements of the drop down list
1	Soil depth	0-50; 50-75; 75-100; 100-150; 150-999
2	Texture	L,SCL,SIL,SL;SC,SIC,CL,C,C,LS,S;SL,SICL,SIC,SC,C;SL,SICL,SIC,SC,C; heavy clay
3	Elevation	0-20; 100-200; 200-1000; 1000-1500; 1500-1800; 2000-9999
4	Rainfall	0-20; 20-50; 50-100; 200-400; 400-500; 500-750; 750-1000; 1000-1200; 1200-1500; 2000-3000
5	pH	0-4; 4-4.9; 5.5-6.4; 6.5-7.5; 7.6-8.5; 8.6-9; 9-14
6	EC	0-3; 3-5; 5-10; 10-15; 15-35; 35-50; 50-999





Subashini et al.

7	Calcareous	Non Calcareous; 0-5; 5-10; 10-99; Slightly; Strong
8	OC	High; Medium; Low
9	CEC	0-10; 10-15; 15-20; 20-30; 30-55; 55-999
10	Soil Drainage	Well; Imperfect; ModerateWell; Well-ModerateWell; Moderate Imperfect; Poor; VeryPoor; Imperfect-Poor; Excessive; Poor-Excessive;
11	Slope	0-3; 3-5; 5-10; 10-15; 15-20; 20-999
12	Gravel	Non Gravelly; 10-15; 15-35; 35-999
13	Coarse fragment	Nil; 5-15; 15-35; 35-50; 50-60; 60-75; 75-999

Table 5. Drop down list for each criteria in the Fertilizer recommendation tab of the tool

S.No.	Criteria	Elements of the drop down list
1	Soil order	Alfisol; Inceptisol; Vertisol; Entisols; Ultisols
2	Season	Rabi; Kharif
3	Crop	Bhendi; Cabbage; Carrot; Cauliflower; Chilli; Cotton; Gingely; Greengram; Groundnut; Maize; Onion; Potato; Ragi; Rice; Sorghum; Sugarcane; Tapioca; Turmeric; Wheat
4	Organic manure	Farm compost; Poultry manure; Farmyard manure; Sheep and goat manure; Steamed bone meal; Horn and hoof manure; Blood meal; Meat meal; Fish meal; Raw bone meal
5	Green Manure	Sun hemp; Dhaincha; Sesbania; Forest tree leaf; Green weeds; Pongamia leaf

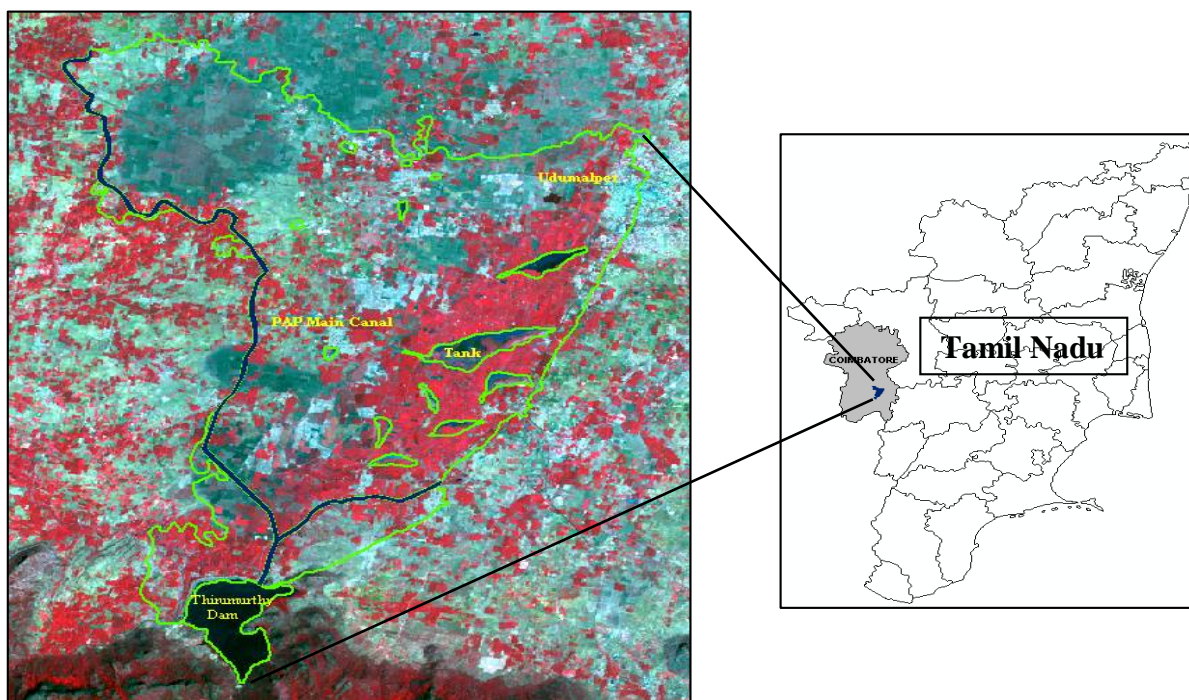


Figure 1. Location map of the test area (Eastern Parambikulam Aliyar Project command area)





Subashini et al.

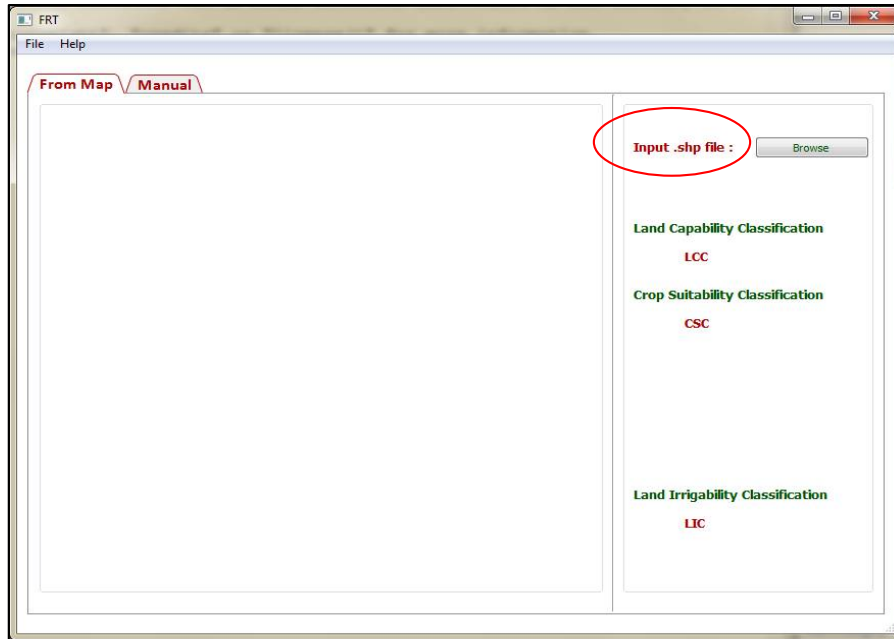


Figure 2. Layout of Interpretative and Fertilizer Recommendation Tool

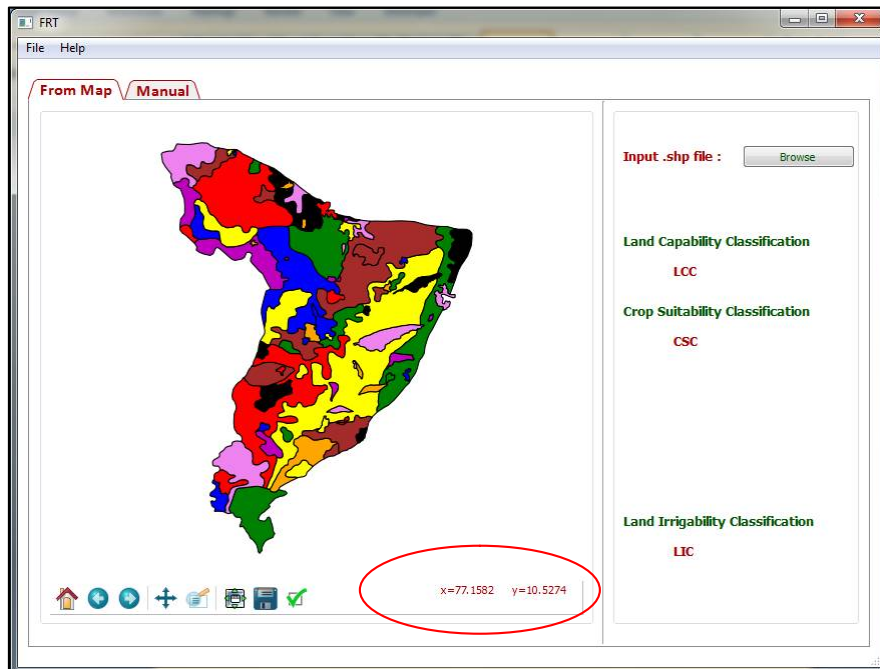


Figure 3. Map display with geographical coordinates



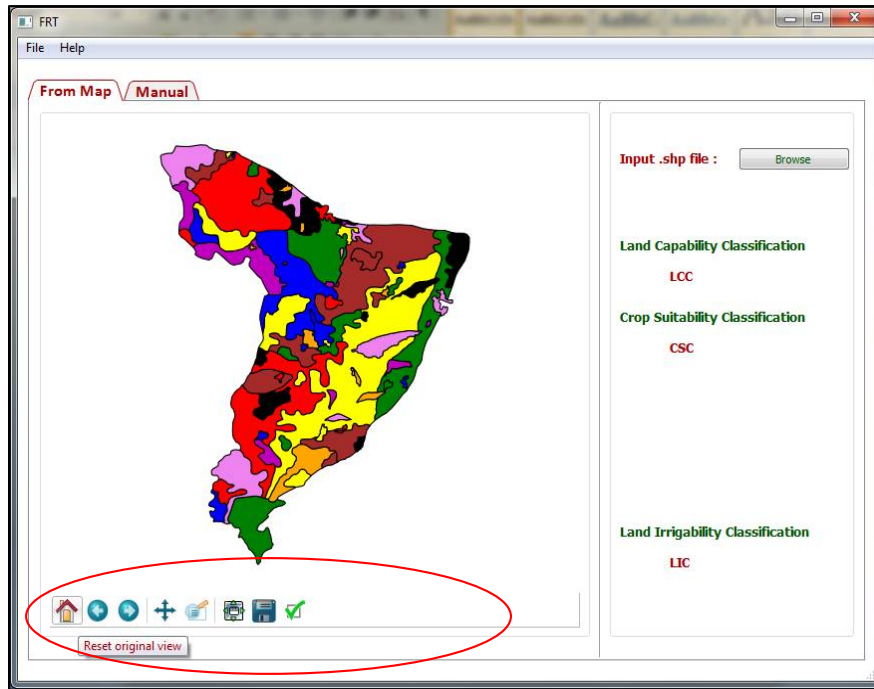


Figure 4. Display toolbar in Map Window

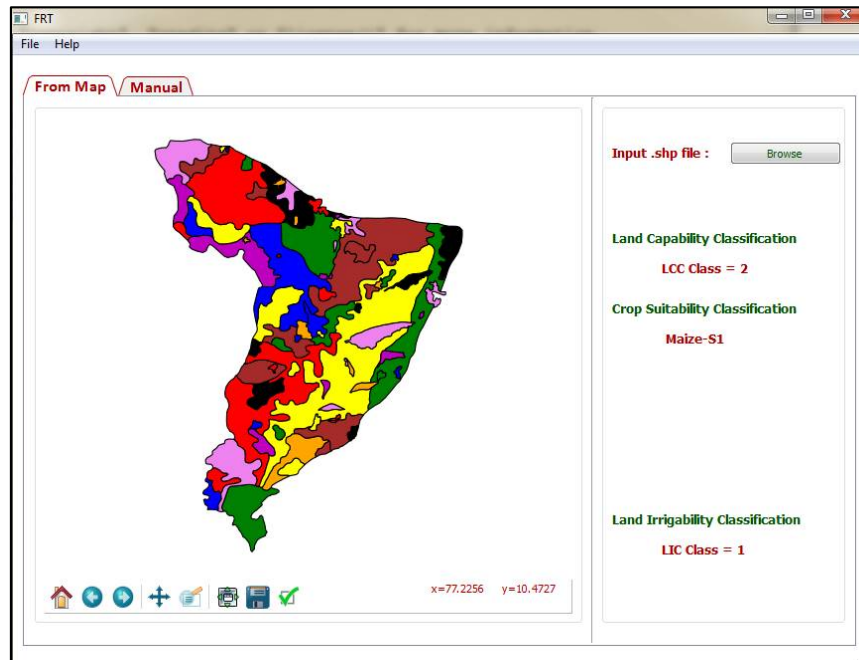


Figure 5. Sample output from the Map Window of the tool



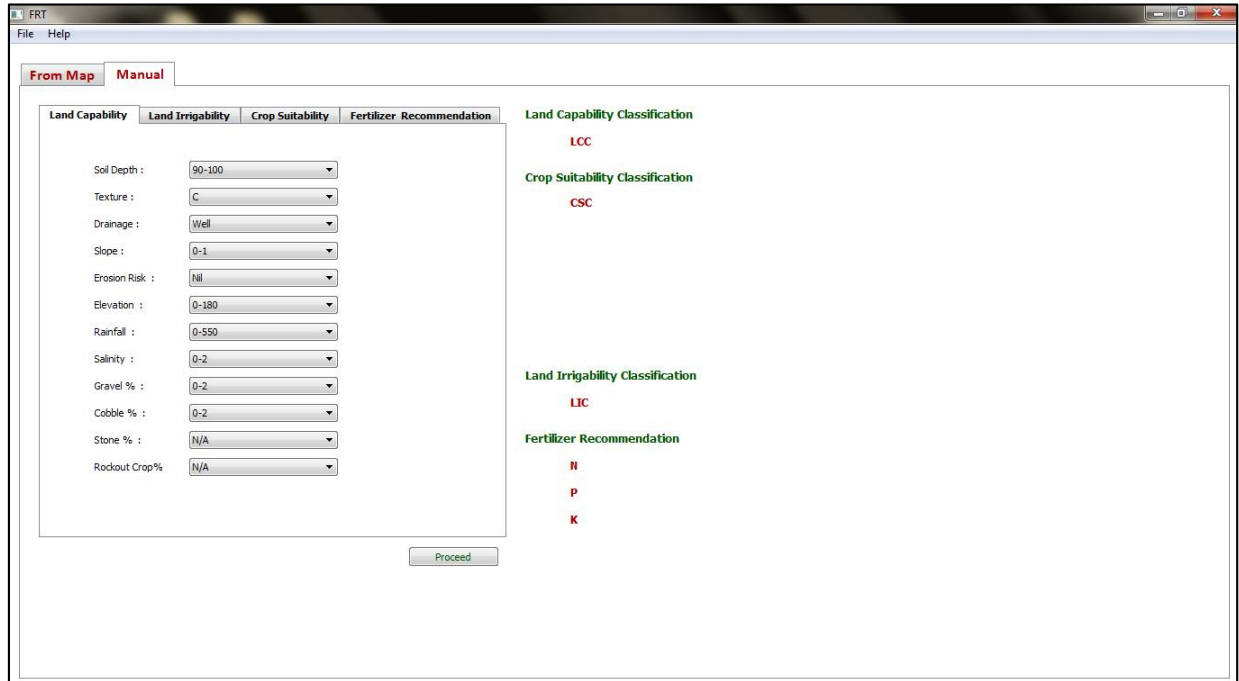


Figure 6. Manual Input window of the tool

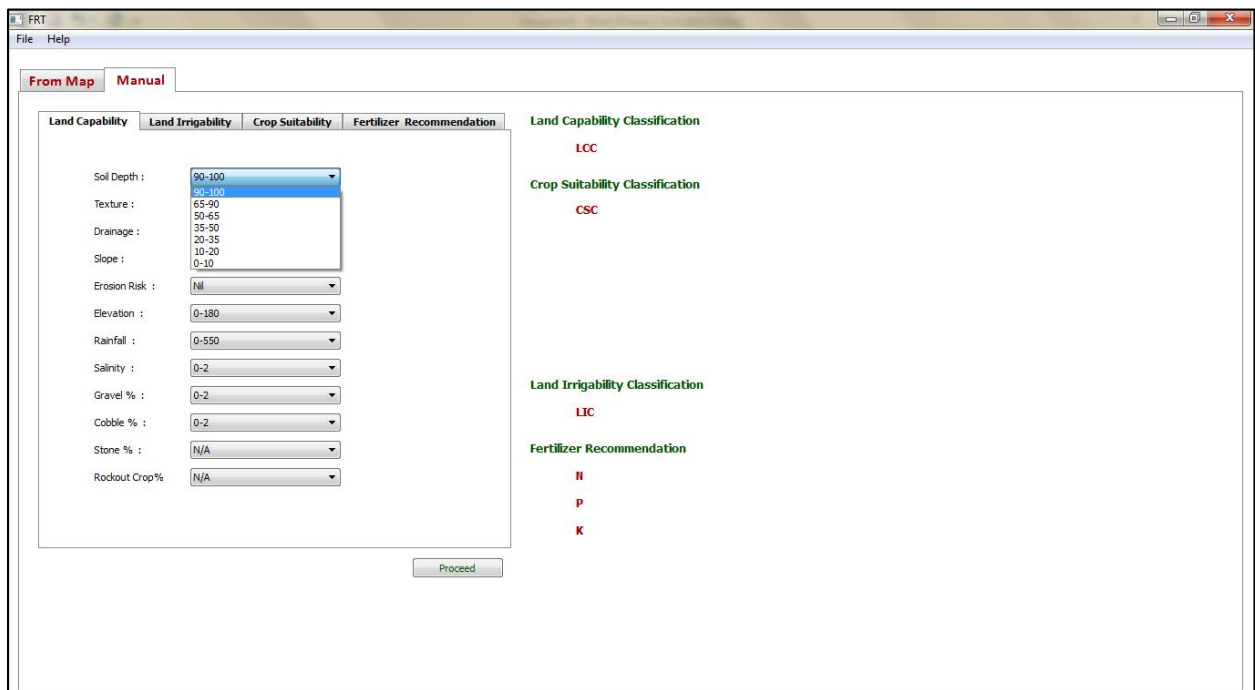


Figure 7. Drop down list for each criteria in Land Capability tab



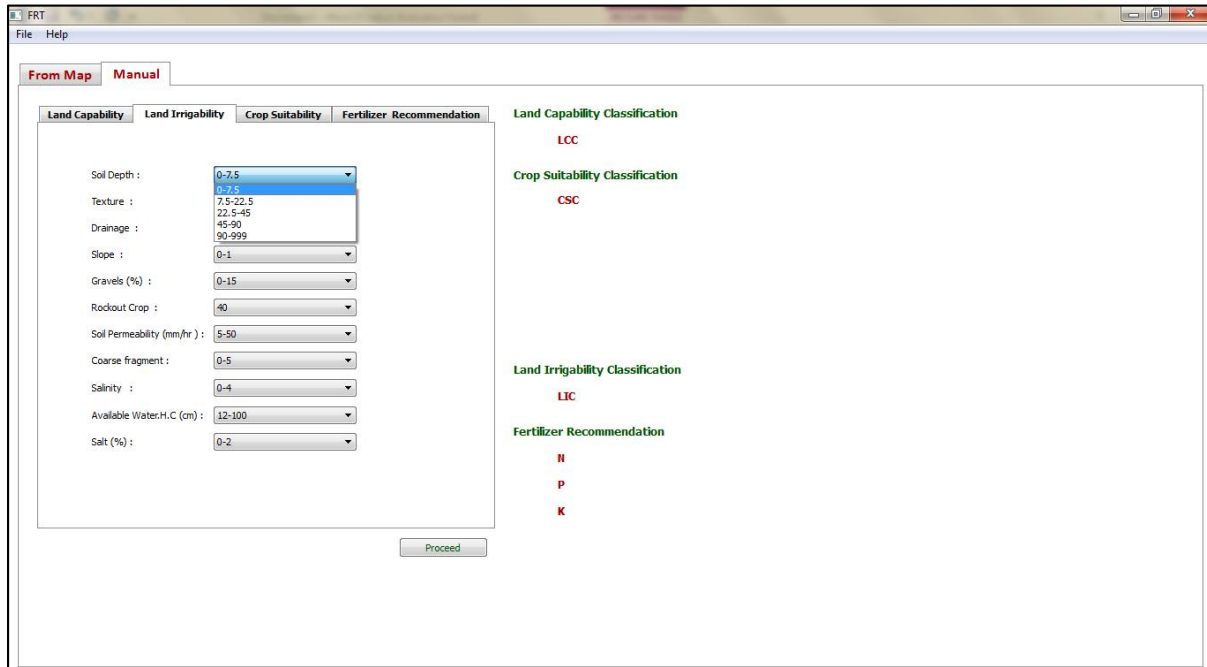


Figure 8. Drop down list for each criteria in Land Irrigability tab

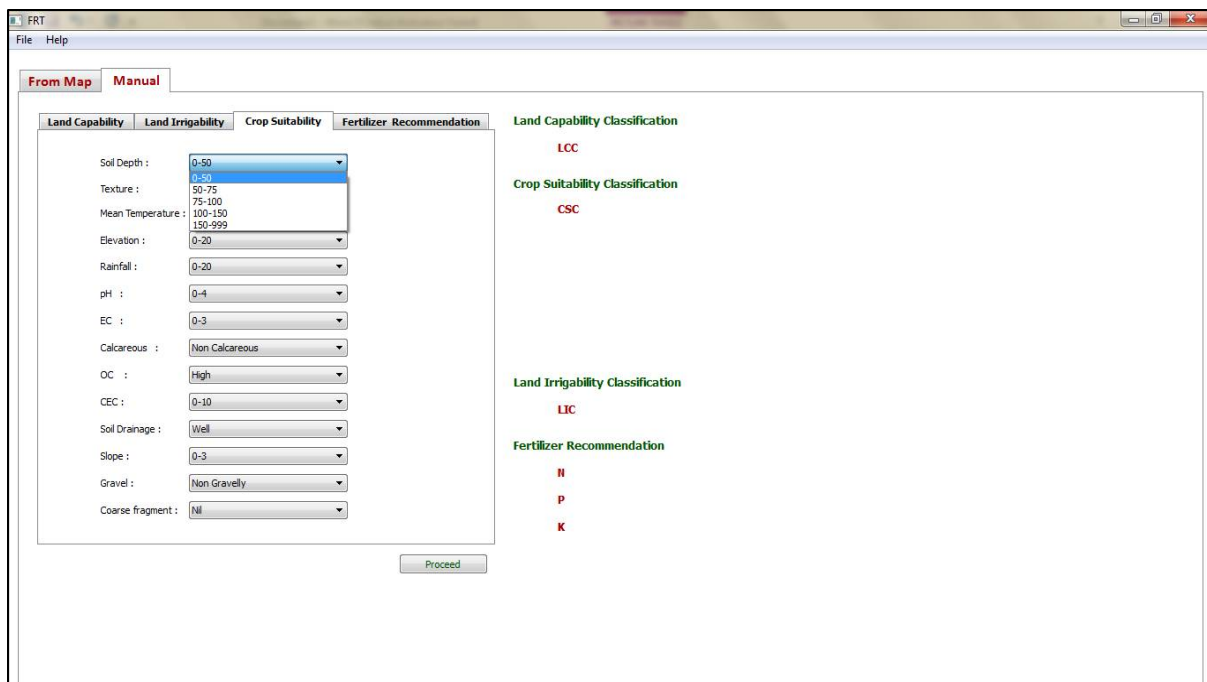


Figure 9. Drop down list for each criteria in Crop Suitability tab



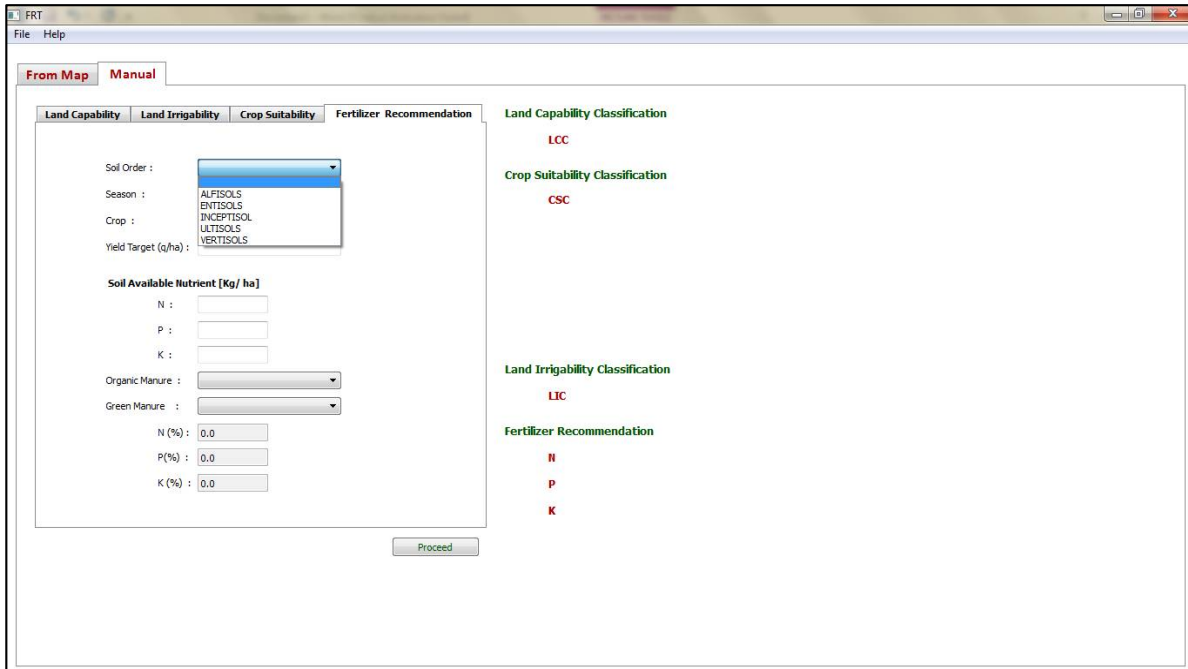


Figure 10. Drop down list for each criteria in Fertilizer Recommendation tab

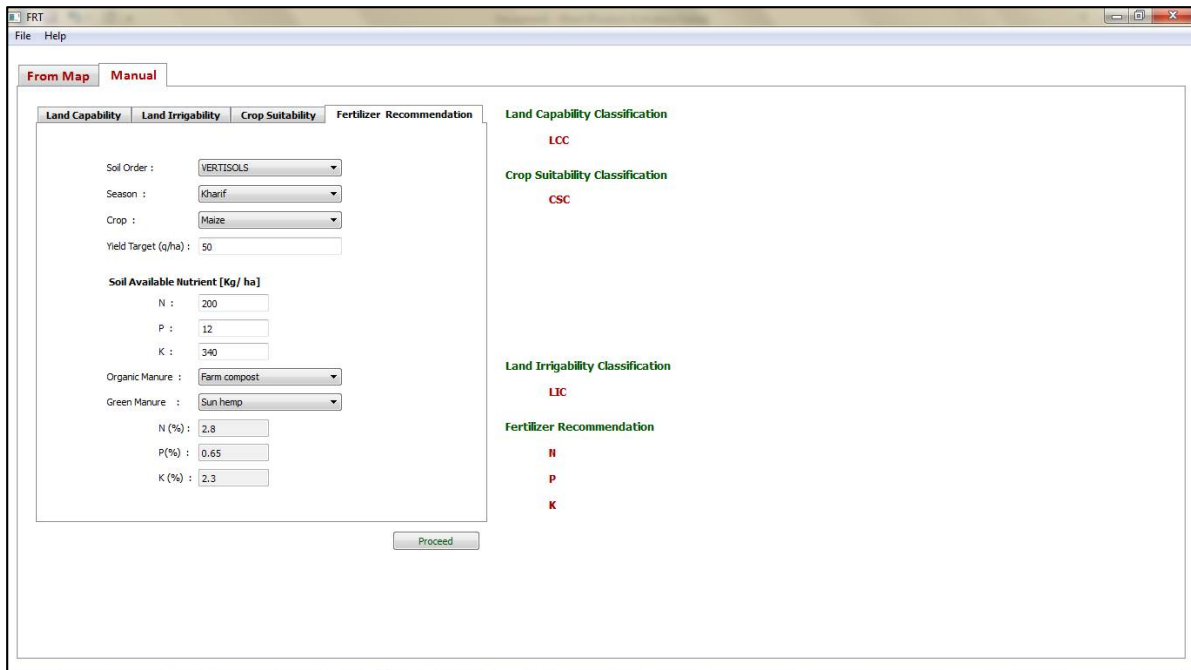


Figure 11. Sample values entered in Fertilizer Recommendation tab





The screenshot shows the 'Manual' window of the FRT software. It features a menu bar with 'File' and 'Help'. Below the menu bar are two tabs: 'From Map' and 'Manual'. The 'Manual' tab is active, showing a sub-menu with 'Land Capability', 'Land Irrigability', 'Crop Suitability', and 'Fertilizer Recommendation'. The 'Fertilizer Recommendation' sub-menu is selected, displaying the following input fields and results:

Input Fields:

- Soil Order: VERTISOLS
- Season: Kharif
- Crop: Maize
- Yield Target (q/ha): 50
- Soil Available Nutrient [Kg/ha]:
 - N: 200
 - P: 12
 - K: 340
- Organic Manure: Farm compost
- Green Manure: Sun hemp
- N (%): 2.8
- P(%): 0.65
- K (%): 2.3

Results:

- Land Capability Classification: LCC Class = 3
- Crop Suitability Classification: Maize-S1
- Land Irrigability Classification: LIC Class = 2
- Fertilizer Recommendation:
 - N: 186.316 (kg/ha)
 - P205: 87.9415 (kg/ha)
 - K20: 105.206 (kg/ha)

A 'Proceed' button is located at the bottom center of the window.

Figure 12. Sample output from the Manual Window of the tool





RESEARCH ARTICLE

Epidemiological and Clinicopathological Evaluation of Chronic Gastritis in Dogs in and Around Chennai City

C.G.Umesh*, A.P.Nambi, S.Kavitha and G.Dhinakar Raj

Centre of Advanced Faculty Training in Veterinary Clinical Medicine, Ethics and Jurisprudence,
Madras Veterinary College, Chennai-600 007, TamilNadu, India.

Received: 10 Aug 2017

Revised: 17 Aug 2017

Accepted: 26 Sep 2017

Address for correspondence

Dr.Umesh.C.G,

Assistant Professor,

Department of Veterinary Clinical Medicine, Ethics and Jurisprudence,

College of Veterinary and Animal Sciences, Pookode, Wayanad – 673 576,

Kerala, India.

Email: umesh03vet@gmail.com/Mob:09562179563,



This is an Open Access Journal / article distributed under the terms of the **Creative Commons Attribution License** (CC BY-NC-ND 3.0) which permits unrestricted use, distribution, and reproduction in any medium, provided the original work is properly cited. All rights reserved.

ABSTRACT

Chronic gastritis in dogs is appeared to be one of the least diagnosed clinical conditions as the definitive diagnosis of it requires detailed diagnostic workup and gastric mucosal biopsy. The present study was aimed to analyse a group of dogs from different regions in Chennai city diagnosed to be having chronic gastritis for its prevalence and various clinicopathological and histopathological changes associated. Thirteen dogs of different age groups and sex presented to Small Animal Medical Outpatient Clinic of the Madras Veterinary College Teaching Hospital, Chennai with clinical signs suggestive of chronic gastritis were selected for the study. After detailed clinical and laboratory examination, animals were subjected to gastroscopic examination under general anaesthesia to collect mucosal biopsy samples for diagnosis and histopathology. Major clinical signs noticed in chronic gastritis were anorexia or inappetence, chronic vomiting, melena and weight loss and minor signs included fever, diarrhoea, haematemesis, pica and abdominal pain. No significant changes were observed in the haematology and serum biochemical parameters in animals with chronic gastritis. The major histopathological changes in gastric tissue were lymphocytic plasmacytic type of gastritis, moderate epithelial injury, accumulation of lymphocytes in the glandular region and fibrosis.

Keywords: Chronic gastritis, Gastric biopsy, Histopathology, Clinicopathological.

INTRODUCTION

Gastritis was a common finding with 35 per cent of dogs investigated for chronic vomiting and 26-48 per cent of asymptomatic dogs affected. The most common form of gastritis in dogs was mild to moderate superficial

12840



**Umesh et al.**

lymphoplasmacytic gastritis with concomitant lymphoid follicle hyperplasia (Simpson, 2010). Chronic gastritis was defined as inflammation of gastric mucosa visible upon microscopy with chronic inflammatory cells like lymphocytes and plasma cells, variable degree of activity like polymorphonuclear cell infiltrate and in some cases glandular atrophy (Redeen, 2010). Chronic gastritis in dogs is mainly characterized by chronic vomiting and especially with bile. Chronic vomiting generally means vomiting intermittently or continuously for at least 7 days (Leib, 2008). In chronic gastritis vomiting is associated with weight loss, decreased appetite and bouts of abdominal pain and vomitus did not contain bile in acute gastritis but bilious vomiting was common in chronic gastritis, due to duodenogastric reflux and pyloric incompetence (Guzelbektes *et al.*, 2008). Chronic gastritis can be found even in asymptomatic animals (Akhtardanesh *et al.*, 2006). Chronic gastritis in dogs had been thought to be an immune-mediated disorder previously but with the discovery that *Helicobacter pylori* was a common cause of gastritis and peptic ulceration in humans, attention had turned to investigation of the potential role of spiral bacteria in chronic gastritis in dogs (Leib, 2005). The underlying cause of chronic gastritis was rarely identified and in the absence of systemic disease, it might be ulcerogenic or irritant drugs, gastric foreign objects, parasites, fungal infections, dietary allergy or intolerance, occult parasitism and reaction to bacterial antigens or unknown pathogens (Simpson, 2005).

MATERIALS AND METHODS

The study consisted of 13 clinical cases of chronic gastritis presented to the Small Animal Medical Outpatient Clinic of the Madras Veterinary College Teaching Hospital, Chennai, India from different parts of Chennai along with 6 apparently healthy animals. Vomiting persisted for more than five days was taken into consideration. The timing, frequency and characteristics of vomitus were recorded. The dogs were screened for other causes of vomiting by detailed physical and laboratory examination. Three milliliters of blood was collected in vacutainer containing Ethylene Diamine Tetra acetic Acid (EDTA) as anticoagulant for haematological investigation. Haematology including haemoglobin (Hb), Packed cell volume (PCV), Red blood cell (RBC), Mean corpuscular volume (MCV), Mean corpuscular haemoglobin (MCH), Mean corpuscular haemoglobin concentration (MCHC), Total Leucocyte counts (TLC) and Differential leucocyte counts (DLC) were estimated as per standard methods (Jain, 1986). Five milliliters of blood was collected from cephalic vein in vacutainer without anticoagulant taking all precautions for avoiding haemolysis as suggested by Kerr (2002). Serum was separated by centrifugation and used for estimation of blood urea nitrogen (BUN) by Diacetyl Monozime method (Marsh *et al.*, 1965), serum creatinine by Jaffe's alkaline picrate method, Serum Glutamic Pyruvic Transaminase (SGPT) by Reitman and Frankel's method, serum total protein (TP) and albumin by modified Biuret and Dumas method (Varley *et al.*, 1980).

Gastroscopy was done as per method described by Tams (2011). The animals were subjected to gastroscopy and gastroscopic biopsy as part of clinical investigation under general anaesthesia after fasting overnight with the owner's agreement. Gastroscopy was performed using a Fiberoptic Videogastroscope with an outer diameter of 9.7 mm, working length 1400mm and working channel diameter of 2.8 mm (KARL STORZ No. 60914 PKS). Gastric biopsy samples taken using biopsy forceps with long oval cups (fenestrated type) from fundus were immediately transferred to a tube with 1ml of 10% formalin, embedded in paraffin blocks, sectioned and stained with hematoxylin and eosin (HE) and examined for histopathological changes of gastric mucosa by a single pathologist. The values of haematological and serum biochemical parameters in the gastritis group were compared with the control group using the non paired 't' test. The data obtained in the study were subjected to statistical analysis as described by Snedecor and Cochran (1994) and discussed.

RESULTS

The prevalence of chronic gastritis in dogs under study was found to be 92.30 per cent i.e. 12 out of 13 clinical cases of gastritis were found to be positive for chronic gastritis through histopathology (Figure 1). Age wise prevalence of



**Umesh et al.**

chronic gastritis in dogs under study was presented in Figure 2. Highest incidence of chronic gastritis were noticed in age group of 2-5 years which consisted of 6 out of 13 dogs (46.15 per cent), followed by three dogs in age group of less than two years (23.08 per cent), two dogs in 5-8 years and more than 8 years group each (15.38 per cent) (Fig.2). Chronic gastritis was detected in 10 male dogs (76.92 per cent) and three female dogs (23.08 per cent). The prevalence of chronic gastritis in different breeds like Labrador, German Shepherd, Spitz, Non-descript, Doberman and Great Dane were 38.46 per cent (5 dogs), 15.38 per cent (2 dogs), 7.69 per cent (one dog), 15.38 per cent (2 dogs), 15.38 per cent (2 dogs), 7.69 per cent (one dog) respectively.

The degrees of occurrence of predominant clinical signs in chronic gastritis included, chronic vomiting in 12 out of 13 dogs (92.30 per cent), anorexia or inappetence in 7 dogs (53.84 per cent), melena in 7 dogs (53.84 per cent), and weight loss in 9 dogs (69.23 per cent). Less commonly fever, abdominal pain, diarrhoea and pica was noticed in five (38.46 per cent), five (38.46 per cent), two (15.38 per cent), 2 dogs (15.38 per cent) respectively (fig.3). The content of vomitus observed in the present study was food material in two dogs (16.67 per cent), blood in four dogs (33.33 per cent), bile in five dogs (41.67 per cent) and foam in one dog (8.33 per cent). The erythron and leukogram of apparently healthy dogs and dogs with chronic gastritis are given in the Tables 1 and 2.

The mean±S.E values of haemogram of dogs with chronic gastritis included Hb (13.48 ± 0.63 g/dl), PCV (38.10 ± 2.08 per cent), RBC count ($5.90 \pm 0.33 \times 10^6$ /cmm), MCV (65.14 ± 1.94 fl), MCH (23.13 ± 0.71 pg) and MCHC (35.56 ± 0.45 g/dl), WBC count ($13.55 \pm 2.20 \times 10^3$ /cmm), Neutrophil, Lymphocyte, Monocyte and Eosinophil counts ($10.77 \pm 1.86 \times 10^3$ /cmm, $2.35 \pm 0.30 \times 10^3$ /cmm, $0.30 \pm 0.07 \times 10^3$ /cmm and $0.35 \pm 0.12 \times 10^3$ /cmm). There was no statistically significant difference observed in values of haemogram and leukogram between apparently healthy animals and animals with chronic gastritis. The mean±S.E values of serum biochemical parameters of apparently healthy dogs and dogs with chronic associated gastritis are presented in the Table 3. The dogs with chronic gastritis had mean±S.E values of Blood urea nitrogen (BUN), Serum Creatinine, SGPT and total protein (TP), albumin and globulin of 32.63 ± 8.34 mg/dl, 1.84 ± 0.57 mg/dl, 85.24 ± 26.57 IU/L, 6.68 ± 0.41 IU/L, 2.05 ± 0.13 g/dl and 4.43 ± 0.44 g/dl respectively. None of the serum biochemical values showed statistically significant difference in their mean values between apparently healthy animals and animals with chronic gastritis.

The major histopathological changes in gastric mucosa of animals with chronic gastritis observed were lymphocytic plasmacytic gastritis (77.78 per cent), (Figure: 4) infiltration of lymphocytes in the glandular region (55.56 per cent), prominent epithelial injury (37.5 per cent), lymphofollicular hyperplasia (12.5 per cent) and fibrosis (22.22 per cent).

DISCUSSION

Several studies have shown that chronic gastritis is common in dogs, with a prevalence ranging from 67–100 per cent in healthy dogs, 74–90 per cent in dogs presented with vomiting and 100 per cent in laboratory Beagles (Simpson, 2009) and a higher prevalence was noticed in pet dogs (Neiger, 2010). Ali Shabestari *et al.* (2008) reported that there was no significant difference in the prevalence between apparently healthy animals and dogs with vomiting. The prevalence was found to be highest in Labrador Retrievers and may be due to the over representation of this breed in the population. Simpson (2005) reported that there appeared to be no breed or sex predisposition to chronic gastritis. The present study strengthens the findings of chronic vomiting as the predominant and most characteristic clinical sign of chronic gastritis as observed in previous researches (Hermanns *et al.*, 1995 and Leib, 2005). The minor signs also should take in to account like inappetence, pica, weight loss, fever, polyphagia, haematemesis or melena when dealing with chronic gastritis cases (Jenkins and Basset, 1997 and Lobetti, 2006). The less specific haematological and serum biochemical findings in the present study underlines the findings of Simpson (2005) who stated that the clinicopathological changes of chronic gastritis were nonspecific.





Umesh et al.

Ali Shabestari *et al.* (2008) reported that lymphocytic plasmacytic gastritis was the most common type of chronic gastritis in dogs. The common histopathological changes in gastritis were the presence of lymphocytic infiltration in all the regions of the tissue, lymphoid follicular hyperplasia and fibrosis from lamina propria. (Happonen *et al.* (1996), Scanziani *et al.* (1997) and Taulescu *et al.* (2008). Lymphocytic infiltration in all the regions of the tissue, lymphoid follicular hyperplasia and fibrosis from lamina propria were (Happonen *et al.* (1996), Scanziani *et al.* (1997) and Taulescu *et al.* (2008).

ACKNOWLEDGEMENTS

The technical support and facilities received from the Dean, Madras Veterinary College, Director of Clinics, TANUVAS, and the Staff of Department of Animal Biotechnology and Centre of Advanced Faculty Training in Veterinary Clinical Medicine, Ethics & Jurisprudence, Madras Veterinary College, Chennai – 600 007, are thankfully acknowledged.

REFERENCES

1. Simpson, K.W., (2010). Diseases of stomach. In: Ettinger, S.J, and E.C. Feldman (eds), Textbook of Veterinary Internal Medicine: Diseases of dogs and cat. 7th ed. W.B.Saunders Co., Philadelphia. pp. 1515-1520.
2. Redeen, S., (2010). Chronic gastritis: Diagnosis, natural history and consequences. Medical dissertation submitted to Linkoping University, Sweden.
3. Leib, M. S., 2008. Diagnostic Approach to Chronic Vomiting in Dogs and Cats and Challenging Cases of Vomiting. In: Proceedings of 80th Western Veterinary Conference, Las Vegas, Noida.
4. Guzelbektes, H., Coskun, A. Ortatagli, M. and Sen, I. (2008). Serum gastrin in dogs with acute or chronic gastritis and positive or negative for *Helicobacter* sp. in the stomach. *Bull. Vet. Inst. Pulawy*, 52 : 357-361.
5. Ali Shabestari, A. S. L., Mohammadi, M. Jamshidi, S. Sasani, F. Bahadori, A. and Oghalaie, A. (2008). Assessment of chronic gastritis in pet dogs and its relation with *Helicobacter* like organisms. *Pak. J. Biol. Sci.*, 11:1143- 1148.
6. Leib, M. S., (2005). Chronic GI disease: A new look at some common problems. In: Proceedings of the North American Veterinary Conference, Orlando, Florida., 19:367-370.
7. Simpson, K.W., (2005). Diseases of stomach, In : BSAVA Manual of Canine and Feline Gastroenterology, 2nd ed. (Eds) E.J. Hall, J.W. Simpson, D.A. Williams, British Small Animal Veterinary Association, England, pp: 165 – 170.
8. Jain, N.C. 1986. Schalm's Veterinary Haematology. 4th ed., Lea and Febiger, Philadelphia. pp: 821 – 837.
9. Kerr, M. G., 2002. Clinical Biochemistry. In: Veterinary Laboratory Medicine, 2nd ed. Blackwell Science Ltd., pp: 69-111.
10. Marsh, W.H., B. Fingerhut and H. Miller, 1965. Non protein nitrogen, urea, urate, creatinine and creatine. In: Practical clinical biochemistry 5th ed. William Heinemann Medical Books Ltd. London. p: 460.
11. Varley, H., A.H. Grawlock and M. Bell, 1980. Practical Clinical Biochemistry. 5th ed. William Heinemann Medical Books Ltd. London, pp : 458 – 484.
12. Tams, T. R., 2011. Gastroscopy. In: Small Animal Endoscopy. St. Louis, C V Mosby, pp: 97–113.
13. Snedecor, G.W. and W.G. Cochran, 1994. Statistical methods. 8th ed. Iowa State University Press, USA.
14. Neiger, R., 2010. *Helicobacter* colonization: is it a problem?. In: Proceedings of North American Veterinary Conference. Pp; 556-559.
15. Hermanns, W., Kregel, K. Breuer, W. and Lechner, J. (1995). *Helicobacter* like organisms: Histopathological examination of gastric biopsies from dogs and cats. *J. Comp. Pathol.*, 112: 307–318.
16. Leib, M. S., (2005). Chronic GI disease: A new look at some common problems. In: Proceedings of the North American Veterinary Conference, Orlando, Florida., 19:367-370.
17. Jenkins, C.C. and Basset, J. R. (1997). *Helicobacter* Infection. *Comp. Cont. Educ. Pract. Vet.*, 19: 267-275.





Umesh et al.

18. Lobetti, R., (2006). Infectious diseases of the GI tract. In : Proceedings of 2006 World Congress: World Small Animal Veterinary Association, Czech Republic, pp. 471–473.

19. Happonen, I., Saari, S. Castren, L. Tyni, O. Hanninen, M. L. and Westermarck, E. (1996). Comparison of diagnostic Methods for detecting gastric *Helicobacter*-like organisms in dogs and cats. *J. Comp. Path.*, 115: 117-127.

20. Scanziani, E., Di Ceglie G. and Crippa, L. (1997). *Helicobacter* infections and stomachs lesions in dogs. *Veterinaria.*, 11:35-39.

21. Taulescu M., Catoi, C. Gal, A. Bolfa, P. and Rus, I. (2008). Morphological aspects in gastritis induced by *Helicobacter pylori* in dogs. *Vet.Med.*,65: 450-456.

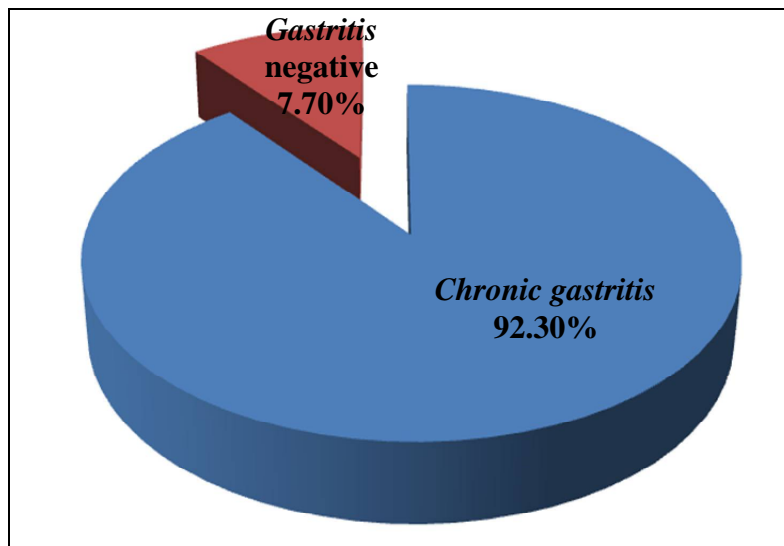


Figure 1.Prevalence of chronic gastritis in dogs under study

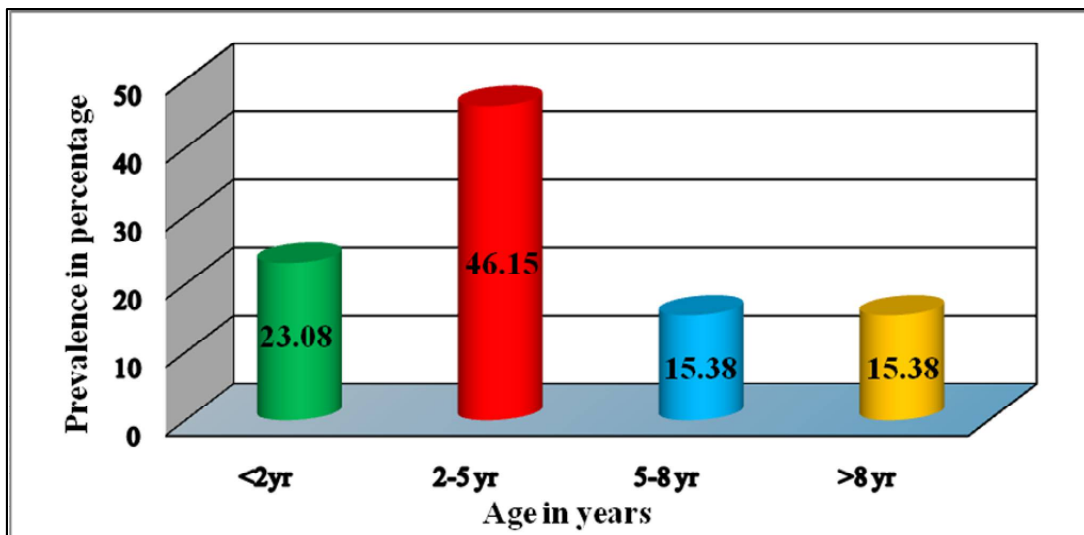


Figure 2.Age wise prevalence of chronic gastritis in dogs under study





Umesh et al.

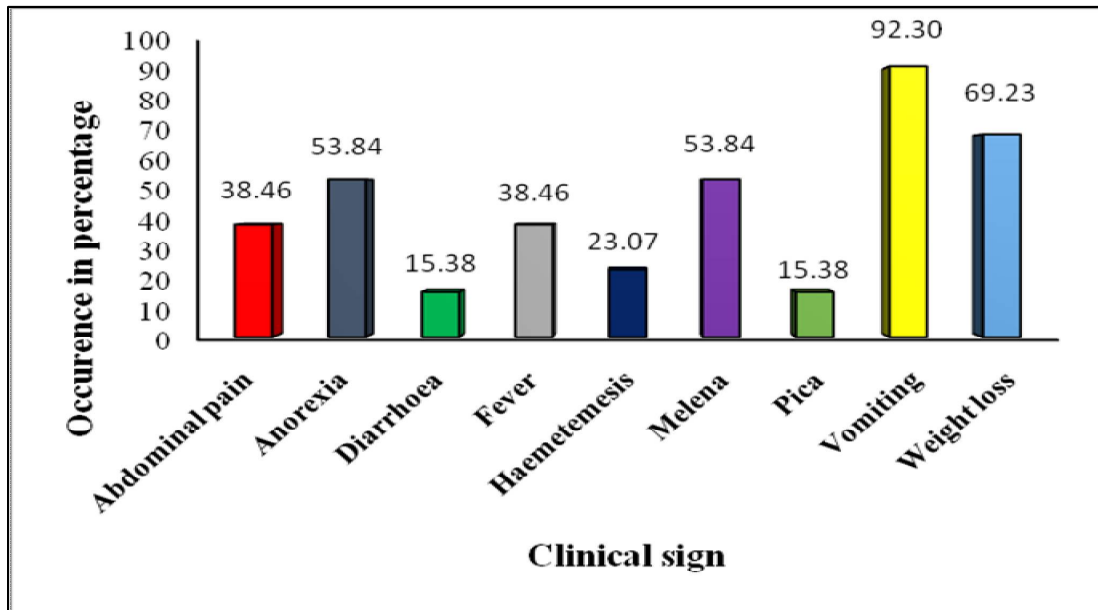


Figure 3.Clinical signs observed in dogs with chronic gastritis

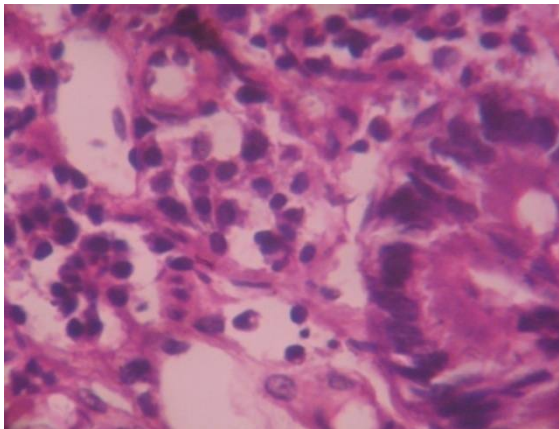


Plate a: Lymphocyte and plasma cell infiltration

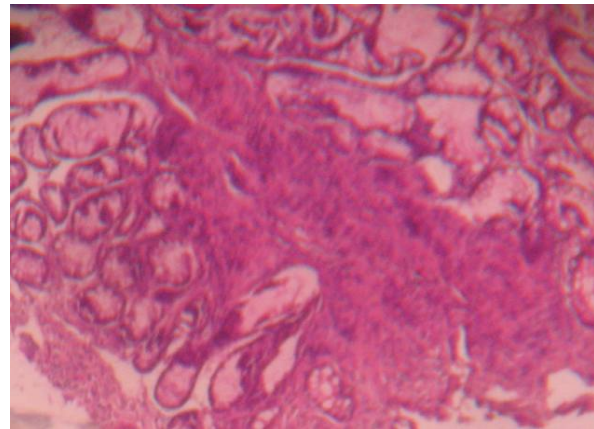


Plate b: Proliferation of fibrous tissue in between the epithelial tissue

Figure 4.Histopathological changes in chronic gastritis





Umesh et al.

Table 1. Erythron of apparently healthy dogs and dogs with chronic gastritis

Parameters	Apparently healthy animals (n = 6)	Chronic gastritis (n = 13)	t
Hb(g / dl)	14.11± 0.80	13.48± 0.63	0.58 ^{NS}
PCV(%)	39.70± 2.57	38.10±2.08	0.45 ^{NS}
RBC(10 ⁶ /cmm)	5.85± 0.34	5.90± 0.33	0.09 ^{NS}
MCV(fl)	67.90±2.70	65.14± 1.94	0.81 ^{NS}
MCH(pg)	24.16± 0.78	23.13± 0.71	0.87 ^{NS}
MCHC(%)	35.63± 0.83	35.56± 0.45	0.09 ^{NS}

NS Non significant (P > 0.05)

Table 2. Leukogram of apparently healthy dogs and dogs with chronic gastritis

Parameters	Apparently healthy animals (n = 6)	Chronic gastritis (n = 13)	t
WBC (10 ³ /cmm)	11.87± 1.13	13.55 ± 2.20	0.50 ^{NS}
Neutrophils (10 ³ /cmm)	8.65± 0.74	10.77± 1.86	0.75 ^{NS}
Lymphocytes(10 ³ /cmm)	2.68± 0.32	2.35± 0.30	0.67 ^{NS}
Monocytes(10 ³ /cmm)	0.33±0.07	0.30± 0.07	0.24 ^{NS}
Eosinophils(10 ³ /cmm)	0.25± 0.06	0.35± 0.12	0.12 ^{NS}

NS Non significant (P > 0.05)

Table 3. Serum biochemistry of apparently healthy dogs and dogs with chronic gastritis

Parameters	Apparently healthy animals (n = 6)	Chronic gastritis (n = 13)	t
BUN (mg / dl)	7.26±0.86	32.63±8.34	2.03 ^{NS}
Creatinine (mg/dl)	0.60±0.13	1.84±0.57	1.45 ^{NS}
SGPT (IU / L)	37.80±3.94	85.24±26.57	1.19 ^{NS}
Total protein (g/dl)	6.84± 0.47	6.68± 0.41	0.23 ^{NS}
Albumin (g / dl)	2.44± 0.10	2.05± 0.13	1.85 ^{NS}
Globulin(g / dl)	4.40± 0.49	4.43± 0.44	0.32 ^{NS}

NS Non significant (P > 0.05)

